NOVEL NON-APOPTOTIC PATHWAY OF CASPASE 3 ACTIVATION DURING MILD OXIDATIVE STRESS

LEOW SAN MIN

B.SC (HONS), NUS

A THESIS SUBMITTED FOR THE DEGREE OF DOCTOR OF PHILOSOPHY

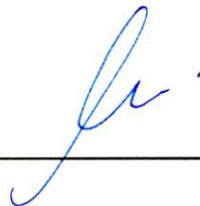## NUS GRADUATE SCHOOL FOR INTEGRATIVE SCIENCES AND ENGINEERING

NATIONAL UNIVERSITY OF SINGAPORE

2012

Declaration

**I hereby declare that the thesis is my original work
and it has been written by me in its entirety. I have
duly acknowledged all the sources of information
which have been used in the thesis**

**This thesis has also not been submitted for any
degree in any university previously.**

Leow San Min

3 January 2013

ACKNOWLEDGEMENTS

I would like to express my heartfelt gratitude to my supervisor, Associate Professor Marie-Veronique Clement, for giving me the opportunity to join her lab as a PhD student and from here embark my journey in the research field. I would like to thank her for being an inspirational and great mentor, and also her words of encouragement and support that spur me on in spite of the difficult moments during the 4 years of my study.

Also, my sincere appreciation goes to my TAC members, Associate Professor Victor Yu Chun Kong, and Dr. Sashi Kesavapany, for their valuable suggestions and help throughout the course of my project.

I would also like to thank my mentor, Michelle, for guiding me in my project during my first year, and my good friends in the lab, Michelle, Charis, Luo Le and Ryan, for the wonderful time we spent together. A big thank to my lab mates, Mui Khin and Dr Alan, for all the help and support they have given me. Special thanks go to Gireedhar and Kai Jun, who have worked along with me, and contributed tremendously to the progress of my project.

Finally, I dedicate this dissertation, however imperfect, to my family and my boyfriend, Eric, for their love and support that see me through good times and bad times.

TABLE OF CONTENTS

SUMMARY

Caspases activation has been established as one of the hallmarks of apoptosis. Nevertheless, non-apoptotic roles of caspases, particularly in vital processes such as cellular differentiation, cell signalling, and cellular remodelling have also been documented in recent years.

In the first part of the study, we compared the effect of caspase 3 activation in cells exposed to a non-toxic dose (50µM) of the oxidative stress inducer, hydrogen peroxide (H_2O_2) to a classical inducer of apoptotic cell death, staurosporine (STS). Our results show that both treatments resulted in activation of caspase 3. Exposure to STS correlated with cell death that was accompanied by the activation of classical apoptotic pathway. On the contrary, activation of caspase 3 by H_2O_2 had no effect on the cells' nucleus morphology and no significant increase in numbers of cells in sub-G1 population. Instead, the cells underwent cell growth arrest up to 72h post-H_2O_2 treatment. While STS activated caspase 3 through the well-established initiator caspase cascade pathway, activation of caspase 3 by H_2O_2 was independent of the initiator caspases. Although STS-activated caspase 3 could transitorily be detected in the cells' nucleus, it ultimately accumulated in the cytosol. In contrast, a sustained nuclear localization of activated caspase 3 was observed in H_2O_2-treated cells.

The second part of the study outlined an unconventional, lysosome-mediated pathway of caspase 3 activation. At 2-4h post-H_2O_2 treatment, lysosomal membrane permeabilization (LMP) was observed. In conjunction with this finding, lysosomal proteases cathepsin B and L were identified as possible upstream activators of caspase 3. Cathepsin inhibitors zFA-FMK and zFY-CHO prevented cleavage and activation of

caspase 3. Iron, peroxynitrite, nitric oxide and p53 were also identified to be upstream factors of LMP and cathepsin-mediated cleavage of caspase 3.

We observed that H_2O_2 treatment induced an increase in lysosomal volume and such increase was prevented by specific caspase 3 inhibitor and molecular silencing of caspase 3. We discovered that Transcription Factor for EB (TFEB), the master gene for lysosome biogenesis, could be regulated by caspase 3. Inhibition of caspase 3 inhibited the expression of TFEB as well as its nuclear localization, which is crucial for its transcriptional role in lysosome biogenesis. We therefore suggest a novel role of caspase 3 in regulating lysosome biogenesis.

LIST OF TABLES

LIST OF FIGURES

ABBREVIATIONS

AEBSF	4-(2-Aminoethyl) benzenesulfonyl fluoride hydrochloride
Apaf-1	Apoptotic protease activating factor-1
Asp	Aspartate
CAD	Caspase-Activated DNase
CARD	Caspase-Recruitment Domain
CM-H_2DCFDA	5-(and-6)-chloromethyl-2´,7´-dichlorodihydrofluorescein diacetate acetyl ester
cPTIO	2-(4-carboxyphenyl)-4,4,5,5-tetramethylimidazoline-1-oxyl-3-oxide
Cys	Cysteine
DAF	4-amino-5-methylamino-2′,7′-difluorofluorescein
DD	Death domain
DED	Death Effector Domain
DFO	Deferoxamine mesylate salt
DFP	Deferiprone
$DIOC_6(3)$	3, 3'-Dihexyloxacarbocyanine Iodide
DISC	Death-inducing signalling complex
DMEM	Dulbecco's Modified Eagle's Medium
DMSO	Dimethyl Sulfoxide
DMTU	Dimethylthiourea
eNOS	Endothelial nitric oxide synthase
ERK	Extracellular-signal-regulated kinases
FACS	Fluorescence-activated cell sorting
FeTPPS	5,10,15,20-Tetrakis(4-sulfonatophenyl)porphyrinato Iron(III), Chloride
HO-1	Heme oxygenase-1
IAP	Inhibitors of apoptosis

IL	Interleukin
JNK	c-Jun N-terminal kinase
LIP	Labile iron pool
LMP	Lysosomal membrane permeabilization
LTD	Long-term depression
MAPK	Mitogen-activated protein kinase
MOMP	Mitochondrial outer membrane permeabilization
mTOR	Mammalian target of rapamycin
mTORC1	mTOR complex 1
NHE-1	Sodium Hydrogen Exchanger-1
nNOS	Neuronal nitric oxide synthase
NOS	Nitric oxide synthase
PARP	Poly (ADP-ribose) polymerase
PFT	Pifithrin-α
PI	Propidium Iodide
PS	Phosphatidylserine
RNS	Reactive Nitrogen Species
ROS	Reactive Oxygen Species
RPMI-1640	Roswell Park Memorial Institute-1640
S.E.M.	Standard error of mean
Sd	Standard deviation
SDS-PAGE	Sodium Dodecyl Sulphate-Polyacrylamide Gel Electrophoresis
Ser	Serine
STS	Staurosporine
TCR	T cell receptor
TFEB	Transcription Factor for EB
TNF	Tumour necrosis factor

CHAPTER 1 INTRODUCTION

1.1 Caspase

1.1.1 The caspase family

Caspases are aspartic acid-specific cysteine protease (Hence the name Caspase: **C**ysteine-**Asp**artate prote**ase**) belongs to the family of interleukin-1β-converting enzyme family. Caspases are synthesized as inactive proenzymes that are distributed in cytoplasm, mitochondrial intermembrane space, and nuclear matrix of most of the cells[1].

In mammalian cells, fourteen caspases have been identified that can be divided into three major groups based on the homology in amino acid sequence and their function (Figure A). The inflammatory caspases (group I) and the initiator caspases (group II) are caspases with long prodomain. The inflammatory caspases (caspase 1, caspase 4, caspase 5, caspase 12, caspase 13 and caspase 14) play important role in cytokine maturation and inflammatory responses[2]. The initiator caspases are divided into those that contain either the Caspase-Recruitment Domain (CARD) (caspase 2 and 9)[3,4], or those that contain the Death Effector Domain (DED) (caspase 8 and 10) at the N-terminal[5,6]. The prodomain dictates how the caspases can be activated. DED and CARD are involved in autoactivation of initiator caspases by facilitating their recruitment into death- or inflammation- inducing signalling complexes[1]. Generally, caspase 8 and 10 with DED can be activated by cell surface receptors while the CARD-containing caspases, i.e. the initiator caspase 2 and 9, as well as the inflammatory caspases 1,4,5, 11 and 12 are activated by environmental insults. The

third group of caspases with short prodomain is known as the effector or executioner

caspases (caspase 3, caspase 6 and caspase 7) or group III caspases[7].
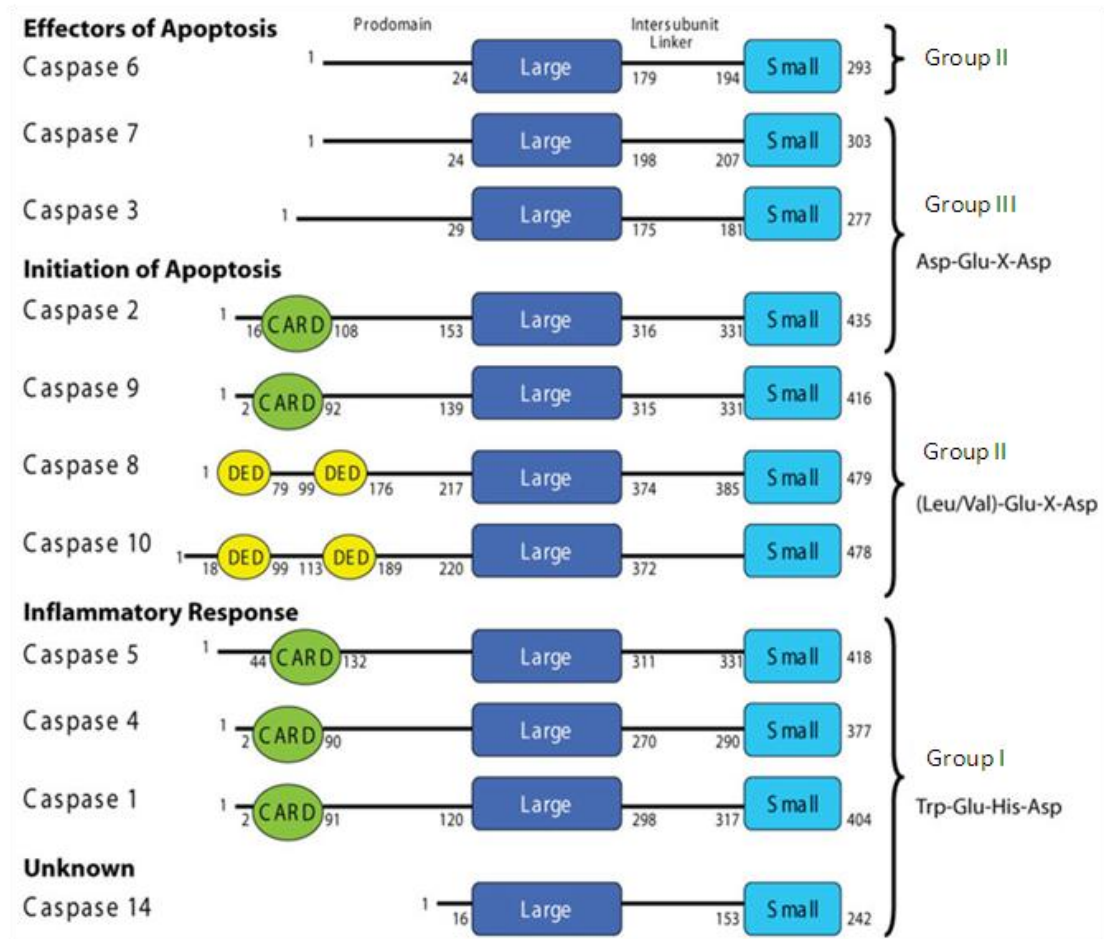
Figure A. The caspase family. Three major groups of caspases. Group I: inflammatory caspases; group II: apoptosis initiator caspases; group III: apoptosis effector caspases. The CARD, the DED, and the large (p20) and small (p10) catalytic subunits are indicated. (Adapted MacKenzie and Clark, 2012[8])

1.1.2 Mechanisms of caspases activation

Caspases are synthesized as inactive zymogens known as procaspases and their activation is tightly controlled. The quaternary structure of an active caspase is composed of two large subunits and two small subunits from the procaspase, forming a tetrameric complex with two active sites (Figure B). The substrate cleavage site of caspases is highly conserved with a tetrapeptide motif with the stringent requirement of an aspartate residue in the P1 position. Caspases cleave their substrate on the carboxyl side of the aspartate residue. The residue at P4 position of the tetrapeptide motif determines the different substrate specificity of different caspases. The catalytic cysteine site consists of a pentapeptide motif (QACXG) and the catalytic reaction is carried out by the cysteine, histidine and glycine residues.
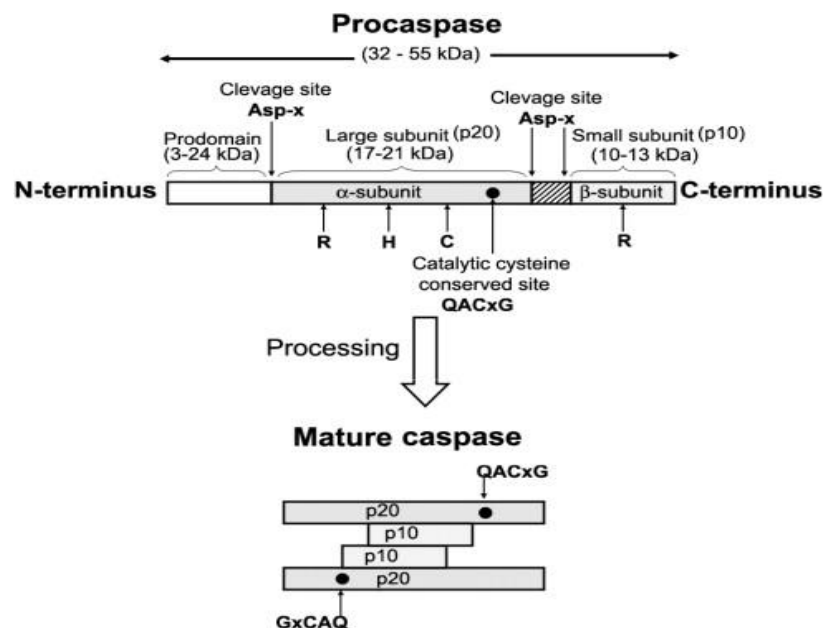
Figure B. Scheme of procaspase activation. Cleavage of the procaspase requires sequential cleavage of the protease, which release the prodomain and the two catalytic subunits. Cleavage at the specific Asp-X bonds leads to the formation of the mature caspase, which comprises the heterotetramer p20 and p10. The residues involved in the formation of the active centre are shown. (Adapted from Chowdhury et al., 2008[1])

Activation of the effector caspases requires sequential proteolysis that separates the prodomain from the large subunit, and the large subunit from the small subunit. Subsequent heterodimerization of the subunits form the active caspase. The cleavage and activation of effector caspase are mediated by the initiator caspases or an activated effector caspase. The effector caspases act as effector of apoptosis through cleavage of cellular substrates that are responsible for biochemical or morphological changes during apoptosis. The activation of initiator caspases involves an assembly of other molecules that either aid in increasing the net concentration and/or induce a conformation change of the procaspase that facilitates their self-activation. Three models are proposed to describe the activation mechanism of initiator caspases: the induced proximity[9], proximity-driven dimerization[10,11], or induced conformation model[12]. As the name suggests, the initiator caspases are the initiator of a caspase cascade and are responsible for activating the effector caspase[13].

1.1.3 Classical pathways of caspase 3 activation during apoptosis

Apoptosis is a genetically regulated mechanism of programmed cell death characterized by cellular changes such as cell shrinkage, chromatin condensation, membrane blebbing, DNA fragmentation, as well as formation of apoptotic bodies which are phagocytised by adjacent cells and phagocytes[14]. It constitutes a common mechanism of cell replacement, tissue remodelling, and removal of damaged cells development, immune regulation and homeostasis of a multi-cellular organism[15]. The process of apoptosis can be initiated by a diverse range of intracellular or extracellular cell signals, such as ionizing radiation, chemotherapeutic agents, oxidative stress, hyperthermia, growth factor or hormone withdrawal, and cytokines[16].

A key feature of apoptosis is the activation of caspases. Inhibition of caspases can lead to induction of necrosis. Compared to necrosis, apoptosis is physiologically advantageous because cellular contents are packed into apoptotic bodies that are recognized and engulfed by phagocytosis, thereby preventing induction of inflammatory response and damage to surrounding tissues. As an executioner caspase, caspase 3 is the critical effector caspase for apoptosis. The human CASP3 gene, homologous to *C. elegans* CED-3 gene was first cloned from human Jurkat T-lymphocytes in 1994[17]. Caspase-3 is either wholly or in part responsible for the proteolysis of a large number of substrates that contain a common Asp- Xaa-Xaa-Asp (DXXD) motif[18], including cytoskeletal proteins[19,20], apoptosis regulators[21], nuclear structural proteins[22], and protein kinases[23]. The cleavage of caspase 3 substrates are responsible for biochemical and morphological changes during apoptosis, such as cell shrinkage and membrane blebbing[22], DNA fragmentation[24], and nuclear condensation[25]. As the central player in the apoptotic machinery, caspase 3 activation

determines cellular sensitivity to diverse apoptotic stimuli, such as doxorubicin[26],
etoposide[26] , and cisplatin[27].

During apoptosis, caspase 3 is activated in the caspase cascade. The caspase cascade
starts with the activation of the initiator caspases 8 and caspase 9 by pro-apoptotic
signals. Once activated, caspase 8 and caspase 9 gain the ability to cleave and activate
caspase 3. Generally, there are three pathways of caspase cascade activation during
apoptosis: the death signal-induced, death receptor mediated pathway (also known as
the extrinsic pathway), the stress-induced, mitochondria-mediate pathway (also
known as the intrinsic pathway), and the less common granzyme pathway. Figure C
illustrates the two more common pathways through which caspase 3 is activated.
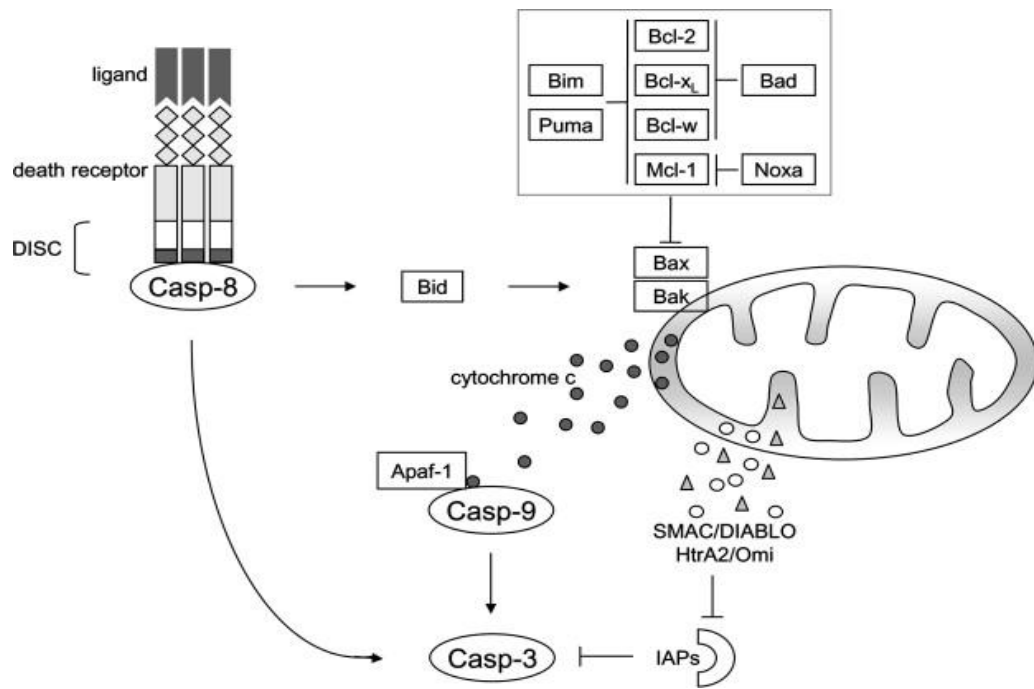
Figure C. The intrinsic and extrinsic pathway of caspase 3 activation. The caspase cascade can be triggered through the extrinsic (death-receptor mediated) pathway or the intrinsic (mitochondrial) pathway. The intrinsic pathway is highly regulated by the Bcl-2 family of proteins. The released mitochondrial proteins Smac/DIABLO and HtrA2/Omi antagonize the inhibitors of apoptosis (IAPs). Cross-talk exists between the two pathways through caspase 8-mediated cleavage of Bid, which then facilitates cytochrome c release. (Adapted from Bruin and Medema, 2008[28])

The extrinsic pathway is initiated by ligands binding to the apoptotic-inducing cell surface receptors known as the death receptors, which are the members of the tumour necrosis factor (TNF) receptor superfamily. The extrinsic pathway can be activated by multiple ligands binding to different death receptors, mediated by different adaptor molecules. However, the pathways to be activated are similar[29]. The homologous cytoplasmic sequence, the death domain (DD) of the death receptor allows the receptor to interact with the DED domain of caspase 8. Binding of ligands to the death receptor induces receptor trimerization, followed by adaptor molecule binding to the DD of the receptor. The adaptor molecule works as a molecular scaffold that juxtaposes multiple procaspase 8 molecules, and together with the death receptors, form the death-inducing signalling complex (DISC). Within DISC, the high local

7

concentration and favourable mutual orientation of multiple caspase 8 enable autoproteolytic activation of caspase 8. Activated caspase 8 then cleaves caspase 3 and results in apoptosis.

On the other hand, the intrinsic pathway of caspase cascade is activated by environmental insults that results in mitochondrial membrane permeabilization (MOMP), which enables cytosolic release of cytochrome c from the intermembrane space of mitochondria. In the cytosol, cytochrome c binds to the scaffolding protein, apoptotic protease activating factor-1 (Apaf-1). The binding of cytochrome c to Apaf-1 induces ATP-dependent conformational change of Apaf-1. Subsequently, Apaf-1 recruits procaspase 9 by binding to the CARD of procaspase 9, leading to the formation of apoptosome complex. Interaction within the apoptosome complex results in conformational change of procaspase 9, which enhances the proteolytic activity of procaspase 9. Mature caspase 9 is released from the multimeric complex and activates caspase 3.

The intrinsic pathway is highly regulated by the Bcl-2 family members. The Bcl-2 family consists of anti-apoptotic proteins such as Bcl-2 and Bcl-XL, and pro-apoptotic proteins such as Bax, Bad and Bid[30]. The Bcl proteins are involved in upstream of apoptosis in induction of caspase cascade. The interplay of these proteins in terms of localization, conformation and/or activity is crucial in regulating the mitochondrial event. Bcl-2 family plays important roles in cross talk of the two pathways. For example, caspase 8 may cleave Bid which then activates Bax, leading to Bax translocation to the mitochondria and initiating the intrinsic apoptotic pathway[31].

Lastly, in the granzyme pathway, caspase 3 is directly cleaved and activated by the serine protease granzyme B. The granzyme pathway is mediated by cytotoxic T cells and usually takes place in tumour cells or virus-infected cells. In this pathway, cells are first permeabilized by perforin, which allows granzyme B to be released from cytotoxic T cells into the target apoptotic cells. In the target cells, granzyme B activates caspase 3 and results in apoptosis[15].

1.1.4 Non-apoptotic functions of caspase 3

In spite of their established role in apoptosis, caspases activation and substrate cleavage have been observed in the absence of cell death, suggesting alternative role of caspases beyond apoptosis. In recent years, mounting evidences have indicated that caspases also play important roles in a variety of non-apoptotic and apoptosis-like vital processes, including cell differentiation, cell signalling, and cellular remodelling. Remarkably, a significant portion of these studies are dedicated to the executioner caspase 3.

Non-apoptotic roles of caspase 3 start to surface when scientists observe constitutive activation of caspase 3 in the absence of cellular stress and pro-apoptotic stimuli[32-34]. Moreover, proteolytic cleavage of known substrates of caspase 3, such as Poly (ADP-ribose) polymerase (PARP), Lamin B, Spectrin and Acinus, can be detected during physiological event such as erythropoiesis and spermatid maturation[35-38]. These are well known substrates of caspase 3 during apoptosis. More importantly, caspase 3 seems to be crucial in maintaining integrity of development. Caspase 3 knockout mice could survive to early perinatal life but with reduction in total skeletal muscle mass and are strikingly smaller compared to the wild-type mice[39]. Studies with caspase knockout mice also indicated that caspase 3 play important roles in osteogenic differentiation of bone marrow stromal stem cells[40], neuronal differentiation of primary derived neuronal stem cells[41], and in proliferation and differentiation of adult hematopoietic stem cells[42].

Non-apoptotic roles of caspase 3 are well established in terminal differentiation that involves compartmentalized cellular degeneration resembling incomplete apoptosis.

During terminal differentiation, cells undergo drastic cellular architecture rearrangement, and these cells lost most of their organelles including mitochondria and nuclei. Nonetheless, cells remain metabolically active despite undergoing such apoptotic-like process. Although the process of terminal differentiation strongly resembles that of apoptosis, there are still distinct differences between terminal differentiation and apoptosis, and this may explain why the cells continue to survive. Whereas apoptotic cells usually exhibit membrane blebbing, there is no evidence of membrane blebbing or the formation of apoptotic bodies in differentiating lens fibre cells or erythroblasts[35]. Compared to apoptosis, the process of terminal differentiation is relatively slow. Enucleation of lens fibre cells[34] and erythroid[43] takes about 3 days to complete.

On the other hand, caspase 3 can also execute its non-apoptotic role in different cellular frameworks that do not exhibit compartmentalized degeneration, by involving in other vital processes of non-degenerative nature. Many of these processes exhibit characteristics of apoptosis in terms of caspases activation and substrate cleavage. However, in many cases such as during differentiation, the timing and intensity of caspases-mediated signals may be critical in determining the cell fate of whether to differentiate or to die.

To date, caspase 3's non-apoptotic functions have been found in cellular differentiation, proliferation, immune functions, neuronal functions, as well as cell motility. Table 1 summarizes recent findings of caspase 3 involvement in non cell death processes.

Table 1. Non-apoptotic functions of caspase 3

Cellular function	Cell type/model/processes	Reference
Differentiation (including terminal differentiation)	Erythroblast	[37]
	Lens epithelial cells	[44]
	Platelets	[45]
	Spermatid	[46]
	Keratinocytes	[47]
	Skeletal muscle	[48]
	Neuronal stem cells	[41]
	Bone marrow stromal stem cells	[40]
	Hematopoietic stem cells	[42]
	Embryonic stem cells	[49]
	Macrophage	[50]
	Glia	[51]
Proliferation	Forebrain cells	[52]
	T cells	[53]
	B cells	[54]
Immune function	Dendritic cell maturation	[55]
	Interleukin (IL)-2 release	[56]
	IL-16 processing	[57]
Neuronal function	Astrocyte cytoskeletal remodelling	[58]
	Dendritic pruning	[59]
	Synaptic plasticity	[60]
Cell motility	Glioblastoma cells	[32]

1.1.5 Regulation of non-apoptotic functions of caspases

The mechanisms to non-apoptotic roles of caspases are less well understood and remain to be fully investigated. It is suggested that the key to caspases' non apoptotic roles could be their selective cleavage specific subsets of substrates, avoiding cell dismantling. For example, during erythroblast differentiation, caspase 3 cleaves GATA-1, a transcription factor specific to erythrocytes. On the other hand, caspase 3 cleaves Mst-1, the transcription factor specific to muscle cells, during myoblast differentiation[48]. The importance of substrate specificity is further shown in proliferating B-cells where caspase 3 cleave p21 but not p27, although p21 and p27 are important proteins in regulating cell cycle progression[54].

Transient and limited caspase activity

In many circumstances, caspase activity might not be regulated in an all-or-nothing manner. There could be fine tune control of caspase activity, such that activation of caspase occurs for a limited period of time and its level is controlled within a certain threshold. This is supported by consistent observation of transient and limited caspase activity in cells where caspases execute their non-apoptotic function, such as differentiation of erythrocytes[61], lens fibre cells[62], and PC12 cells[63].

It is suggested that such controlled caspase activation regulates the substrate cleavage specificity of caspases for specific cellular function. Caspases have different affinities towards different substrates. Transient or low level of caspase activity favours the cleavage of the substrates that exhibit highest affinity[64]. Interestingly, different level of caspase activity may change their cleavage pattern such that the substrates change their functions from anti- to pro-apoptotic as the caspase activity increases[65,66]. For

example, RasGAP, a regulator of Ras- and Rho-dependent pathways, is differentially cleaved under different concentration of activated caspase 3. At low caspase 3 activation, caspase 3 cleaves RasGAP to generate an N-terminal fragment with anti-apoptotic properties. As the caspase activity increases, the fragment is further cleaved into two pro-apoptotic fragments that potentiate DNA damage-induced apoptosis in cells[67,68]. Similarly, the transcription factor STAT3 is reported to possess multiple caspase cleavage sites that are cleaved under different concentration of caspases. This may contribute to differential modulation of STAT3 signalling under apoptotic and non-apoptotic conditions[69].

On the other hand, it is suggested that some substrates are activated by low caspase activation but are inactivated by high caspase activation during apoptosis. One example is the transcription factor NF-kB, which is usually cleaved and inactivated by caspase 3 during apoptosis, and hence inactivates its survival pathway[70]. However, it is now known that during inflammatory response, NF-kB can also be activated by limited activation of caspase 3 through through a PARP-1–mediated mechanism in the absence of apoptosis, leading to NF-kB nuclear translocation and gene transcription activity[71,72].

Several mechanisms have been accounted to achieve a transient and limited caspase activity, including post-translational modification of caspases and inhibition of caspase activity by anti-apoptotic proteins. Caspases activity can be altered by post-translation modification, such as phosphorylation[73] or s-nitrosylation[74]. The inhibitor of apoptosis proteins (IAPs) are endogenous negative regulators of caspases activity by binding to activated caspase and inhibit their activities[75,76]. It is proposed that IAP

play important roles in controlling the extent of caspase activation; to not induce cell death but is sufficient to carry out its non-apoptotic function. In Drosophila, mutations in dbruce (*Dropsophila* IAP) result in spermatid individualization defects and male sterility[46]. Although caspase 3 is required for spermatid differentiation, excessive caspase activity could damage the spermatid nuclei, and this is prevented by dburce. Upon exposure to recorded birdsong, the brief caspase 3 activity found in the zebra finch auditory forebrain is proposed to play important role in memory and learning. In unstimulated forebrain, activated caspase 3 is present but bound to the endogenous inhibitor BIRC4 (XIAP), suggesting an IAP-regulated mechanism for rapid release of activated caspase 3 upon exposure to novel song[59].

Compartmentalized activation of caspase

During apoptosis, a global activation of caspase result in cleavage of many substrates, leading to cell dismantling and apoptosis. In contrast, compartmentalized caspase activation ensures that caspase process specific substrates in specific compartment. A classic example of spatial regulation of caspase activation leading to its specific roles is exemplified in megakaryocytes, where different caspase 3 distributions were found in cells destined for platelet formation and cells destined for cell death. Granular labelling of activated caspase 3 was detected in megakaryocytes during platelet formation, whereas uniform diffused staining of activated caspase 3 was detected in apoptotic megakaryocytes[45].

Regulation at level of substrate cleavage

Other than controlling the activation level and sequestration of activated caspase 3 compartment, caspases can be post-translationally modified or bounded to adaptor

proteins to change their affinity towards specific subset of substrates[73,77]. Similarly, caspase substrates can also be modified to reduce/increase their affinity of cleavage by caspases. For example, phosphorylation of presenilin-2, a substrate of caspase 3 during apoptosis, was found to protect it from caspase 3 cleavage[78]. On the other hand, the timing and intensity of substrate cleavage seems to be critical in determining the cell fate. For example, caspase 3 is reported to cleave Caspase-Activated DNase (CAD) during *in vitro* skeletal muscle differentiation and *in vivo* regeneration, resulting in DNA strand breaks and damage[79,80]. Importantly, such cleavage of CAD by caspase 3 is also a common mechanism during apoptosis. However, it is found that the caspase 3-mediated DNA damage/strand breaks only occurs for a short period and occurs during early stages of the skeletal muscle differentiation[81]. Therefore, whereas prolonged DNA damage/strand break results in apoptosis, transient DNA damage could signal the cells to differentiation.

1.2   Oxidative stress and caspase activation

1.2.1   Oxidative stress

Although the reactive oxygen species (ROS) play essential role in maintaining cellular homeostasis and vital function, their reactivity also causes potential biological damage, damage cellular lipids, proteins or DNA, inhibiting their normal function. Oxidative stress is a biochemical condition characterized by a pro-oxidant state of the cells, which is achieved by disruption in redox state and imbalance between ROS production and elimination[82]. However, in recent years it is also shown that physiological important redox signalling involves a temporary disturbance in the cell redox steady state[83]. Also, interventional trials have shown that shifting the balance by providing more antioxidants has limited protection effect during oxidative stress. This suggests that oxidative stress is not merely a global imbalance of oxidants and antioxidants. Hence, a new definition of oxidative stress as "a disruption of redox signalling and control" has been proposed[83].

In response to oxidative stress, the cells undergo a plethora of cell fate, including growth arrest, gene transcription, initiation of signal transduction pathways, and repair of ROS-induced DNA damage[84,85] . The end result of oxidative stress could be cell death, apoptosis or necrosis, or cellular senescence, or cells could even continue to survive and proliferate[85]. Increased or sustained oxidative stress has also been observed in many pathological condition, such as in cancer, neurodegenerative diseases, chronic inflammatory processes, type II diabetes and in aging[86,87]. The differences in the outcome depend on the cellular genetic background, the species of ROS involved, and the intensity and duration of oxidative stress[88]. It has been reported that the effect of oxidative stress is dose-dependent: low level of ROS

promotes cell proliferation and survival, while high level of ROS promote cell death[89].

In fact, low level or physiological level of ROS is implicated in signal transduction network known as redox signalling. This is attributed to the ability of low level of ROS to reversibly modify critical residues of macromolecules such as lipids, proteins and DNA. Such reversible modification of ROS is able to modulate the macromolecules' activity and function in signal transduction. On the other hand, excessive ROS attacks macromolecules in an irreversible manner. Such unspecific attack of ROS often results in irreversible oxidative damage and succumb the cells to unfavourable cell fate such as cell death or senescence.

1.2.2 ROS-mediated caspase activation

The link between oxidative stress/ ROS and caspase activation is well established on the premise of apoptosis. Classic inducers of apoptosis, such as Fas[90,91], TNF[92], TRAIL, and staurosporine[93] have been shown to activate caspase cascade in different cell lines through mechanisms involving ROS. Also, exogenous addition of oxidants such as H_2O_2 has been shown to induce caspase activation and result in apoptosis[94]. It is believed that ROS are able to modulate caspase activity, through multiple mechanisms that could cross talk and may be dependent of each other. Generally, ROS mediates caspase activation through signalling pathway, while ROS inhibition of caspase activation occurs through direct modification of caspases molecules. Nevertheless, it has also been shown that ROS mediates caspase 9 activation by oxidatively modified caspase 9. This facilitates the interaction between caspase 9 and Apaf-1 through the formation of disulfide bond within a complex, essentially promoting apoptosome formation and caspase 9 activation[95]. On the other hand, it is postulated that caspase could be involved in ROS generation, as intracellular oxidation has been observed in cells undergoing apoptosis in response to non-oxidative trigger.

How ROS modulate caspases activation is intriguing. ROS are broad-spectrum molecules that have multiple targets and engage in multiple signalling pathways. It has been shown that ROS are able to modify both pro- and anti-apoptotic factors[96]. Hence, ROS signalling to caspase activation is likely to be complex and involves multiple pathways. Organelles prone to oxidative stress, such as the mitochondria, lysosome, and endoplasmic reticulum, are sensors to oxidative stress that further elicit series of complex pathways. In addition, DNA damage and activation of the

Mitogen-activated protein kinase (MAPK) pathways are important response during ROS-induced apoptosis. Ultimately, most of these pathways converge on the mitochondrial pathway leading to caspase cascade activation.

As the major site of intracellular ROS generation, mitochondria are particularly susceptible to the damaging effects of ROS. One of the consequences of ROS-induced mitochondria damage is mitochondrial outer membrane permeabilization (MOMP). Cytochrome c is release to facilitate apoptosome formation and caspase 9 activation, and consequently caspase 3 activation. MOMP is a point of no return for caspase activation and cell death. Activation of caspase cascade during oxidative stress through the mitochondrial pathway is supported by various experimental evidences[97,98]. Components within mitochondria sensitive to oxidative damage include the respiratory chain complexes[99,100], voltage-dependent anion channel[101], and cardiolipin[102]. Disruption or oxidation of these components may promote cytochrome *c* release and collapse of the mitochondrial transmembrane potential, and ultimately activation of the caspase cascade.

Other than MOMP and cytochrome c release, ROS could trigger caspase cascade through modulation of components in the activating signalling complexes. For example, Apaf-1 has been found to be oxidized by ROS, which promotes apoptosome formation and consequently leading to activation of caspase 9 and 3[103].

1.2.3 Caspase 3 activation during mild oxidative stress

Despite the well-established pathways of caspase 3 activation by ROS leading to apoptosis, our lab has recently demonstrated that caspase 3 can be activated during mild oxidative without leading to cell death[104]. Mild oxidative stress elicited by 50μM H_2O_2 induced caspase 3 activation that was responsible for sustained repression of Sodium Hydrogen Exchanger-1 (NHE-1) protein expression, which has been implicated in cell proliferation and transformation[105]. Not only that the study was the first highlighting the role of caspases 3 in the oxidative repression of gene expression, it also revealed an alternative pathway of caspase 3 activation through iron-dependent mechanism in the absence of cell death. It is proposed that the decrease in NHE-1 expression by activation of caspase 3 may be critical in arresting cell growth during mild oxidative stress, even in the absence of cell death.

One of the characteristics of cancer cells is their ability to evade apoptosis, which results in uncontrolled proliferation. Surprisingly, in a number of viable cancer cells, constitutive caspases activities have been observed[32]. This implies that caspases have important roles in tumour progression other than their implication in apoptosis. Consistent with this observation, chronic oxidative stress or increased ROS level has been observed in many cancer cells[106,107]. Therefore, understanding the implications of caspase activation during mild oxidative stress may be important in shedding some light on the mechanisms of tumorigenesis.

1.3 Aim of study

Caspase activation has been closely associated with apoptosis. In recent years, evidences that caspases are involved in a numbers of non-apoptotic processes have surfaced. For example, caspases are required in cellular function such as differentiation and proliferation of specific cell types. This means that caspases play important roles in the control of life and death. Nevertheless, how caspases are regulated as well as the pathway leading to their non-apoptotic roles is poorly understood.

Previous study in our lab provided evidences that caspase 3 could have a non-apoptotic roles in regulating gene expression during mild oxidative stress. When cells were treated with 50μM H_2O_2, NHE-1 gene expression was down-regulated. This down-regulation of NHE-1 gene was caspase 3 and 6 dependent[104]. Not only so, caspase 3 is also involved in ROS generation. Furthermore, although H_2O_2 treatment activated caspase 3 and 6, there was no apoptosis.

The aim of our present study is to unravel the pathway leading to caspase 3 activation in the absence of cell death during mild oxidative stress. Also, the alternative role of caspase 3 besides apoptosis was explored.

CHAPTER 2 MATERIALS AND METHODS

2.1 Materials

2.1.1 Chemicals and reagents

Company	Chemical and reagents
Hyclone, UT, USA	Dulbecco's modified Eagle's medium (DMEM), Roswell Park Memorial Institute-1640 (RPMI-1640) Foetal bovine serum (FBS), Phosphate Buffered Saline (PBS), Trypsin, L-glutamine
Lonza (Walkersville, MD, USA)	Gentamicin Sulphate
Sigma-Aldrich, MO, USA	Aprotinin, Pepstatin A, Phenylmethanesulfonyl Fluoride (PMSF), Leupeptin, Sodium Vanadate, Dimethylsulfoxide (DMSO), Deferoxamine mesylate salt (DFO), o-Phenantroline monohydrate (PHEN), Dithiothereitol (DTT), Staurosporine (STS), Dimethylthiourea (DMTU), Triton X-100, Propidium Iodide, RNAse A, Crystal Violet, Bovine Serum Albumin (BSA), Carbonyl cyanide m-chlorophenylhydrazone (CICCP), Pepstatin A, 4-(2-Aminoethyl) benzenesulfonyl fluoride hydrochloride (AEBSF)
Acros Organics, Geel, Belgium	Deferiprone (DFP)
Merck KGaA, Darmstadt, Germany	Methanol, Hydrogen peroxide, Sodium Dodecyl Sulphate (SDS)
R&D system	zDEVD-FMK, zIETD-FMK, z-LEHD,FMK, zVAD-FMK, zFA-FMK,QVD-OPH
Enzo Life Sciences	Ac-DEVD-AFC, Ac-IETD-AFC, Ac-LEHD-AFC, Pifithrin-α (PFT)
Cell Signaling Technology (Beverly, MA, USA)	Chaps cell extract buffer
BD Pharmingen, USA	Cell lysis buffer (1X)
Molecular Probes (Molecular Probes Inc., Eugene, OR, USA)	5-(and-6)-chloromethyl 2',7'-dichlorodihydrofluorescein diacetate acetyl ester (CM-H_2DCFDA),4-Amino-5-Methylamino-2',7'-Difluorofluorescein Diacetate (DAF-FM Diacetate), Hoechst 34580, Lysotracker® DND-99, Acridine Orange, 3, 3'-Dihexyloxacarbocyanine Iodide (DIOC$_6$(3))
Pierce Biotechnology, Rockford, IL, USA	Coomassie Plus^{TM} Protein assay reagent, Restore^{TM} Western Blot Stripping buffer, Supersignal West Pico chemiluminescent substrate

Company	
A.G. Scientific, Inc., CA, USA	2-(4-carboxyphenyl)-4,4,5,5-tetramethylimidazoline-1-oxyl-3-oxide (cPTIO)
Calbiochem (Merck KGaA, Darmstadt, Germany)	5,10,15,20-Tetrakis(4-sulfonatophenyl)porphyrinato Iron (III), Chloride (FeTPPS), zFY-CHO, Cathepsin G inhibitor I
Invitrogen, CA, USA	Opti-MEM®I reduced serum medium, Lipofectamine^{TM} RNAiMAX
Santa Cruz Biotechnology, CA, USA	Calpeptin

2.1.2 Antibodies

Company	Antibodies
Cell Signaling Technology (Beverly, MA, USA)	Rabbit polyclonal anti-caspase 3 (#9662) Rabbit monoclonal anti-cleaved caspase 3 (#9664) Rabbit monoclonal anti-caspase 8 (#4790) Mouse monoclonal anti-caspase 9 (#9508) Mouse monoclonal anti-p53 (#2524) Rabbit polyclonal anti-phospho p53 (Ser15) (#9284)
DakoCytomation (Glostrup, Denmark)	Polyclonal Goat Anti-Rabbit Immunogluobulins/HRP (P0448)
Pierce (Pierce, Thermo Fisher Scientific Inc, Rockford, IL, USA)	Horseradish peroxidase (HRP)-conjugated goat anti-mouse secondary antibody (#31430)
Sigma-Aldrich (St Louis, USA)	Mouse monoclonal Anti-β-actin (A5441)
Abcam (Cambridge, UK)	Rabbit polyclonal anti-cathepsin B (ab33538) Mouse polyclonal anti-cathepsin L (ab6314) Rabbit polyclonal anti-active caspase 3 (ab13847) Rabbit polyclonal anti-p21 (ab7960) Rabbit polyclonal anti-Lamin B1 (ab16048)
Santa Cruz Biotechnology, CA, USA	Rabbit polyclonal anti-SOD1 (sc-11407) Rabbit polyclonal anti-TFEB (sc-48784) Rabbit polyclonal anti-HO-1 (sc-10789)
Molecular Probes (Molecular Probes Inc., Eugene, OR, USA)	Rhodamine Red^{TM}-X goat anti-rabbit IgG (R6394)

2.1.3 Cell lines and cultures

L6 rat myoblasts stably transfected with full length proximal 1.1kb of NHE-1 promoter were obtained from Dr. Larry Fliegel (Department of Biochemistry, University of Alberta, Canada)[108]. L6 myoblasts were maintained in Dulbecco's modified Eagle's medium (DMEM) supplemented with 10% FBS, 2mM L-glutamine, 0.25mg/ml Geneticin (G418 sulfate), and 1mM Gentamicin Sulfate at 37ºC, with 5% CO_2 in a humidified atmosphere. For experiment with serum starved condition, cells were grown in DMEM with 0.5% FBS.

2.2 Methods

2.2.1 Treatment of cells with H_2O_2 and other compounds

A stock solution of 10mM H_2O_2 was prepared by diluting 30% (v/v) H_2O_2 solution with 1X PBS. Diluted H_2O_2 in 1X PBS was added into the medium to attain the final concentration required in the experiments. Stock solutions of caspase peptide inhibitors (zVAD-FMK, zDEVD-FMK, QVD-OPH, zIETD-FMK, zLEHD-FMK), DFO, zFA-FMK, zFY-CHO, cathepsin G inhibitor I, pepstatin A, and calpeptin were dissolved in DMSO. Stock solutions of DFP, DMTU, cPTIO, AEBSF, and FeTPPS were dissolved in 1XPBS. For treatment of cells with compounds with DMSO, a vehicle control (DMSO) was included in the experimental setup.

2.2.2 Morphology studies

The morphology of the cells was analyzed by under Nikon Eclipse TS100. Morphology pictures are taken with Nikon DS-Fi1c at the magnification of 10X.

2.2.3 Luciferase Gene Reporter Assay

NHE-1 promoter activity of stably transfected cells were assessed with single-luciferase assay (Promega, Madison, WI) according to manufacturer's instructions. Adherent cells were lysed with 100µl reporter lysis buffer at room temperature and lysate harvested were incubated on ice for 10min. For single luciferase assay, 10µl cell lysate was added to 50µl luciferase substrate. Bioluminescence generated was measured using a Sirius luminometer (Berthold, Pforzheim, Germany). Luminescence readings obtained were normalized to protein concentration of the lysate, which was measured using the Coomassie Plus^{TM} Protein assay reagent.

2.2.4 Caspase Activity Assay

After treatment, cells were harvested and were lysed with 1X Cell Lysis Buffer (10mM Tris-HCl at pH 7.5, 10mM NaH2PO4/NaHPO4, 130mM NaCl, 1% Triton X-100, 10mM sodium pyrophosphate) (BD Biosciences Pharmingen, San Diego, CA). After centrifugation at 12,000rpm, 4°C for 5 min, 40µl cell lysate was added to 44µl of reaction mixture consists of: 4µl of specific caspase substrate (1mM (stock conc), caspase 8 substrate: Ac-LETD-AFC, caspase 3 substrate: Ac-DEVD-AFC and caspase 9 substrate: Ac-LEHD-AFC) and 40µl of 2X Reaction Buffer (10mM HEPES, pH 7.4, 2mM EDTA, 6mM DTT, 10mM KCl and 1.5mM MgCl$_2$) supplemented with protease inhibitors (1mM phenylmethylsulfonyl fluoride (PMSF), 10µg/ml aprotinin, 10µg/ml pepstatin A, 20µg/ml leupeptin), into a 96-well microplate. Samples were incubated at 37°C for 1h and fluorescence was read at an excitation wavelength of 400 nm and an emission wavelength of 505 nm using Spectrofluoro Plus spectrofluorometer (TECAN, GmbH, Grodig, Austria). Caspase

activity was normalized against protein concentration of each sample and expressed as relative fluorescence unit per microgram of protein (RFU/µg).

2.2.5 Cell viability estimation by Crystal Violet Assay

Crystal violet assay was used to estimate the number of viable and adherent cells. Cells were grown on 6-well plates and were subjected to various treatments. After washing with 1X PBS, cells were stained with 0.5ml crystal violet solution (0.75% (w/v) crystal violet, 50% (v/v) ethanol, 1.75% (v/v) formaldehyde, 0.25% (w/v) NaCl) for 10min. Excess crystal violet solution was carefully washed away with water and the plates were left to air-dry. Each well was then added with 1ml of 1%SDS/PBS to solubilize the dye retained in the adherent cells. 50µl of cell lysate from each well was transferred into separate wells of 96-well microplate and the absorbance was measured at 595nm using Spectrafluor Plus spectrofluorometer (TECAN, GmbH, Grödig, Austria). Cell density at each time point (with or without treatments) was expressed as the percentage relative to the density of control untreated cells at time zero.

2.2.6 DNA Fragmentation Assay/Cell cycle analysis

Cells harvested were centrifuged at 2500rpm for 5min. Cell pellet were washed twice with 1XPBS and were resuspended in ice-cold PBS/1%FBS. Cells were then fixed with 70% ethanol and were left at 4°C for at least 30min. After fixation, cells were centrifuged at 10,000rpm for 5min at 4ºC. The cell pellet was washed twice with ice-cold 1% FBS/PBS before staining with 500µl of PI/RNaseA staining solution for 30min at 37ºC. The samples were then subjected for flow cytometry analysis using the excitation wavelength of 488nm and emission wavelength of 610nm on the flow

cytometer (BD FACSCanto II, BD Biosciences, CA, USA). Flow cytometry data was analyzed with Cyflogic^{TM} software (CyFlo Ltd, Finland).

2.2.7 SDS-PAGE and Immunoblotting

Cells harvested were lysed with Chaps cell extract buffer (Cell Signalling Technology (Beverly, MA, USA)) supplemented with 1mM PMSF and 5mM DTT. Before measurement of protein concentration, the lysate was centrifuged at 14,000rpm for 10min to remove the debris. Protein quantification was performed using the Coomassie Plus™ Protein assay reagent (PIERCE, Thermo Fisher Scientific Inc, Rockford, IL, USA).

For detection of protein of interest, 50μg of total protein per sample was subjected to SDS-PAGE with 15% (v/v) acrylamide resolving gel at 110V using the Bio-Rad Mini-PROTEAN 3 Cell (CA, USA). Protein samples were mixed with the 5x loading dye (0.313M Tris HCl (pH 6.8), 10% SDS (w/v), 0.05% bromophenol blue, 50% glycerol and 0.5M DTT) and heated at 95°C for 5min before loading. Kaleidoscope pre-stained standards (Bio-Rad, CA, USA) was used to estimate the molecular sizes of the proteins bands obtained. The resolved proteins were transferred onto a nitrocellulose membrane by the wet transfer method at 350mA for 1h using the Bio-Rad Mini Trans-Blot Electrophoretic Transfer Cell (CA, USA) in an ice-bath. Blocking was done in 5% fat-free milk in Tris-buffered saline /Tween 20 (TBST) (20 mM Tris-HCl, pH 7.6, 137mM NaCl, 0.1% Tween 20), at room temperature for 1h. The membrane was washed with TBST to remove excess milk before incubated with primary antibodies (diluted in 5% (w/v) BSA) overnight at 4°C. After washing off the unbound primary antibody with TBST, the membrane was subsequently incubated with

the respective horse radish peroxidase conjugated secondary antibodies (diluted in 5% (w/v) milk) for 1h at room temperature. Probed protein of interest was detected with enhanced chemiluminscence using SuperSignal Chemiluminescent Substrate (PIERCE, IL, USA) with Kodak Biomax MR X-ray film. For re-probing of the same membrane for different proteins, membrane was stripped with Restore Western Blot Stripping Buffer for 10min at 37ºC, before incubation with primary and secondary antibody for another protein. For densitometric analysis, the bands obtained were scanned with EPSON Perfection 1250 and analyzed by FujiFilm Multigauge V3.0. The band density for proteins was normalized against the band density of β-actin.

2.2.8   RNA Interference (RNAi) Assay

Cellular transfection of siRNA was performed using Lipofectamine® RNAiMAX (Invitrogen, Carlsbad, CA, USA) according to the manufacturer's protocol. Cells were seeded and grown for at least 24h before transfection. For transfection, medium was replaced with DMEM/10% FBS without antibiotics. siRNA of specific gene or control siRNA was mixed with the Lipofectamine® RNAiMAX in Opti-MEM®I reduced serum medium (Invitrogen, Carlsbad, CA, USA). The mixture was incubated for 20min. resuspended thoroughly, and was subsequently added drop-wise into each well. At 8h post-transfection, cells were washed with 1XPBS and replaced with fresh DMEM/10%FBS medium. Cells were harvested for various assays at 24h or 48h post-transfection.

siRNA for caspase 3 (ON-TARGETplus SMARTpool - Rat CASP3), p53 (ON-TARGETplus SMARTpool - Rat TP53), and cathepsin B (ON-TARGETplus SMARTpool - Rat CTSB) were purchased from Dharmacon (Thermo Scientific, IL,

USA). A negative control siRNA (QIAGEN, Valencia, CA, USA) that is non-homologous to any known gene sequence was used as a negative control.

2.2.9   Nuclear-Cytoplasmic Fractionation

Nuclear-cytoplasmic fractionation was performed with the NE-PER Nuclear and Cytoplasmic Extraction Reagents (PIERCE, Thermo Fisher Scientific Inc, Rockford, USA) according to manufacturer's protocol. Briefly, cells harvested were centrifuged at 2200rpm, 5min at 4ºC. Pellet collected was resuspended in 200µl of ice-cold CERI buffer by vortexing at maximum speed for 15s. 11µl CERII buffer was added and the resuspension was vortexed for 5s before centrifugation at 16,000g for 5min at 4ºC. The supernatant was collected as the cytosolic fraction. The nuclear pellet was lysed in 100µl of ice-cold NER buffer. The resuspension was vortexed for 15s and subsequently incubated on ice for 20min. Debris was removed by centrifugation at 16,000g for 10min at 4ºC and the supernatant was collected as the nuclear extract.

2.2.10 Immunofluorescence Assay using Confocal Microscopy

For immunofluorescence assay, cells were seeded on cover slips on 12-well plate. Cells were fixed with 4% paraformaldehyde for 30min at room temperature. After fixation, cells were washed with 1XPBS twice to remove excess paraformaldehyde. After washing with 100mM NH_4Cl for 5min twice and washing with 1XPBS, cells were permeabilized with 0.2% TX-100 (Sigma-Aldrich, LO, USA) for 10min at room temperature. Cells were then incubated with primary antibody of the protein of interest for 2h at room temperature. After washing with PBS, cells were incubated with Rhodamine Red™-X goat anti-rabbit IgG R6394 (Molecular Probes Inc., Eugene, OR, USA) and with Hoechst 34580 (Molecular Probes Inc., Eugene, OR,

USA) for 1h. The cells were washed three times with 1XPBS before the cover slip was mounted for confocal analysis using Olympus FluoView1000 (FV1000; Olympus, Japan) with identical acquisition parameters for the same image session. Pictures are analyzed with Olympus FLUOVIEW Ver1.7a Viewer.

2.2.11 Intracellular ROS/RNS Measurement by flow cytometry

Cells were trypsinized and were centrifuged at 2500 rpm for 5min to collect the cell pellet. Cell pellet was resuspended and incubated with 5µM CM-H$_2$DCFDA (for ROS measurement) or DAF-FM Diacetate (for RNS measurement) at 37ºC in dark. After 15min, cell suspension was centrifuged at 2500rpm for 5min and washed with PBS twice to remove excess dye. Cells were resuspended in 500µl PBS and were subjected to flow cytometry analysis of DCF or DAF fluorescence using the FITC channel on the flow cytometer (BD FACSCanto II, BD Biosciences, CA, USA). Flow cytometry data was analyzed with Cyflogic^{TM} software (CyFlo Ltd, Finland).

2.2.12 Analysis of lysosomal membrane permeabilization with the Acridine Orange assay

Cells were incubated with a solution of 10µM Acridine Orange (Molecular Probes Inc., Eugene, OR, USA) for 30min at 37ºC before treatment with H$_2$O$_2$. At various time points, cells were trypsinized and were centrifuged at 2500 rpm for 5min to collect the cell pellet. Cells were resuspended in 500µl PBS and were subjected to flow cytometry analysis of Acridine Orange fluorescence using the FITC-A channel (BD FACSCanto II, BD Biosciences, CA, USA).

2.2.13 Analysis of lysosomal volume with Lysotracker and Acridine orange staining

Lysosomal volume was assessed by immunofluorescence with Lysotracker® Red DND-99 (Molecular Probes Inc., Eugene, OR, USA) or by flow cytometry with Lysotracker DND99 or Acridine Orange staining. For immunofluorescence, cells were seeded on cover slips on 12-well plate. After treatments with H_2O_2 or drugs, cells were incubated with a solution containing 75nM Lysotracker® Red DND-99for 45min, 37ºC. Cells were then fixed with 4% paraformaldehyde for 30min at room temperature. After fixation, cells were washed with 1X PBS twice to remove excess paraformaldehyde. After washing with PBS, the cover slip was mounted for confocal analysis using Olympus FluoView1000 (FV1000; Olympus, Japan) confocal microscope with identical acquisition parameters for the same image session. For flow cytometry analysis of lysosomal volume, cells were exposed to a solution of 75nM Lysotracker® Red DND-99 for 45min or 10μM Acridine Orange for 30min after treatment with H_2O_2. Cells were then trypsinized and were centrifuged at 2500 rpm for 5min to collect the cell pellet. Cells were resuspended in 500μl 1X PBS and were subjected to flow cytometry analysis of Lysotracker or Acridine Orange fluorescence under the PerCP-A channel (BD FACSCanto II, BD Biosciences, CA, USA). Flow cytometry data was analyzed with Cyflogic^{TM} software (CyFlo Ltd, Finland).

2.2.14 Analysis of Mitochondrial Outer Membrane Permeabilization with $DIOC_6(3)$

Cells were trypsinized and were centrifuged at 2500 rpm for 5min to collect the cell pellet. Cell pellet was resuspended and incubated with 10nM $DIOC_6(3)$ (Molecular

Probes Inc., Eugene, OR, USA) at 37ºC in dark. After 15min, cell suspension was centrifuged at 2500rpm for 5min and washed with PBS twice to remove excess dye. Cells were resuspended in 500µl PBS and were subjected to flow cytometry analysis using the FITC-A channel on the flow cytometer (BD FACSCanto II, BD Biosciences, CA, USA). Flow cytometry data was analyzed with Cyflogic^{TM} software (CyFlo Ltd, Finland).

2.2.15 Statistical Analysis

Data are presented as mean ± standard error of mean (S.E.M.) where n≥3. Student's t-test was performed when appropriate, using the Microsoft Excel software, with p-value of less than 0.05 considered significant. In the event of n=2, data are presented as mean ± standard deviation (Sd).

CHAPTER 3 RESULTS

3.1 Characterization of non-classical caspase 3 activation upon H_2O_2 treatment

3.1.1 Exposure of L6 myoblasts to non-toxic does of H_2O_2 results in caspase 3 activation

Exogenous addition of H_2O_2 to cells may result in a physiological or pathological outcome, depending on the H_2O_2 concentration. At low dosage, H_2O_2 acts as second messenger in cell signalling, its mechanism includes oxidation of redox-sensitive cysteine residues of protein kinases and transcription factors[109]. At high dose, H_2O_2 can cause apoptosis and necrosis[110]. In the present study, we aimed to establish a setting whereby H_2O_2 elicits a mild oxidative stress without inducing cell death.

L6 myoblasts were seeded in DMEM containing 10% FBS overnight before exposure to 50μM H_2O_2. After 1 hour, cells were recovered in fresh 10% FBS medium (Figure 1A). To show that 50μM H_2O_2 does not induce cell death, we used the well-established apoptotic inducer, staurosporine (STS) as a positive control for apoptosis. STS was discovered in 1977 in a culture of an actinomycete (*Streptomyces* strain AM-2282(T))[111], and was first shown to be a potent inhibitor of protein kinases[112,113]. STS was shown to induce apoptosis in a variety of cell lines and has since been used as an apoptotic trigger. STS induces apoptosis through multiple signalling pathways, including arrest of cell cycle progression[114-116], caspase activation[117,118], cathepsins-related mechanisms[119,120], and focal adhesion disassembly[121].

To determine if the cells undergo apoptosis after H_2O_2 treatment, we assessed morphological and biochemical hallmarks of apoptosis, including observation of cell morphology, inspection of nuclear fragmentation, and determination of the percentage of cells in subG1 phase by cell cycle profiling. L6 myoblasts exposed to 1μM STS showed shrunken and rounded cell morphology at 24h and 48h, while cells exposed to 50μM H_2O_2 maintained a normal morphology that was comparable to the control untreated cells (Figure 1B). Staining of cell nuclei with the Hoechst 34580 nucleic acid stain enables observation of cell nuclei under the fluorescence microscope. The nuclei of L6 myoblasts remained intact when cells were exposed to 50μM H_2O_2 for 24h and 48h while nuclei condensation and nuclear fragmentation were observed in STS-treated cells (Figure 1C).

The degree of nuclei fragmentation was quantitatively measured by use of a DNA intercalating dye, Propidium Iodide (PI), in Fluorescence-absorbent cell scanner (FACS) analysis of cell cycle (Figure 1D). In apoptotic cells where DNA are fragmented, a high population of cells show reduced DNA content, as fragmented DNA leaks out of the cells when cells are permeabilized. This is shown as the subG1 phase on cell cycle profile. In this phase, the DNA content is lower than that in the G1 phase (n). Therefore, the subG1 phase of cell cycle profile corresponds to the population of apoptotic cells with fragmented DNA. At 24h and 48h, the basal level of apoptotic cells was 2-4% of the whole population. Upon treatment with H_2O_2, there was a slight increase of 2% in the percentage of subG1 cells; however, the increase was statistically insignificant (Figure 1D). In contrast, STS-treated samples recorded an increase of close to 7 fold in percentage of cells in the subG1 phase compared to control cells. The percentage of apoptotic cells upon STS treatment was 14.6% and

20.7% at 24h and 48h respectively (Figure 1D). This indicated that a significant percentage of STS-treated cells underwent apoptosis.

A)
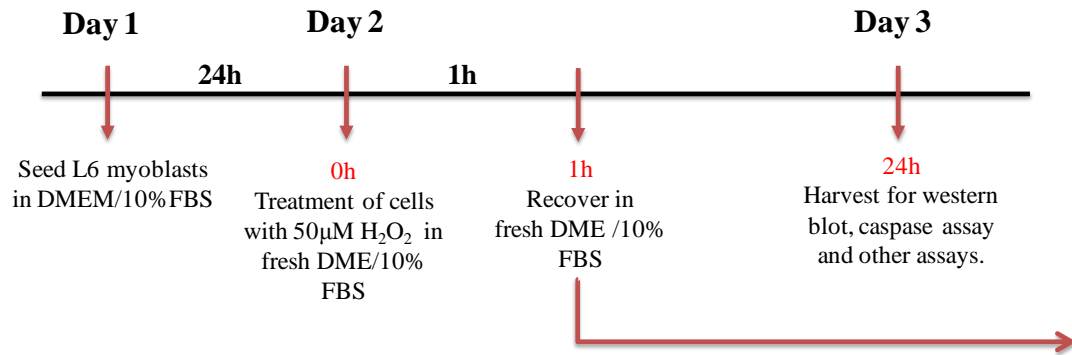
B)
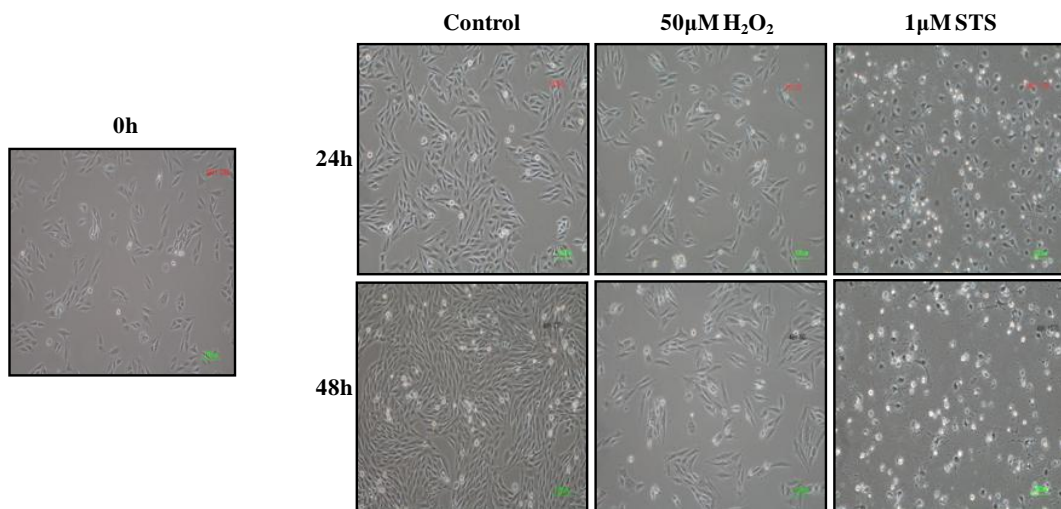
C)
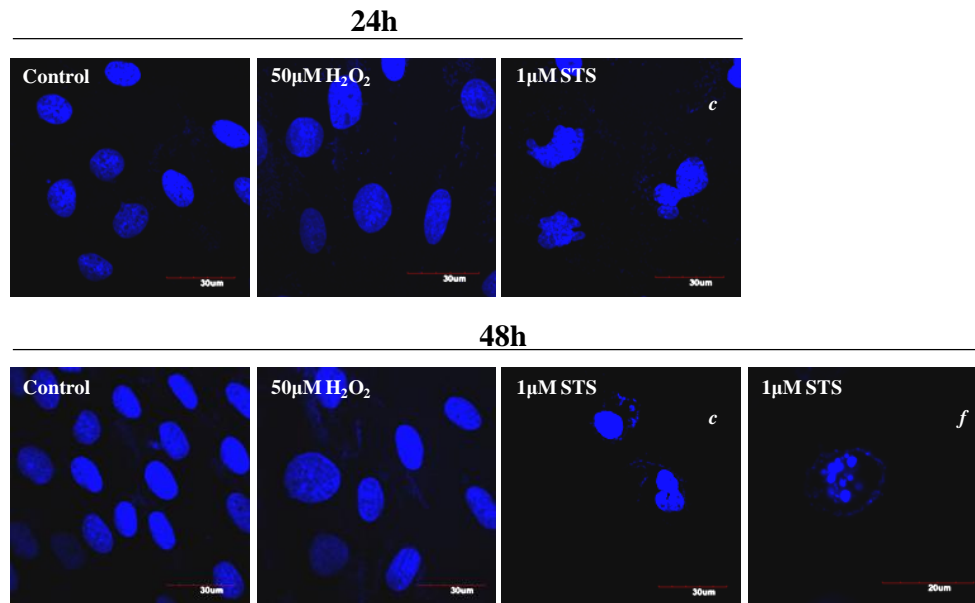
D)
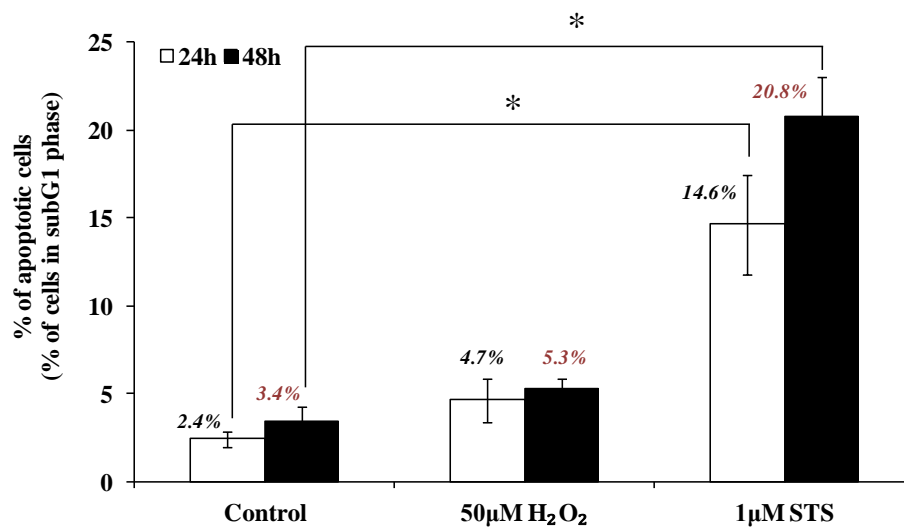
Figure 1. Effect of H₂O₂ and STS on cellular morphology and survival.
(A) Basic experimental setup of the project: exposure of L6 myoblasts to 50μM H₂O₂. L6 myoblasts were treated with 50μM H₂O₂ and 1μM STS for 24 and 48 hours. (B) Cell morphology was observed under a phase contrast microscope. (C) Cell nuclei were stained with Hoechst 34580 nucleic acid stain and nuclear morphology was observed under a confocal microscope. *c*: nuclear condensation; *f*: nuclear fragmentation. (D) Cells were stained with the propidium iodide (PI) dye for cell cycle profile analysis. Percentage of cells in subG1 phase was tabulated as percentage of apoptotic cells. The data represent the means of three independent experiment ± S.E.M., *P < 0.05. Pictures shown are representative of at least 3 independent experiments.

Although H_2O_2 treatment had no effect on cellular morphology, we observed a decrease in cell density in both H_2O_2 and STS-treated culture plates. In STS-treated culture plate, there was a significant population of cells floating in the medium, indicating that cells were undergoing a certain degree of anoikis, i.e. cell death due to loss of attachment (Figure 1B). In comparison, most cells remained attached to the culture plate even after treatment with H_2O_2, suggesting that H_2O_2 treatment did not induce apoptosis or anoikis, but a retarded cell growth (Figure 1B). A quantitative measurement of cell growth was achieved by crystal violet staining of adherent cells (Figure 2). While control untreated cells showed an exponential growth pattern, H_2O_2-treated cells showed no increase in cell number, suggesting an arrested cell proliferation up to 72 hours (Figure 2A). Figure 2B showed the representative cell cycle profile for H_2O_2- and STS-treated cells. The cell cycle profile of H_2O_2-treated cells was comparable to the control untreated cells at 24h and 48h and no obvious cell cycle arrest was observed. When the numbers in each cell cycle phase were tabulated and represented as numbered graph, we found that there was no relative increase in G1, S or G2/M phase for H_2O_2-treated cells (Figure 2C, D and E). This suggests that H_2O_2-induced cell growth arrest was not due to cell cycle arrest. In contrast, STS-treated cells had a decreased population in the G1 phase at 24h and 48h, and increased population in the S phase at 48h.

A)

B)

24h

48h
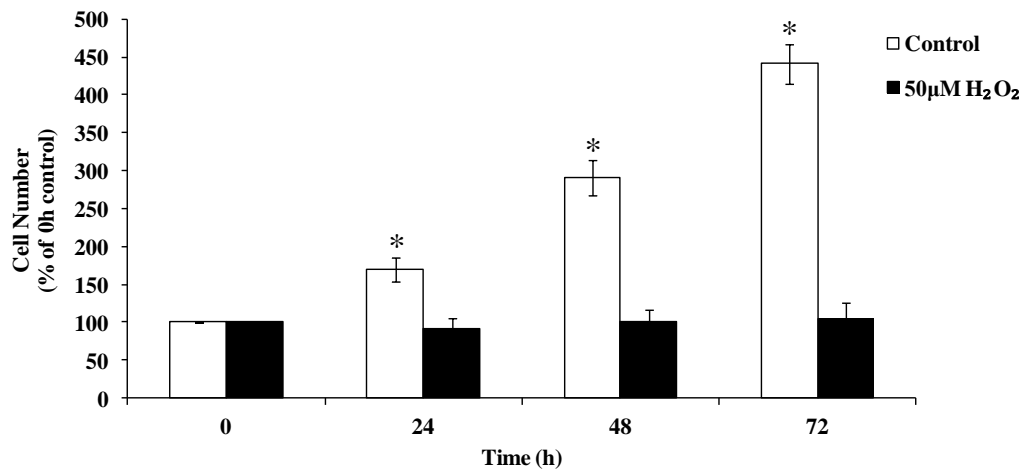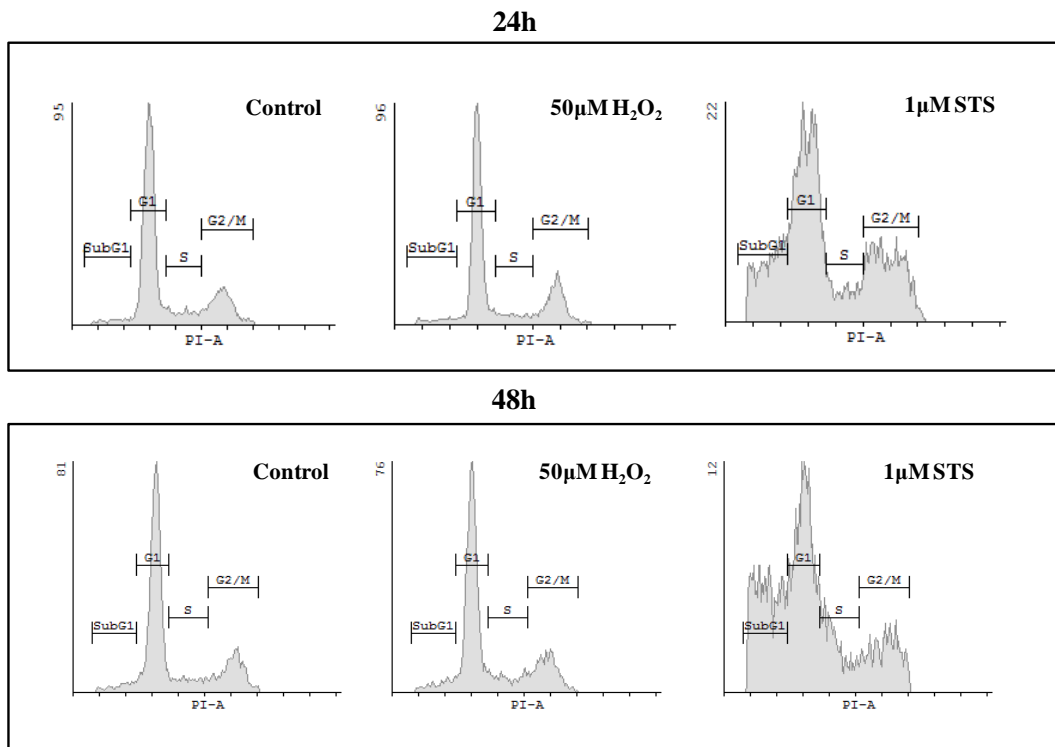
C)
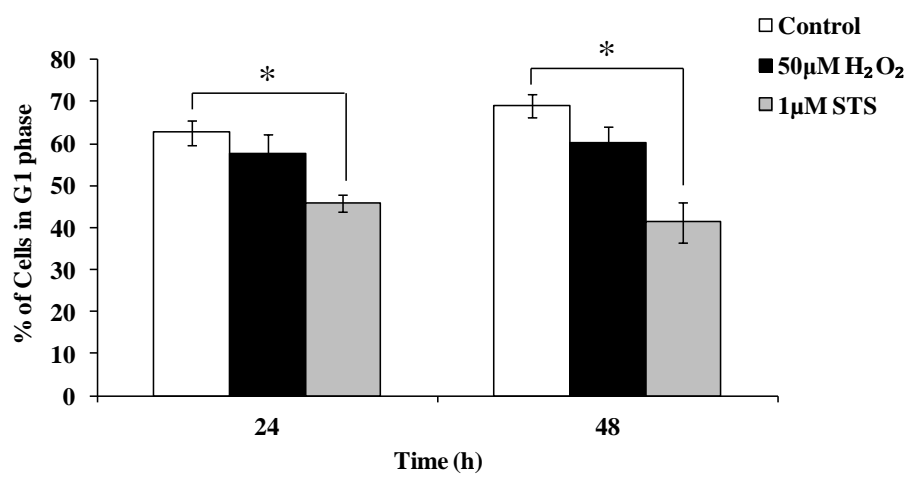
D)
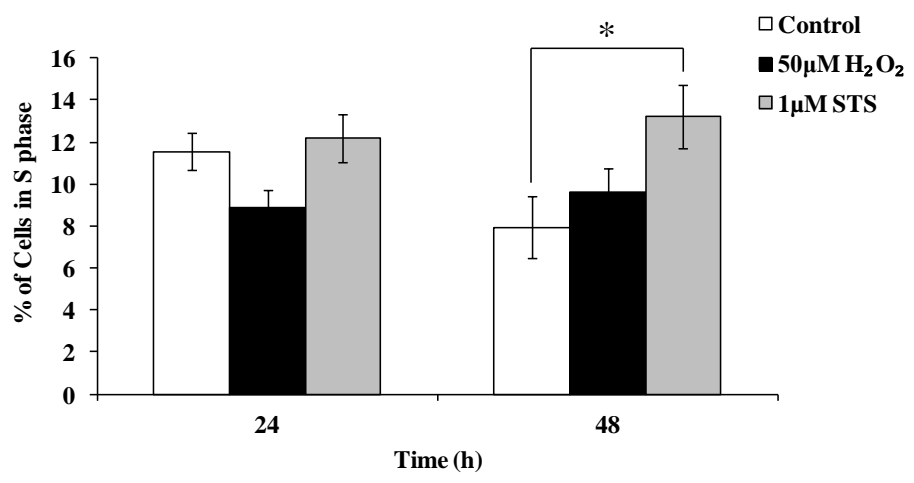
E)
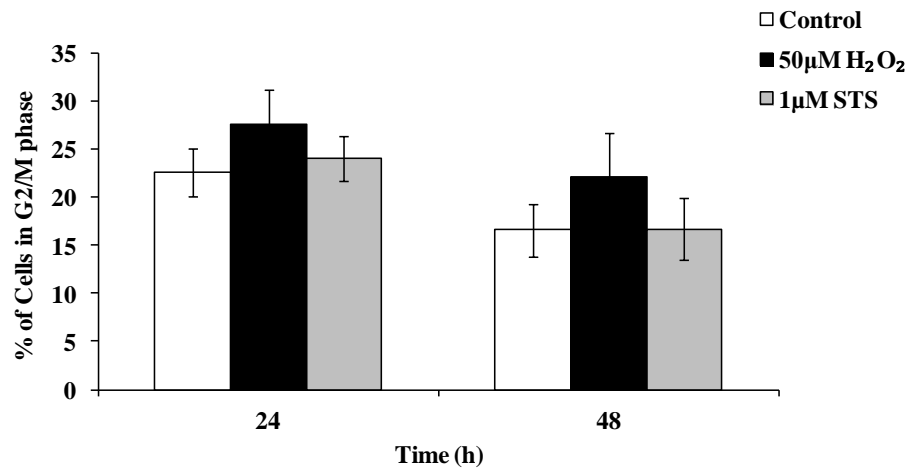
Figure 2. H$_2$O$_2$ treatment resulted in decreased cell growth without inducing cell cycle arrest. (A) Cells were treated with 50μM H$_2$O$_2$ for indicated time points and were stained with crystal violet to quantify adherent cell density. The data are the means of four independent experiments ± S.E.M., *$P < 0.05$.

(B) Cell cycle profile analysis of cells treated with 50μM H$_2$O$_2$ or 1μM STS for 24 or 48 hours. Graphs shown are representative of four independent experiments.

The percentage of cells in (C) G1, (D) S, and (E) G2/M phase from FACS analysis of cell cycle was tabulated. The data are the means of four independent experiments ± S.E.M., *$P < 0.05$.

Lastly, we assessed the occurrence of Mitochondrial Outer Membrane Permeabilization (MOMP) upon treatment of H_2O_2 and STS. MOMP is a crucial step in the intrinsic pathway of apoptosis and is generally considered as a "point of no return" to cell death. It leads to cytosolic release of pro-apoptotic proteins, driving the activation of caspase cascade through apoptosome formation. After MOMP, activated caspase 3 cleaves the p75 subunit of mitochondrial respiratory chain complex I, producing ROS and discrupting the mitochondrial membrane potential[122]. Hence, MOMP is characterized by loss of mitochondrial membrane integrity and a drop in mitochondrial membrane potential. The fall in mitochondrial membrane potential can be measured by use of a cationic lipophilic dye, $DIOC_6(3)$. The accumulation of $DIOC_6(3)$ in the mitochondria matrix is driven by the mitochondrial membrane potential[123]. Disruption to the mitochondrial membrane integrity and mitochondrial membrane potential results in decreased uptake of $DIOC_6(3)$ to the mitochondria. Hence, the occurrence of MOMP is evident by a decrease in $DIOC_6(3)$ staining. To artificially induce MOMP, we used an oxidative phosphorylation uncoupler, CICCP. Figure 3 showed that both STS and CICCP treatment resulted in 10-15% decrease in the $DIOC_6(3)$ fluorescence intensity. In contrast, there was no change to the fluorescence intensity after H_2O_2 treatment. This indicates that mitochondrial membrane was intact upon H_2O_2 treatment, further confirming that H_2O_2 did not induce apoptosis.
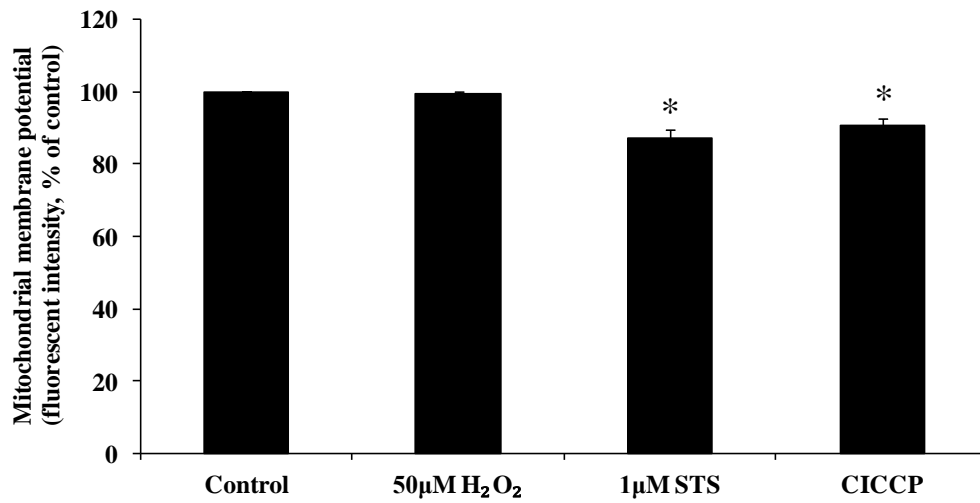
Figure 3. STS treatment, but not H$_2$O$_2$, induced Mitochondrial Outer Membrane Permeabilization. Cells were treated with 50μM H$_2$O$_2$, 1μM STS or 20μM CICCP for 4 hours before they were stained with 10nM DIOC$_6$(3) dye. Green mitochondrial fluorescence of 10,000 cells per sample was determined by flow cytometry using the FITC-A channel. The data are the means of four independent experiments ± S.E.M., *$P < 0.05$.

We proceeded to analyze caspase 3 activation by H_2O_2 by measurement of caspase 3 activity with a fluorogenic substrate Ac-DEVD-AFC, and Western Blot analysis of caspase 3 cleavage. Both H_2O_2 and STS treatment resulted in time-dependent caspase 3 activation when measured using Ac-DEVD-AFC (Figure 4). For H_2O_2-treated cells, the increase of caspase 3 activity was first detected at 8h, increasing by 2 fold as compared to the control. Caspase 3 activity continued to increase and peaked at 24h with about 5 fold increase compared to the control (Figure 4A). Compared to H_2O_2, STS-induced caspase 3 activity started earlier at 6h, gradually increased and peaked at 12h with about 30 fold increase compared to the control (Figure 4A). Using Western Blot analysis, cleavage of caspase 3 was evident by the detection of a 17kda band on the Western Blot, which represents the p17 fragment of activated caspase 3. H_2O_2-induced caspase 3 cleavage was detected at 9h, which then gradually increased and peaked at 18-24 hours post-treatment (Figure 4B). This is similar to its caspase 3 activity profile observed using Ac-DEVD-AFC. For STS-treated cells, cleavage of caspase 3 were detected as early as 3-4h, which then gradually increased and peaked at 12-18 hours post-treatment (Figure 4B). Again, this is similar to its caspase 3 activity profile observed using Ac-DEVD-AFC.

A)
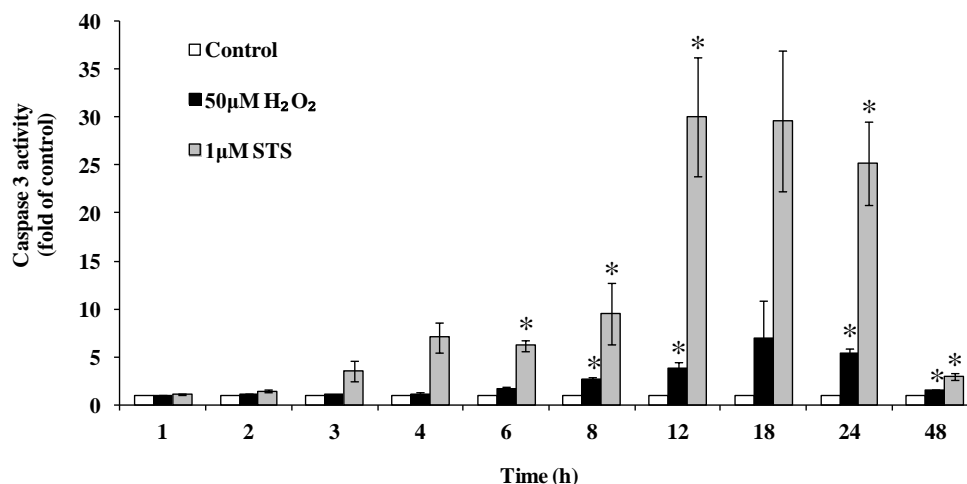
B)
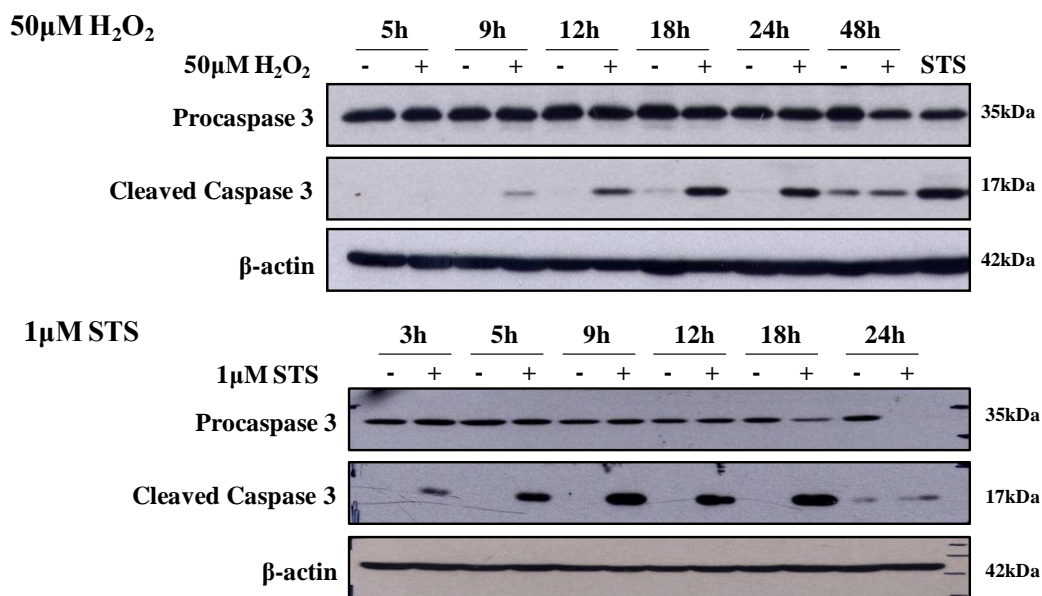
Figure 4. H₂O₂ and STS treatment resulted in time-dependent caspase 3 activation. (A) Caspase 3 activity in cells exposed to 50μM H₂O₂ or 1μM STS for indicated time points, measured with the fluorogenic substrate Ac-DEVD-AFC. The data are the means of three independent experiments ± S.E.M., *$P < 0.05$, compared to control at respective time points.

(B) Western Blot analysis of caspase 3 cleavage in cells exposed to 50μM H₂O₂ or 1μM STS for indicated time points. Western Blots shown are representative of three independent experiments.

3.1.2   Localization of activated caspase 3 upon H₂O₂ treatment

Having established that H_2O_2 treatment induced caspase 3 activation in a non-cell death condition, we next assessed the localization of cleaved (activated) caspase 3. Cells were incubated with a primary antibody purchased from Abcam (ab13847), which is specific to the cleaved fragment activated caspase 3, p17 and p12. Subsequently, cells were incubated with a secondary antibody conjugated to Rhodamine. Immunofluorescence study showed a striking difference between STS and H_2O_2-treated cells in terms of cleaved caspase 3 localization (Figure 5A). At 12h, staining of activated caspase 3 in red was observed mainly in the nuclei of STS-treated cells. At 24h post treatment, such staining was observable in both H_2O_2- and STS-treated cells, but in different cellular compartment. For H_2O_2 treated cells, cleaved caspase 3 accumulated mainly in the nuclei, whereas for STS-treated cells, cleaved caspase 3 accumulated mainly in the cytoplasm. At 48h, intensity of cleaved caspase 3 staining decreased in H_2O_2-treated cells but nevertheless remained in the nuclei. For STS-treated cells, cleaved caspase 3 remained in the cytoplasm (Figure 5A).

To validate the specificity of the staining, we co-incubated the cells with the primary antibody ab13847 and its corresponding blocking peptide. Nuclear staining of cleaved caspase 3 upon H_2O_2 treatment was completely blocked by co-incubation with the blocking peptide, suggesting that the staining was specific and associated with not background staining (Figure 5B). We then performed an immunofluorescence study with two different primary antibody purchased from different company, ab13847 and cell signalling #9664. Incubation with either antibody in H_2O_2-treated cells revealed a

red nuclear staining (Figure 5C). Such findings confirmed the localization of activated caspase 3 in the nucleus of H_2O_2-treated cells.

A)

Hoechst | Cleaved Caspase 3 | Hoechst + cleaved caspase 3 | Merged with TI

48h — Control, 50μM H₂O₂, 1μM STS

Negative Control (50μM H₂O₂)

B)

50μM H₂O₂

50μM H₂O₂ (with blocking peptide)

Cleaved caspase 3 | Hoechst + cleaved caspase 3

Cleaved caspase 3 | Hoechst + cleaved caspase 3
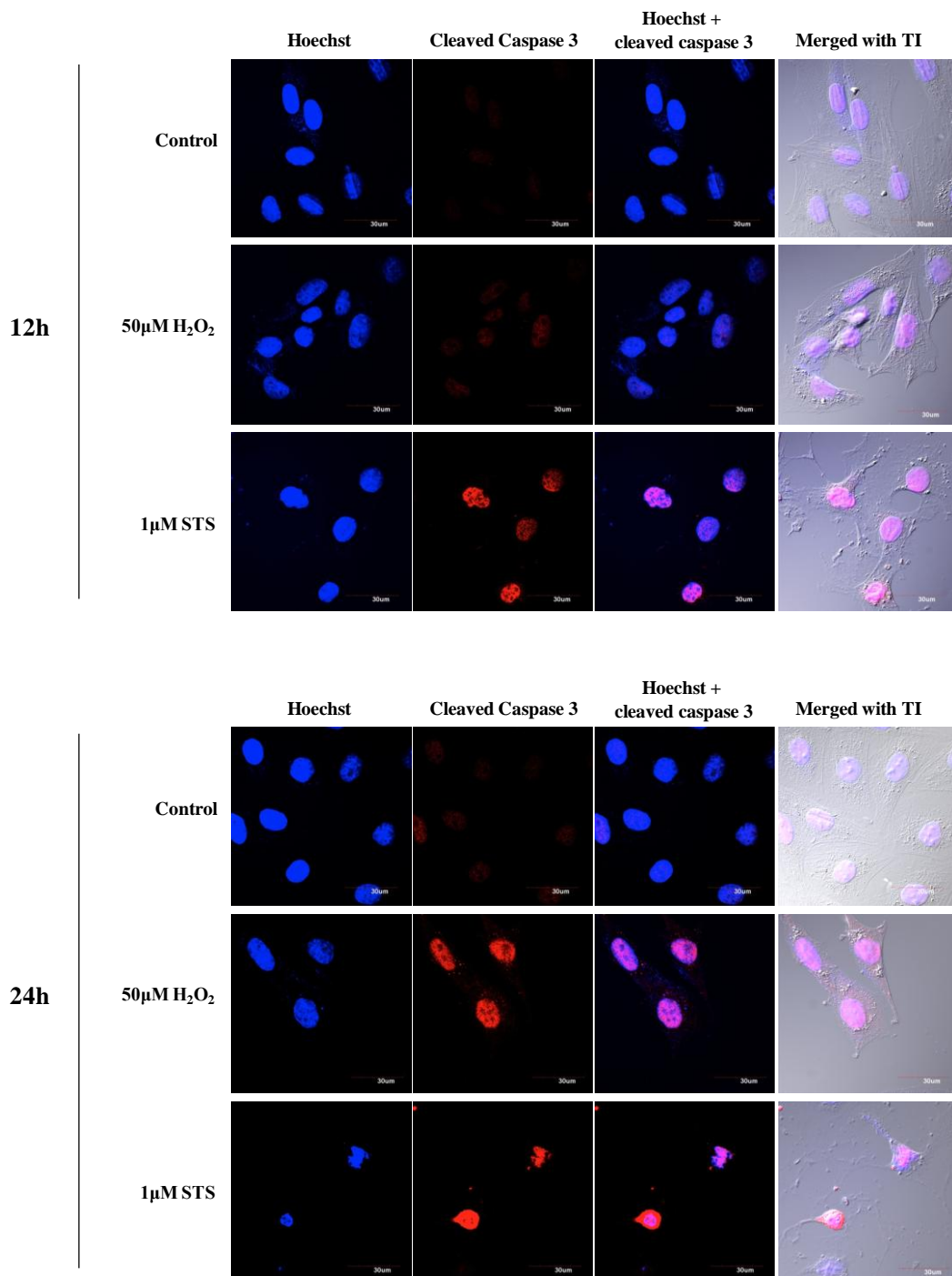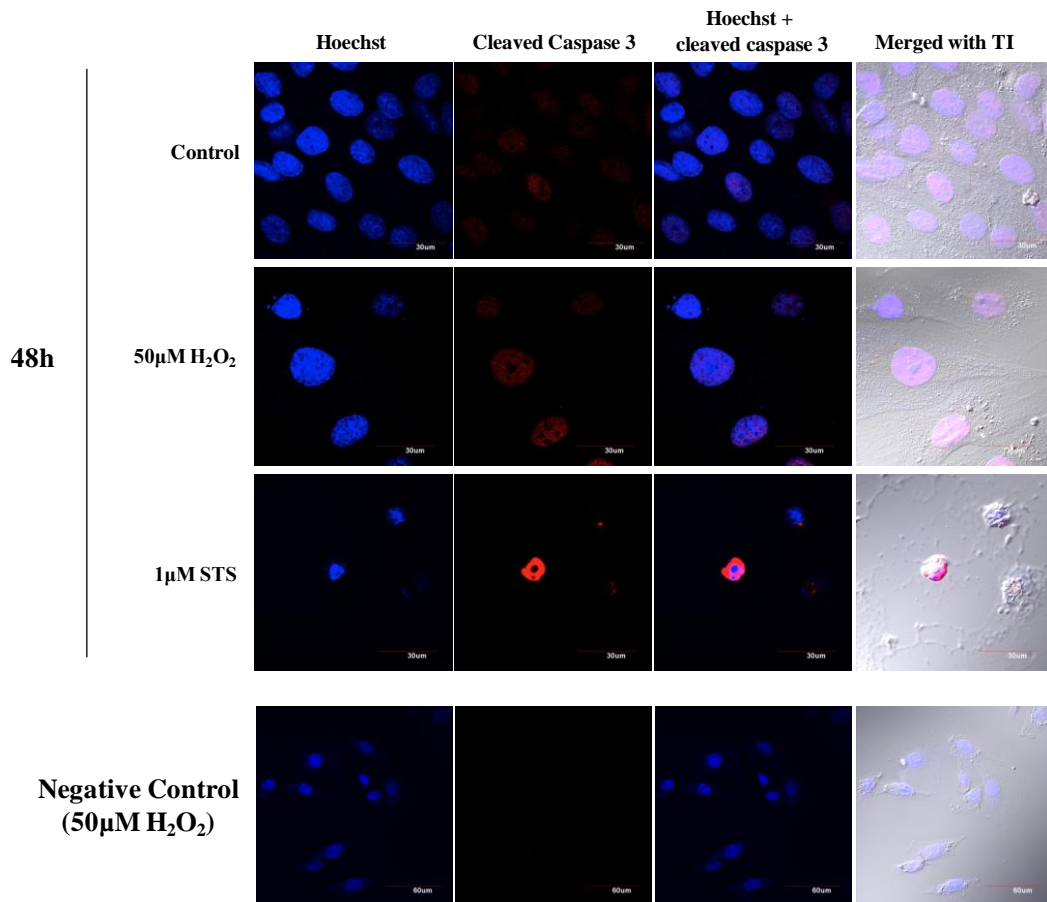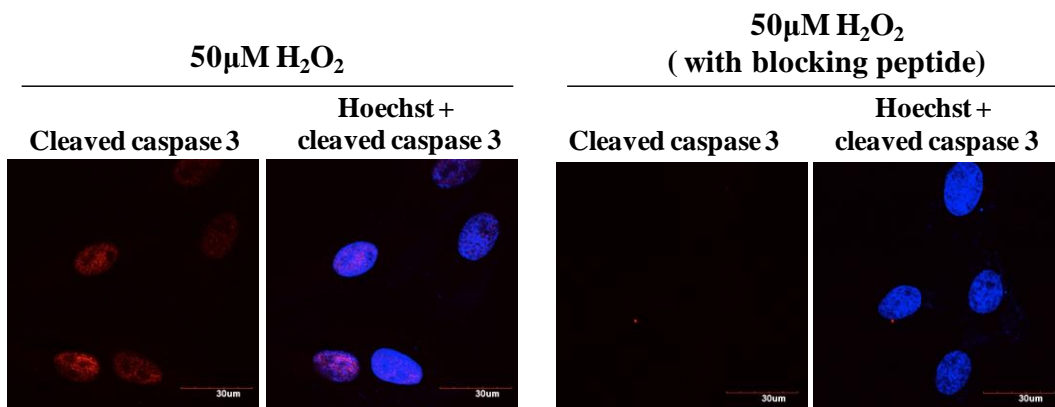
C)
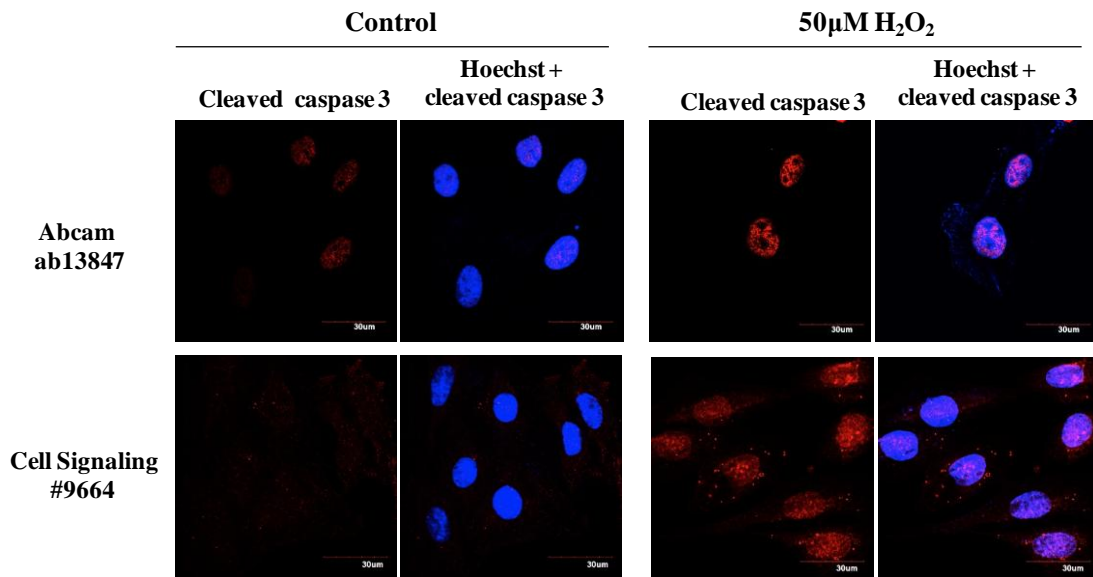
Figure 5. Sub-cellular localization of cleaved caspase 3 after H_2O_2 and STS treatment. (A) L6 myoblast were treated with 50μM H_2O_2 or 1μM STS for 12, 24 or 48 hours. After fixation, cells were incubated with primary antibody specific to the p17 fragment and p12 fragment of activated (cleaved) caspase 3 (Abcam ab13847), followed by confocal microscopy analysis. Immunofluorescence images shown are representative of three independent experiments. Negative control refers to samples incubated in blocking buffer without primary antibody. (TI: Transmitted Light Image) (B) Cells were treated with 50μM H_2O_2 for 24 hours. After fixation, cells were incubated with Abcam ab13847 and the antibody-specific blocking peptide, followed by confocal microscopy analysis. (C) Cells were treated with 50μM H_2O_2 for 24 hours. After fixation, cells were stained with two different primary antibodies, Abcam ab13847 or Cell Signalling #9664, both recognize activated caspase 3.

3.1.3 H_2O_2-induced caspase 3 activation was initiator caspase-independent

Because of their proteolytic nature, caspases are synthesized as inactive zymogens that are activated in a highly regulated proteolytic cascade. Activation of caspases involves proteolytic cleavage of themselves or each other, depending on their position in the proteolytic hierarchy. Classical apoptosis scenario involves self activation of initiator caspases, usually caspase 8 or 9, and activation of the executioner caspases by the activated initiator caspases. L6 myoblasts were treated with H_2O_2 or STS for different time points and were harvested for caspase activity assay and Western Blot analysis of caspase 8 and 9 cleavage. STS as the classical apoptosis inducer activated both caspase 8 and 9 (Figure 6A, B and C). In contrast, initiator caspase 8 and 9 were not activated upon H_2O_2 treatment (Fig 6A, B and D). This finding was intriguing as initiator caspases are generally activated prior to executioner caspase so as to mediate the cleavage of executioner caspases. The absence of caspase 8 and 9 activation in H_2O_2 system led us to deduce that H_2O_2-induced caspase 3 activation was caspase-independent. To confirm, L6 myoblasts were pre-incubated with specific peptide inhibitors of caspase 8, zIETD-FMK, or caspase 9, zLEHD-FMK, before treatment with H_2O_2 and STS. These peptide inhibitors specifically and irreversibly inhibit its corresponding caspases through a covalent thioether adduct with the cysteine of the active site. Pre-incubation with zLEHD-FMK was able to decrease cleavage of caspase 3 by STS treatment (Figure 7A). In contrast, both z-IETD-FMK and zLEHD-FMK had no effect on H_2O_2-induced caspase 3 cleavage (Figure 7B). Moreover, control experiment showed that the dose of zIETD-FMK and zLEHD-FMK used were sufficient to inhibit caspase 8 and 9 activity induced by STS treatment (Figure 7C and D). Such findings suggest that H_2O_2-mediated caspase 3 cleavage was independent of the initiator caspases. Interestingly, upon STS treatment, we could not detect the

usual p18 and p10 cleaved fragment of caspase 8. Instead, a 30kda band was detected on Western Blot, suggesting that an alternative cleavage pattern of caspase 8 by STS treatment in L6 myoblasts. Such alternative cleavage pathway has been found recently and was described in details by Hoffmann et al.[124].

A)
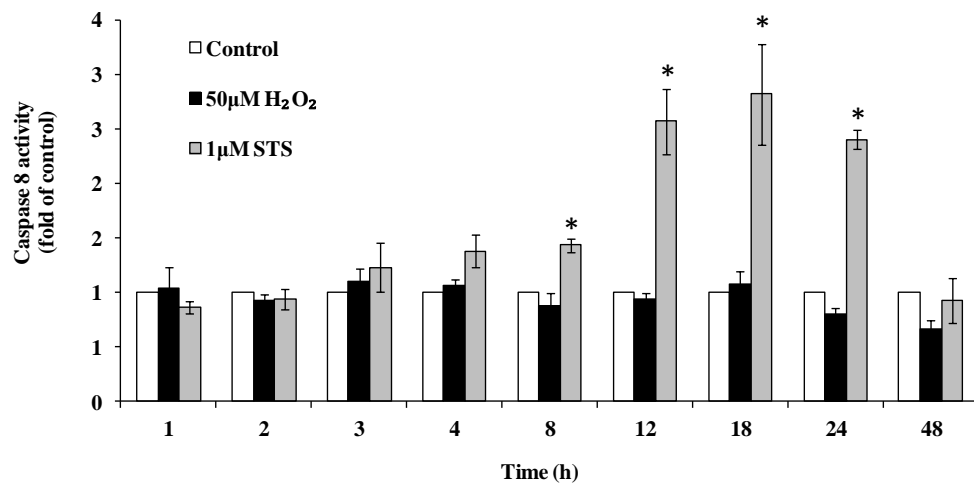
B)
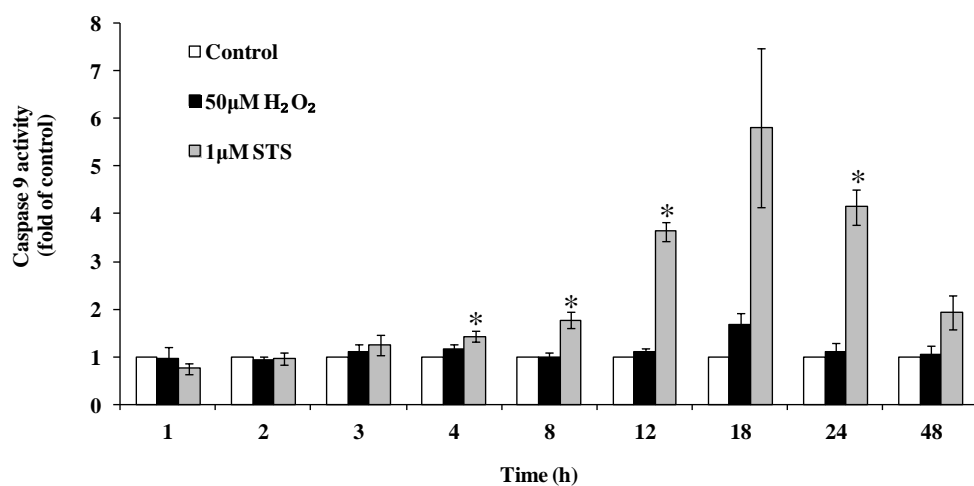
C)
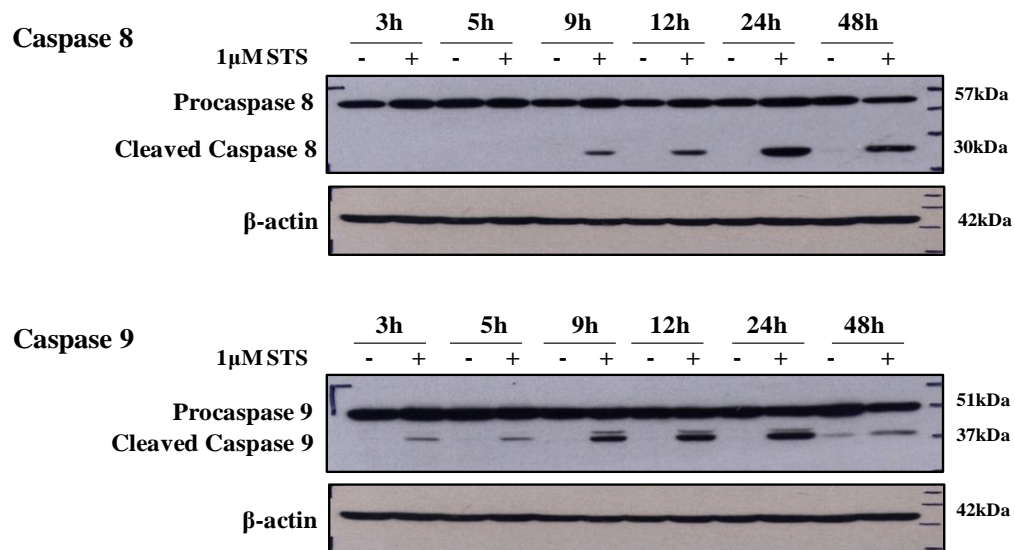
D)
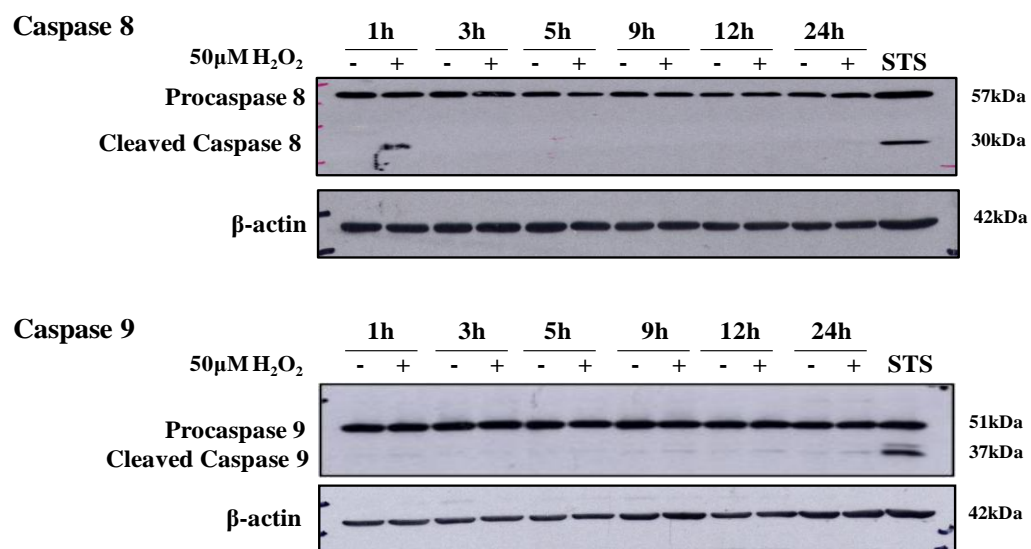
Figure 6. STS treatment, but not H₂O₂ treatment, activated the initiator caspases 8 and 9. (A) Caspase 8 activity in cells exposed to 50μM H_2O_2 or 1μM STS for indicated time points, measured with the fluoregenic substrate Ac-IETD-AFC. The data are the means of four independent experiments ± S.E.M., *$P < 0.05$. (B) Caspase 9 activity in cells exposed to 50μM H_2O_2 or 1μM STS for indicated time points, measured with the fluoregenic substrate Ac-LEHD-AFC. The data are the means of three independent experiments ± S.E.M., *$P < 0.05$, as compared to control at respective time points. (C) Cells were treated with 1μM STS for indicated time points and were harvested for Western Blot analysis of caspase 8 and 9 cleavage. Western Blot shown is representative of three independent experiments. (D) Cells were treated with 50μM H_2O_2 for indicated time points and were harvested for Western Blot analysis of caspase 8 and 9 cleavage. STS-treated lysate was included as a positive control. Western Blot shown is representative of three independent experiments.

A)

DMSO   **z-IETD**   **z-LEHD**

1μM STS   -   +   -   +   -   +

Procaspase 3   35kDa

Cleaved Caspase 3   17kDa

β-actin   42kDa

B)

DMSO   **z-IETD**   **z-LEHD**

50μM H$_2$O$_2$ -   +   -   +   -   +

Procaspase 3   35kDa

Cleaved Caspase 3   17kDa

β-actin   42kDa
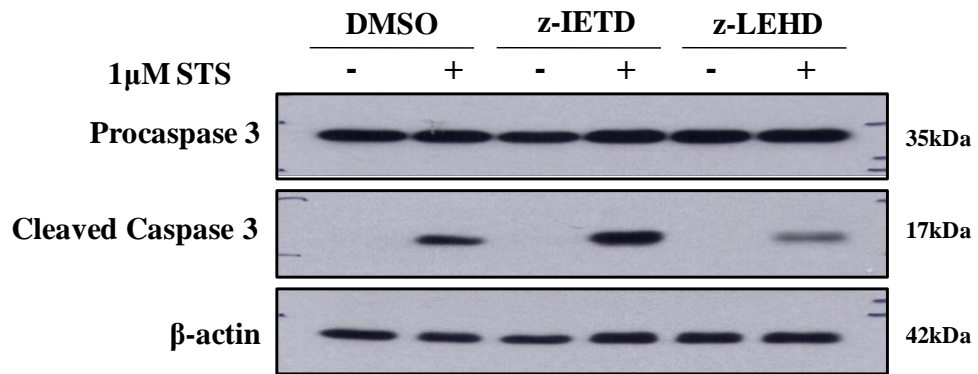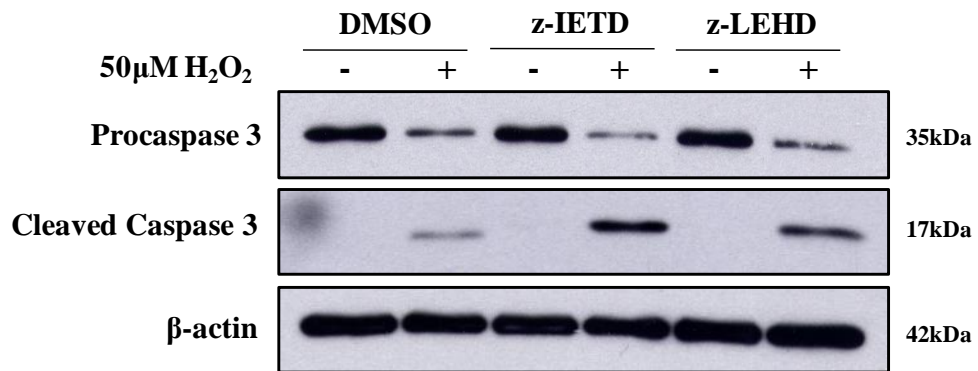
C)
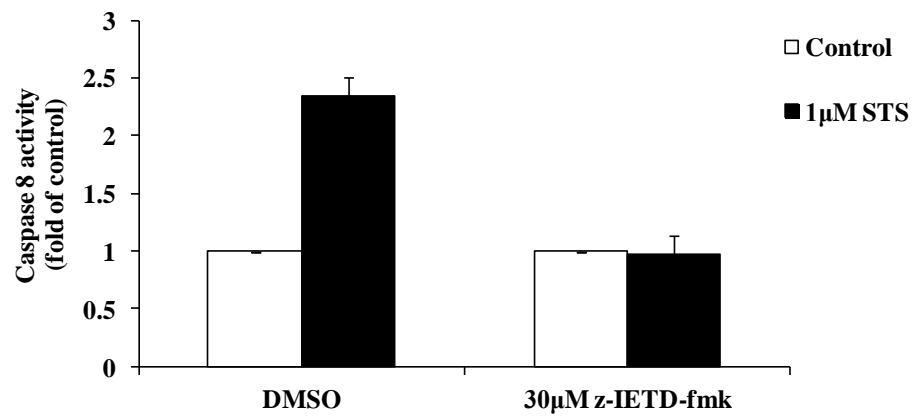
D)
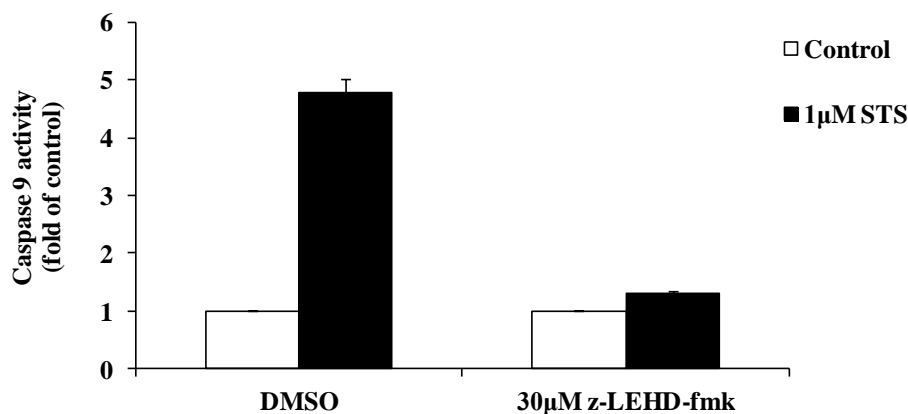
Figure 7. Caspase 3 activation upon H_2O_2 treatment was not prevented by inhibition of the initiator caspases 8 and 9. (A) Cell were pre-treated with 30μM of specific caspase inhibitors, z-IETD-FMK (caspase 8) or z-LEHD-FMK (caspase 9), for 2 hours before exposure to 1μM STS. After 5 hours, cells were harvested and subjected to Western Blot analysis. Western Blot shown is representative of three independent experiments. (B) Cell were pre-treated with 30μM of specific caspase inhibitors, z-IETD-FMK (caspase 8) or z-LEHD-FMK (caspase 9), for 2 hours before exposure to 50μM H_2O_2. After 24 hours, cells were harvested and were subjected to Western Blot analysis of caspase 3 cleavage. Western Blot shown is representative of three independent experiments. (C) Caspase 8 activity in cells treated with 1μM STS for 24 hours, with or without z-IETD-FMK pre-treatment. (D) Caspase 9 activity in cells treated with 1μM STS for 24 hours, with or without z-LEHD-FMK pre-treatment.

Next, L6 myoblasts were pre-incubated with the pan-caspase inhibitors zVAD-FMK for 2 hours before exposure to 50μM H_2O_2 or 1μM STS (Figure 8). Cleavage of caspase 3 by STS treatment was decreased in the presence of 25μM and 50μM zVAD-FMK (Figure 8A). In contrast, pre-incubation with the same dose of zVAD-FMK did not inhibit caspase 3 cleavage by H_2O_2 treatment (Figure 8B). Again, control experiment showed that 25μM zVAD-FMK was sufficient to inhibit caspase 3, 8 and 9 activity induced by STS (Figure 8C, D and E). Also, although zVAD-FMK was unable to decrease H_2O_2-induced caspase 3 processing, it could block caspase 3 activity completely (Figure 8F). This suggests that zVAD-FMK could direct inhibit the activated caspase 3 while not affecting its processing from the pro-enzyme. Based on these results, we concluded that H_2O_2-mediated caspase 3 cleavage could be independent of another caspase. Although both STS and H_2O_2 treatment led to caspase 3 activation, such caspase 3 activation differed in terms of magnitude, time of activation, as well as their upstream mechanisms. A summary of H_2O_2- and STS-mediated caspase 3 activation is presented in Table 2.

A)
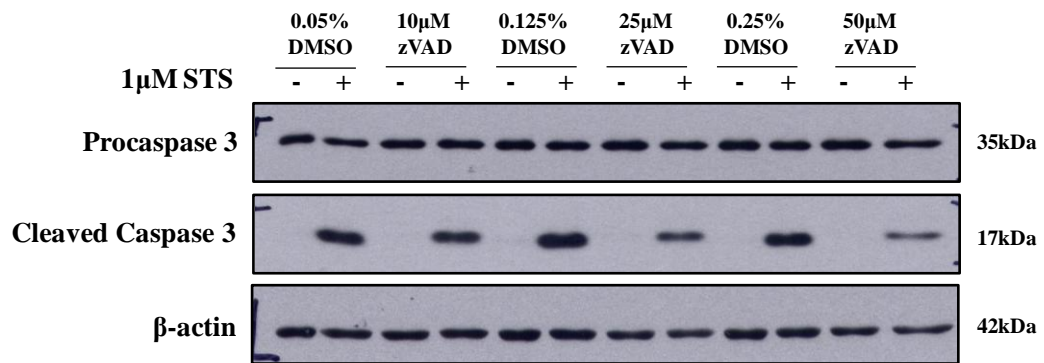
B)
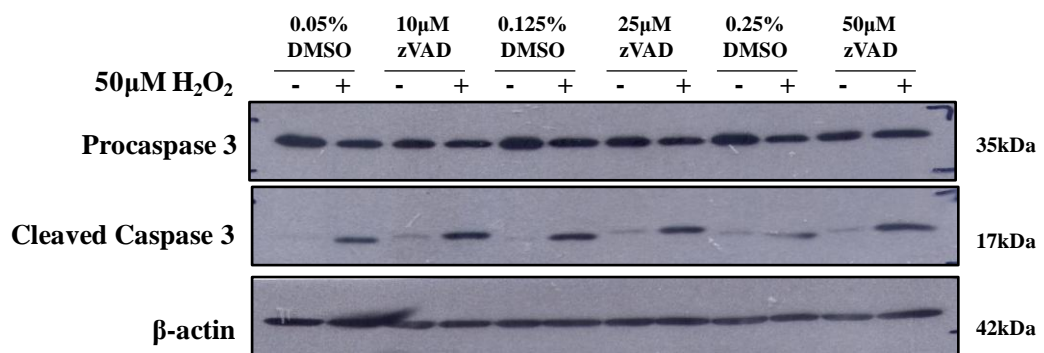
C)
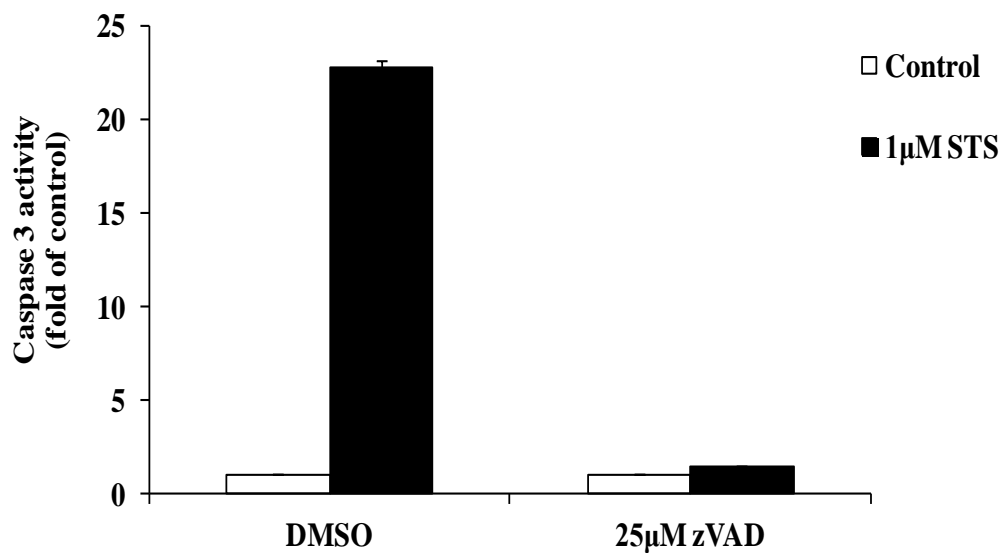
D)
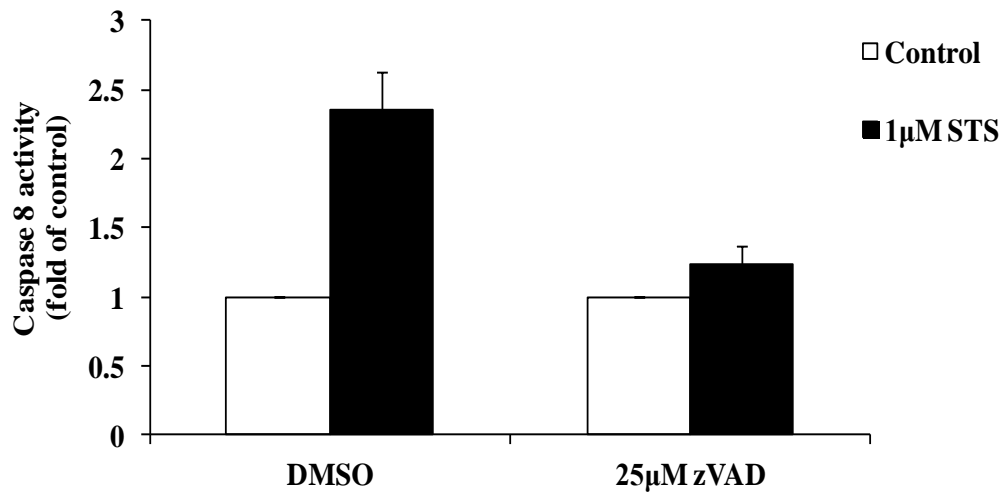
E)
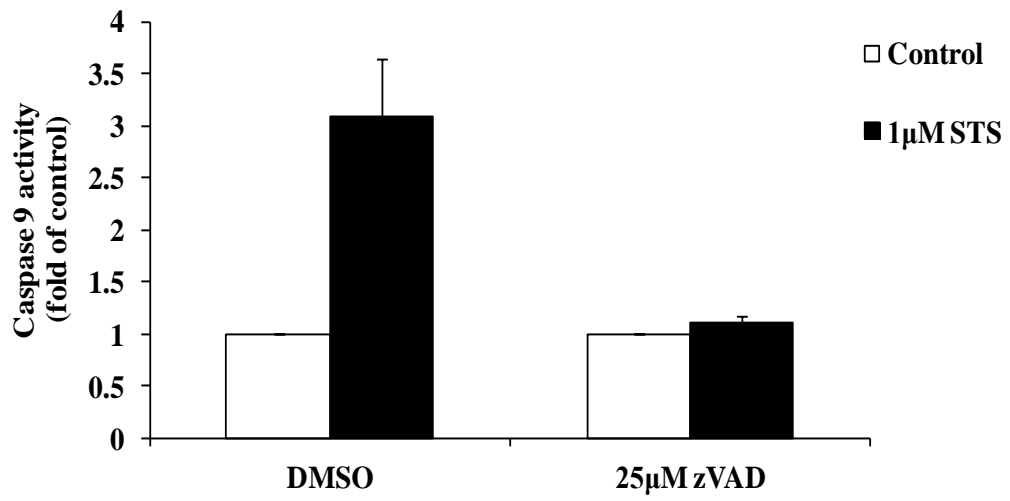
8F)
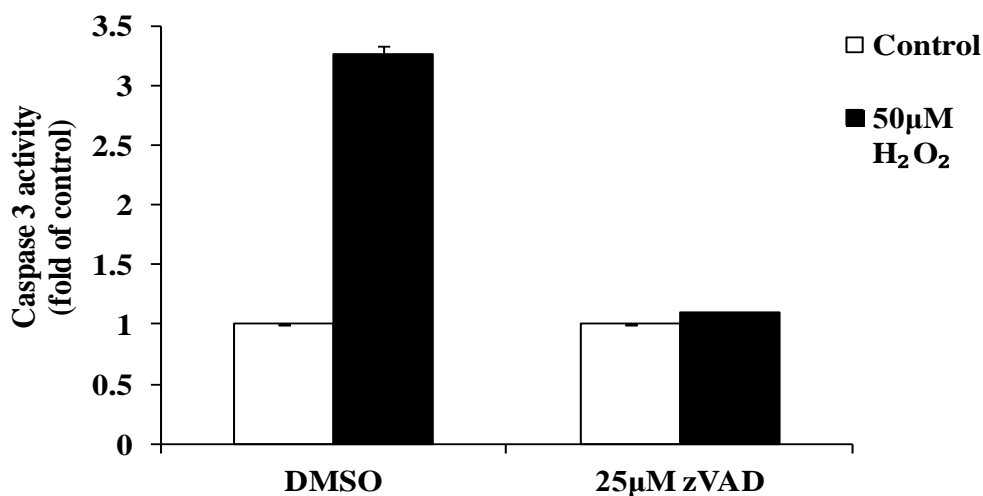
Figure 8. Caspase 3 activation upon H_2O_2 treatment is caspase-independent. L6 myoblasts were pre-treated with increasing doses of the pan-caspase inhibitor, zVAD-fmk, for 2 hours before exposure to (A) 1μM STS or (B) 50μM H_2O_2. After 24 hours, cells were harvested and subjected to Western Blot analysis of caspase 3 cleavage. Western Blots shown are representative of two independent experiments.

Cells were pre-treated with 25μM zVAD-FMK before exposure to 1μM STS. After 24 hours, cells were harvested for (C) caspase 3, (D) caspase 8, and (E) caspase 9 activity assay.

(F) Cells were pre-treated with 25μM zVAD-FMK before exposure to 50μM H_2O_2. At 24 hours-post H_2O_2 treatment, cells were harvested for caspase 3 activity assay.

Table 2. Summary of H₂O₂- and STS- induced caspase 3 activation. (* time of activation, # highest fold of activation)

Caspase 3 activation		H_2O_2	STS
	Time [*]	~ 8h	~ 3h
	Magnitude [#]	~ 4-7X	~ 25-30X
Caspase 8 activation		no	yes
Caspase 9 activation		no	yes
Effect of caspase 8/9 inhibitor on caspase 3 activation		no	yes
Effect of pan caspase inhibitor on caspase 3 activation		no	yes
MOMP		no	yes
Apoptosis		no	yes

3.2   Mechanism of H$_2$O$_2$-induced caspase 3 activation

3.2.1   H$_2$O$_2$-induced caspase 3 activation is dependent on lysosomal cathepsins B and L

3.2.1A A non-caspase cysteine protease is responsible for H$_2$O$_2$-induced caspase 3 activation

In section 3.1, we have shown that H$_2$O$_2$-induced caspase 3 activation was independent on the conventional caspase proteolysis cascade. This suggests an alternative path to caspase 3 activation without the involvement of the initiator caspases 8 and 9 (Figure 9). As caspase 3 is synthesized as an inactive proenzyme, its full activation requires proteolytic cleavage of the protein into functional fragments (p17 and p12), which then oligomerize to form the active enzyme. Therefore, a protease activity should exists upstream of caspase 3.
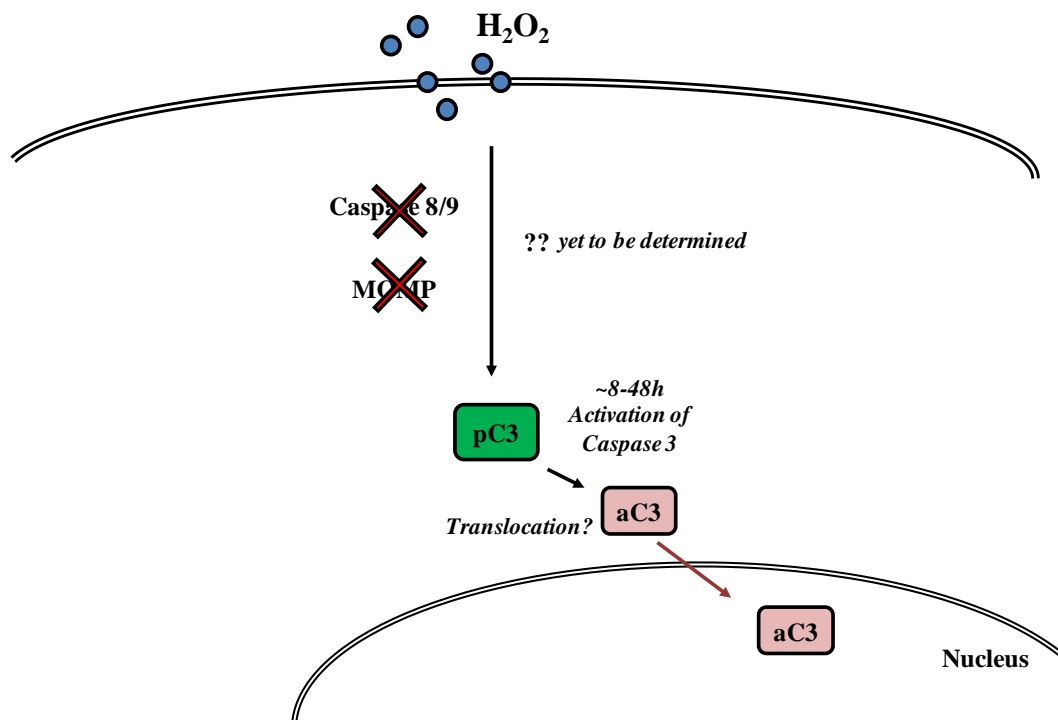
Figure 9. An unconventional path to caspase 3 activation upon H$_2$O$_2$ treatment. Upon H$_2$O$_2$ treatment, caspase 3 was activated. Activated caspase 3 was translocated into the nucleus. The activation of caspase 3 occurred in absence of MOMP and was independent of the initiator caspases 8 and 9. The protease upstream of caspase 3 is yet to be determined.

There are 3 major families of proteases, serine, aspartate, and cysteine proteases. Besides the well-established caspase activation in a caspase cascade, other protease-mediated caspase 3 activation has been reported in the literature. It has been shown that caspase activation and apoptosis was inhibited by serine protease and aspartatic inhibitor, especially when caspase activation and apoptosis were not affected by pan caspase inhibitors. Several reports have highlighted the importance of serine proteases during DNA damage-induced apoptosis. It has been shown that in PC12 cells, the serine protease inhibitors, AEBSF (also known as Pefabloc) and *N*-tosyl-l-phenylalanine chloromethyl ketone (TLCK) could act upstream of caspase to delay

DNA damage-induced neuronal cell death, by preventing mitochondrial event such as cytochrome c release or loss of transmembrane potential[125]. Another study has shown that AEBSF could block caspase activation, PARP degradation and apoptosis in melanoma cell lines, IGRmyc-3 and IGR39D, neuroblastoma cell line IMR32, as well as a rat-derived fibroblast. While such effect of AEBSF was observed in DNA damage-induced apoptosis by etoposide and irradiation, its protective effect was not extended to TNF-α-induced apoptosis[126]. Besides DNA damage-induced apoptosis, serine inhibitors APF, TLCK, and AEBSF were also reported to inhibit caspase activation and apoptosis caused by hypoxia reoxygenation[127].

On the other hand, the aspartate inhibitor Pepstatin A has been shown in several studies to inhibit caspase activation and apoptosis. For example, in human foreskin fibroblast, Pepstatin A prevented cytochrome c release and caspase activation and thereby delaying staurosporine-induced cell death[120]. It was also shown that, in both naive, and Nerve Growth Factor-treated, PC12 cells, Pepstatin A provided a protective effect from cell death caused by oxygen and glucose deprivation when used alone or in combinations with zVAD-FMK[128]. In contrast, pre-incubation with zVAD-FMK alone was unable to rescue the cells from cell death[128].

To investigate the involvement of serine proteases and aspartate proteases in H_2O_2-induced caspase 3 activation, we pre-incubated the cells with the broad-spectrum serine protease inhibitor, AEBSF or the aspartate inhibitor Pepstatin A before treatment with 50μM H_2O_2. Pre-incubation with up to 200μM, of AEBSF did not decrease caspase 3 activity (Figure 10). We did not increase the dose of AEBSF as a higher dose would stress the cells and resulted in cell death. Similarly, pre-incubation

of cells with Pepstatin A, did not inhibit caspase 3 activity (Figure 11), suggesting

that H_2O_2-mediated caspase 3 activation was independent of both serine and aspartate

protease.
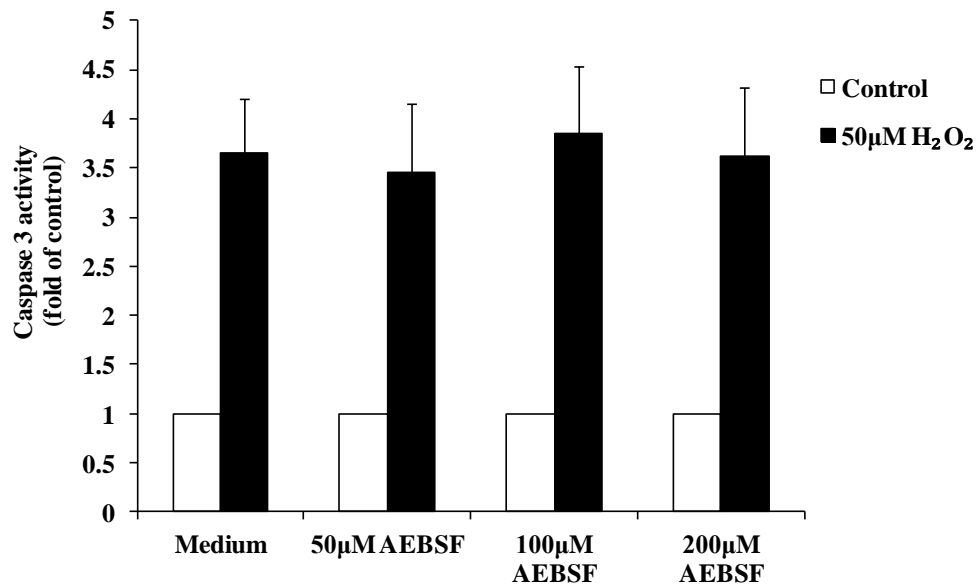
Figure 10. Caspase 3 activation upon H_2O_2 treatment was independent of serine protease. Cells were pre-treated with 50, 100 or 200μM of a broad-spectrum serine protease inhibitor, AEBSF, for 2 hours before exposure to 50μM H_2O_2. After 24 hours, cells were harvested for caspase 3 activity assay analysis. The data are the means of three independent experiments ± S.E.M.
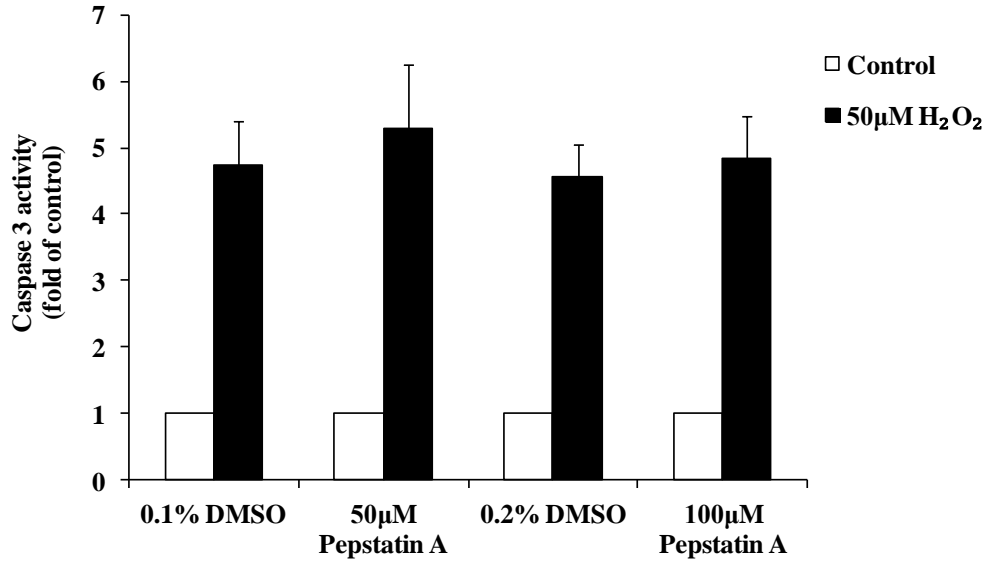
Figure 11. Caspase 3 activation upon H_2O_2 treatment was independent of aspartate protease. Cells were pre-treated with 50 or 100μM of a broad-spectrum aspartate protease inhibitor, Pepstatin A, for 2 hours before exposure to 50μM H_2O_2. After 24 hours, cells were harvested for caspase 3 activity assay analysis. The data are the means of three independent experiments ± S.E.M.

In Figure 8B, we showed that up to 50μM, zVAD-FMK was unable to prevent caspase 3 cleavage by H_2O_2 treatment. However, 50μM zVAD-FMK was sufficient to inhibit caspase 3 cleavage induced by STS treatment, despite the fact that STS-induced caspase 3 cleavage was much higher than that induced by the H_2O_2 treatment (Figure 8A). When we pre-incubated the cells with 100μM of zVAD-FMK, H_2O_2-induced caspase 3 cleavage was prevented (Figure 12). The difference between the effect of 50 μM and 100μM zVAD-FMK could be explained by the unspecific inhibitory effect of zVAD-FMK at high dose. It has been well documented that zVAD-FMK cross-inhibits other proteases, such as calpains and cathepsins, particularly at the typical doses used for caspase inhibition (100 μM)[129,130]. In fact, it was believed that, at such a high dose, zVAD-FMK functioned as a broad-spectrum cysteine protease inhibitor.
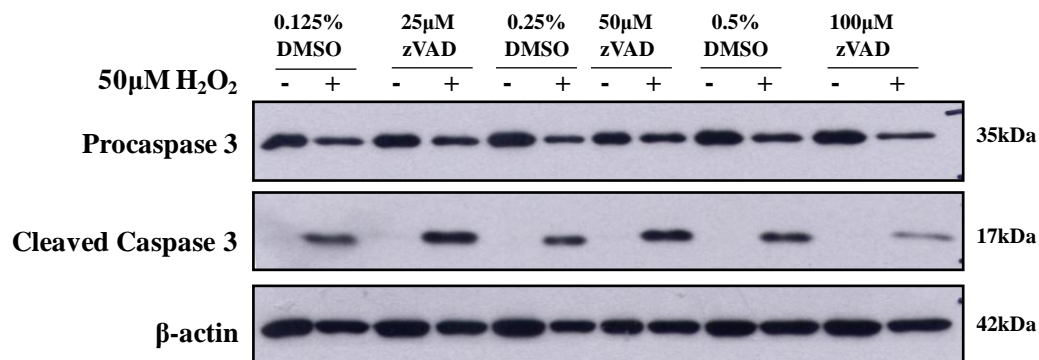
Figure 12. Caspase 3 cleavage upon H_2O_2 treatment was decreased by 100μM zVAD-FMK. L6 myoblasts were pre-treated with 25, 50 or 100μM pan-caspase inhibitor, zVAD-fmk, for 2 hours before exposure to 50μM H_2O_2. After 24 hours, cells were harvested and subjected to Western Blot analysis of caspase 3 cleavage. Western Blot shown is representative of two independent experiments.

3.2.1B Inhibition of cathepsin B and L prevented caspase 3 activation by H_2O_2

treatment

The cysteine protease family consists of three major groups: caspases, cathepsins (part of its family) and calpains. While the roles of caspases in apoptosis are well established, it has also been shown that cathepsins and calpains are involved in apoptosis[131].

The calcium-activated cysteine protease, calpain, plays an important role in ER stress-mediated apoptotic pathway. The involvement of calpain in apoptosis is supported by attenuation of apoptosis through pharmacological inhibition of calpain[132]. Calpain can be a negative regulator as well as a positive regulator of caspase 3 activation. It has been shown that calpain could cleave procaspase 7, 8 and 9 leading to their inactivation[133]. On the other hand, calpain could cleave Bid to its pro-apoptotic truncated form, resulting in MOMP and caspase cascade activation[134,135]. To determine if calpain is the upstream activator of caspase 3 in our system, we pre-incubated the cells with Calpeptin, a cell permeable calpain inhibitor before treatment with H_2O_2 (Figure 13). We found that caspase 3 activation was unaffected in the presence of Calpeptin. This suggests calpain is not involved in caspase 3 activation.
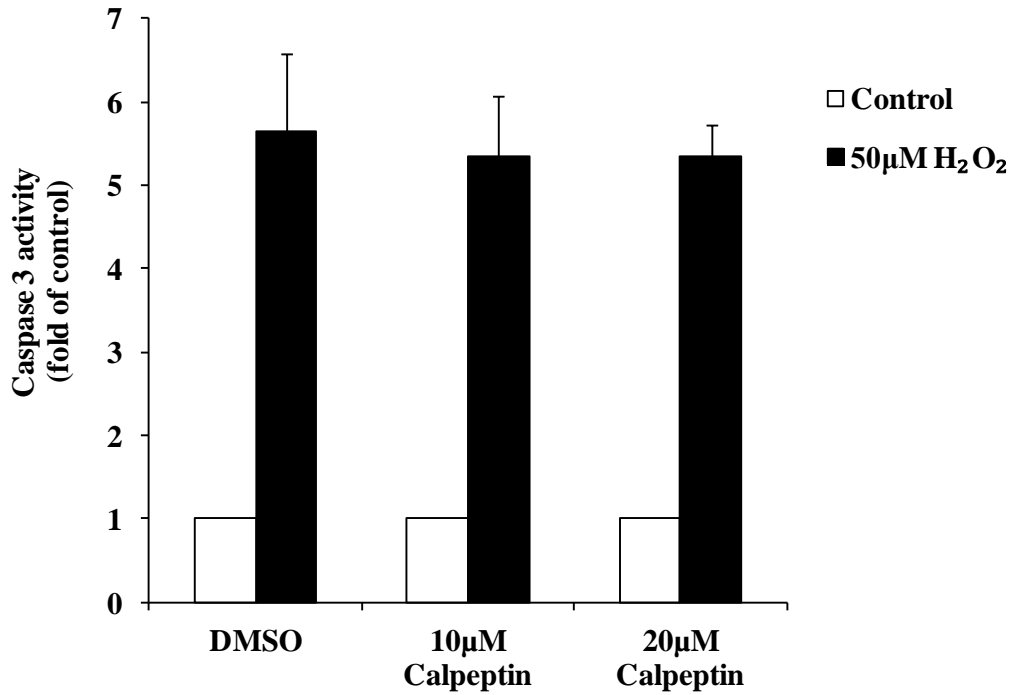
Figure 13. Caspase 3 activation upon H_2O_2 treatment was independent of calpain. L6 myoblasts were pre-treated with 10 or 20μM of calpain inhibitor, Calpeptin, for 2 hours before exposure to 50μM H_2O_2. After 24 hours, cells were harvested for caspase 3 activity assay analysis. The data are the means of three independent experiments ± S.E.M.

The involvement of cathepsins in cell death has been well reported, as discussed in Section 1. Also, *in vitro* cleavage of caspases by cathepsins has also been reported[136,137]. To test if the H_2O_2-induced caspase 3 activation is dependent on cathepsin, we pre-incubated the cells with zFA-FMK, an inhibitor specific to cathepsin B and L, before treatment with 50µM H_2O_2. Pre-incubation with zFA-FMK inhibited both caspase 3 activity and cleavage in a dose-dependent manner (Figure 14). Similarly, pre-incubation of cells with inhibitor specific to cathepsin L, zFY-CHO inhibited caspase 3 activity and cleavage dose-dependently at 50µM and 100µM (Figure 15). Inhibiton of caspase 3 activation by zFA-FMK was more efficient than zFY-CHO, suggesting that both cathepsin B and L played a role in caspase 3 activation. Furthermore, silencing of cathepsin B resulted in a decrease in caspase 3 activation in H_2O_2-treated cells, thereby confirming that cathepsin B was involved in H_2O_2-mediated caspase 3 activation (Figure 16). It was also noted that silencing of cathepsin B in untreated cells activated caspase 3 (Figure 16B). Despite the caspase 3 activation, silencing of cathepsin B was not affecting cell survival, and the reason and possible outcome of this mild caspase 3 activation is yet to be investigated (Figure 16C). As zFA-FMK and zFY-CHO could inhibit both caspase 3 activity and cleavage, this indicates that the inhibitors were acting upstream of caspase 3, instead of acting directly on the caspase 3 protein that have already been activated.

A)
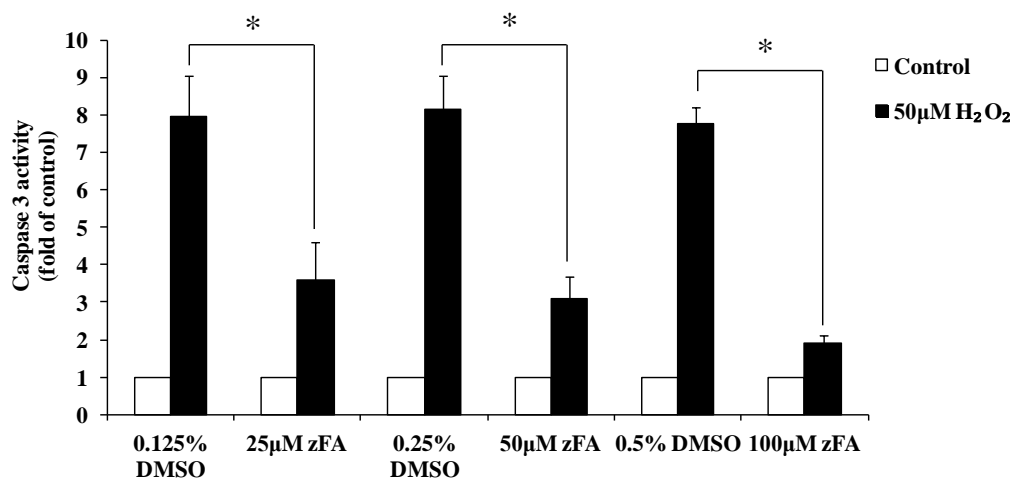
B)
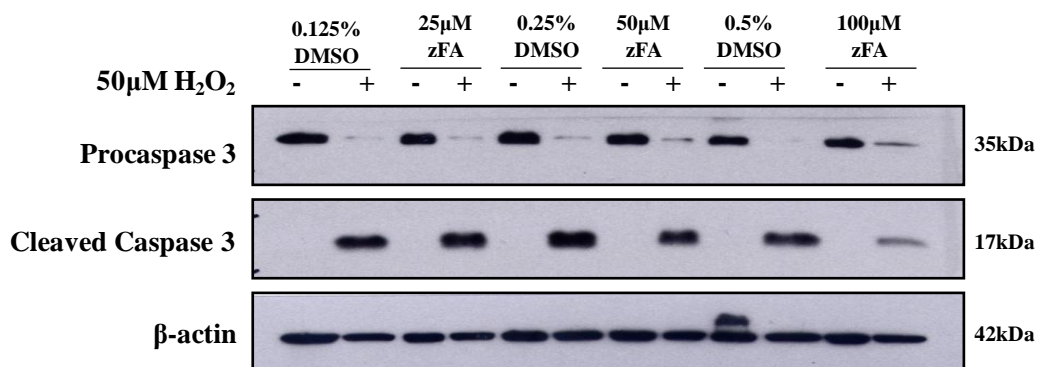
Figure 14. Caspase 3 activation upon H₂O₂ treatment was inhibited by zFA-FMK. Cells were pre-treated with 25, 50 or 100μM zFA-FMK for 2 hours before exposure to 50μM H₂O₂. After 24 hours, cells were harvested for (A) caspase 3 activity assay and (B) Western Blot analysis. The data are the means of three independent experiments ± S.E.M., *$P < 0.05$. Western blot shown is representative of three independent experiments.

A)
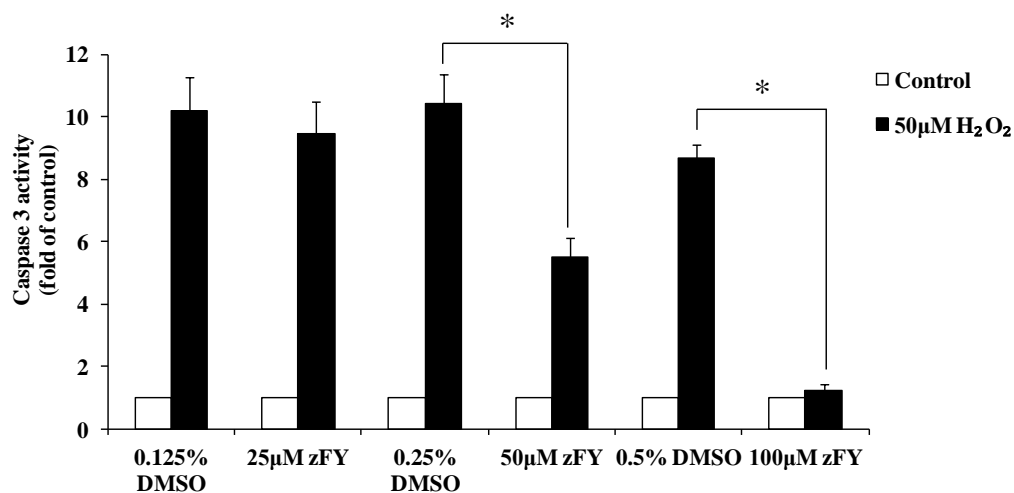
B)
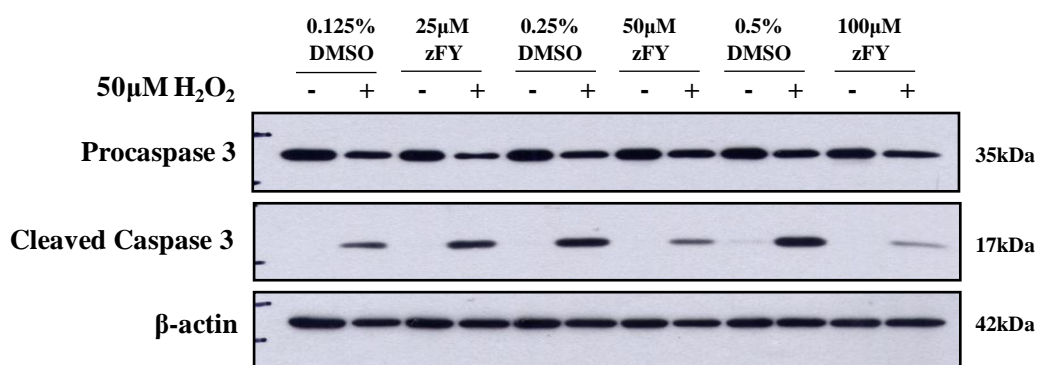
Figure 15. Caspase 3 activation upon H₂O₂ treatment was inhibited by zFY-CHO. Cells were pre-treated with 25, 50 or 100μM zFY-CHO for 2 hours before exposure to 50μM H₂O₂. After 24 hours, cells were harvested for (A) caspase 3 activity assay and (B) Western Blot analysis. The data are the means of three independent experiments ± S.E.M., *P < 0.05. Western blot shown is representative of three independent experiments.

A)
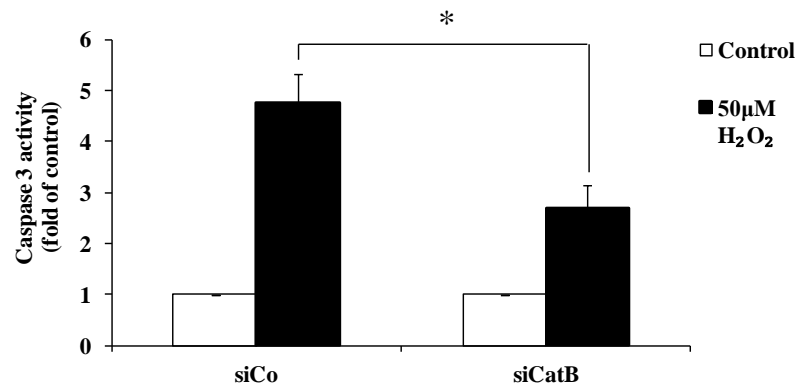
B)
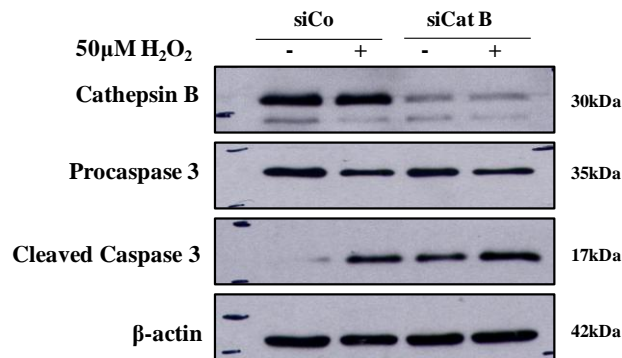
C)
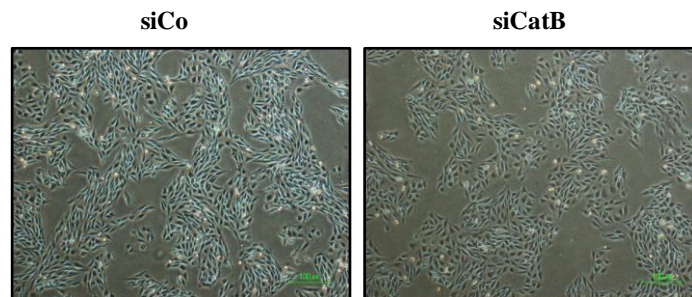
Figure 16. Knock-down of Cathepsin B decreased caspase 3 activation by H_2O_2 treatment. Cell were transiently transfected with siRNA specific to cathepsin B (siCatB) or negative control siRNA (siCo). Cells were treated with 50μM H_2O_2 24h post-transfection. At 24h post-H_2O_2 treatment, cells were harvested for (A) caspase 3 activity assay and (B) Western Blot analysis. (C) Cell morphology after silencing of cathepsin B was observed under a phase contrast microscope. The data are the means of three independent experiments ± S.E.M., *$P < 0.05$. Western blot indicating knock-down efficiency of cathepsin B is representative of four independent experiments. Pictures shown are representative of three independent experiments.

To eliminate the possibility that the inhibitors used (zFA-FMK or zFY-CHO) might cross-inhibit caspase 3 activity, the inhibitors' effect on the enzymatic activity of activated caspase 3 were tested. zFA-FMK or zFY-CHO were added to STS-treated cell lysates, which contained fully activated caspase 3, on a 96-well plate. The mixture of inhibitors and lysate were then added to enzymatic reaction containing the fluorogenic substrate of caspase 3, Ac-DEVD-AFC, and measured for caspase 3 activity. There was no inhibition of caspase 3 activity with addition of zFA-FMK or zFY-CHO, up to 100μM (Figure 17). In contrast, caspase 3 activity was completely abrogated with 25μM of the pan-caspase inhibitor, zVAD-FMK (Figure 17). The results indicate that both zFA-FMK and zFY-CHO did not have a direct inhibitory effect on caspase 3.
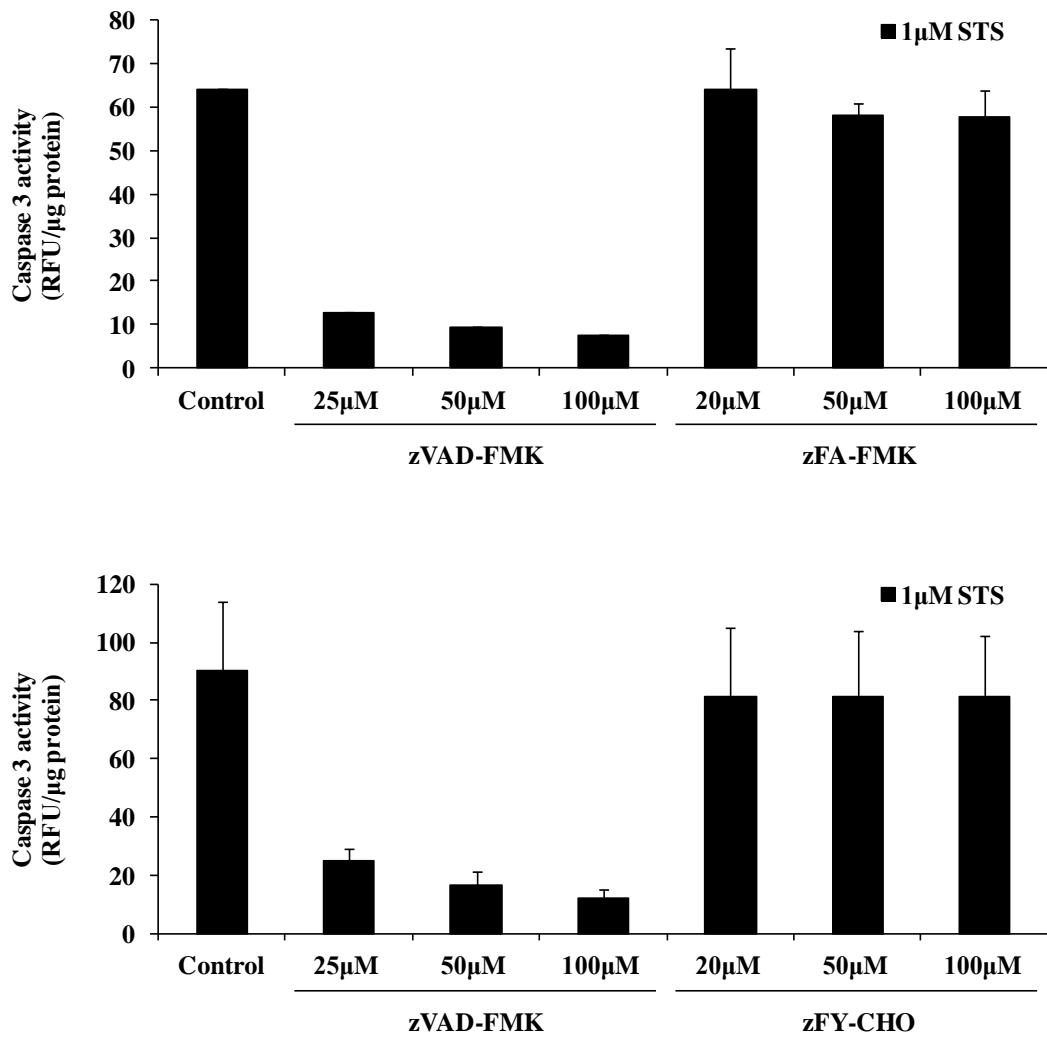
Figure 17. *In vitro* caspase activity assay with zFA-FMK and zFY-CHO. Cells were treated with 1μM STS and were harvested after 24 hours. Cell lysate was added with increasing dose of zVAD-FMK, zFA-FMK or zFY-CHO. Caspase 3 activity in the lysate was then measured with the fluorogenic substrate Ac-DEVD-AFC.

To determine whether the inhibitory effects of zFA-FMK or zFY-CHO were restricted to H_2O_2 treatment, we serum starved the cells for 24 hours. We found that serum starvation resulted in caspase 3 activation at a similar level to that induced by H_2O_2 treatment (Figure 18). Although caspase 3 was activated, these treatments did not lead to cell death, as evident by the observation of cell morphology and nuclei staining. Upon serum starvation, cellular morphology characteristic of apoptotic cells, such as cell shrinkage was not detected (Figure 19A). Similarly, cell nuclei remained intact with minimal signs of nuclei condensation and fragmentation sighted (Figure 19B). zFA-FMK or zFY-CHO was added to serum starved cells and results showed that serum starvation-induced caspase 3 activity could be effectively blocked by zFA-FMK or zFY-CHO (Figure 20). This confirmed that the involvement of cathepsin B and L in caspase 3 activation was not limited to the pathway induced by H_2O_2 treatment.
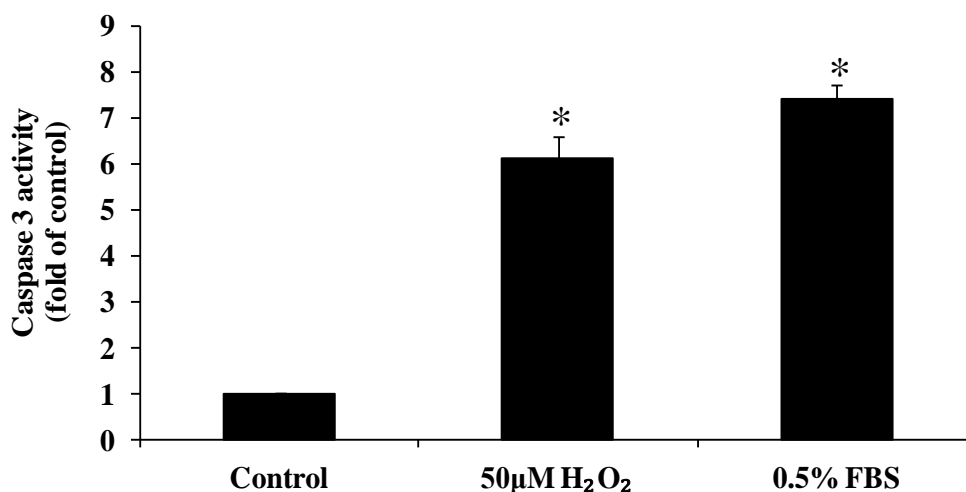
Figure 18. Serum starvation induced caspase 3 activation. Cell were treated 50μM H_2O_2 for 24 hours, or serum-starved overnight. Cells were harvested for caspase 3 activity assay. The data are the means of three independent experiments ± S.E.M., *P < 0.05, as compared to control.

A)
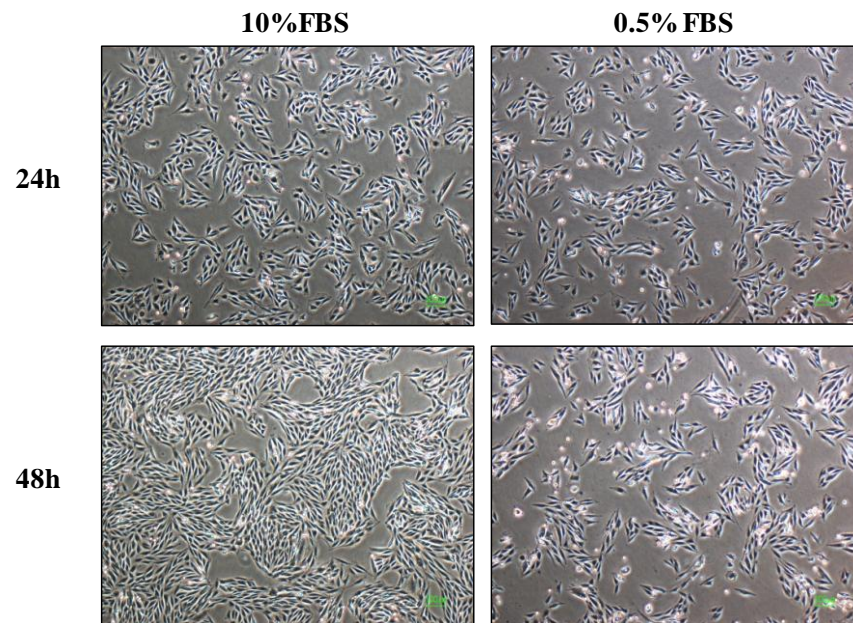
B)
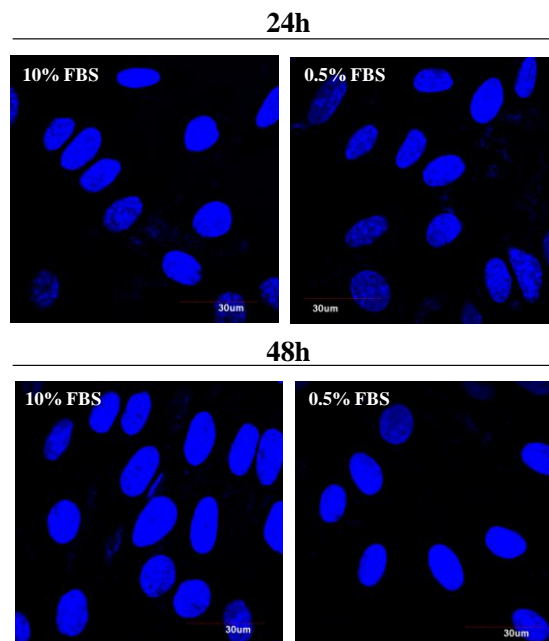
Figure 19. Effect of serum starvation on cellular morphology. Cells were serum-starved for 24 or 48 hours. (A) Cell morphology was observed under a phase contrast microscope. (B) Cell nuclei were stained with Hoechst stain and nuclear morphology was observed under a confocal microscope. Pictures shown are representative of at least 3 independent experiments
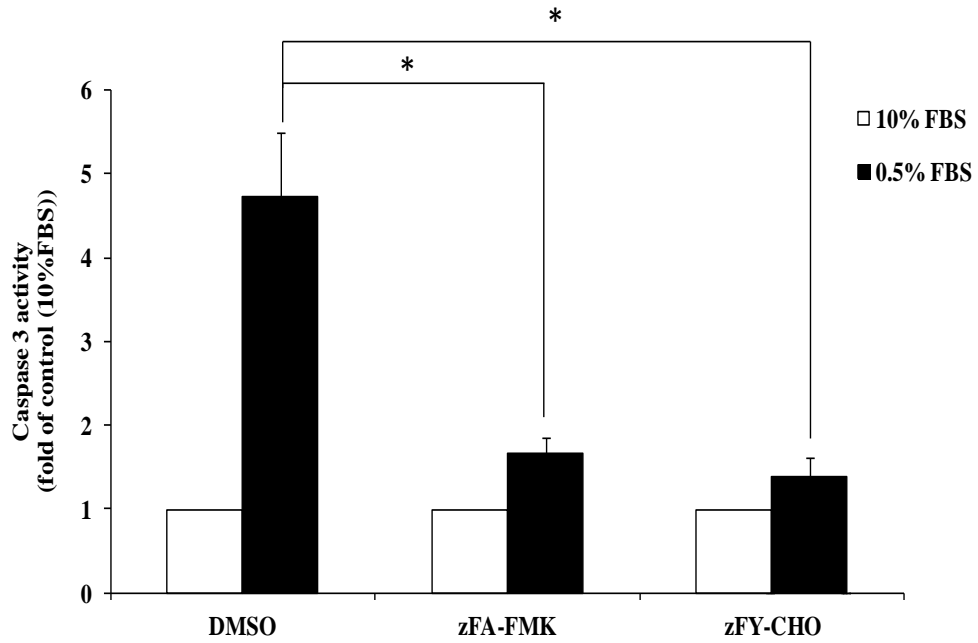
Figure 20. Inhibition of Cathepsin B and L decreased serum starvation-induced caspase 3 activation. Cells were serum starved overnight and were treated with 50μM of zFA-FMK or zFY-CHO. Cells were harvested for caspase 3 activity assay analysis. The data are the means of four independent experiments ± S.E.M., *$P <$ 0.05.

3.2.1C Cathepsin B was translocated into the cytoplasm upon H$_2$O$_2$ treatment

Having established the involvement of cathepsin B and L in H$_2$O$_2$-mediated caspase 3 activation, we next examined their protein expression. Cells were treated with H$_2$O$_2$ at different time points and were harvested for cathepsin B and L Western Blot analysis. Western Blot of cathepsin B detected three bands, which corresponds to the procathepsin B (40kda), the mature cathepsin B in single-chain form (30kda), and the heavy chain of the double-chain form (25kda) (Figure 21A). The double-chain form is the proteolytic product of the mature single-chain form. Both double-chain and single-chain forms of cathepsin B are considered as the mature cathepsin B with fully activated enzymatic properties. Densitometric analysis of Cathepsin B protein expression revealed a steady increase in the protein level of the single-chain form of mature cathepsin B at 24h and 48h (Figure 21B). The protein level of the heavy-chain form and procathepsin B remained unchanged until 24h post-H$_2$O$_2$ treatment. At 48h post-H$_2$O$_2$ treatment, there was an increase in the protein level of both heavy chain and procathepsin B (Figure 21C and D). For cathepsin L, a single band at 25kda as the mature cathepsin L was detected (Figure 22A). Densitometric analysis showed that there was no change in the overall cathepsin L protein expression over time (Figure 22B).

A)
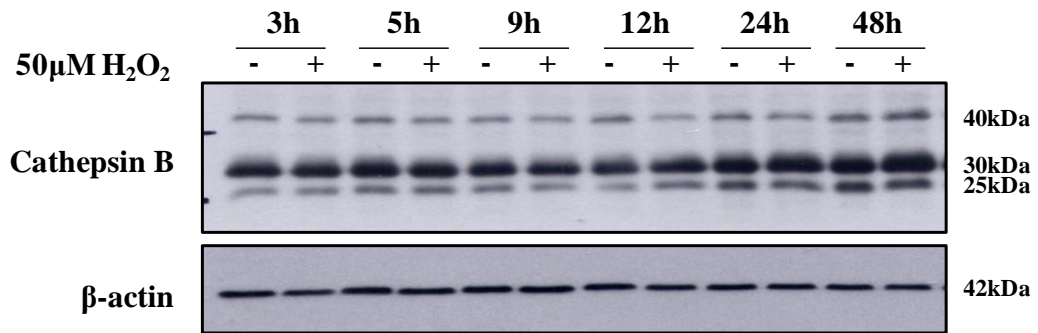
B)
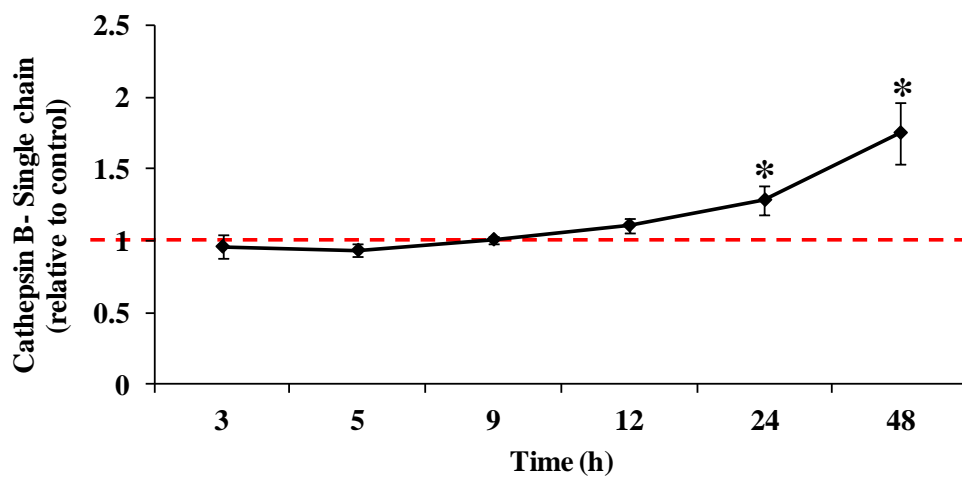
C)
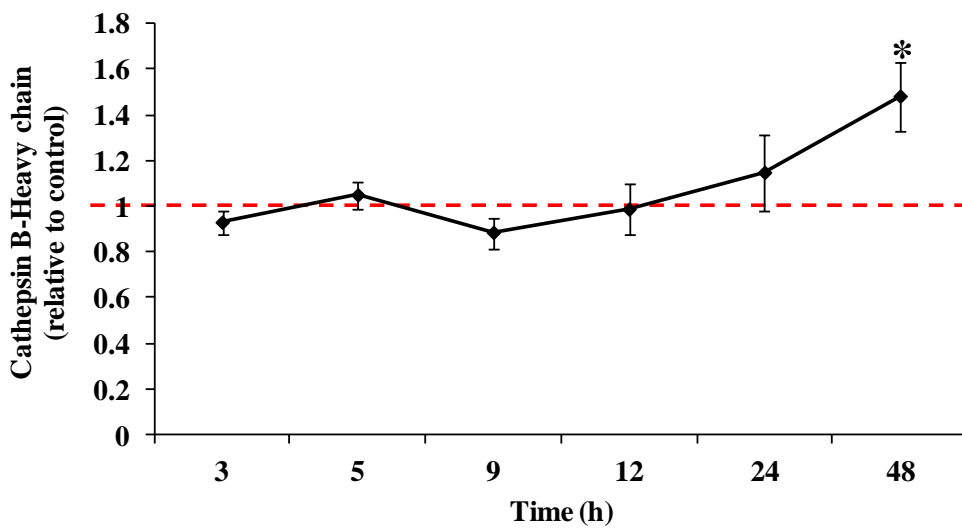
D)
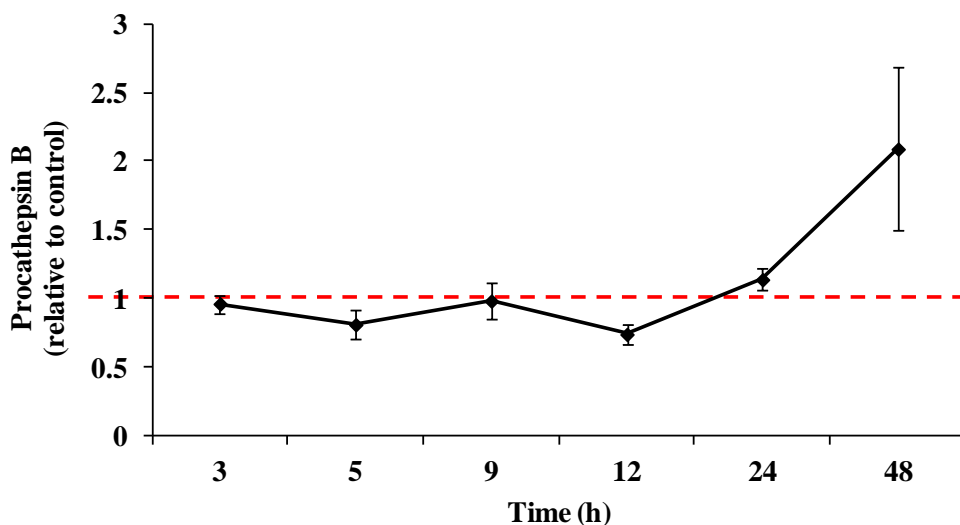
Figure 21. Expression of cathepsin B protein upon H_2O_2 treatment. (A) Cells were treated with 50μM H_2O_2 for indicated time points and were harvested for Western Blot analysis of cathepsin B protein expression level. Densitometric analysis of (B) single chain, or (C) double chain, heavy form or mature cathepsin B, expression, normalized to loading control β-actin. The change in mature cathepsin B protein expression was shown as a fold difference relative to control cells at respective time points. The data are the means of five independent experiments ± S.E.M., *$P < 0.05$.
(C) Densitometric analysis of procathepsin B expression, normalized to loading control β-actin. The change in procathepsin B protein expression was shown as a fold difference relative to control cells at respective time points. The data are the means of two independent experiments ± Sd.

A)
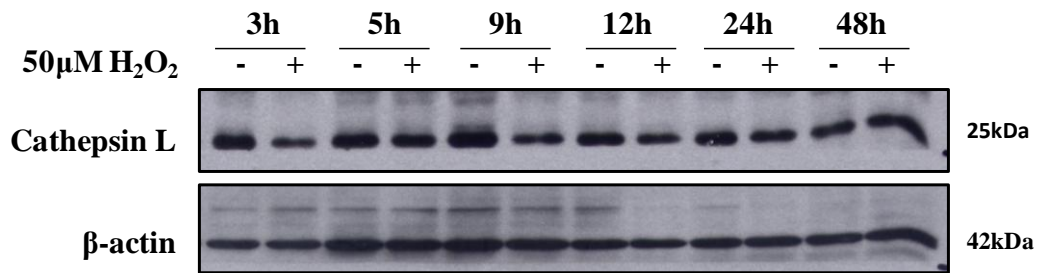
B)
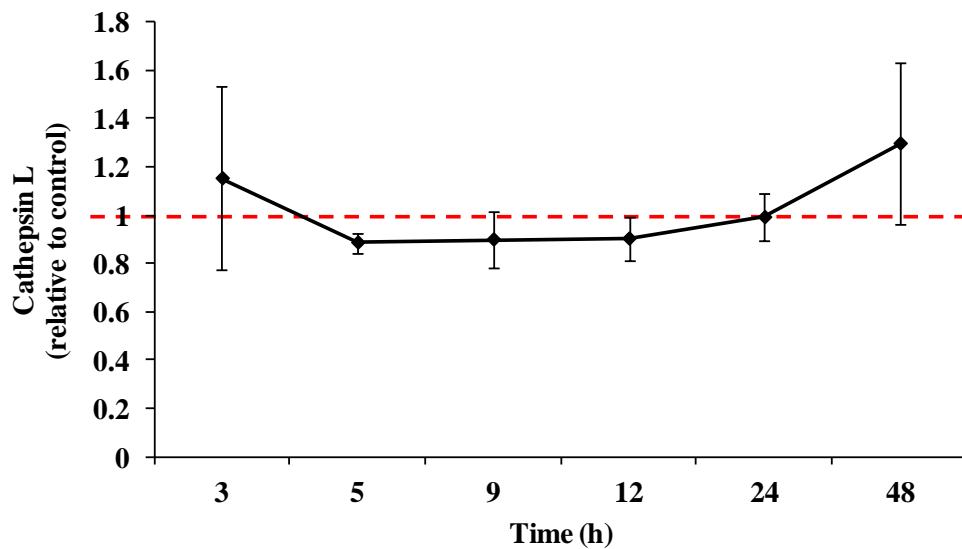
Figure 22. Expression of cathepsin L protein upon H₂O₂ treatment. (A) Cells were treated with 50µM H₂O₂ for indicated time points and were harvested for Western Blot analysis of mature cathepsin L protein expression level. (B) Densitometric analysis of mature cathepsin L expression, normalized to loading control β-actin. The change in mature cathepsin L protein expression was shown as a fold difference relative to control cells at respective time points. The data are the means of three independent ± S.E.M.

Both cathepsin B and L are lysosomal proteases while caspase 3 is a cytosolic protein. Cytoplasmic relocalization of cathepsins is therefore necessary for the proteolytic action to take place. Cathepsin B localization was assessed by immunofluorescence. Cells treated with 50μM H_2O_2 were incubated with a primary antibody specific to cathepsin B and were observed under the confocal microscope. Figure 23A showed the typical staining of lysosomes with LysoTracker® Red DND-99. Figure 23B showed that, in control untreated cells the red staining of cathepsin B was typical of the staining of lysosomes, as shown in Figure 23A. However, in H_2O_2-treated cells, it showed a diffused cytoplasmic staining, indicating that cathepsin B has translocated into the cytoplasm after H_2O_2 treatment (Figure 23B).

A)
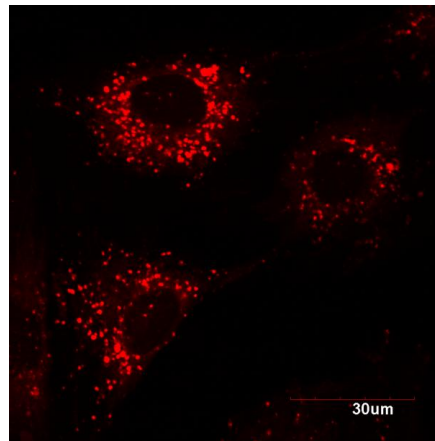
B)
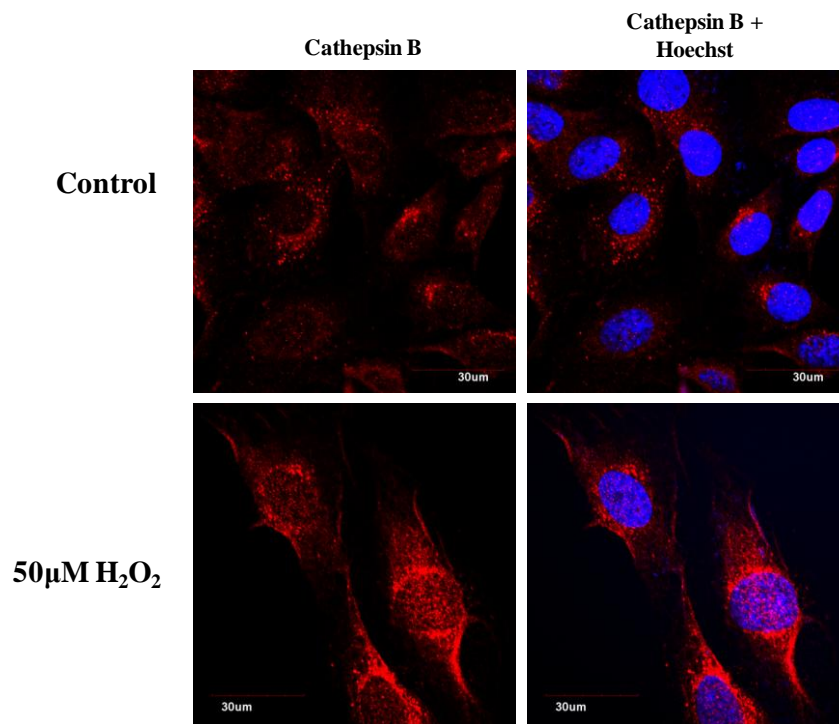
Figure 23. Cathepsin B translocated from the lysosomes into the cytoplasm upon H₂O₂ treatment. (A) L6 myoblasts were incubated with a diluted LysoTracker® Red DND-99 solution (75nM) for 45min, 37°C, followed by observation under a confocal microscope. (B) L6 myoblasts were treated with 50μM H₂O₂ for 24 hours. After fixation, cells were incubated with primary antibody specific to cathepsin B, followed by observation under a confocal microscope. Nuclei were stained blue with Hoechst 34580 nucleic acid stain.

Next, we investigate the occurrence of lysosomal membrane permeabilization (LMP) as cathepsins release is always associated with LMP, or vice versa. LMP was quantified by Acridine Orange staining. Figure 24 showed a simple illustration of the working mechanism of Acridine Orange. The lysosomotropic probe Acridine Orange is a metachromatic fluorophore that accumulates in acidic organelles and displays a red to orange fluorescence when excited by blue light. On lysosomal rupture, the dye is released into the cytosol where its fluorescence spectrum changes from red to green. Therefore, a decrease in red fluorescence or an increase in green fluorescence indicates LMP has taken place.
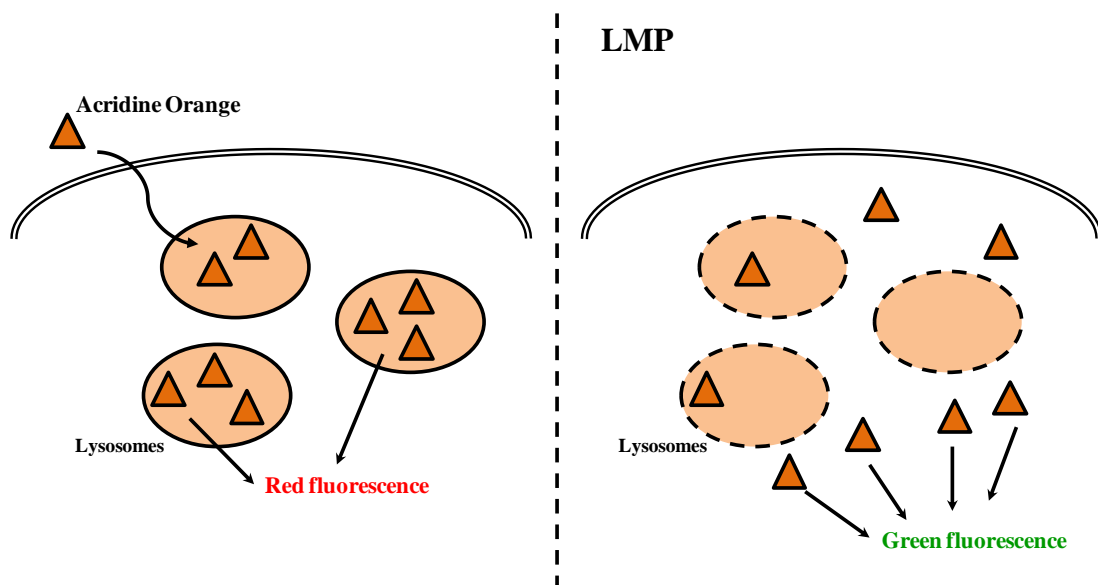
Figure 24. Graphical illustration of the working mechanism of Acridine Orange lysosomal staining assay.

To measure LMP in our system, cells were pre-stained with Acridine Orange for 30min prior to H_2O_2 treatment. Time kinetic study of FACS analysis of Acridine Orange cytosolic green fluorescence revealed an increase of 8% and 14% in the fluorescence intensity at 2h and 4h respectively (Figure 25). This indicates that LMP has taken place at 2-4h post-H_2O_2 treatment. Such increase in green fluorescence gradually subsided after 4h and the fluorescence intensity was decreased to basal level at 18h. After 24h, a decrease in green fluorescence was observed and at 48h, the decrease was about 17% from the control (Figure 25).
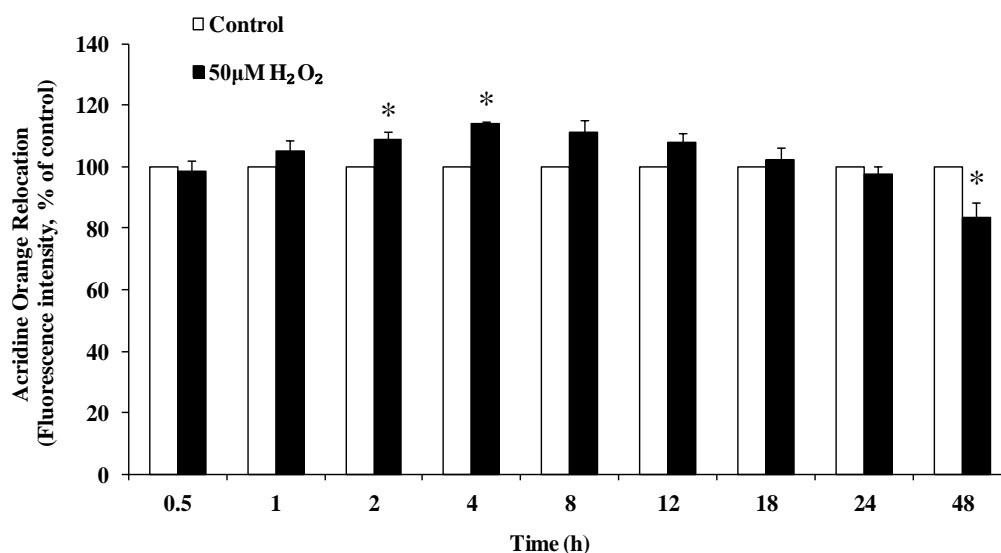
Figure 25. H_2O_2 treatment resulted in lysosomal membrane permeabilization at 2-4h. Cells were exposed to an Acridine Orange solution (10μM) for 30 min at 37°C, before cells were treated with 50μM H_2O_2 for indicated time points. Green cytosolic fluorescence of 10,000 cells per sample was determined by flow cytometry using the FITC-A channel. The data are the means of four independent experiments ± S.E.M., *$P < 0.05$, as compared to control at respective time points.

3.2.2 H_2O_2-induced caspase 3 activation was redox-regulated

We have established a pathway of cathepsin-mediated caspase 3 activation via LMP in the absence of cell death. Still, the question remains as how a transient dose of H_2O_2 could result in the generation of such signalling pathway. The time gap between the earliest event of LMP detected (2h) and H_2O_2 treatment (0h) suggests the existence of an upstream reaction before LMP (Figure 26).
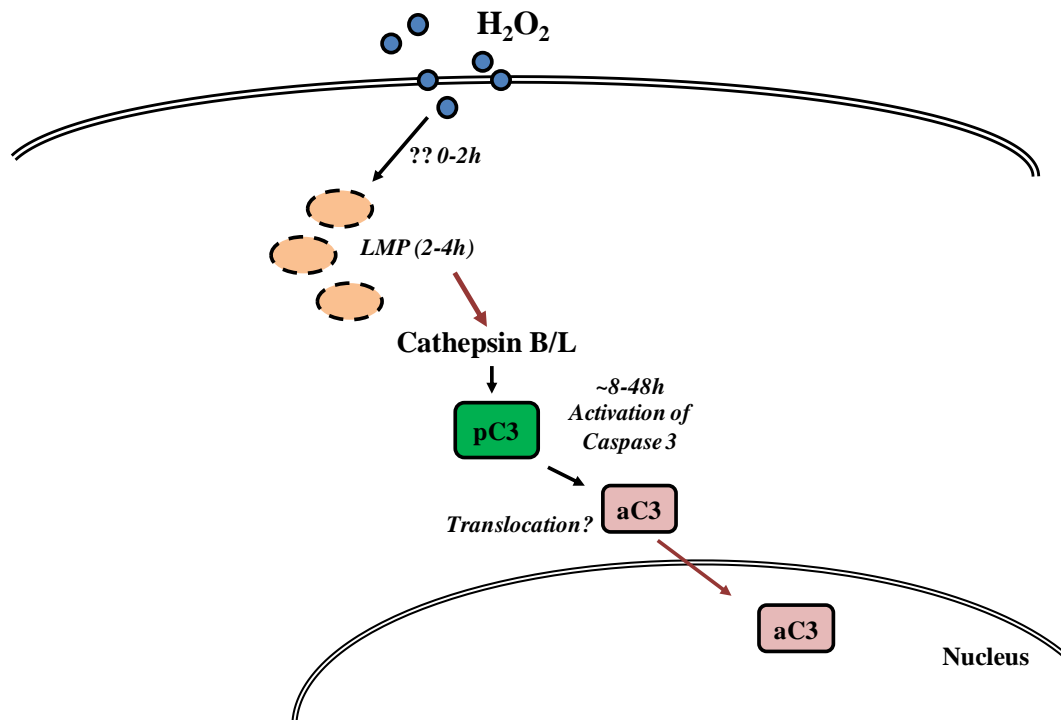
Figure 26. An upstream reaction led to cathepsin-dependent caspase 3 activation. H_2O_2 treatment triggered LMP at 2-4h. The occurrence of LMP resulted in cathepsin B and L release, which cleaved and activated caspase 3 at 8-48h. An upstream pathway(s) was postulated to be mediating H_2O_2 effect at 0-2h leading to LMP. (pC3: procaspase 3, aC3: activated caspase 3)

When exogenously added H_2O_2 diffuse across the membrane bilayer, it is expected to cause a disturbance to the intracellular redox balance. Depending on the dose of H_2O_2, such disturbance could be reversed by the cellular antioxidant system, or it could be irreversible. Again, the irreversible effect of H_2O_2 on redox balance could have diverse effects on the cells, depending on the amount of H_2O_2. Such effects could be the generation of a signalling pathway, induction of oxidative stress, and/or cell death.

In our system, 50μM H_2O_2 induced an oxidative stress to the cells as evident by the up-regulation of Heme Oxygenase 1 (HO-1) protein (Figure 27). HO-1 is a stress-responsive protein induced by a variety of oxidative challenges[138,139] and therefore can be used as a marker for oxidative stress. Both 50 and 150μM H_2O_2 treatment caused an up-regulation of the HO-1 protein at 4 and 24 hours-post treatment (Figure 27A). Such up-regulation was not observed in STS-treated cells. It was observed that upon 50μM H_2O_2 treatment, the up-regulation of HO-1 protein expression was sustained up to 48 hours (Figure 27B). This also indicates that 50μM H_2O_2 treatment induced a sustained oxidative stress which lasted for at least 48 hours.

A)
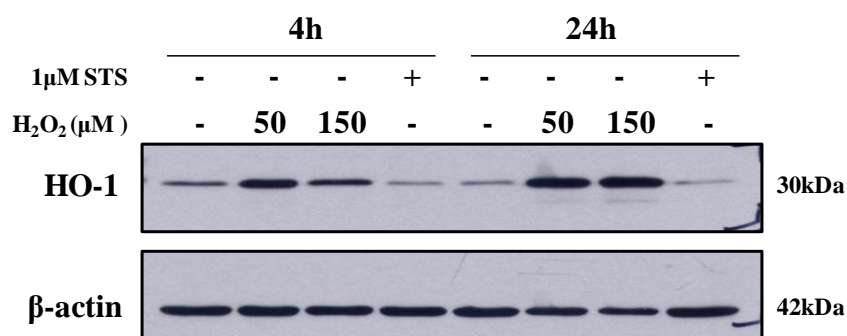
B)
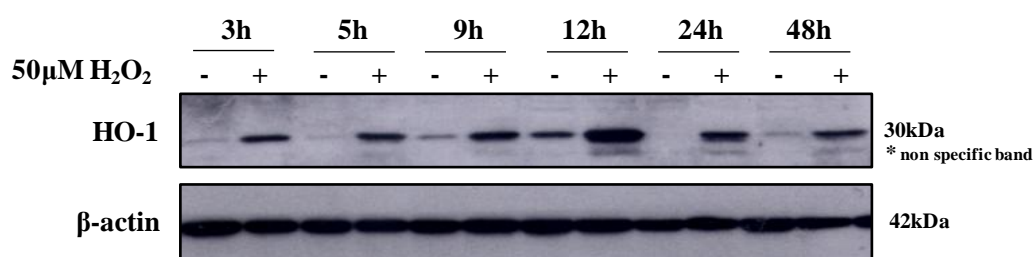
Figure 27. Up-regulation of HO-1 upon H₂O₂ treatment. (A) L6 myoblasts were treated with 50 or 150µM H₂O₂, or 1µM STS for 4 and 24 hours. Cells were harvested for Western Blot analysis of Heme Oxygenase 1 (HO-1) expression. (B) Cells were treated with 50µM H₂O₂ for indicated time points and were harvested for Western Blot analysis of HO-1 expression. Western Blots are representative of two independent experiments.

The up-regulation of HO-1 protein expression is associated with change in cellular redox state. We hypothesized that the upstream reaction before LMP could be redox-regulated. Due to its chemical structure, H_2O_2 has mild oxidation property. Most of the physiological and pathological actions of H_2O_2 are mediated through its more reactive by-products of oxygen species. Both iron and ROS are known mediators of LMP[140], however it should be noted that iron is also an essential mediator of H_2O_2 reaction. In this section, we investigate the possible involvement of iron and a second ROS/RNS in the activation of caspase 3.

3.2.2A Iron chelation prevented H_2O_2-induced caspase 3 activation

When the cells were pre-incubated with an iron chelator, Deferiprone (DFP), the up-regulation of HO-1 was partially inhibited, but not completely (Figure 28). This indicates that oxidative stress induced by H_2O_2 treatment was partially mediated through a reaction with iron. This suggests that iron was an important factor in ROS generation through reaction with H_2O_2. However, it is not known if it was also significant in its role in iron-mediated caspase 3 activation. We hypothesized the following involvement of iron in caspase 3 activation: 1) iron was required in a catalyzed reaction (e.g. Fenton's reaction) to generate a reactive H_2O_2 by- product which carries out the subsequent reaction, 2) iron was required in the upstream activation of caspase 3, or 3) iron had a direct effect on caspase 3 activity.
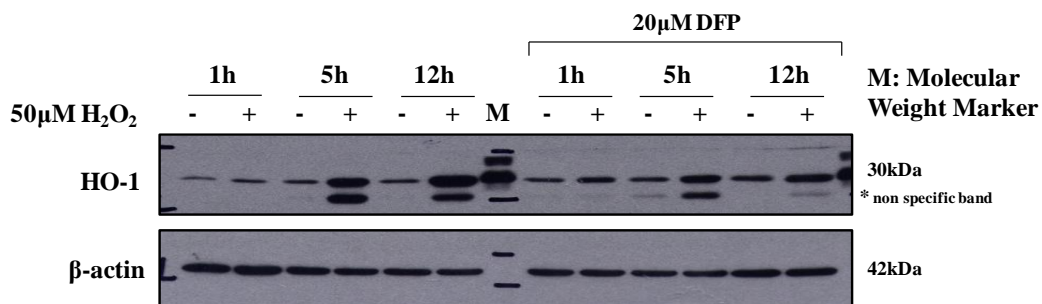
Figure 28. Iron chelation decreased H_2O_2-induced HO-1 up-regulation. Cells were pre-treated with 20μM iron chelator Deferiprone (DFP) for 2 hours before exposure to 50μM H_2O_2. Cells were harvested at indicated time points for Western Blot analysis of HO-1.

To evaluate the importance of iron in caspase 3 activation, cells were pre-incubated with either of the two iron chelators, Deferoxamine (DFO) or DFP as measured for caspase 3 activity and cleavage. Upon iron chelation, H_2O_2-induced caspase 3 activity and caspase 3 cleavage was almost completely abrogated (Figure 29). In contrast, iron chelation had no effect on STS-induced caspase 3 activation. Compared to DFO, DFP is more soluble and enters the cells readily and efficiently to reach the major intracellular sites of iron accumulation. Entry of DFO into the cells is much slower and requires more incubation time to reach significant concentration in the cell[141]. Since the cell oxidative response was detected as early as 1h after addition of H_2O_2, DFO was unsuitable as the iron chelator in our system to measure the effect of iron as an upstream species in caspase 3 activity. LMP was therefore measured using DFP as the iron chelator. LMP was completely inhibited when cells were pre-incubated with DFP (Figure 30).

Subsequently, DFP was added to cells at various time points before or after exposure to H_2O_2. Results showed that only with addition of DFP at 0h, meaning a co-existence of H_2O_2 and DFP, caspase 3 activity and cleavage was completely inhibited, whereas addition of iron chelator after H_2O_2 exposure had no effect (Figure 31).

A)
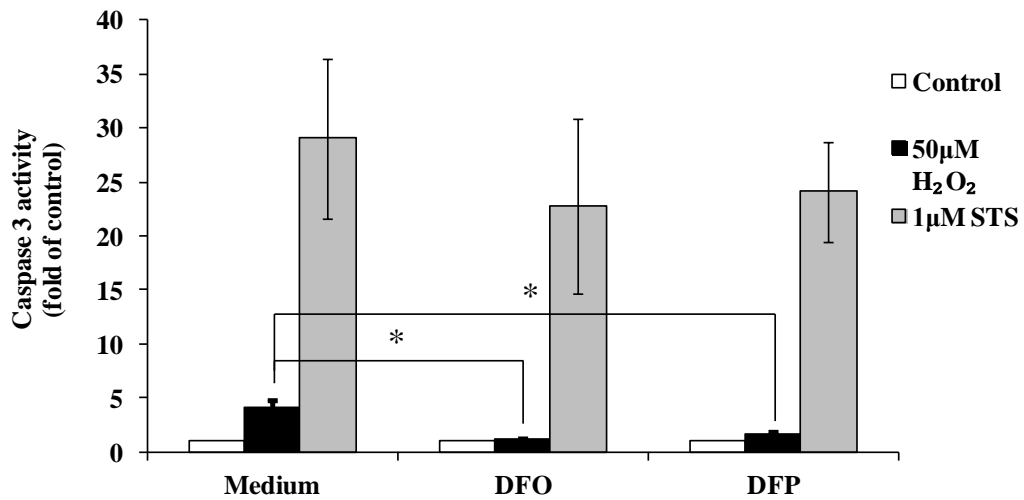
B)
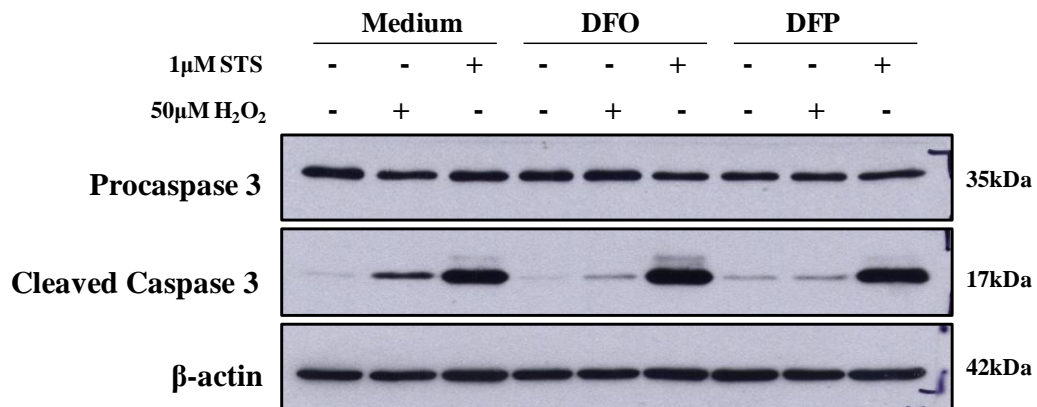
Figure 29. Iron chelation prevented caspase 3 activation. L6 myoblasts were pre-treated with iron chelators, Deferoxamine (DFO, 20μM) or Deferiprone (DFP, 50μM), for 2 hours before exposure to 50μM H_2O_2 or 1μM STS. After 24 hours, cells were harvested for (A) caspase 3 activity assay and (B) Western Blot analysis of caspase 3 cleavage. The data are the means of three independent experiments ± S.E.M., $*P < 0.05$.

A)
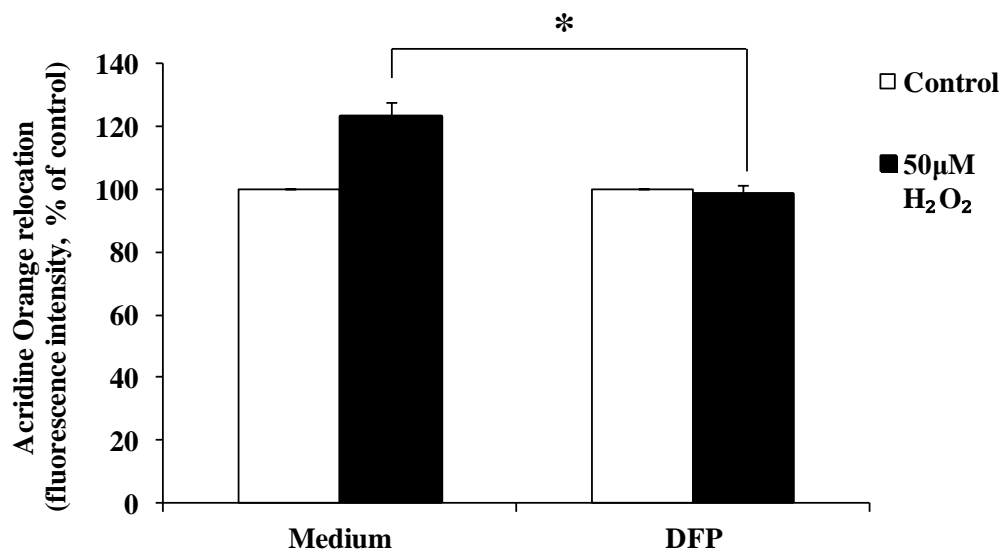
B)
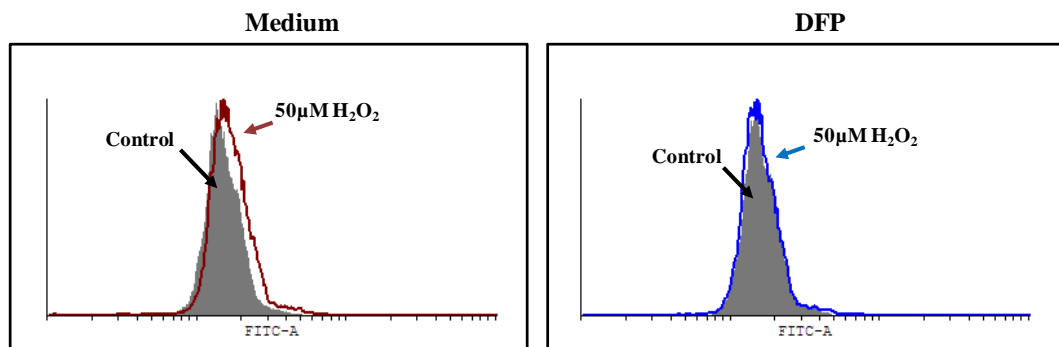
Figure 30. LMP was inhibited by iron chelation. (A) L6 myoblasts were exposed to 10μM Acridine Orange and 50μM DFP for 30 min at 37°C, before treatment with 50μM H_2O_2 for 4 hours. Green cytosolic fluorescence of 10,000 cells per sample was determined by flow cytometry using the FITC-A channel. The data are the means of three independent experiments ± S.E.M., *$P < 0.05$. (B) A representative flow cytometry histogram from three experiments is shown.

A)

B)

Figure 31. Iron chelation at the first hour of reaction inhibited caspase 3 activation. L6 myoblasts were exposed to 50μM H_2O_2 and were co- or post-treated with DFP at different time points. At 24h post-H_2O_2 treatment, cells were harvested for (A) caspase 3 activity assay and (B) Western Blot analysis. The data are the means of three independent experiments $\pm$ S.E.M., *$P < 0.05$. Western blot shown is representative of three independent experiments.

The uptake of H_2O_2 into the cells is a time-dependent process. Given that the culture medium contains iron, one may argue that the reaction of H_2O_2 with iron could happen intracellular or extracellular. The culture medium used in experiments, DMEM contains Ferric Nitrate ($Fe(NO_3)_3 \cdot 9H_2O$) with the concentration of 0.1mg/L or 0.25μM. However, it is unlikely that the H_2O_2-iron reaction took place in the medium. Firstly, the low concentration of iron in the medium means that it is unlikely to be the rate-limiting factor for the reaction to take place. Secondly, ferric iron is the stable oxidative state of iron that does not react with another oxidation agent, such as H_2O_2. Therefore, we hypothesized that the iron content in the medium did not take part in H_2O_2-mediated signalling.

To test the hypothesis, cells were treated with H_2O_2 in RPMI-1640 and were harvested at indicated time points. The RPMI-1640 is an iron-free medium, thereby preventing any chance of H_2O_2 reacting with extracellular iron before entering the cells. Result shows that, at 24h post-H_2O_2 treatment, there was no difference in the morphology of cells treated in DMEM or RPMI (Figure 32A). There was also no difference in caspase 3 activation between cells treated with H_2O_2 in DMEM or RPMI. H_2O_2 treatment in cells cultured in DMEM or RPMI resulted in a caspase 3 activation of 5.4 fold (Figure 32B). Cells were then treated with H_2O_2 in RPMI and harvested at different time points. Result shows that upon H_2O_2 treatment, caspase 3 was activated in a time-dependent manner. The maximum activation was registered at 24h post H_2O_2 treatment (Figure 32C). These result supported our hypothesis that extracellular iron in the medium was not involved in the H_2O_2-mediated signalling.

A)
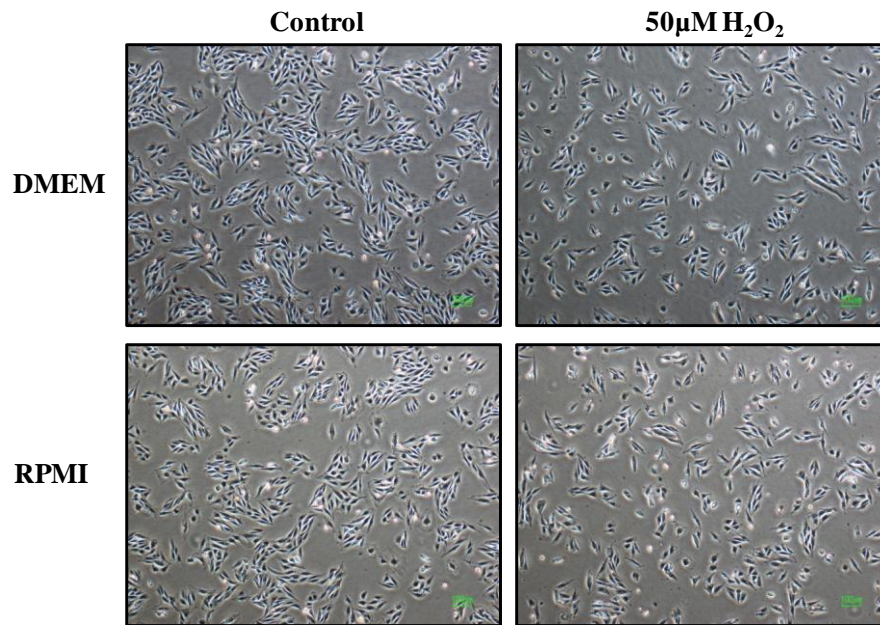
B)
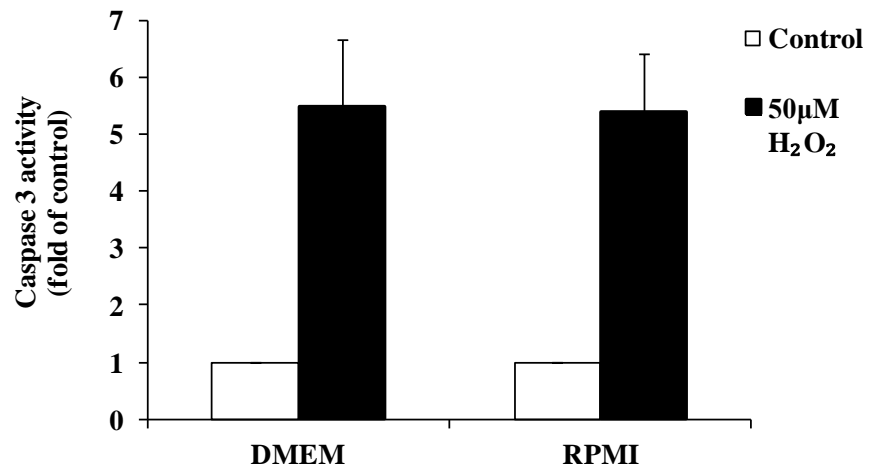
C)
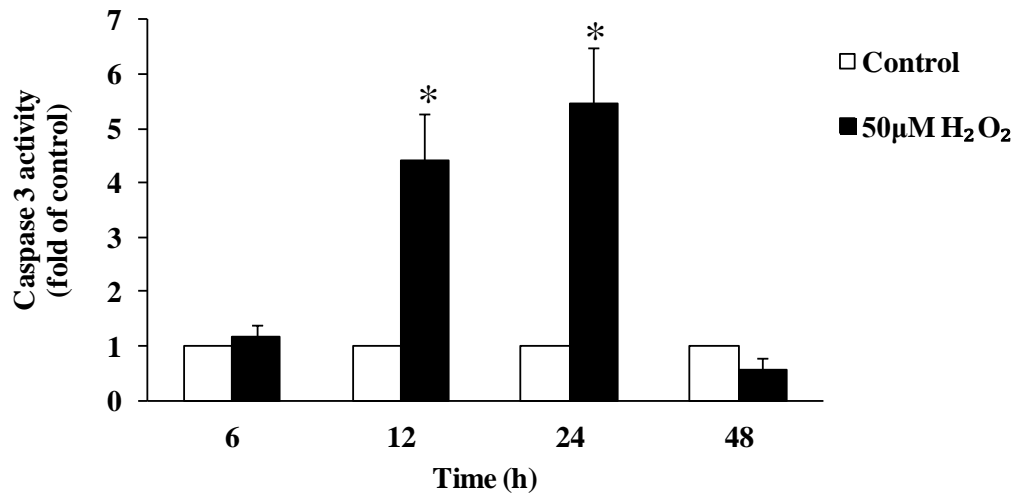
Figure 32. Extracellular iron was not required in caspase 3 activation by H_2O_2 treatment. Cells were treated with 50μM H_2O_2 in DMEM or RPMI for 24 hours. (A) Cell morphology was observed under a phase contrast microscope. Pictures shown are representative of three independent experiments. (B) Cells were harvested for caspase 3 activity assay. The data are the means of three independent experiments ± S.E.M. (C) Cells were treated with 50μM H_2O_2 in RPMI for indicated time points, and were harvested for caspase 3 activity assay analysis. The data are the means of three independent experiments ± S.E.M., $*P < 0.05$, as compared to control at respective time points.

3.2.2B Peroxynitrite and nitric oxide were involved in caspase 3 activation by H_2O_2

Having established the involvement of intracellular iron in H_2O_2-mediated caspase 3 activation, we next investigate the involvement of ROS/ reactive nitrogen species (RNS) in caspase 3 activation. Two widely used fluorophore, CM-H_2DCFDA (or in short, DCF) and DAF-FM Diacetate (or in short, DAF) were used to detect any increase in ROS or RNS after H_2O_2 treatment. Both DCF and DAF are redox sensitive dye that fluoresces when oxidized by intracellular ROS or RNS. The increase in DCF and DAF fluorescence was measured by FACS analysis and the fluorescence intensity correlates to the ROS or RNS level in cells.

At 0.5 to 1 hour after H_2O_2 treatment, an increase in DCF fluorescence was detected, but the increase was statistically insignificant (Figure 33A). Subsequently, there was an overall increase in the DCF fluorescence starting from 2h to 48h post-H_2O_2 treatment (Figure 33B). Such increase in DCF staining ranged from 130-160% relative to the control. Figure 33C shows an alternate graphical representation of DCF fluorescence staining.

A)
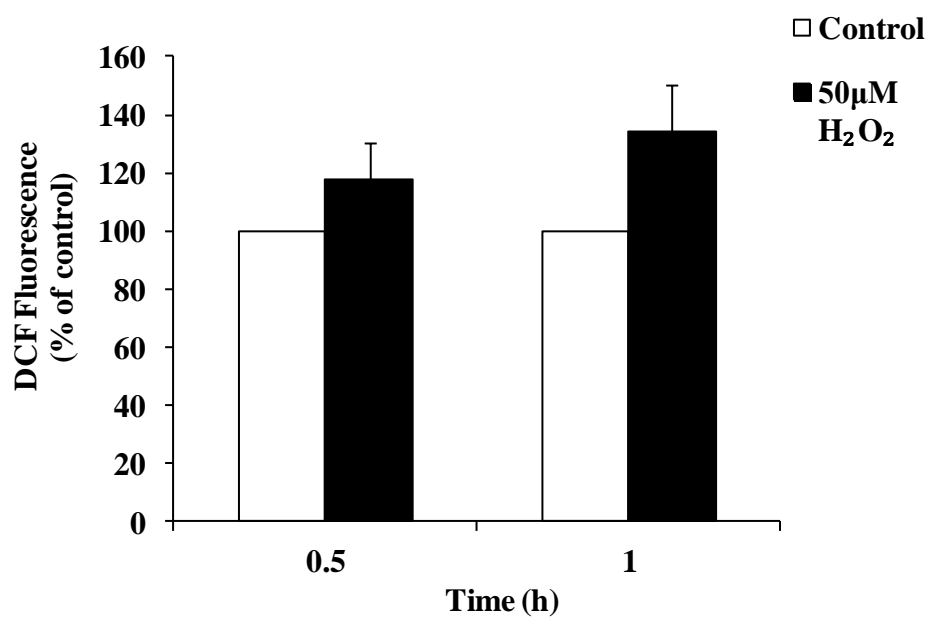
B)
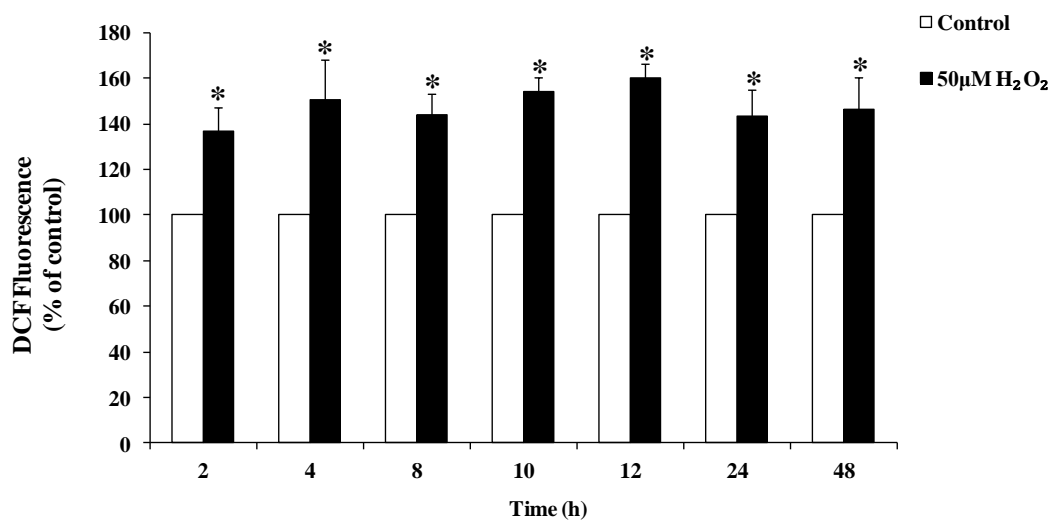
C)
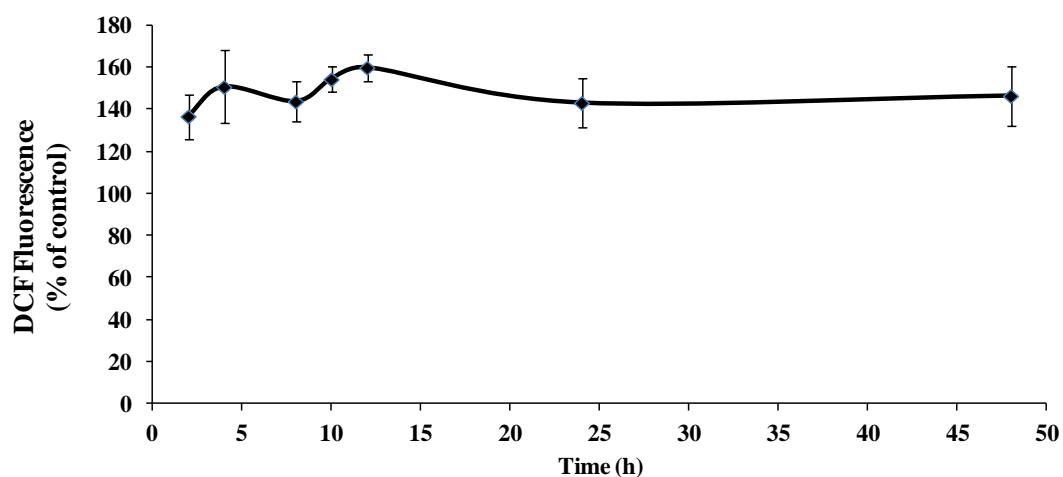
Figure 33. ROS measurement upon H$_2$O$_2$ treatment using the CM-H$_2$DCFDA probe. Cells were treated with 50μM H$_2$O$_2$ for (A) 0.5h and 1h or (B) 2h, 4h, 6h, 8h, 12h, 24h and 48h, and were incubated with CM-H$_2$DCFDA for 20min, 37°C. Green cytosolic fluorescence of 10,000 cells per sample was determined by flow cytometry using the FITC-A channel. The data are the means of five independent experiments ± S.E.M., *$P < 0.05$, as compared to control at respective time points.
(C) An alternative representation of (B).

A time kinetic study of DAF staining revealed an overall increase in nitric oxide level after H_2O_2 treatment. As with DCF staining, the increase in DAF fluorescence at 0.5-1h post-H_2O_2 treatment was statistically insignificant (Figure 34A). The increase of DAF fluorescence was also sustained from 2h to 48h post-H_2O_2 treatment (Figure 34B). The increase in DAF fluorescence ranged from 140-240% relative to the control. Figure 34C shows an alternate graphical representation of DAF staining. A prominent peak of the fluorescence intensity can be observed from the graph. At that point (10h post-H_2O_2 treatment), the increase in DAF fluorescence was 240% relative to the control.

A)
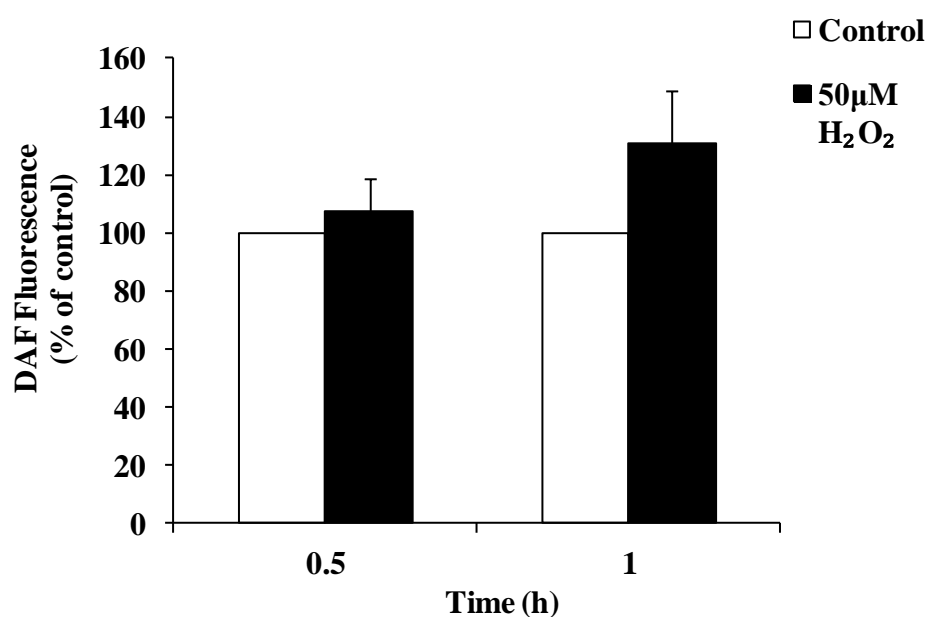
B)
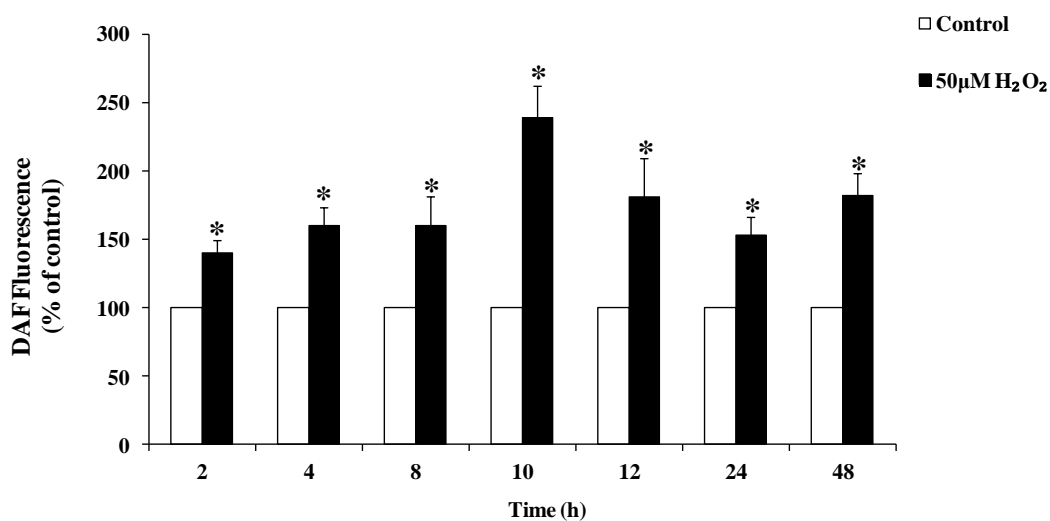
C)
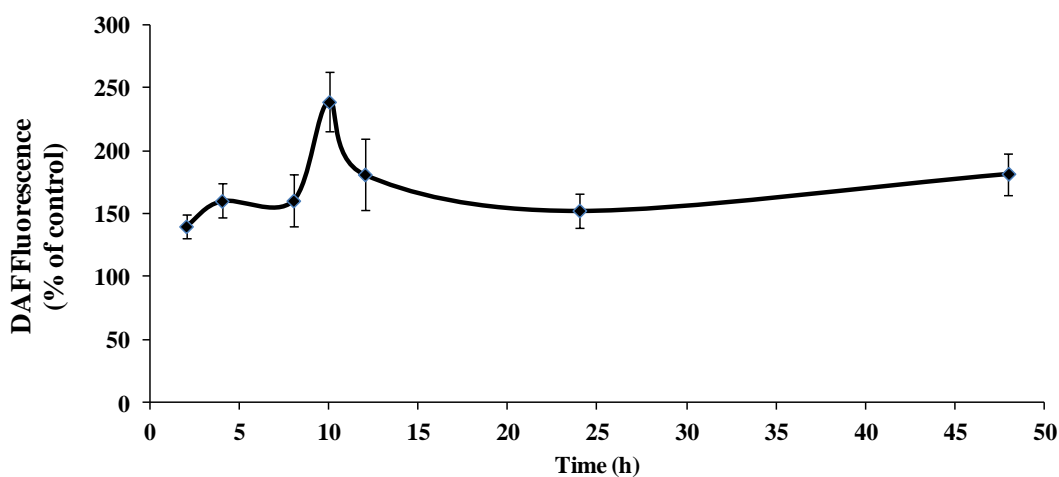
Figure 34. Nitric Oxide measurement upon H₂O₂ treatment using the DAF-FM Diacetate probe. Cells were treated with 50μM H₂O₂ for (A) 0.5h and 1h or (B) 2h ,4h ,6h ,8h ,12h ,24h and 48h, and were incubated with DAF-FM Diacetate for 20min, 37°C. Green cytosolic fluorescence of 10,000 cells per sample was determined by flow cytometry using the FITC-A channel. The data are the means of five independent experiments ± S.E.M., *$P < 0.05$, as compared to control at respective time points.
(C) An alternative representation of (B).

While DAF is specific for nitric oxide (NO•) detection; DCF detects a wide range of ROS. Based on the specificity of the dyes, we deduced the possible species of ROS and RNS produced: DCF detects peroxyl radical (ROO•), hydroxyl radical (OH•), peroxynitrite (ONOO$^-$) and H_2O_2, while DAF detects NO•. Next, we predicted that as the immediate product of H_2O_2 in the Fenton's reaction, OH• was involved in caspase 3 activation. Surprisingly, pre-incubation of cells with Dimethylthiourea (DMTU), a potent OH• scavenger had no effect on H_2O_2-induced caspase 3 activation. This is with regard to both caspase 3 activity (Figure 35A) and caspase 3 cleavage (Figure 35B). Eliminating OH•, we next assessed the possibility of ONOO$^-$ and NO• involvement in caspase 3 activation.

A)
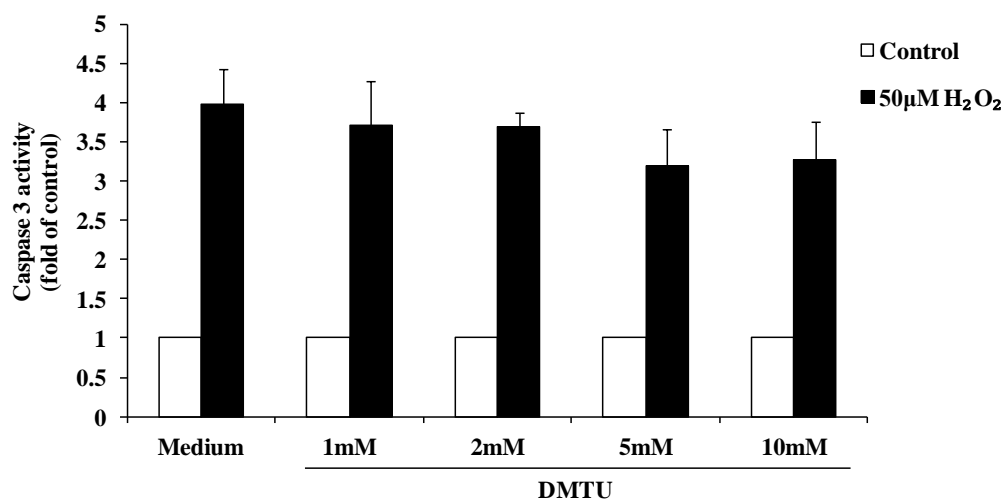
B)
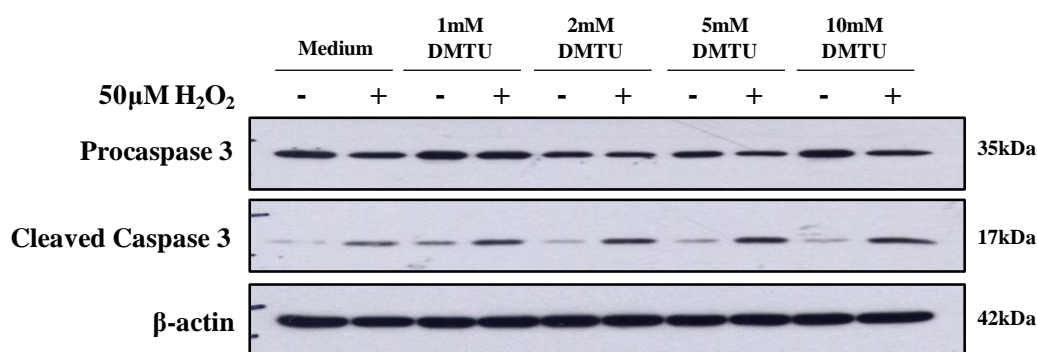
Figure 35. Scavenging OH• did not prevent caspase 3 activation. L6 myoblasts were pre-treated with increasing dose of DMTU before exposure to 50μM H₂O₂. At 24h post-H₂O₂ treatment, cells were harvested for (A) caspase 3 activity assay and (B) Western Blot analysis. The data are the means of three independent experiments ± S.E.M.

Cells were incubated with a peroxynitrite decomposition catalyst, FeTPPS, before treatment with H_2O_2. Incubation with FeTPPS abrogated caspase 3 activation and cleavage in a dose-dependent manner (Figure 36). Besides caspase 3 activity, LMP was also prevented by FeTPPS (Figure 37).

A)
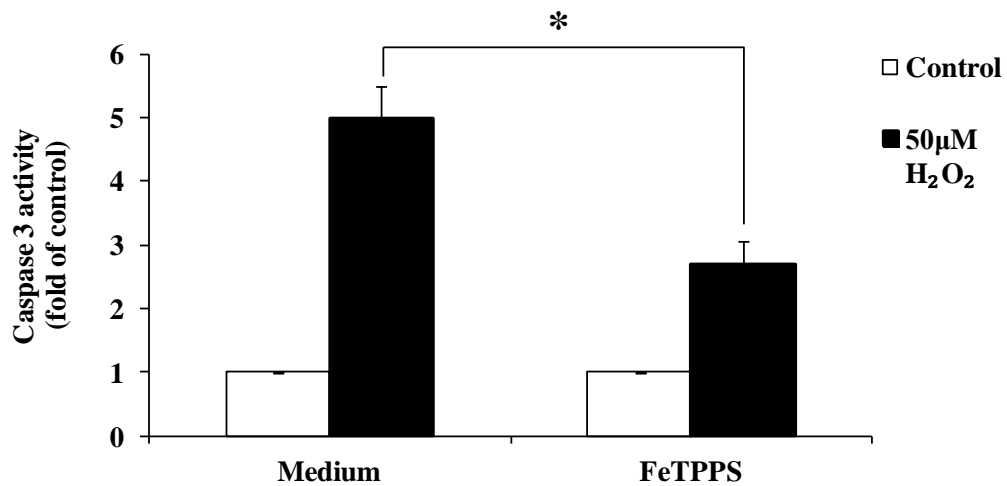
B)
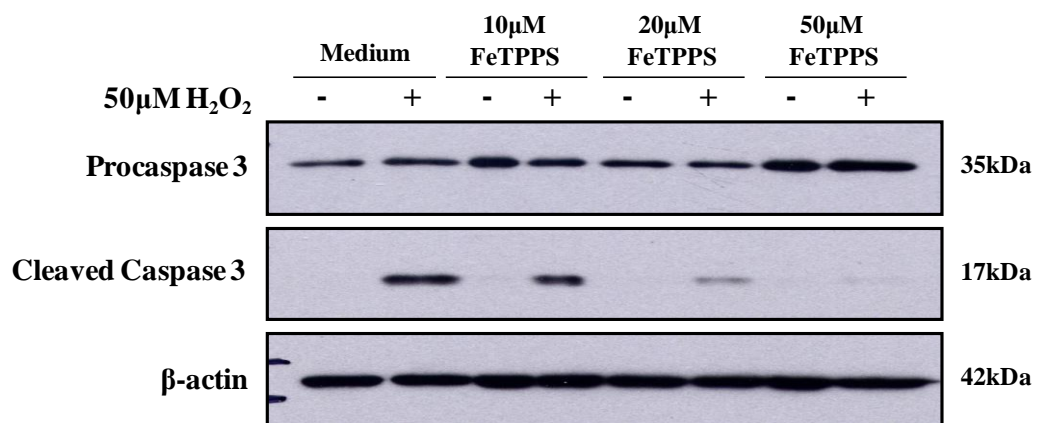
Figure 36. H_2O_2-mediated caspase 3 activation required ONOO⁻. L6 myoblasts were pre-treated with various doses of peroxynitrite decomposition catalyst, FeTPPS, before exposure to 50µM H_2O_2. At 24h post-H_2O_2 treatment, cells were harvested for (A) caspase 3 activity assay and (B) Western Blot analysis. The data are the mea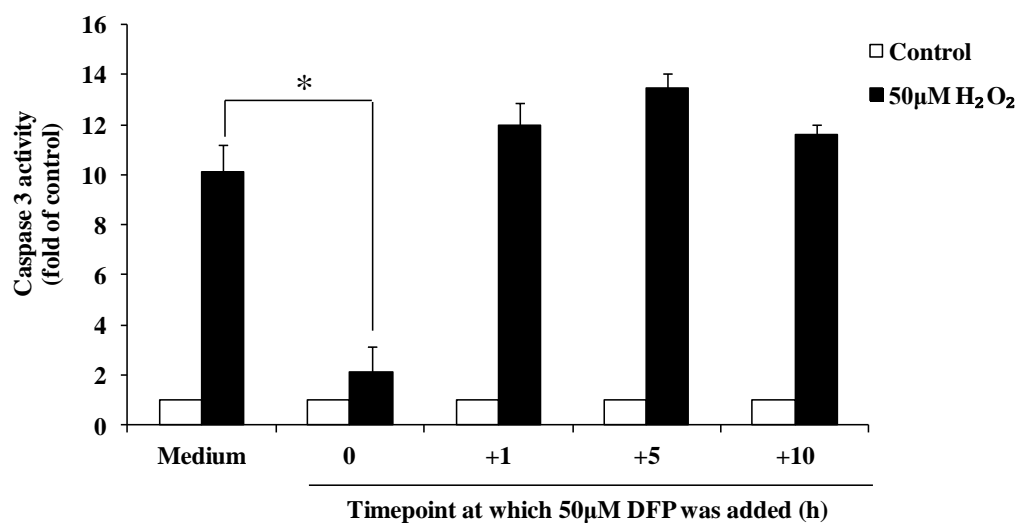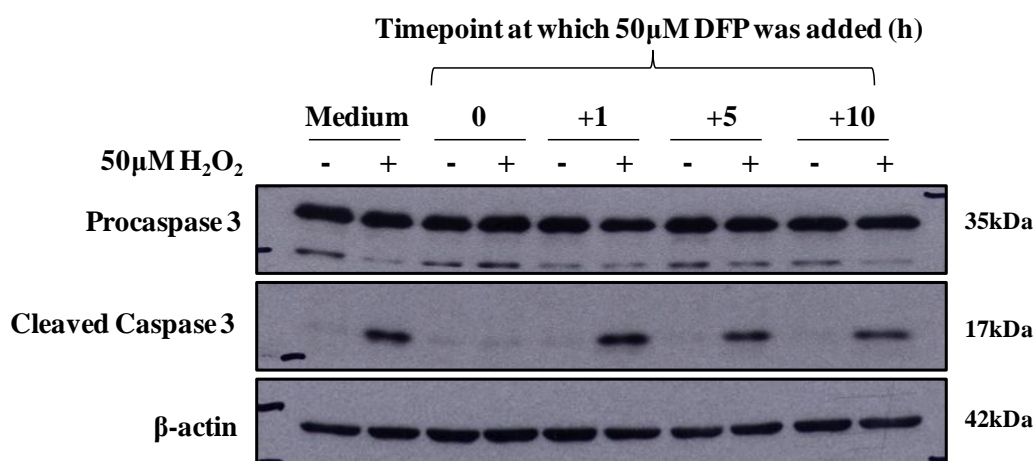ns of three independent experiments ± S.E.M., *P < 0.05. Western Blot shown is representative of two independent experiments.

A)
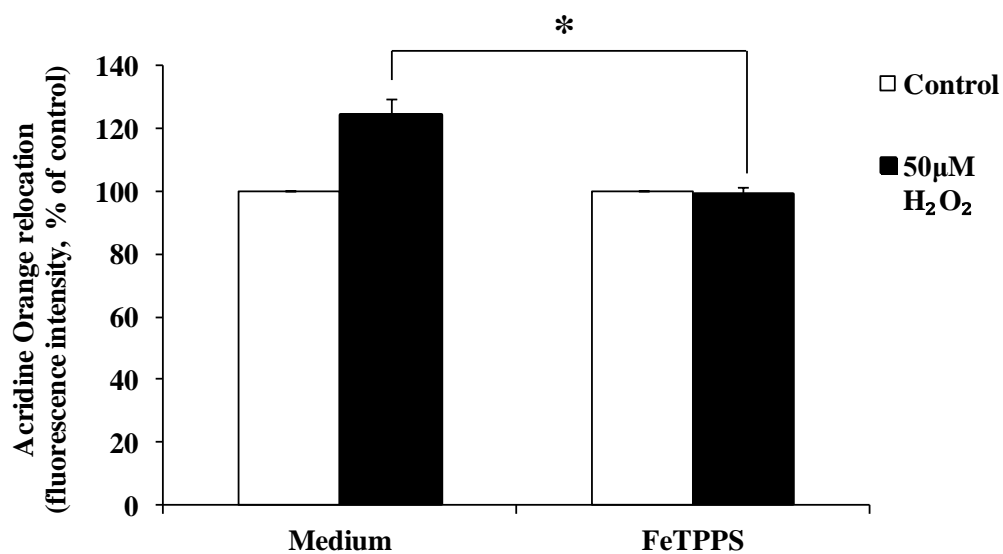
B)
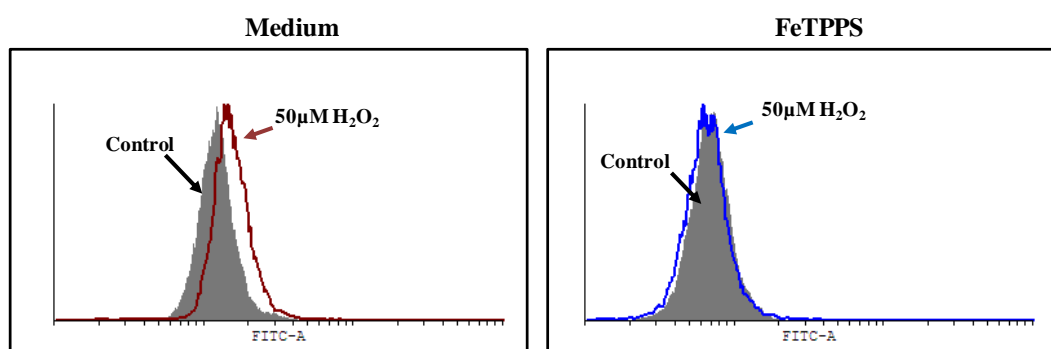
Figure 37. LMP was inhibited by ONOO⁻ chelation. Cells were exposed to 10μM Acridine Orange and 50μM FeTPPS for 30 min at 37°C, before cells were treated with 50μM H_2O_2 for 4 hours. Green cytosolic fluorescence of 10,000 cells per sample was determined by flow cytometry using the FITC-A channel. (A) The data are the means of three independent experiments ± S.E.M., *$P < 0.05$. (B) A representative flow cytometry histogram from three experiments is shown.

NO• chelation was achieved by cPTIO. At 100μM and 200μM, pre-treatment with cPTIO decreased caspase 3 activation by H_2O_2, but was not able to arrest it completely. At 200μM, cPTIO decreased H_2O_2-induced caspase 3 activity from 7 to 3 fold, a reduction close to 60% (Figure 38). We did not increase the dose of cPTIO over 200μM because a higher dose resulted in cell death (data not shown). cPTIO also did not inhibit LMP completely. Using 200μM cPTIO, a 60% reduction (from 118% to 108% over the control) of the fluorescence intensity was achieved (Figure 39).
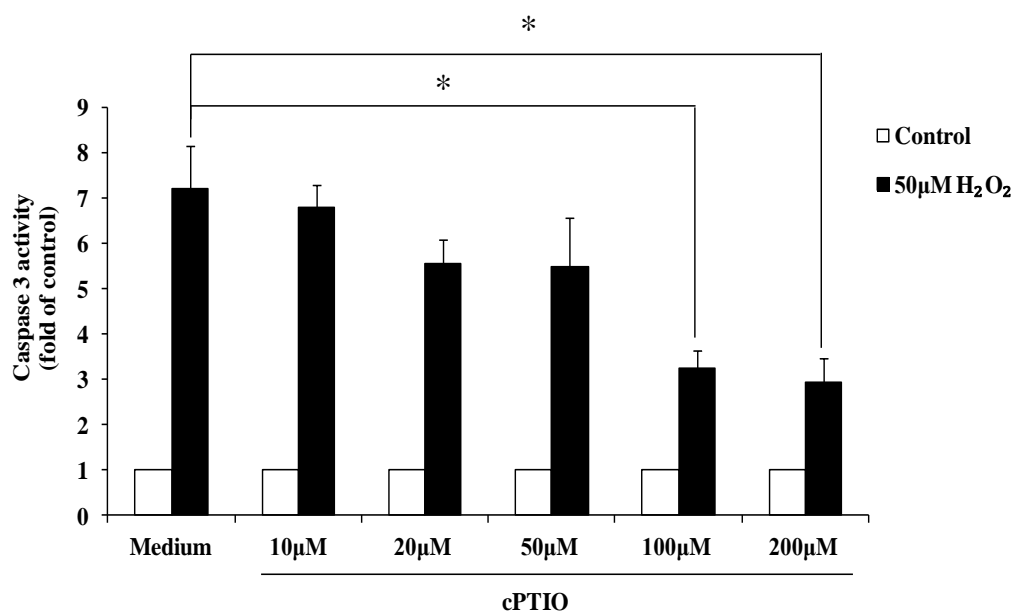
Figure 38. NO• chelation inhibited caspase 3 activation by H_2O_2 treatment. Cell were pre-treated with 10, 20, 50 100 or 200μM nitric oxide chelator, cPTIO, for 2h before exposure to 50μM H_2O_2. After 24h, cells were harvested for caspase 3 activity assay analysis. The data are the means of three independent experiments ± S.E.M., *$P < 0.05$.

A)
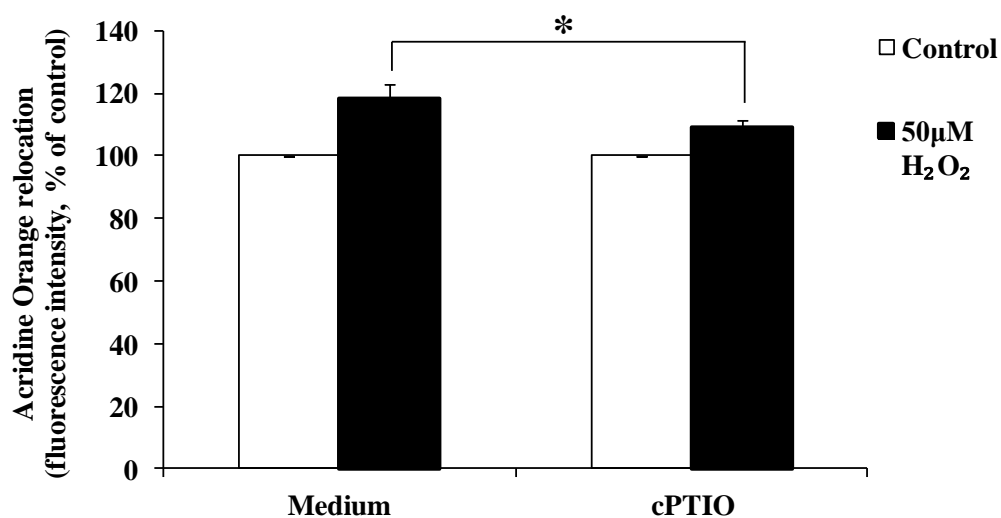
B)
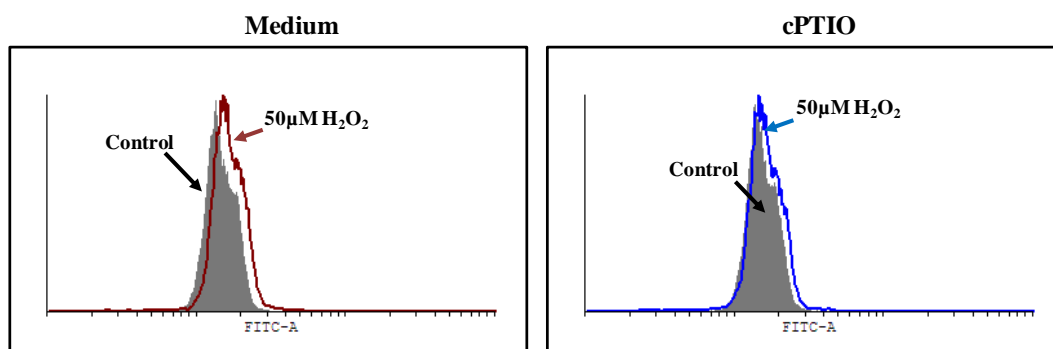
Figure 39. LMP was inhibited by NO• chelation. Cells were exposed to 10μM Acridine Orange and 200μM cPTIO for 30 min at 37°C, before cells were treated with 50μM H_2O_2 for 4h. Green cytosolic fluorescence of 10,000 cells per sample was determined by flow cytometry using the FITC-A channel. (A) The data are the means of three independent experiments ± S.E.M., $*P < 0.05$. (B) A representative flow cytometry histogram from three experiments is shown.

In summary, results in this section showed that caspase 3 activation by H_2O_2 was redox-regulated. Iron, peroxynitrite and nitric oxide were required for LMP and caspase 3 activation. While iron was only required in the first hour of reaction, constant presence of peroxynitrite was required for sustained caspase 3 activation. Figure 40 showed the summarized pathway of the redox-regulated caspase 3 activation by H_2O_2.
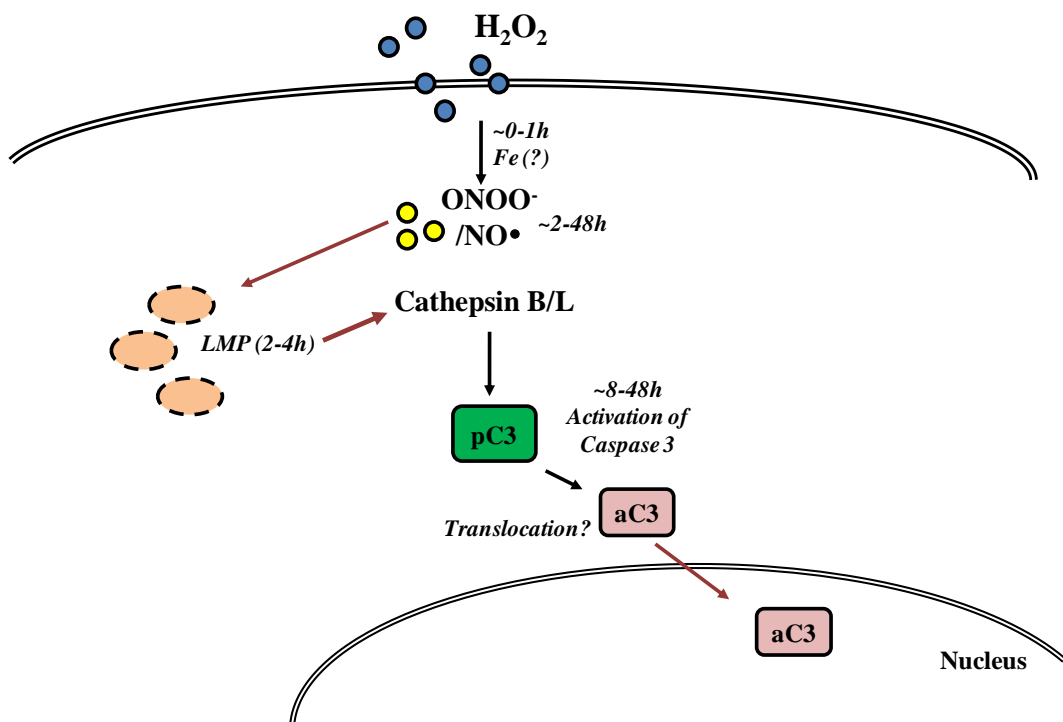
Figure 40. Iron, ONOO⁻, and NO• were upstream of LMP and caspase 3 activation. Upon H_2O_2 treatment, there was an increase in ROS/RNS level from 2-48h. Such increase in ROS/RNS level was postulated to be iron-dependent. Iron, ONOO⁻, and NO• were found to be inducing LMP leading to caspase 3 activation. (pC3: procaspase 3, aC3: activated caspase 3)

3.2.3 H$_2$O$_2$-induced caspase 3 activation is p53-dependent

As a key regulator of cell fate, p53 is the master gene that response to various stress signals including oxidative stress and DNA damage. As a tumour suppressor, p53 plays pivotal role in the cell protective mechanism to genome instability. For example, in case of DNA damage, the p53-mediated DNA damage responses pathway is activated. Such p53-meadiated response elicits diverse responses, ranging from cell growth arrest, cellular senescence and apoptosis.

On the other hand, ROS is known to be one of the major sources of DNA damage. ROS has the ability to modify cellular biomolecules, including DNA, leading to DNA damage and dysfunction. For example, DNA base damage is caused by the reaction of hydroxyl radicals with DNA bases through the mechanisms of addition and abstraction, which leads to the formation of various OH-adduct radical of bases[142]. Through the same mechanisms, hydroxyl radicals attack the DNA sugar and cause DNA sugar damage[142]. Similar to OH•, ONOO$^-$ is able to cause oxidative modification to DNA bases, particularly Guanine, and the sugar-phosphate backbone[143]. The effect of NO• on DNA damage is mostly mediated through its oxidation product with O$_2$, N$_2$O$_3$[143,144]. N$_2$O$_3$ cause DNA damage through nitrosation of amines on DNA bases, eventually leads to deamination of the bases. The change in structure caused by deamination converts the original base to a different molecule. The potential consequences of such change are base mutation or single strand breaks, depending on the modified nucleoside[143].

Nevertheless, the response of p53 to ROS is not limited to ROS-induced DNA damage, but depends on the level of oxidative stress instead. At low level of oxidative

stress, p53 plays an antioxidant role and promote cell survival[145]. At high level of oxidative stress, p53 plays a pro-oxidant role and promote cell death[145].

Based on these arguments, it is natural to assume that p53 is involved in our system. Firstly, H_2O_2 treatment resulted in DNA damage as evident by the phosphorylation of γ-H2AX and increased comet tail length in the comet assay (Appendix A). Secondly, H_2O_2 treatment resulted in cell growth arrest (Figure 2). Thirdly, H_2O_2 treatment induced a pro-oxidant state in cell with sustained production of ROS and nitric oxide (Figure 33 and 34). Hence, we explore the possibility of p53 is involved in the activation of caspase 3.

3.2.3A H_2O_2 treatment resulted in activation of p53

The two benchmarks of p53 activation is an increase in the protein level of p53, caused by the stabilization of the p53 protein[146], and phosphorylation of p53 at serine 15[147,148]. The phosphorylation site serine 15 was also reported to be phosphorylated during oxidative stress. For example, Chen et al. has shown that 100μM H_2O_2 leads to p53 phosphorylation on Ser-15 in an ATM kinase-dependent manner, resulting in p53 stabilization, transcription of p21Cip1/Waf1 (p21) and apoptosis[149].

To investigate the involvement of p53 in our system, we first looked at p53 protein expression after H_2O_2 treatment. Western Blot analysis showed that, upon H_2O_2 treatment, there was an increase in the expression level of total p53 protein as well as the phosphorylation level at serine 15 (Figure 41A). Densitometric analysis of five independent experiments revealed a decreasing pattern in p53 protein expression over time after the first hour (Figure 41B). At 1 hour post-H_2O_2 treatment, the increase in

p53 protein level was 1.4 fold of the control. There was a gradual decline in the protein level after 1 hour, and at 9h, p53 protein level was reduced to basal level.

Densitometric analysis of p53 phosphorylation level (as normalized to loading control β-actin) showed that phosphorylation at serine 15 was increased from 1h to 24h post-H_2O_2 treatment (Figure 41C). Maximum phosphorylation was observed at 1h and 3h, with an increase of approximately nine folds relative to the control. After the maximum phosphorylation at 3h, the phosphorylation level steadily decreased. At 48h, the phosphorylation level decreased to basal level. When we normalized the phosphorylation level to total p53 protein level, a peak of phosphorylation was observed at 3h (Figure 41D). This is due to higher p53 protein level at 1h as compared to 3h. When normalized to total p53 protein level, the increase in phosphorylation level was 5.2 fold and 9.2 fold at 1h and 3h respectively. After 3h, the phosphorylation level decreased steadily and reached the basal level at 48h.

A)

B)

C)

111
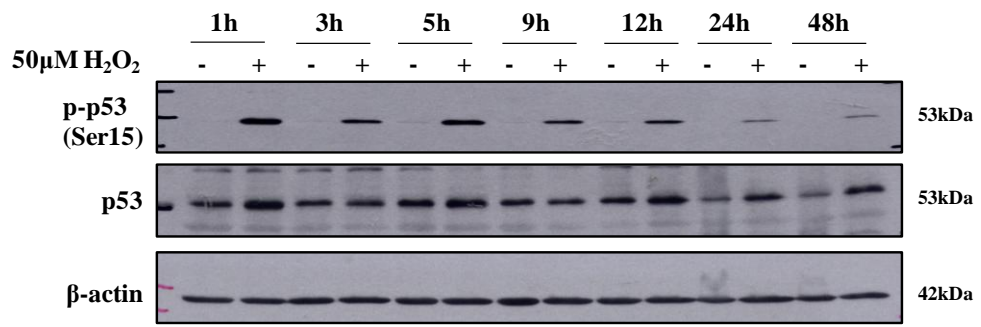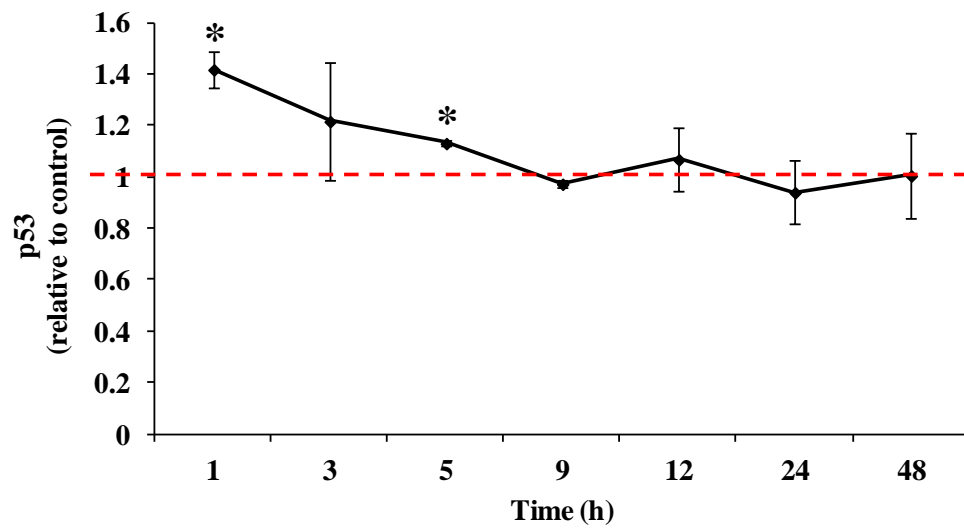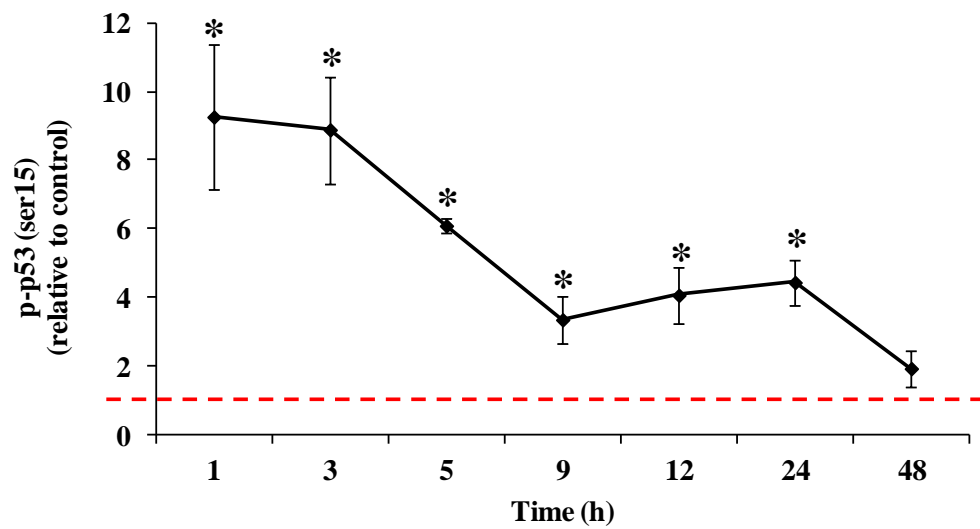
D)
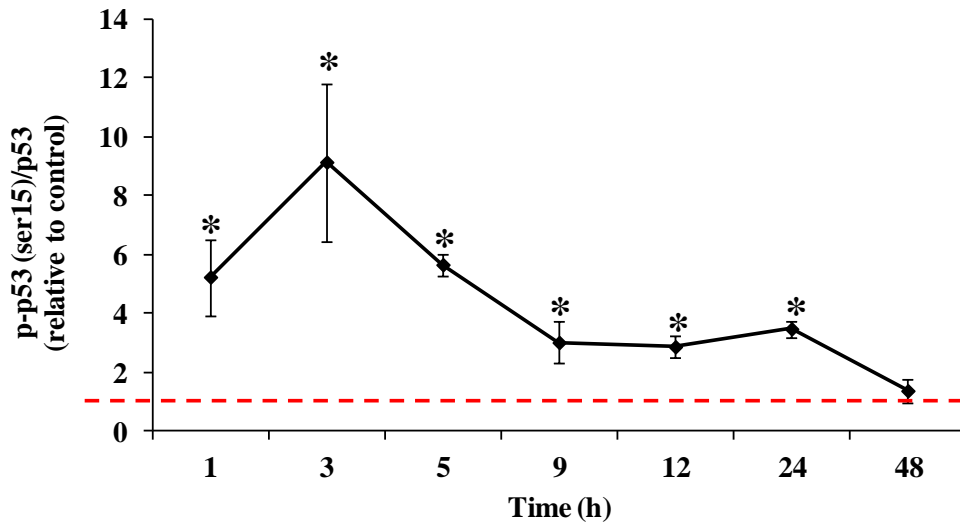
Figure 41. H₂O₂ treatment induced phosphorylation of p53 at ser15. (A) L6 myoblasts were treated with 50μM H_2O_2 for indicated time points and were harvested for Western Blot analysis of p53 protein level. Western Blot shown is representative of five independent experiments.

Densitometric analysis of (B) total p53 protein expression, normalized to loading control β-actin, (C) p53 phosphorylation level on ser15, normalized to loading control β-actin, (D) p53 phosphorylation level on ser15, normalized to the densitometric value of total p53 protein expression as calculated in (B). The change in total p53 protein expression and phosphorylation level was shown as a fold difference relative to control cells at respective time points. The data are the means of five independent experiments ± S.E.M., $*P < 0.05$.
.

3.2.3B Inhibition of p53 decreased H_2O_2-induced caspase 3 activation

Having shown that p53 was activated upon H_2O_2 treatment, we then examined the effect of such activation on caspase 3 activation. p53 was silenced by specific siRNA before cells were treated with 50μM H_2O_2. At 24h post-H_2O_2 treatment, cells were harvested for caspase 3 activity assay and Western Blot analysis. It was found that silencing of p53 resulted in decrease in caspase 3 activity (Figure 42A) and caspase 3 cleavage (Figure 42B). However caspase 3 activity was not completely inhibited by p53 silencing. In case of p53 knock down, the activity of caspase 3 decreased from 4.3 fold to 2.7 fold, a decrease of less than 50% (Figure 42A). It is also noted that silencing of p53 alone resulted in caspase 3 cleavage, although the reason and possible outcome of this caspase 3 activation is yet to be investigated (Figure 42B). Such caspase 3 activation effected by p53 knock down did not affect cell morphology and cell density. Instead, the decrease in cell density by H_2O_2 treatment was reverted by knock-down of p53 (Figure 42C). The results support that p53 was responsible for H_2O_2-induced cell growth arrest. Nevertheless, analysis by the densitometry of the Western Blot of p21, the reported downstream gene in of p53 in p53-mediated cell cycle arrest pathway, showed no increase in protein expression over time (Figure 43). This further supported our earlier deduction that decreased proliferation of H_2O_2-treated cells was not due to cell cycle arrest. Finally, silencing of p53 prevented LMP event at 4h post-H_2O_2 treatment (Figure 44). However, the inhibition of LMP by p53 knock down was also incomplete.

113

A)

B)

C)

	Control	50μM H$_2$O$_2$
siCo		
sip53		
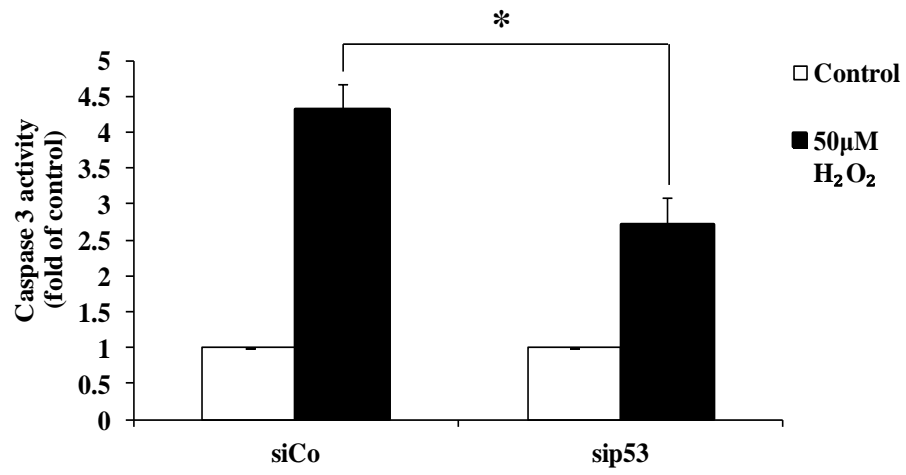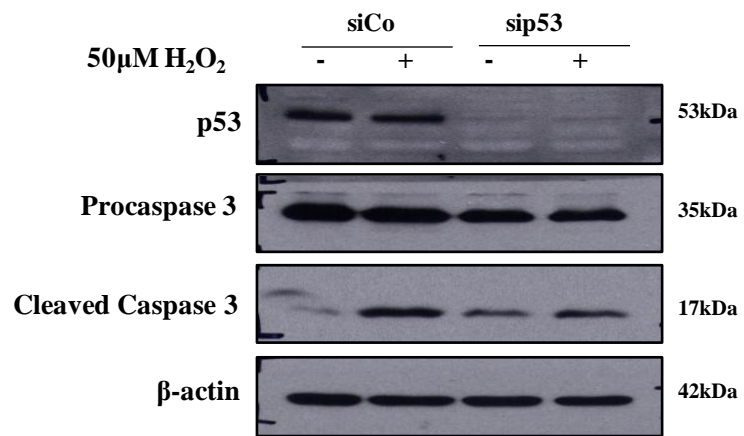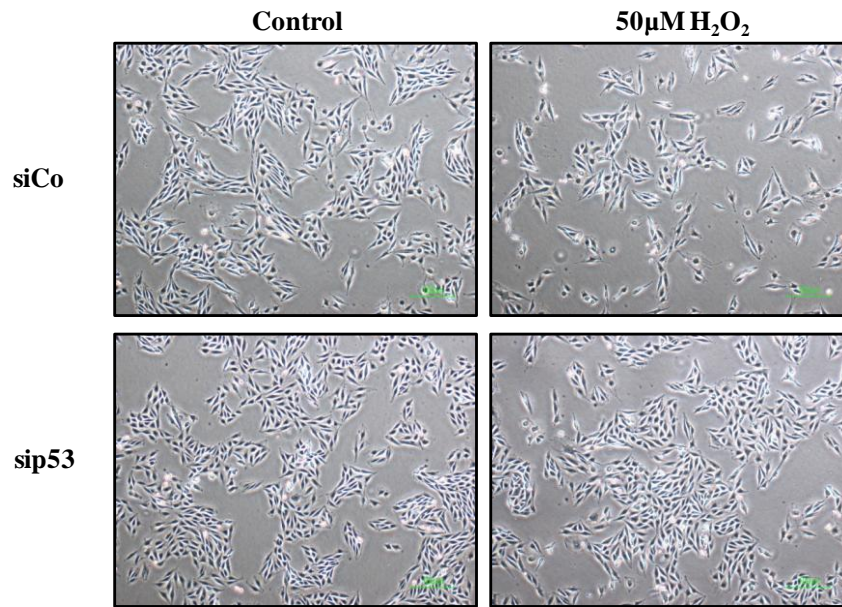
Figure 42. Knock-down of p53 decreased caspase 3 activation by H$_2$O$_2$ treatment. L6 myoblasts were transiently transfected with siRNA specific to p53 (sip53) or negative control siRNA (siCo) for 24 hours before exposure to 50μM H$_2$O$_2$. After 24 hours, cells were harvested for (A) caspase 3 activity assay and (B) Western Blot analysis. The data are the means of three independent experiments ± S.E.M., *P < 0.05. Western blot is representative of three independent experiments.
(C) Cell morphology was observed under a phase contrast microscope. Pictures shown are representative of three independent experiments.

A)
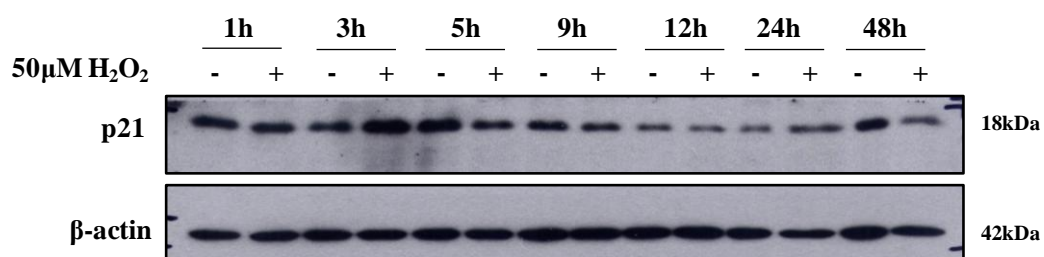
B)
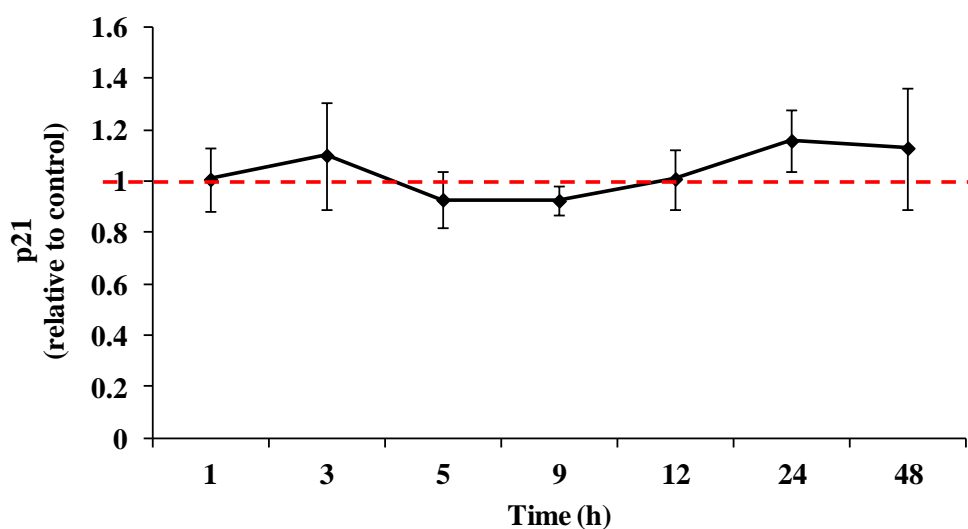
Figure 43. p21 expression upon H₂O₂ treatment. (A) L6 myoblasts were treated with 50μM H₂O₂ for indicated time points and were harvested for Western Blot analysis of p21 protein level. Western Blot shown is representative of five independent experiments.

(B) Densitometric analysis of p21 expression, normalized to loading control β-actin. The change in p21 protein expression was shown as a fold difference relative to control cells at respective time points. The data are the means of five independent experiments ± S.E.M.

A)
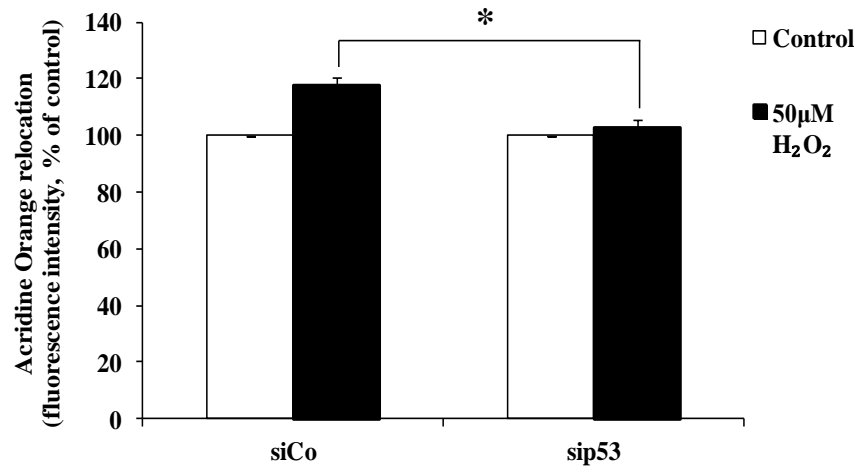
B)
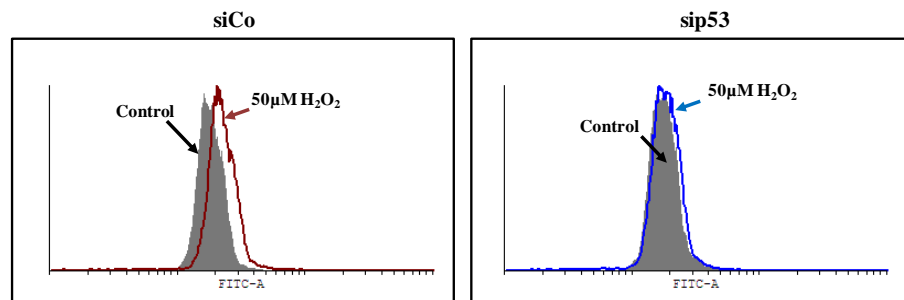
C)
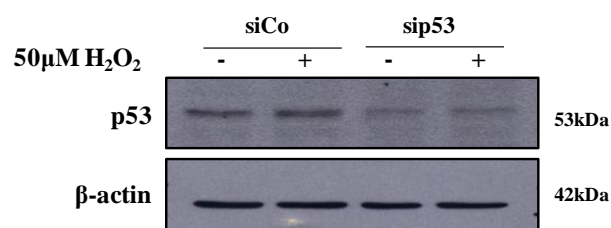
Figure 44. LMP was inhibited by p53 knock-down. Cells were transiently transfected with siRNA specific to p53 (sip53) or negative control siRNA (siCo). At 24h post-transfection, Cells were exposed to 10μM Acridine Orange for 30 min at 37°C, before cells were treated with 50μM H_2O_2 for 4h. Green cytosolic fluorescence of 10,000 cells per sample was determined by flow cytometry using the FITC-A channel. (A) The data are the means of three independent experiments ± S.E.M., *$P <$ 0.05. (B) A representative flow cytometry histogram from three experiments is shown. (C) Western Blot indicating knock-down efficiency of p53 is representative of three independent experiments.

We next assessed the cellular localization of phosphorylated- and total p53 (Figure 45). In L6 myoblasts, p53 protein was detected in the nucleus and cytoplasm, with the protein found primarily in the nucleus (Figure 45). Although not detected in the previous Western Blot, but when under a higher exposure and with higher amount of protein loaded, it was found that nuclear p53 was phosphorylated at serine 15 at normal untreated condition. Upon H_2O_2 treatment, the phosphorylation further increased for both nuclear and cytoplasmic pool of p53. The amount of phosphorylated p53 was higher in the nuclear fraction than the cytosolic fraction (Figure 45)
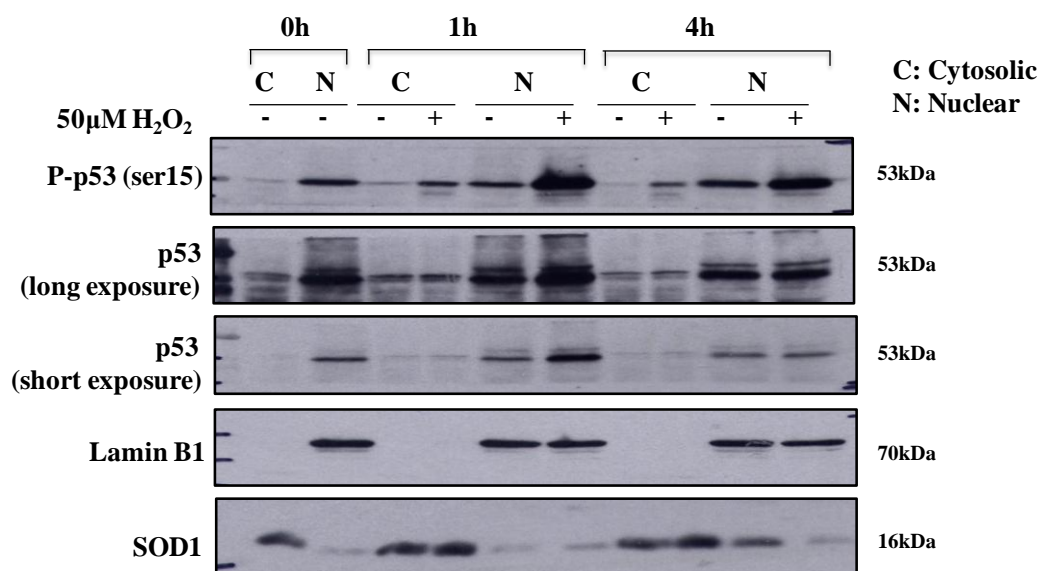
Figure 45. H_2O_2 treatment resulted in increase in phosphorylation of both the cytosolic and the nuclear p53. Cells were exposed to 50μM H_2O_2 for 1h or 4h, and were subjected to cytoplasmic-nuclear fractionation and subsequently Western Blot analysis. Lamin B1 is the marker for nuclear fraction and Superoxide Dismutase 1 (SOD1) is the marker for cytoplasmic fraction. Western Blot shown is representative of two independent experiments. (C: Cytosolic, N: Nuclear).

3.2.3C p53 mediated caspase 3 activation via its non transcriptional pathway

As a transcription factor, p53 can promote apoptosis by transcriptional activation of the pro-apoptotic genes of the Bcl-2 family[150], or by transcriptional repression of anti-apoptotic genes, such as *survivin*[151]. Although controversial, the transcriptional-independent role of p53 in apoptosis has also been proposed. The mechanism of p53 non-transcriptional role in apoptosis mainly involves the intrinsic pathway. It has been reported that a cytoplasmic localized p53 could directly activate Bax, leading to its translocation into the mitochondria[152]. A mitochondrial localized p53 could physically interact with Bcl-XL and Bcl-2, thereby suppressing their anti-apoptotic properties[153]. Eventually, the p53 non-transcriptional apoptosis mechanism initiates MOMP and subsequently activates the caspase cascade. Figure 46A showed a simple illustration of the proposed models of p53-mediated apoptosis, via the transcriptional or non-transcriptional mechanisms.

When cells were treated with $50 \mu M$ H_2O_2, p53 was activated. This activation of p53 was responsible for inducing LMP and subsequently leading to caspase 3 activation. We hypothesized that caspase 3 activation induced by p53 could be dependent or independent of its transcriptional activity (Figure 46B).

A)

Cyotoxic Drug → p53 → *Transcriptional activation* → NOXA/ PUMA → MOMP → APOSTOSIS

Non-Transcriptional Mechanism

B)

H_2O_2 → p53 → *Transcriptional activation* → ? → LMP → CASPASE 3 ACTIVATION

Pifithrin-α

Non-Transcriptional Mechanism
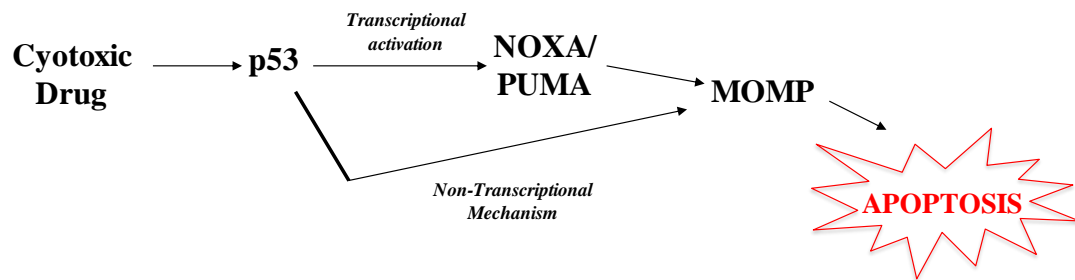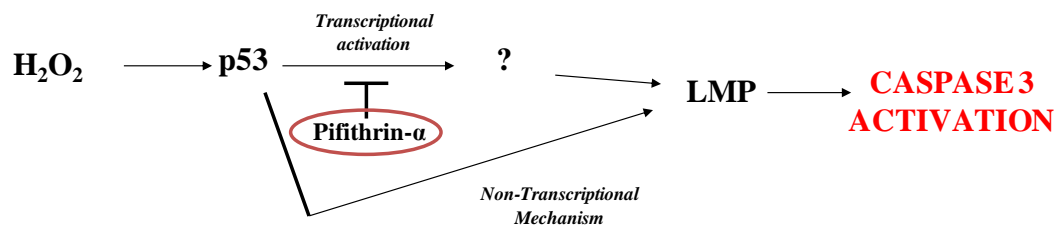
Figure 46. p53 pathway in H_2O_2-induced caspase 3 activation could be transcriptional-dependent or –independent. (A) The established p53-dependent pathway in apoptosis. p53 could have a transcriptional-dependent role in apoptosis, by up-regulating pro-apoptotic genes that facilitate the event of MOMP and caspase cascade activation. The transcriptional-independent role of p53 in apoptosis lies in its ability to directly induce MOMP, leading to caspase cascade activation and apoptosis. (B) Hypothesized pathways of p53-dependent caspase 3 activation upon 50μM H_2O_2 treatment. Pifithrin-α was used to determine if p53 could activate caspase 3 through a transcriptional-dependent or –independent mechanism.

To test the non-transcriptional activity of p53 in our system, we pre-incubated the cells with Pifithrin-α (PFT), a small molecule inhibitor of p53 transcriptional activity[154], and examined caspase 3 cleavage and activity upon H_2O_2 treatment. p21 expression was greatly reduced in cells treated with PFT (Figure 47B), this is similar to the effect on p21 expression with p53 silencing (Figure 47A). This proves that p53 transcriptional activity was inhibited by PFT. However, in the same Western Blot, caspase 3 cleavage was not prevented by pre-treatment with PFT (Figure 47B). Moreover, caspase 3 activity assay confirmed that H_2O_2-induced caspase 3 activation was unaffected by PFT (Figure 47C).

These results were in contrast with our earlier findings in that silencing of p53 could inhibit both caspase 3 cleavage and activity (Figure 42). In view of the results, we proposed that p53-mediated caspase 3 activation in our system was transcriptional-independent.

A)
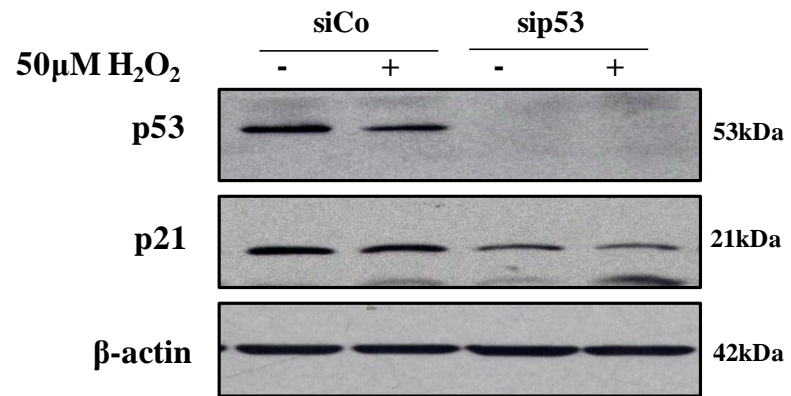
B)
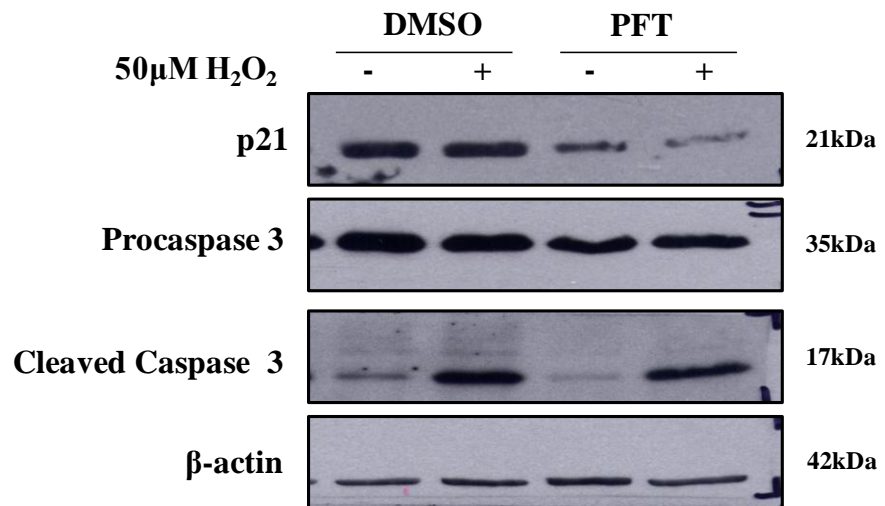
C)
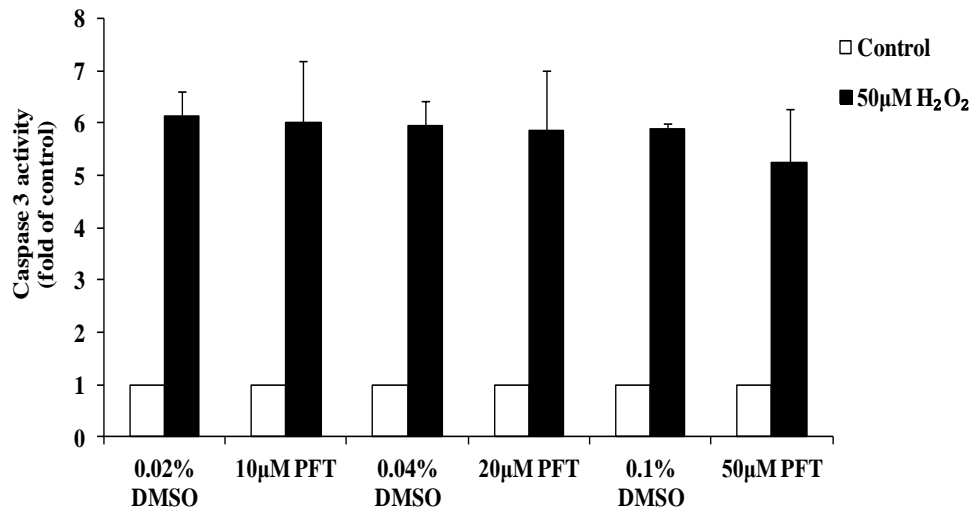
Figure 47. Inhibiting transcriptional activity of p53 by Pifithrin-α (PFT) did not prevent caspase 3 activation. (A) L6 myoblasts were transiently transfected with siRNA specific to p53 (sip53) or negative control siRNA (siCo) for 24h before exposure to 50μM H_2O_2. After 24h, cells were harvested for Western Blot analysis of p21 expression. (B) Cells were pre-treated with 50μM PFT before exposure to 50μM H_2O_2. 24 hours post-H_2O_2 treatment, cells were harvested for Western Blot analysis of caspase 3 cleavage and p21 expression. Western Blots shown are representative of two independent experiments. (C) Cells were pre-treated with increasing dose of PFT before exposure to 50μM H_2O_2. At 24h post-H_2O_2 treatment, cells were harvested for caspase 3 activity assay analysis. The data are the means of three independent experiments ± S.E.M.

3.2.3D p53 activation upon H_2O_2 treatment was ROS/RNS dependent

As shown in Figure 48, LMP-caspase 3 activation and H_2O_2 was connected by a p53- and ROS/RNS-mediated pathway. Both p53 and ROS/RNS were upstream of the LMP-caspase 3 activation. The activation of p53 and production of ROS/RNS could be detected as early as 1-2 h. The relation between p53 and ROS is an interdependent one. While ROS can be the upstream signal that triggers p53 activation, it is also generated as part of the p53 downstream signalling pathway[145]. To understand the relation between p53 and ROS/RNS in our system, we inhibit p53 to examine its effect on the ROS/RNS and vice versa.
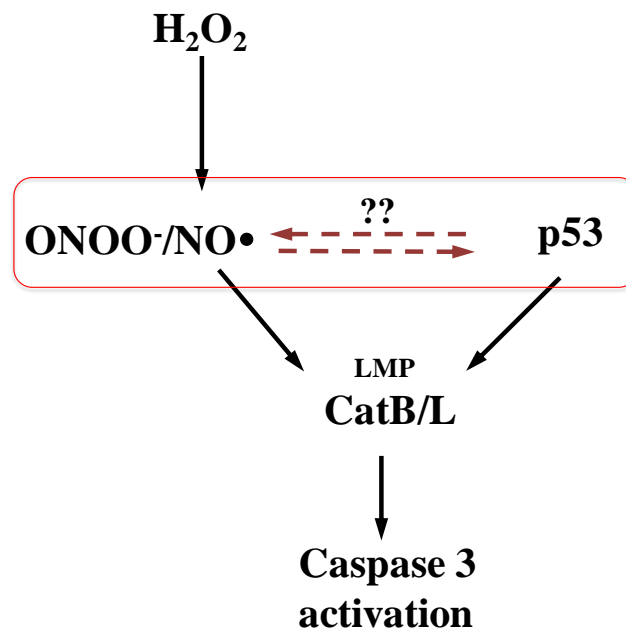
Figure 48. The relation between p53 and ROS/RNS as upstream activators of H_2O_2-induced caspase 3 activation. As upstream activators of LMP and caspase 3, the position of p53 and ROS/RNS in the pathway is not yet determined. Activation of p53 could be ROS/RNS dependent, or vice versa.

Cells were pre-treated with 20µM iron chelator, DFP and were harvested for Western Blot analysis of p53 expression at 1h, 5h and 12h post-H_2O_2 treatment. Pre-incubation with DFP decreased p53 phosphorylation significantly at the three time points measured (Figure 49). The same was observed for cells pre-treated with the peroxynitrite decomposition catalyst, FeTPPS. There was a decreased in phosphorylation of p53 at 1h, 5h, and 12h post-H_2O_2 treatment (Figure 50). In comparison, p53 phosphorylation was relatively unaffected by cPTIO (Figure 51). The inhibitory effect of FeTPPS on p53 phosphorylation at 1h was rather surprising. Indeed, as previously shown in Figure 33A, although there was an increase in DCF fluorescence at 1h, such increase was statistically insignificant due to variation between independent experiments. This suggests that minute amount of peroxynitrite might be sufficient to influence p53 phosphorylation status.
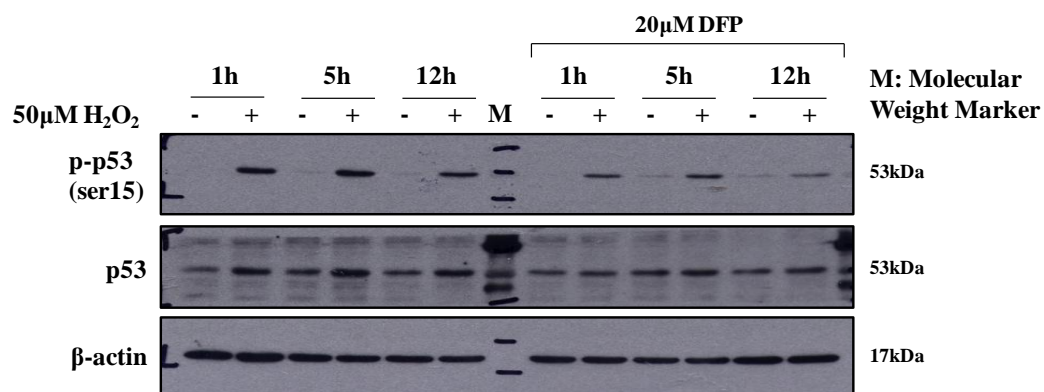
Figure 49. Iron chelation decreased p53 phosphorylation. Cells were pre-treated with 20µM iron chelator DFP for 2h before exposure to 50µM H_2O_2. Cells were harvested at indicated time points for Western Blot analysis. Western Blot shown is representative of three independent experiments.
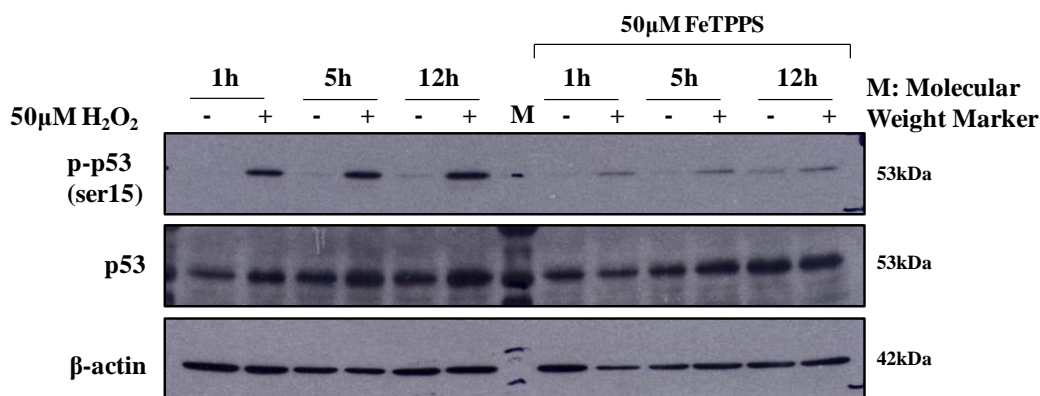
Figure 50. Peroxynitrite chelation decreased p53 phosphorylation. Cells were pre-treated with 50μM FeTPPS for 2h before exposure to 50μM H_2O_2. Cells were harvested at indicated time points for Western Blot analysis. Western Blot shown is representative of two independent experiments.
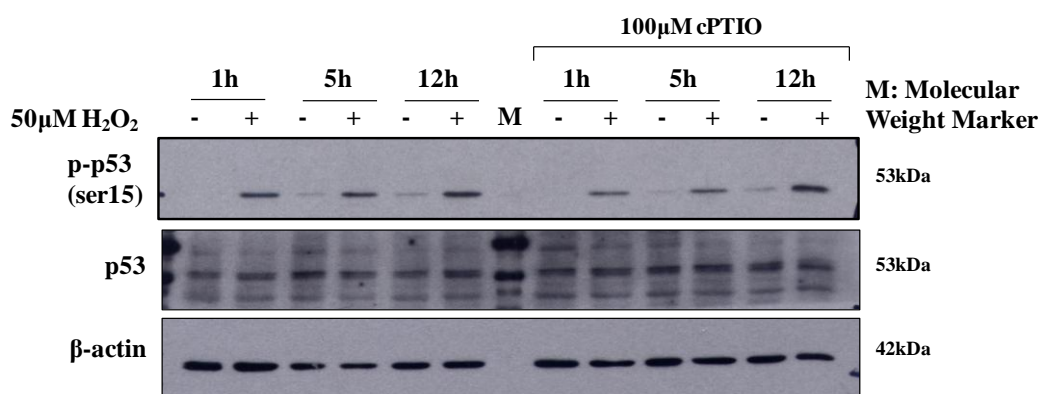
Figure 51. Nitric Oxide chelation had minimal effect on p53 phosphorylation. Cells were pre-treated with 100μM nitric oxide chelator, cPTIO for 2h before exposure to 50μM H_2O_2. Cells were harvested at indicated time points for Western Blot analysis. Western Blot shown is representative of two independent experiments.

Next, we silenced p53 and harvested the cells for DCF and DAF staining analysis. Figure 52 showed the ROS and RNS production in cells transfected with sip53 or negative control siRNA after H_2O_2 treatment. The percentage of DCF and DAF fluorescence was normalized to their respective control (i.e. to cells transfected with sip53 or negative control siRNA, without H_2O_2 treatment). Results showed that at 2h and 4h, both ROS and nitric oxide production upon H_2O_2 treatment was unaffected by p53 silencing (Figure 52). At 12h post-H_2O_2 treatment, it was observed that p53 knock-down cells had higher ROS production compared to negative control siRNA-transfected cells (Figure 52A). On the other hand, nitric oxide production at 12h was unaffected by p53 knock-down (Figure 52B).

A)
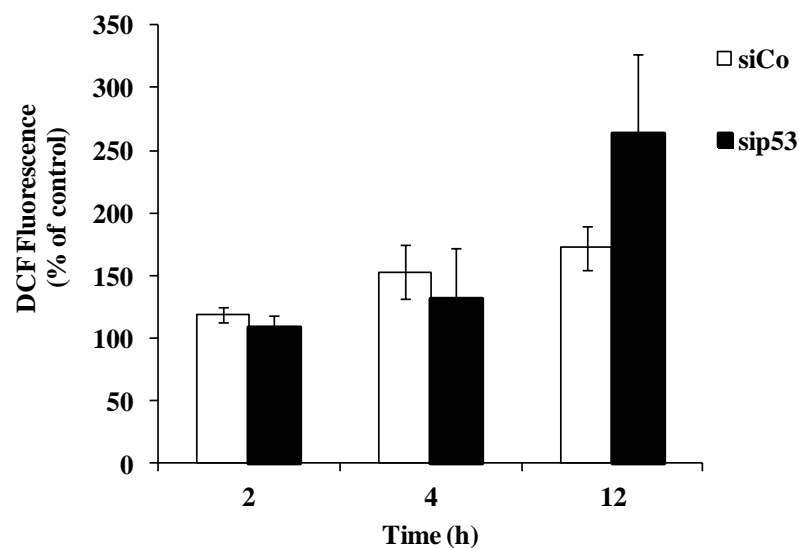
B)
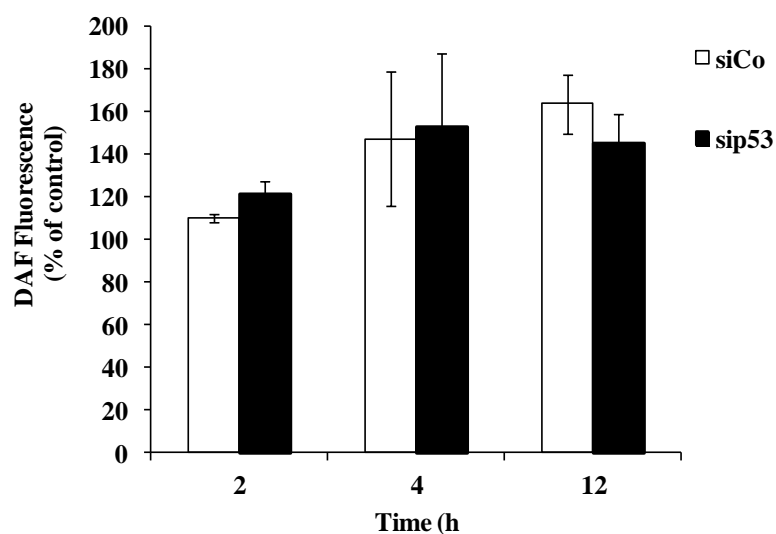
C)
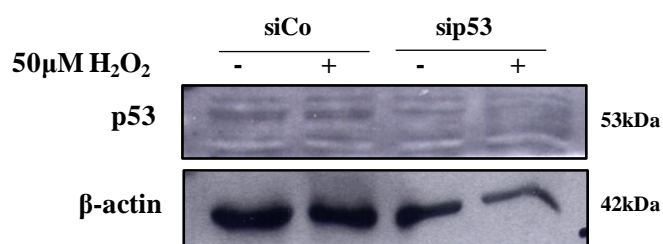
Figure 52. H₂O₂-induced ROS/RNS production was unimpeded by p53 knock-down. L6 myoblasts were transiently transfected with siRNA specific to p53 (sip53) or negative control siRNA (siCo) for 24h before exposure to 50μM H_2O_2. At 2h, 4h, and 12h post H_2O_2 treatment, cells were harvested for (A) CM-H₂DCFDA and (B) DAF-FM staining. Green cytosolic fluorescence of 10,000 cells per sample was determined by flow cytometry using the FITC-A channel. The data are the means of two independent experiments ± Sd, normalized to control (sip53 or siCo, without H_2O_2 treatment) at respective time points. (C) Western Blot indicating knock-down efficiency of p53 is representative of two independent experiments.

3.3 An alternative function of caspase 3 activation in absence of cell death

We have demonstrated an alternative pathway of caspase 3 activation during oxidative stress by H_2O_2. H_2O_2- and STS-induced caspase 3 activations differed in terms of time of activation, magnitude of activation and also their dependency on the upstream initiator caspases for activation. The different upstream pathways leading to caspase 3 activation in H_2O_2 and STS treatment is presented in Figure 53. While it is highly likely that STS induced caspase 3 activation is via the classical extrinsic pathway, H_2O_2-induced caspase 3 activation was shown to be ROS and p53 dependent. Also, such activation requires LMP and the release of cathepsin B and L. More importantly, not only was caspase 3 activated via a non-classical pathway, H_2O_2 treatment did not result in apoptosis.

We need to ask if this alternative activation pathway is simply a redundant pathway for caspase 3 activation or does caspase 3 have a different function when activated via this pathway; especially since its has been shown in our study that cell death does not occur with caspase 3 activation.

1µM STS → MOMP → Caspase 9 → Caspase 3 → APOPTOSIS

Nuclear + cytoplasmic localization

⇩ *cleaves*

PARP
Lamin A/C
Gelsolin

- -

50µM H$_2$O$_2$ —$\overset{p53}{\underset{ROS/RNS}{\longrightarrow}}$ LMP → Cathepsin B/L → Caspase 3 → **??**

Nuclear localization

✗ *cleaves*

PARP
Lamin A/C
Gelsolin
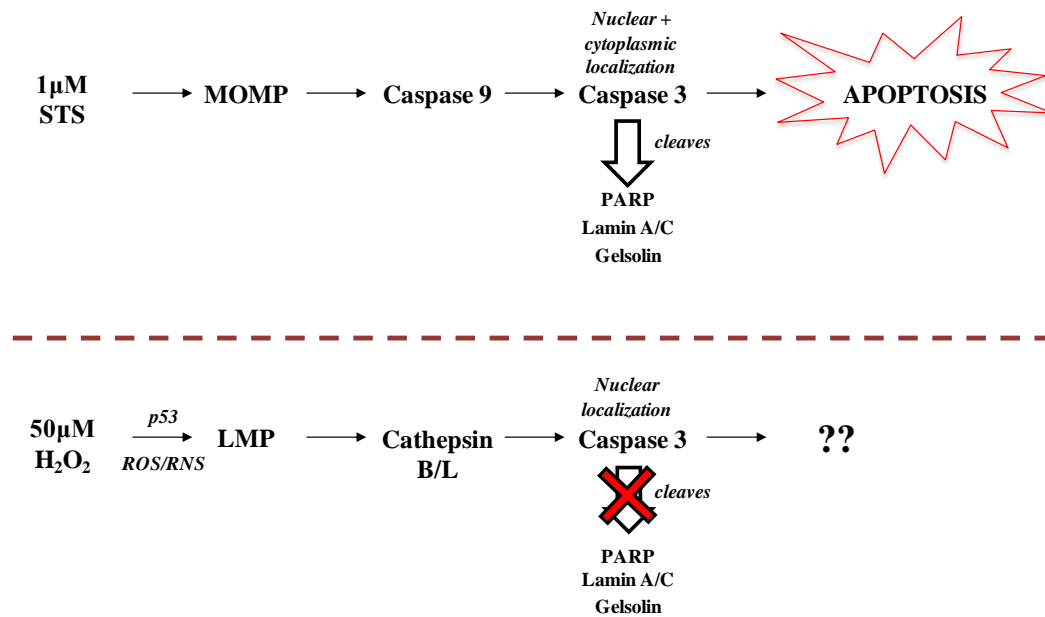
Figure 53. Alternative function of activated caspase 3 in non-apoptotic condition. While STS treatment resulted in caspase 3 activation and apoptosis, H$_2$O$_2$ treatment resulted in caspase 3 activation without inducing cell death. While activated caspase 3 in STS treatment cleaved the classical apoptotic substrates such as PARP, Lamin A/C and Gelsolin; activated caspase 3 in H$_2$O$_2$ treatment did not result in such cleavage (Appendix B). With the distinct difference with STS-activated caspase 3 in terms of upstream pathway, cleavage of substrates as well as localization of the activated enzyme, caspase 3 activated by H$_2$O$_2$ may have an alternative function in cells.

3.3.1   H₂O₂-induced caspase 3 activation was involved in lysosomal biogenesis

3.3.1A H₂O₂ treatment resulted in an increase in lysosome biogenesis

When we incubated the cells with LysoTracker® Red DND-99, under the confocal microscope, we observed a significant increase in the lysotracker staining over time in cells treated with H_2O_2, especially at 12h, 24h and 48h post-treatment (Figure 54A). The increase in lysotracker staining indicates increase in lysosome numbers which also suggesting an increase in lysosome biogenesis. A quantitative measurement of such lysosomes increase was obtained when cells were stained with LysoTracker® Red DND-99 and the red lysosomal fluorescence was assessed by FACS analysis (Figure 54B). Result shows that there was a gradual increase in relative fold of lysotracker fluorescence intensity of H_2O_2-treated cells as compared to the control cells at 8–48h (Figure 54B). The same trend of fluorescence increment was observed when cells were stained with Acridine Orange, a metachromatic dye that exhibit a red fluorescence when accumulates in lysosomes. When measured by FACS analysis, it was shown that the Acridine Orange-induced red lysosomal fluorescence steadily increased from 8-48h (Figure 54C).   Together, the results confirmed that H_2O_2 treatment led to a lysosome biogenesis in cells.

A)
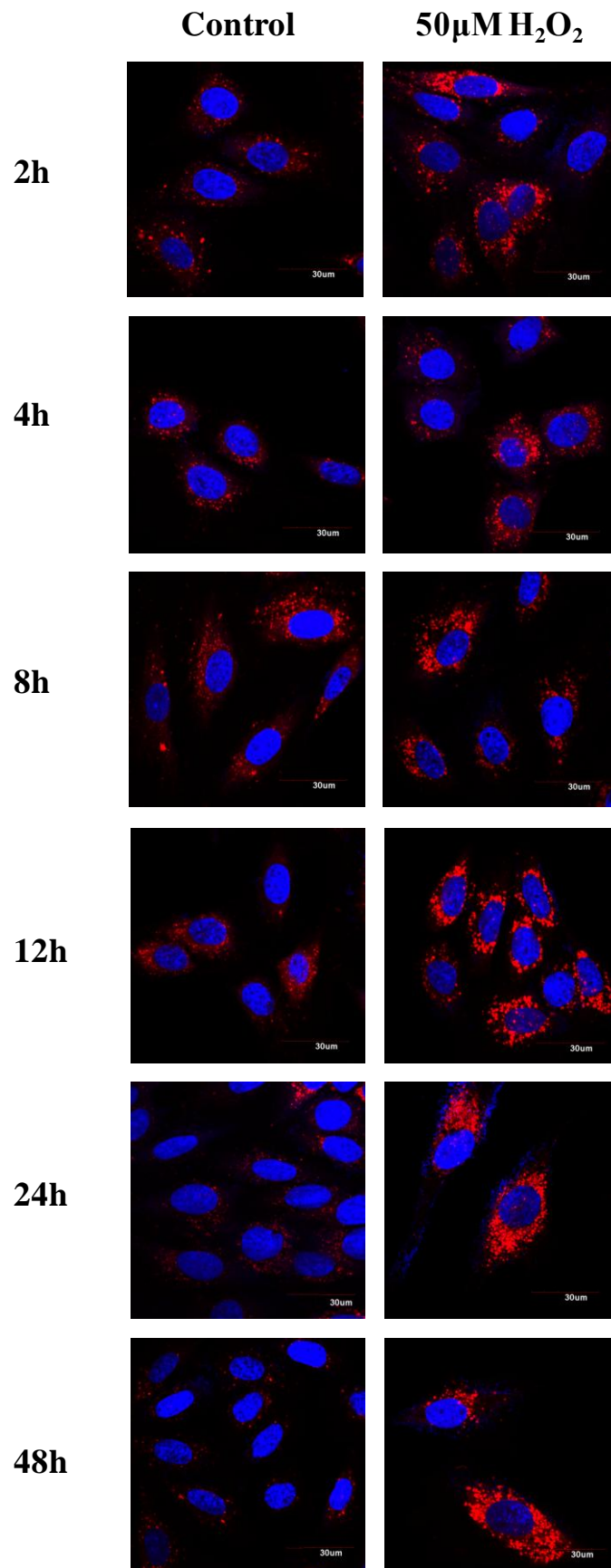
B)
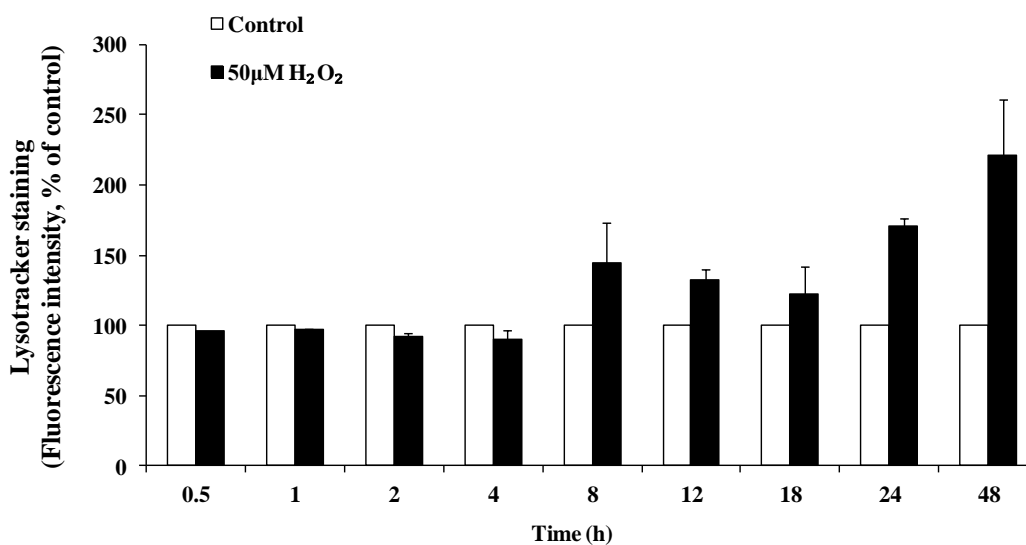
C)
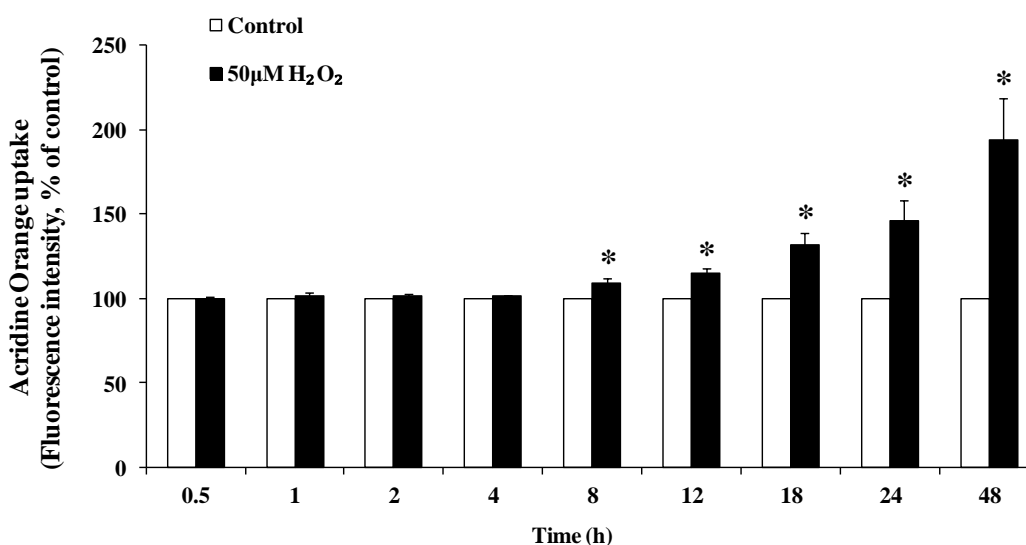
Figure 54. H₂O₂ treatment resulted in time-dependent increase in lysosome biogenesis. Cells were treated with 50μM H₂O₂ for indicated time points and were incubated with a diluted LysoTracker® Red DND-99 solution (75nM) for 45min, 37°C. (A) After fixation, red lysosomal fluorescence was analyzed under the confocal microscope. (B) Red lysosomal fluorescence of 10,000 cells per sample was determined by flow cytometry using the PerCP-A channel. The data are the means of two independent experiments with duplicates ± SD.

(C) Cells were treated with 50μM H₂O₂ for indicated time points and were exposed to an Acridine Orange solution (10μM) for 30min, 37°C at 24h post-H₂O₂ treatment. Red lysosomal fluorescence of 10,000 cells per sample was determined by flow cytometry using the PerCP-A channel. The data are the means of four independent experiments ± S.E.M., *$P < 0.05$.

3.3.1B Inhibition of caspase 3 decreased H$_2$O$_2$-induced lysosome biogenesis

When cells were pre-incubated with QVD-OPH, a broad spectrum caspase inhibitor prior to H$_2$O$_2$ treatment and LysoTracker® Red DND-99 staining, it was found that this pre-incubation with QVD-OPH could greatly reduce the increase in lysotracker staining due to H$_2$O$_2$ (Figure 55A). Such decrease in lysotracker staining was also achieved by pre-treatment of cells with the caspase 3-specific inhibitor, zDEVD-FMK (Figure 55B). Finally, we silenced caspase 3 and measured the Acridine Orange staining by flow cytometry 24 hours after H$_2$O$_2$ treatment (Figure 55C). Upon caspase 3 knock-down, H$_2$O$_2$-induced increase in Acridine Orange red fluorescence was decreased from 148% to 124%. In conclusion, we deduced that increase in lysosome biogenesis was a consequence of caspase 3 activation.

A)

Control | 50μM H₂O₂

DMSO

QVD-OPH

B)

Control | 50μM H₂O₂

DMSO
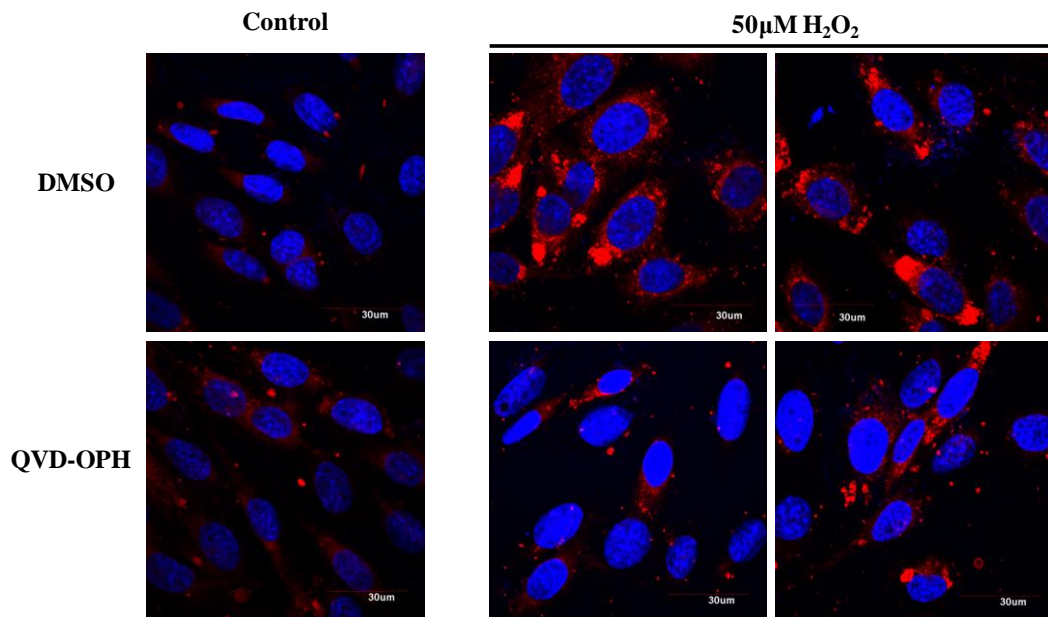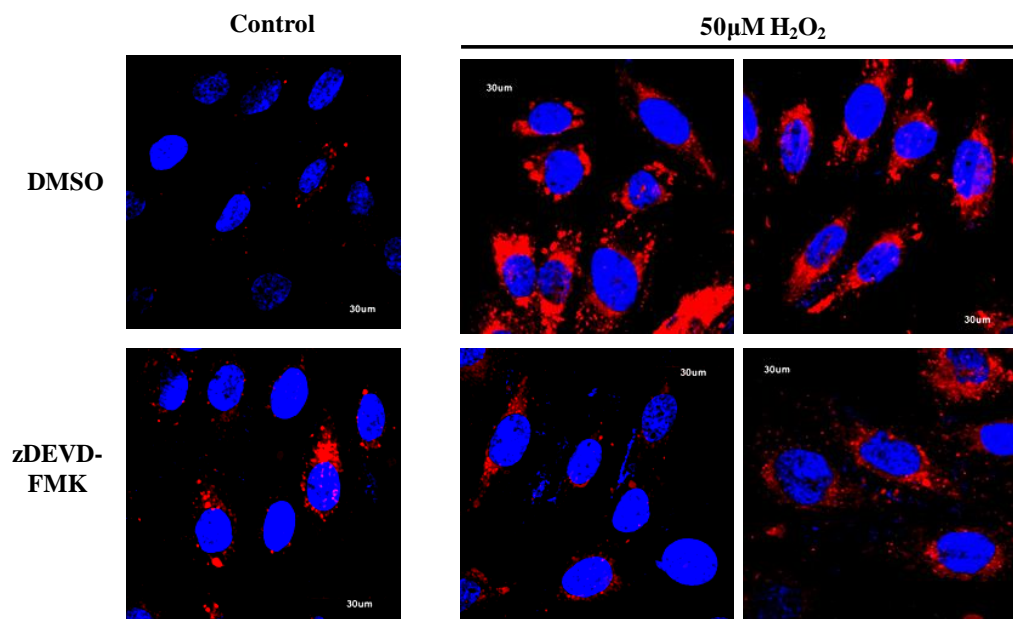
zDEVD-FMK

C)
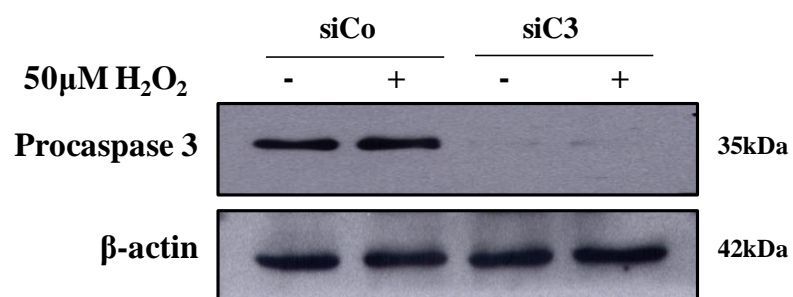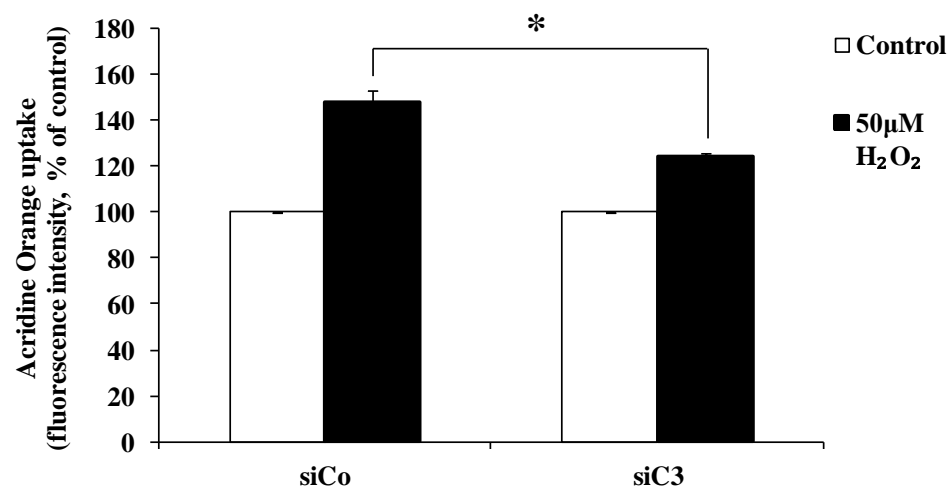
D)
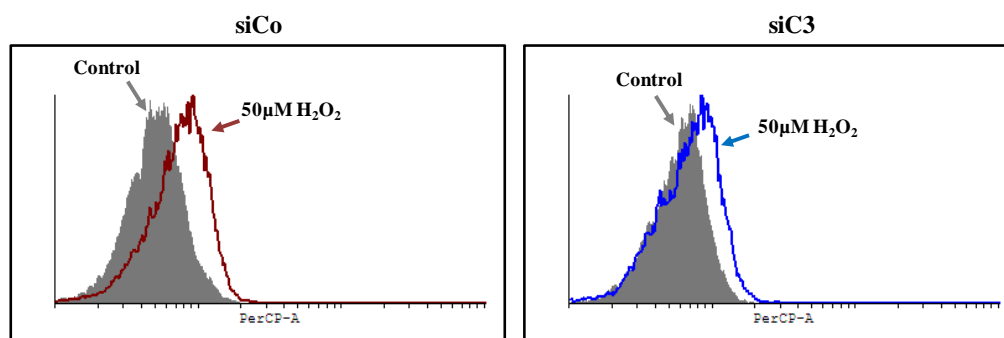
Figure 55. Effect of caspase 3 inhibition on H_2O_2 – induced lysosome biogenesis.
L6 myoblasts were pretreated with (A) 10μM QVD-OPH or (B) 20μM zDEVD-FMK, for 2 hours before treated with 50μM H_2O_2 for 24 hours. Cells were then exposed to a diluted LysoTracker® Red DND-99 solution (75nM) for 45min, 37°C. After fixation, red lysosomal fluorescence was analyzed under confocal microscope. Immunofluorescence images are representative of two independent experiments.
(C) Cells were transiently transfected with siRNA specific to caspase 3 (siC3) or negative control siRNA (siCo). Cells were treated with 50μM H_2O_2 at 24 hours post-transfection. At 24h post-H_2O_2 treatment, cells were exposed to 10μM Acridine Orange for 30 min at 37°C, Red lysosomal fluorescence of 10,000 cells per sample was determined by flow cytometry using the PerCP-A channel. The data are the means of three independent experiments ± S.E.M., *$P < 0.05$. Western Blot indicating knock-down efficiency of caspase 3 is representative of three independent experiments. (D) A representative flow cytometry histogram from three experiments is shown.

The transcription factor for EB (TFEB) had been identified as the master gene for lysosomal biogenesis[155]. TFEB over expression in cultured cells resulted in increased lysosomal biogenesis as well as cellular clearance of macromolecules such as glycosaminoglycans[155]. Recent findings suggest that TFEB translocates into the nucleus to initiate lysosomal biogenesis and lysosomal gene transcription. In our system, when cells were treated with 50μM H_2O_2, there was an enhanced nuclear localization of TFEB (Figure 56A). As a comparison, cytoplasmic staining of TFEB was observed in the control untreated cells. H_2O_2 treatment not only resulted in translocation of TFEB, but also increased the overall expression of TFEB. This was shown as the higher fluorescence intensity of TFEB in the treated cells compared to the control cells.

Although the role of caspases in lysosomal biogenesis was unreported, we speculate that caspase 3 might be involved in the TFEB pathway. We pre-incubated the cells with a pan caspase inhibitor QVD-OPH and the caspase 3-specific inhibitor zDEVD-FMK before H_2O_2 treatment. In the presence of both inhibitors, the increase in TFEB expression as well as the nuclear translocation of TFEB was greatly reduced (Figure 56B and 56C). The result supports a potential role of caspase 3 in lysosomal biogenesis, by regulating the expression and localization of TFEB.

A)
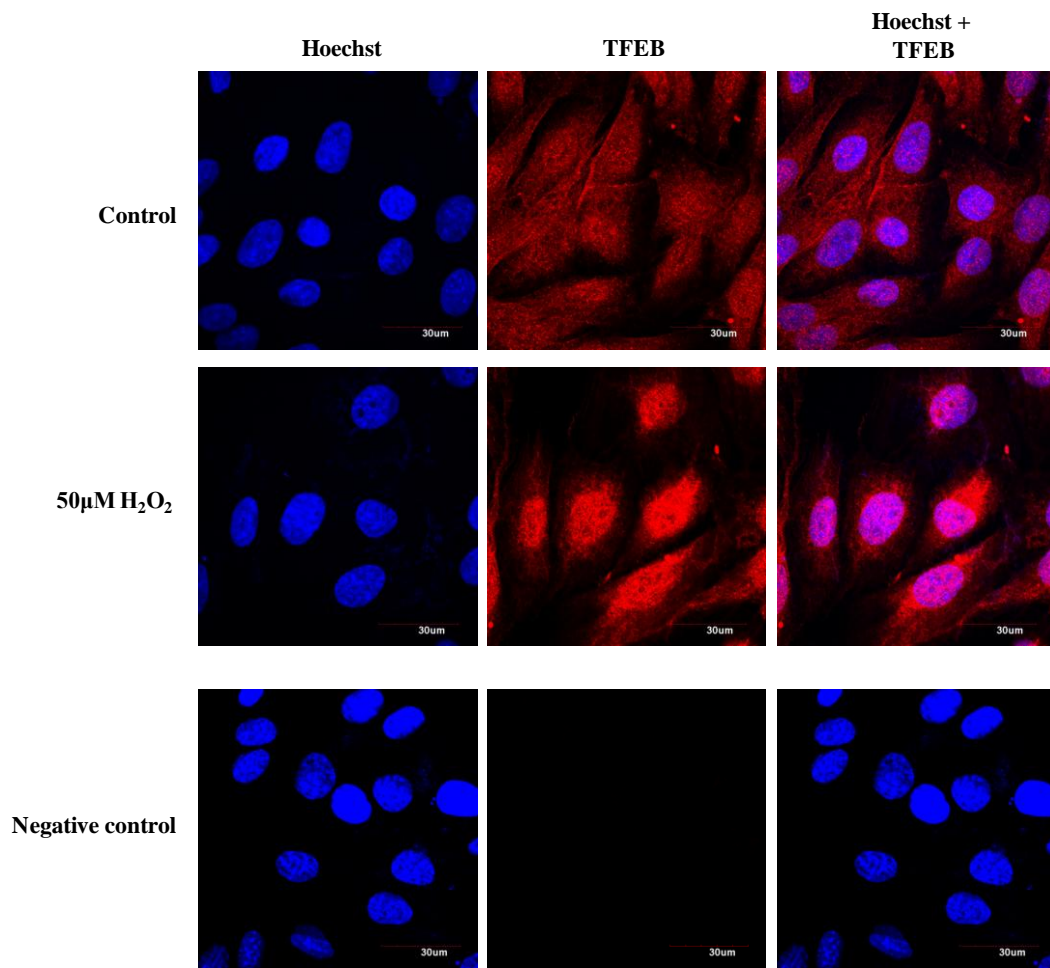
B)
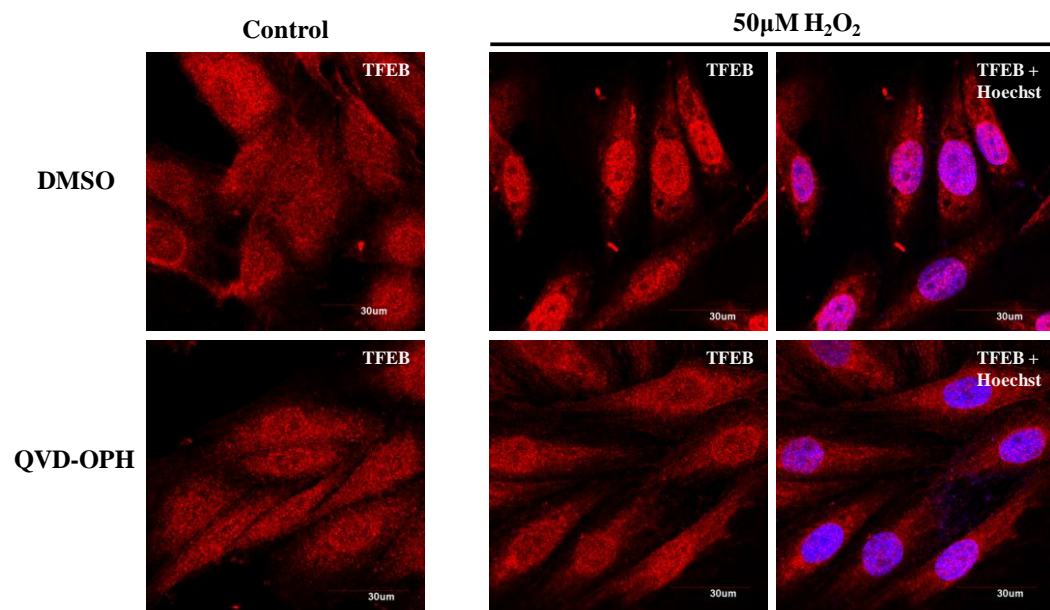
C)
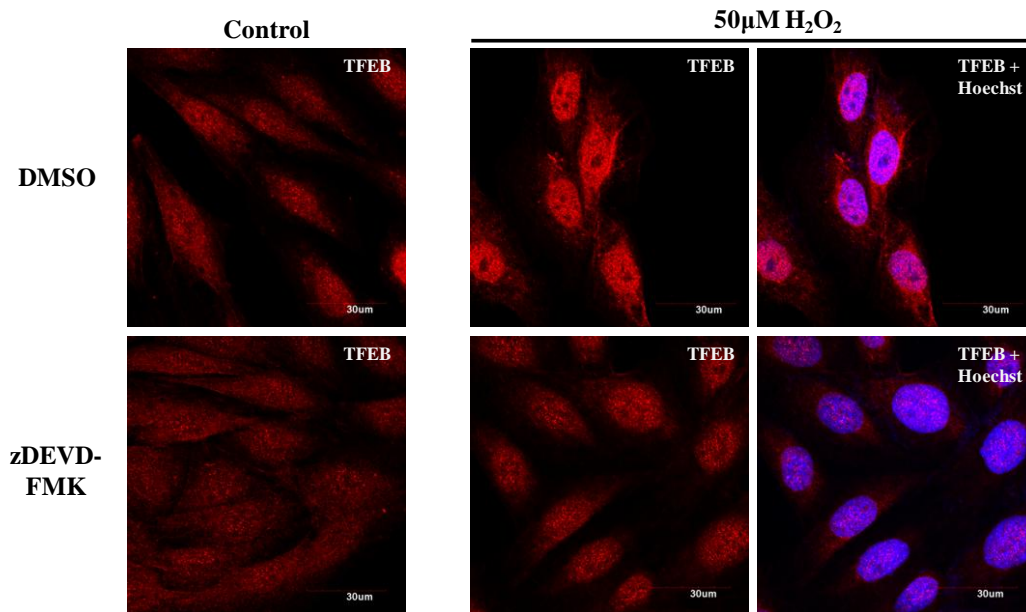
Figure 56. Caspase 3 inhibition impeded TFEB up-regulation and nuclear translocation. (A) L6 myoblasts were treated with 50µM H_2O_2 24 hours. After fixation, cells were incubated with primary antibody specific to TFEB followed by confocal microscopy analysis. Immunofluorescence images shown are representative of three independent experiments. Negative control refers to samples incubated in blocking buffer without primary antibody.
Cells were pretreated with (B) 10µM QVD-OPH or (C) 20µM zDEVD-FMK, for 2 hours before treated with 50µM H_2O_2 for 24 hours. Cells were then were incubated with TFEB specific primary antibody followed by confocal microscopy analysis. Immunofluorescence images are representative of two independent experiments.

3.3.2   NHE-1 promoter activity was unaffected by caspase 3 activation

Our previous study in lab demonstrated a new role of caspase 3 in sustaining repression of protein expression upon mild oxidative stress and in the absence of cell death. In a serum starved condition, 50μM H_2O_2 treatment on L61.1 cells resulted in caspase 3 activation that subsequently led to NHE-1 gene repression[104]. Without activation of caspase 3, H_2O_2 elicited a mild oxidative stress that resulted in transient and reversible inhibition of the NHE-1 promoter activity, but was insufficient to effect down-regulation of protein levels. With the activation of caspase 3, a sustained repression of both NHE-1 promoter activity and protein expression was achieved[104].

As the finding was performed in a serum starvation condition, it was of interest to examine the effect of caspase 3 activation on NHE-1 promoter activity in our system, in which cells were cultured and treated in 10% FBS medium. The study of NHE-1 promoter activity could be easily performed as the same cell line was used in our study. L6 myoblasts were stably transfected with the full length 1.1kb proximal fragment of the mouse NHE-1 gene promoter, which was inserted 5' to the luciferase gene (Figure 57)[108]. NHE-1 promoter activity was quantified by the luciferase enzyme production, as measured by luciferase assay as described in Materials and Methods (Section 2.2.3).
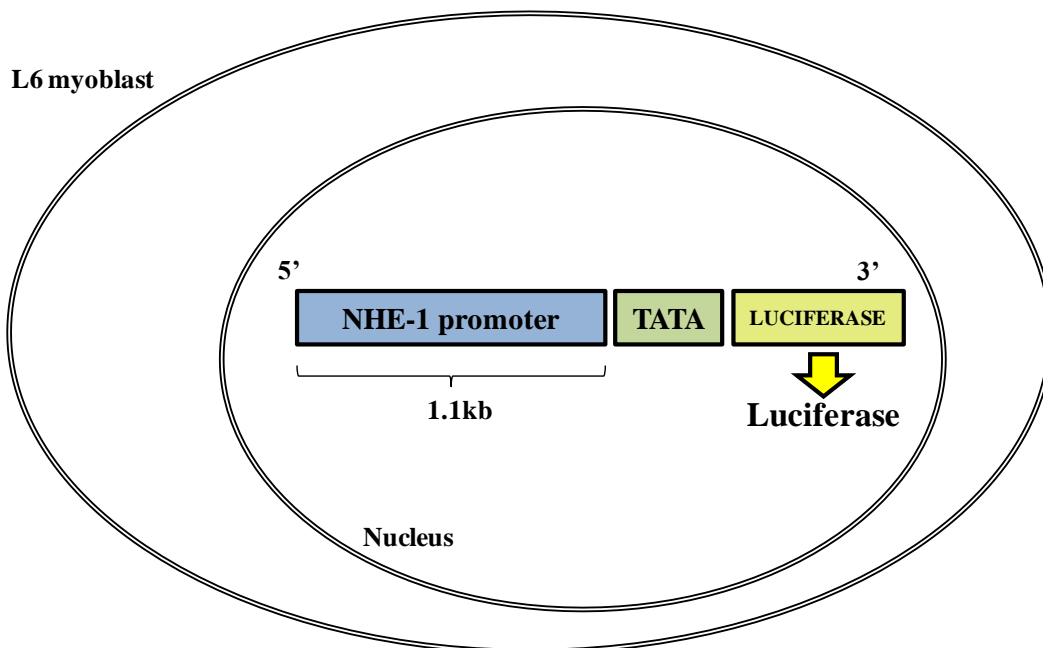
Figure 57. Stable expression of the full length 1.1kb mouse NHE-1 gene promoter by L6 myoblasts. L6 myoblasts were stably transfected with the full length 1.1kb proximal fragment of the mouse NHE-1 gene promoter which inserted 5' to the luciferase reporter gene. Therefore, NHE-1 gene promoter activity can be quantified using the luciferase assay as the production of luciferase enzyme is correlated to the activity of NHE-1 promoter.

NHE-1 promoter activity was decreased in a dose-dependent manner when cells were exposed to increasing dose of H_2O_2 (Figure 58A). Similar finding was observed with cells treated with H_2O_2 in a serum starved condition, a dose-dependent decrease in NHE-1 promoter activity was achieved by addition of H_2O_2 (Figure 58B). Notably, such decrease in NHE-1 promoter activity required twice as much dose in cells treated in 10% FBS than the serum starved cells. For example, while 50μM H_2O_2 treatment induced a 40% decrease in NHE-1 promoter activity in cells treated in physiological condition (10% serum), such decrease could be achieved with 25μM H_2O_2 in serum-starved cells.

A)
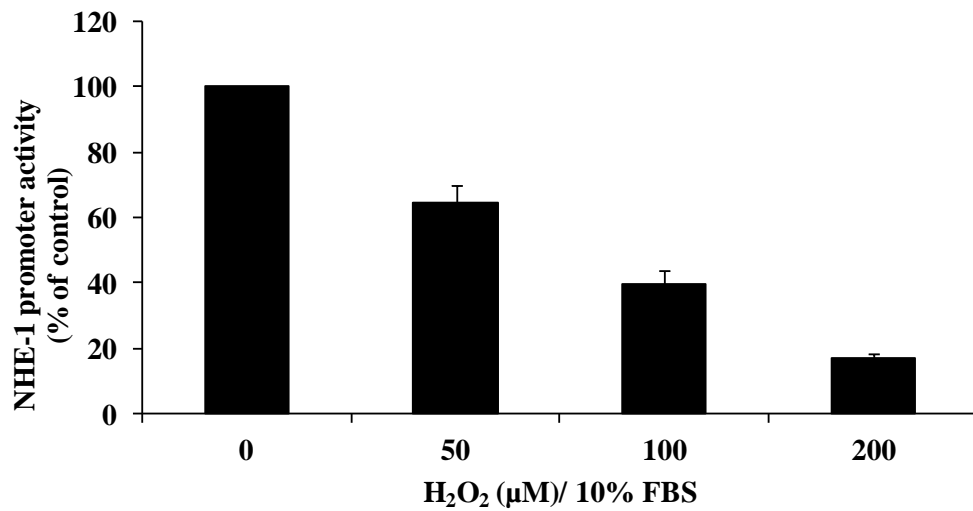
B)
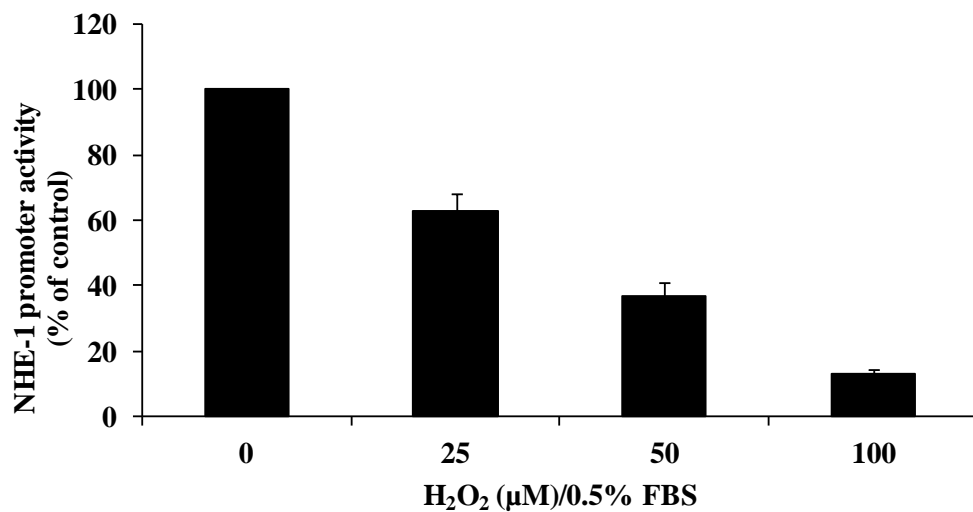
Figure 58. H$_2$O$_2$ down-regulated NHE-1 promoter activity in a dose-dependent manner. (A) Cells were treated with increasing doses of H$_2$O$_2$ for 24 hours and were harvested for luciferase assay to quantify NHE-1 promoter activity. (B) Cells were serum-starved over night before treatment with increasing doses of H$_2$O$_2$ for 24 hours. Cells were then harvested for luciferase assay to quantify NHE-1 promoter activity. The data are the means of four independent experiments ± S.E.M., *$P < 0.05$.

To see if caspase 3 was involved in NHE-1 gene repression in our system, we inhibited caspase 3 activity with the pan caspase inhibitor QVD-OPH and caspase 3 inhibitor zDEVD-FMK and examined NHE-1 promoter activity. At 48h, a recovery in NHE-1 promoter activity was observed, as compared to that at 24h (Figure 59A). It is found that both QVD-OPH and zDEVD-FMK was unable to rescue NHE-1 promoter activity repression by H_2O_2 (Figure 59A). As the dose of QVD-OPH and zDEVD-FMK was sufficient to inhibit caspase 3 activity induce by H_2O_2 (Figure 59B), we thus conclude that caspase 3 activation was not involved in NHE-1 promoter activity repression.

A)
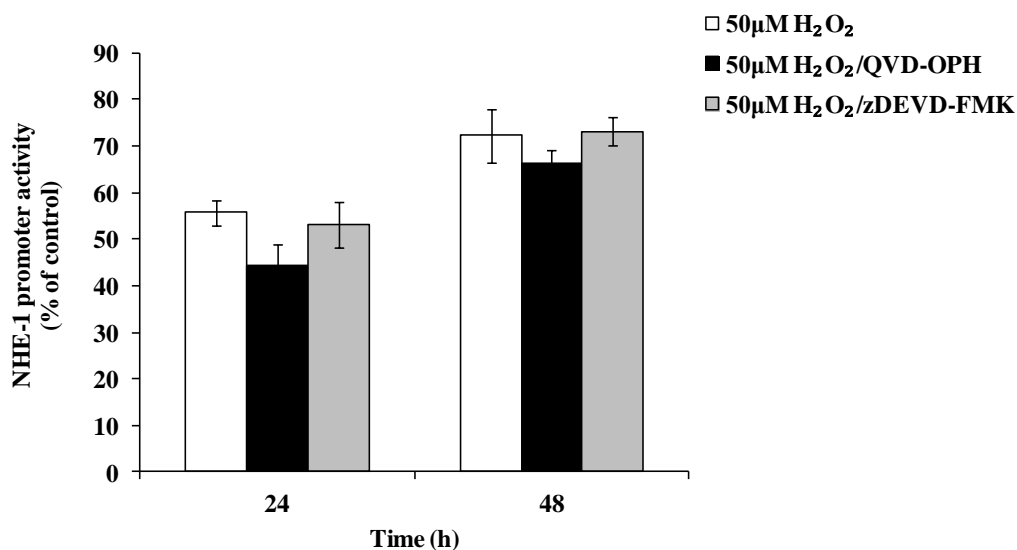
B)
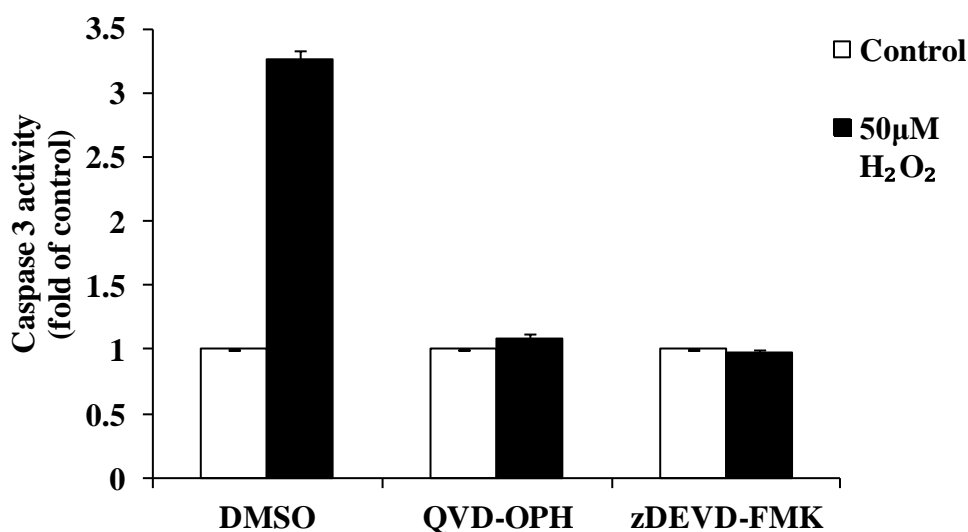
Figure 59. H₂O₂-induced down-regulation of NHE-1 promoter activity was unaffected by caspase 3 inhibition. Cells were pre-treated with 10μM QVD-OPH or 20μM zDEVD-FMK before exposure to 50μM H₂O₂. (A) After 24h and 48h, cells were harvested for luciferase assay. The data are the means of three independent experiments ± S.E.M. (B) At 24h post-H₂O₂ treatment, cells were harvested for caspase 3 activity assay.

CHAPTER 4 DISCUSSION

For a long time, caspases activation has been solely implicated in apoptosis. In recent years, increasing numbers of studies are dedicated to understanding the alternative roles of caspases in a physiological context beyond apoptosis, particularly in cellular function and development. Our present study is a valuable example of how caspase 3 is involved in a non-apoptotic role. Based on the previous study by Kumar et al.,[104] we pursued the upstream pathway leading to caspase 3 activation in a non-apoptotic condition.

Our present study demonstrated that transient exposure to H_2O_2 can elicit an elaborated and complicated signalling response, leading to caspase 3 activation. In our system, caspase 3 was activated independently of the initiator caspases. The activation of caspase 3 was, instead, mediated by peroxynitrite, nitric oxide and p53, which converged on the occurrence of lysosomal membrane permeabilization (LMP). As a result of LMP, cathepsin B and L are released into the cytosol. We postulated that cathepsin B and L could directly cleave and activate caspase 3 in our system. Lastly, we also proposed a novel role of caspase 3 in lysosome biogenesis by regulating the expression and localization of the master gene TFEB.

4.1 H₂O₂ induced caspase 3 activation by a non classical pathway in the absence of cell death

ROS are one of the most important inducer/mediator in apoptosis[156]. Studies that manipulated oxidation level and intracellular antioxidant system have clearly affirmed the roles of ROS in apoptosis based on the following observations: (1) Exogenous addition of ROS or depletion of intracellular antioxidants resulted in apoptosis in various cell types[157-159] (2) Many apoptotic drugs generate ROS that compromise the mitochondrial membrane integrity, leading to cytochrome c release and caspase activation, and subsequently cell death. (3) In these cases, apoptotic drugs-induced apoptosis can be inhibited by antioxidants, ROS scavengers or over-expression of antioxidant genes[158,160,161] (4) Many regulatory genes in cell survival and apoptosis, such as p53[162,163], NF-kB[164] are redox-regulated. (5) Increase in intracellular ROS is a general feature in apoptosis[165].

ROS are one of the most reproducible inducers of caspases cascade, although its exact mechanism is yet to be clearly illustrated. As caspases are cysteine-dependent proteases, it is also expected that they might be redox-sensitive and could be redox-regulated[163]. Despite the mounting evidences of ROS involvement in apoptosis, ROS inhibition of apoptosis was also well reported. For example, although ROS level was often elevated in apoptotic cells, prolonged or excessive oxidative stress can actually prevent caspase activation[163]. Generally, low level of ROS leads to cell survival and proliferation, moderate level of ROS results in apoptosis, high level of ROS results in massive cell death or necrosis. Figure 60 summarizes the effect of ROS on caspase through multiple mechanisms, leading to apoptosis or cell survival.

(A)
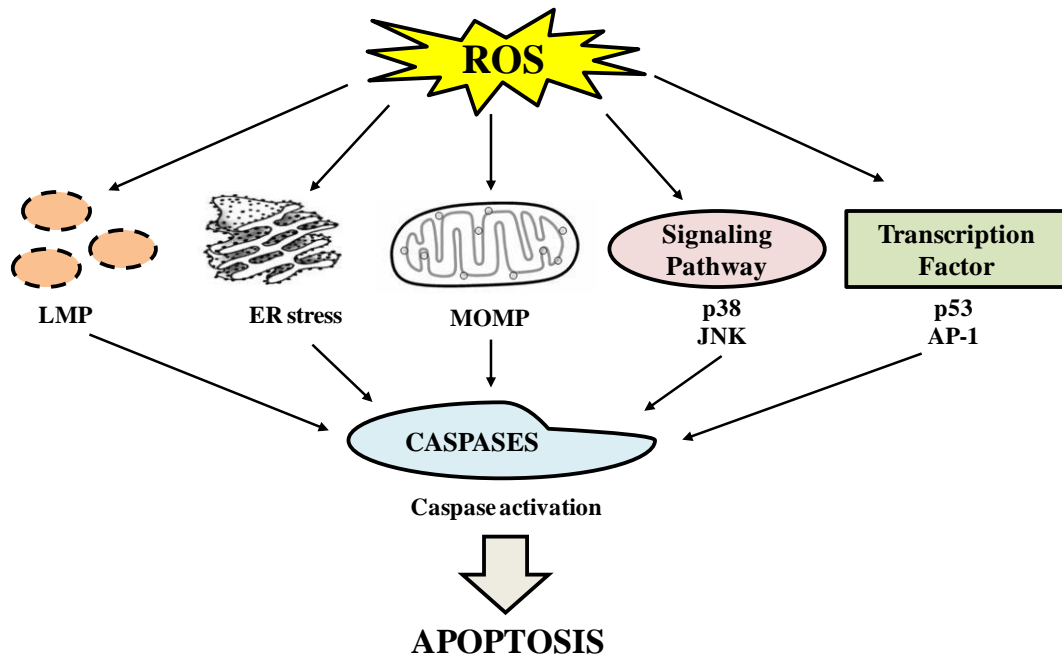
(B)
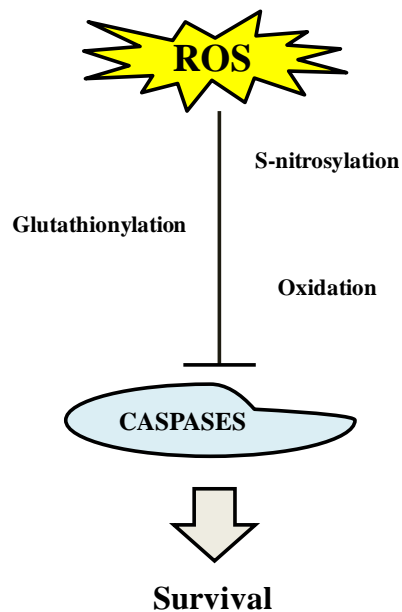
Figure 60. Redox regulation of caspase activation. Caspases can be activated or inhibited by ROS, depending on the concentration and species of ROS in action. (A) ROS induces caspases activation via multiple pathways that are non-exclusive, leading to apoptosis. (B) Caspases contain redox-sensitive residues that can be modified by ROS. Common redox modifications of caspases are s-nitrosylation, oxidation and glutationylation. Often, these redox modifications lead to inactivation of caspases and promote cell survival.

Exogenous H_2O_2 is widely used in studies where oxidant-dependent signalling is concerned. Compared to its derivatives such as OH•, H_2O_2 traverse the membranes readily and survives long enough to induce a redox change distant from its site of production[166]. Therefore, H_2O_2 is a convenient tool to induce oxidative stress. Many studies have utilized exogenous H_2O_2 to induce caspase 3 activation and most of these reports focused on H_2O_2 inducing apoptosis by activating the caspase cascade. Nevertheless, this does not mean that H_2O_2 or ROS necessarily activates caspase and results in cell death. It should be noted that negative results were often less reported than positive results. In our study, H_2O_2 induced activation of caspase 3 in absence of cell death. Compared to the classical inducer of apoptosis, STS-induced and H_2O_2-induced caspase 3 activation were different in several aspects.

STS induces caspase 3 activation through the intrinsic pathway, as evident by the temporal pattern of caspases activation and the inhibitory effect of zVAD-FMK and zLEHD-FMK on caspase 3 activation. Amplification of the caspase cascade was also observed with the activation of caspase 8 a few hours after caspase 3 activation. In contrast, there was no activation of caspase 8 and caspase 9 when cells are exposed to 50μM H_2O_2. H_2O_2-induced caspase 3 cleavage was unimpeded by the caspases inhibitors. Also, although caspase 3 was activated, there was no amplification of the caspase cascade. In term of localization, activated caspase 3 in STS system was detected in both nucleus and cytoplasm, while activated caspase 3 in H_2O_2 system was mainly detected in the nucleus. In comparison with the caspase 3 activation of STS, the magnitude of H_2O_2-induced caspase 3 activation was much lower and started much later. Lastly, while STS-induced caspase 3 contributed to apoptosis, H_2O_2-

induced caspase 3 did not result in apoptosis. Together, these differences outline a unique pathway of caspase 3 activation during mild oxidative stress.

In recent years, there have been new evidence of caspases activation and cleavage of their substrates in the absence of cell death, demonstrating caspases' alternative roles in cellular physiological functions beyond apoptosis[167]. To dates, non-apoptotic roles of caspases have been reported in inflammatory response[168], immune cell proliferation[169,170], and differentiation of various cell types[40,41,48]. The ability of caspase to carry out its non-apoptotic roles relies on various mechanisms that act singularly or in combination for restricted cleavage and limiting execution of apoptosis (Figure 61). For our study, we demonstrate that caspase 3 activated during mild oxidative stress happen in the context of cell survival and could have a non-apoptotic purpose. We also outlined several distinct features of the caspase 3 activation in our system, these are: a caspase-independent upstream pathway, sustained nuclear localization, and low concentration of caspase 3 activity. These distinct features could be important regulatory mechanisms for caspase 3 to execute its non-apoptotic roles in our system.
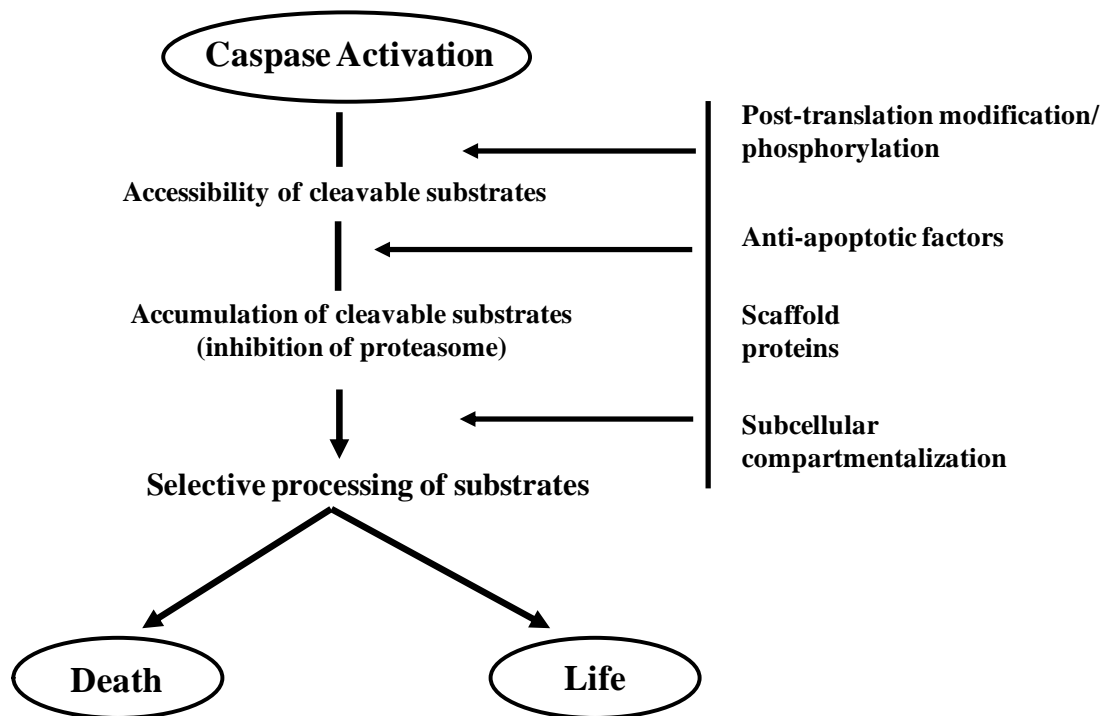
Figure 61. Caspases' functions in cell survival and cell death require extensive regulatory mechanisms. The key to caspases execution of their non apoptotic functions is restricted cleavage of specific target proteins, which is governed by caspase activity and accessibility of target proteins. Caspases activity may be regulated by post-translational modifications of caspases. Accessibility of the target substrate is restricted by specific subcellular compartmentalization of caspases, or substrate protection by scaffold proteins or anti-apoptotic factors. (Adapted from Launay et al., 2005[13])

4.1.1 A threshold of caspase 3 activity in apoptosis

In our study, one striking difference between H_2O_2 and STS induced caspase 3 activation is the magnitude of activation. This was measured by the fold of caspase 3 activity and the amount of cleaved caspase 3 on Western Blot. We postulated that the difference in magnitude of caspase 3 activation was a main determinant in cell fate decision, i.e. there be a critical activation threshold for caspase 3 to carry out its pro-apoptotic role.

Studies have shown that low and transient caspase 3 activation could serve a physiological role instead of activating the cell death machinery[171,172]. It seems that cells can continue to survive in the presence of a certain level of effector caspase activity[171]. For example, immunohistochemical study showed that in glioblastoma cells, two subsets of cells with different caspase 3 activity was found to have different cell fate[32]. The subset of cells with weak to moderate caspase 3 activity does not exhibit any apoptotic morphology, while the subset of cells with strong caspase 3 activity was found with typical apoptotic morphology[32]. The same study also showed that NCH89 *ex vivo* glioblastoma cells have a constitutive, moderate caspase 3 activity that can be significantly blocked by caspase inhibitors. This constitutive, moderate caspase 3 activity was insufficient to induce apoptotic, but was required for tumour migration and invasion[32]. When the cells were cultured *in vitro*, treatment with STS was able to further increase the constitutive caspase 3 activity and result in apoptosis[32]. This is congruent with our study where low level of caspase 3 activity (by 50μM H_2O_2) did not result in apoptosis but high level of caspase 3 activity (by 1μM STS) does.

In our study, the difference of the level of caspase 3 activity was also reflected by the different subsets of caspase substrate cleaved in H_2O_2 and STS treatment. We examined the protein profile of common substrates of caspase 3 in apoptosis, Lamin A/C, PARP, and Gelsolin, and found that they are all cleaved under STS treatment but not under H_2O_2 treatment. We proposed that the level of activated caspase 3 affects its ability in substrate cleavage. It has been shown that RasGAP was cleaved differentially by different concentration of active caspase 3[67]. Under low concentration of active caspase 3, RasGAP was cleaved to generate an N fragment that has an anti-apoptotic function. At higher concentrations of active caspase 3, the N-fragment is further processed into N1 and N2 fragments, which are pro-apoptotic. N1 and N2 fragments potentiate the cells to result in DNA-damage induced apoptosis. This differential cleavage of RasGAP seems to be a regulatory mechanism by caspase 3 to control the extent its own activation in the context of cell survival, as partial cleavage of RasGAP blocks the caspase amplification effect of the C fragment[67].

4.1.2 Sustained nuclear localization of activated caspase 3

Despite the cytoplasmic localization of its proenzyme form, caspase 3 has been shown to be involved in nuclear morphological changes in apoptotic cells[173,174]. A number of caspase 3 substrates are also found to be localized in the nucleus[175,176]. It is therefore proposed that caspase 3 translocates into the nucleus once it is activated. This translocation is an important event during apoptosis.

Several mechanisms have been proposed for the translocation of activated caspase 3 into the nucleus. An earlier study reported a passive diffusion of activated caspase 3 into the nucleus in caspase 9-dependent manner[177], but this was rebutted by recent reports. Another study proposed that activated caspase 3 translocates with a substrate-like protein into the nucleus with the aid of AKAP95 (A-Kinase-Anchoring Protein 95) as the potential carrier[178]. A more recent study suggested that p3-recognition-based specific cleavage of caspase 3 disrupts its crm-1-independent nuclear export signal, thereby enables its nuclear entry after activation[179]. To date, the exact mechanism of caspase 3 nuclear translocation remains elusive.

In our study, time kinetic analysis of immunofluorescence showed that H_2O_2-induced activated caspase 3 had a sustained nuclear localization. At 24h, where the activation of caspase 3 by H_2O_2 was at its maximum, the fluorescence of activated caspase 3 was observed in the nucleus. Even at 48h, when the fluorescence detection becomes more difficult due to the decreased amount of activated enzyme, it was still observed in the nucleus. In comparison, STS-treated cells, at 12h, the fluorescence of activated caspase 3 was detected only in the nucleus. At 24h and 48h, both nuclear and cytoplasmic localization of activated caspase 3 was detected. Notably, cytoplasmic

localization of activated caspase 3 was only found in apoptotic bodies with highly fragmented nuclei, while nuclear localization of activated caspase 3 was found in cells with condensed nuclei. In apoptotic bodies, activated caspase 3 was found in the cytoplasm but not the nucleus. Our study raised two important points: (1) sustained nuclear localization of activated caspase 3 for non-apoptotic cells, (2) the relocation of activated caspase 3 from nucleus to cytoplasm for apoptotic cells.

The localization of activated caspase 3 in the nucleus could be an important mechanism that restricts it from cleaving substrates for apoptosis purpose. This feature could have a physiological function. Constitutive expression of activated caspase 3 has been found in the nuclei of Bergmann glia and a subpopulation of astrocytes in the cerebellar cortex, hippocampus, and spinal cord of rats[180]. Such expression of activated caspase 3 was unrelated to apoptosis. Also, PARP, the important substrate of caspase 3 during apoptosis, was not cleaved[180]. Another study showed that activated caspase 3 was localized in the nuclei of NeuN-positive immature neurons in the proliferative regions of immature rat forebrain[52]. These activated caspase 3-containing cells were not undergoing apoptosis, but instead was dividing and in process of differentiating into mature neurons[52].

These studies bring out several important messages: firstly, nuclear localization of caspase 3 does not necessarily correlate with apoptosis. Secondly, nuclear retention of activated caspase 3 could have a physiological relevance. Nevertheless, the exact mechanism of how this nucleus-retained caspase 3 exert its non-apoptotic role is still unknown. One hypothesis is that caspase 3 could be participating in secondary processing of transcription factors. Several transcription factors from the FOXO

family contain conserved caspase 3 cleavage site[181]. Also, Kumar et al. showed that nuclear localization of caspase 3 was essential for ROS production and down-regulation of NHE-1 gene expression[104].

It has also been shown that altered nuclear event (i.e. nuclear fragmentation and condensation) was dependent on caspase 3 activation. Caspase 3 deficient cells undergo apoptosis without nuclear fragmentation[174]. The cleavage of NuMA and Lamin A/C by caspase 3 is particularly important for nuclear fragmentation[182]. In our study, the nuclei of H_2O_2-treated cells remained intact probably because caspase 3 did not cleave any substrate that maintains the nuclear membrane. Cleavage of Lamin A/C was found in STS-treated cells, but such cleavage was not found in H_2O_2-treated cells. What regulates caspase 3 from cleaving the substrates in altered nuclear event? A concentration-dependent effect of activated caspase 3 could be the key in cleaving the right substrates. In our study, H_2O_2-induced caspase 3 activation might be too low to cleave the Lamin A/C, therefore the nuclei remain intact. It has also been suggested that caspase 3 in the nuclei could be bounded to specific nuclear structure or scaffolding proteins, thereby preventing it to cleave the wrong substrates.

While H_2O_2-induced activated caspase 3 was retained in the nucleus, STS-induced activated caspase 3 was relocated into the cytoplasm at 24h and 48h. One may hypothesize that this relocation could be a consequence of total disruption of the cytoplasmic-nuclear barrier. It has been shown that during apoptosis, the nuclear-cytoplasmic barrier as well as the nuclear transport system was disrupted, leading to increased permeability of the nuclear pore. As a result, soluble proteins that are normally restricted to the nucleus or cytoplasm are distributed throughout the cells[177].

That is, in case of total disruption of the cytoplasmic-nuclear barrier, one should expect that the protein can be distributed evenly throughout the cells. However, we found that in apoptotic bodies, activated caspase 3 was only found in the cytoplasm. This suggests that activated caspase 3 can be re-transported out to the cytoplasm to cleave cytoplasmic substrates. Possible mechanisms could be directional diffusion of activated caspase 3 through the altered nuclear pore complexes from the nucleus to the cytoplasm, or activated caspase 3 could be actively transported out to the cytoplasm.

Although the exact mechanism is not known, the cytoplasmic redistribution of activated caspase 3 could be important for apoptotic morphological change and apoptotic body formation[183,184]. The effector phase of apoptosis is characterized by sequential events starting with altered nuclear event, followed by cytoplasmic event and finally apoptotic body formation[185]. The cytoplasmic event involves caspase 3-mediated cytoskeletal reorganization and disintegration by cleavage of structural proteins such as gelsolin[183], and caspase-3 mediated phosphatidylserine (PS) externalization[186]. This cytoplasmic structural change is critical to package the cells into membrane-bound apoptotic bodies that display PS on its outer surface. The formation of apoptotic bodies prevents leakage of cytoplasmic content to the surrounding tissues. This, together with its rapid phagocytosis by neighbouring cells, including macrophages and parenchymal cells, via recognition of the PS residue, prevents inflammation response or autoimmune reaction[187].

4.1.3 Alternative pathway for alternative cell fate?

The activation of effector caspases by the initiator caspases through the intrinsic pathway or extrinsic pathway is well established. When compared to the effector caspases, the initiator caspases are highly specific in substrate recognition. They cleave relatively few proteins other than their own proenzyme and their downstream effector caspases[188,189]. Therefore initiator caspases have specific roles, and we stand to reason that the initiator caspases have highest efficiency in cleaving their effector caspases.

However, instead of the classical caspase cascade, why do cells sometimes decide to utilize an alternative, lower efficiency, pathway in activating caspase 3? We hypothesize that the alternative pathway might be one of the regulatory factors of caspase's non apoptotic roles. As other protease may cleave caspase 3 less efficiently, the alternative pathway could be a way to control the level of activated caspase 3 in cells. Initiator caspases results in rapid, excessive effector caspase activation, suitable as a coarse control of caspase activation. However, a non caspase protease with lower efficiency can be used as fine control. This hypothesis was supported by Juan et al.'s study on the effect of thrombin on platelets and pancreatic acinar cells[172]. In their study, they reported a sequential and bimodal mode of caspase 3 activation by different concentration of thrombin. The early phase of caspase 3 activation induced by 1U/ml thrombin occurred independently of the initiator caspases 8, 9 and 10, and independently of mitochondrial-induced apoptosis[172]. The delayed phase of caspase 3 activation was mediated by mitochondrial event and caspase 9. At the same time, apoptosis was activated. The early phase of caspase 3 activation can be achieved by using a low and physiological dose of thrombin (0.01U/ml). They also showed that

this caspase-independent, non apoptotic caspase activation was required for platelet aggregation and pancreatic amylase secretion[172]. In L6 myoblasts, when we increased the dose of H_2O_2 to 100µM and 150µM, cells underwent apoptosis. The activation of caspase 3 was at least 2 fold more than that induced by 50µM H_2O_2 (Appendix C). Preliminary findings show that in 100µM and 150µM H_2O_2-treated cells, activation of caspase 8 and 9 was detected. We speculated that caspase 3 activation in 100µM and 150µM-treated cells were activated in a classical caspase cascade.

There are also studies that reported alternative caspase 3 activation pathway leading to apoptosis. In P39 cells, the reduction in ATP resulted in lysosomal membrane permeabilization. The release of lysosomal enzymes was responsible for the activation of caspase 3, which was independent of the mitochondrial event and initiator caspases activation[190]. Another study showed that cisplatin induced caspase 3 activation was mediated by p53 and this p53-mediated caspase 3 activation was independent of the initiator caspases and mitochondrial dysfunction[191]. On the other hand, classical caspase cascade has been observed in physiological, non-apoptotic condition. It was reported that caspase 3 required for the differentiation of muscle progenitor cells into myofibres was activated by caspase 9[192]. Interestingly, caspase 9 activation was independent of mitochondrial event. These studies reinforce the idea that regulation of caspase 3 activation is coordinated by different regulatory mechanisms rather than conforming strictly to the caspase cascade model.

In summary, we proposed that caspase 3 activation has a threshold level which dictates whether the cells are survive or undergo apoptosis. The classical caspase cascade pathway, with its rapid response and high efficiency is likely to serve as the

coarse control for caspase activation. Alternative activation pathways, such as the one we have proposed, probably act as fine control for the cell. The alternative activation pathways may be less efficient; however, a lower activation of caspase 3 that was sufficient for physiological function but insufficient for apoptotic function can be achieved. Furthermore, nuclear sequestration of caspase 3 could be an additional regulating mechanism of caspases' roles; determining the consequences of caspase 3 activation when it is above or below the threshold level.

4.2 A lysosome-mediated pathway of caspase 3 activation

In our study, we discovered an alternative pathway leading to caspase 3 activation involving lysosomal membrane permeabilization (LMP). H_2O_2 (50µM) activated caspase 3 in the absence of initiator caspases activation and mitochondrial event. We found that LMP release of cathepsin B and L was a crucial event in our study of caspase 3 activation. This cytosolic release of cathepsin B and L enabled the proteases to cleave and activate caspase 3. Using pharmacological inhibitors and molecular silencing approach, we identified four upstream candidates for LMP: iron, peroxynitrite, nitric oxide and p53. The inhibition of each of these four candidates inhibited both LMP and caspase 3 activation through pathways that are dependent and independent of each other's. Our results suggest that, instead of the conventional mitochondria-mediated pathway of caspase activation, we proposed that lysosomes are the main player in our system.

4.2.1 Lysosomal membrane permeabilization as a regulated event

Lysosomal membrane permeabilization is a common event in both apoptosis and necrosis. Partial LMP, a limited release of lysosomal contents to the cytoplasm, activates the caspase cascade and result in apoptosis. On the other hand, massive LMP involves a generalized lysosomal rupture and uncontrolled release of lysosomal contents to the cytoplasm, leading to caspase-independent necrosis[193]. Many classical apoptotic inducers, such as activation of death receptors of TNF receptor family[194,195], STS[119], etoposide[196], growth factor withdrawal[195], p53 activation[197], H_2O_2[198,199], all employ partial LMP as part of their apoptotic pathway.

The propagation of apoptosis via LMP is believed to proceed both dependently and also independently of mitochondrial event. The release of cathepsins from the lysosome is a major event after lysosomal membrane destabilization and is responsible for cleaving various protein substrates. The cleavage of the pro-apoptotic proteins Bid and Bax[196,200,201] as well as the anti-apoptotic Bcl-2, Bcl-XL and MCL-1[202] by cathepsins result in mitochondrial event and subsequently activation of the caspase cascade. Figure 62 demonstrates how lysosome can participate in cell death, via caspase dependent or-independent pathway.
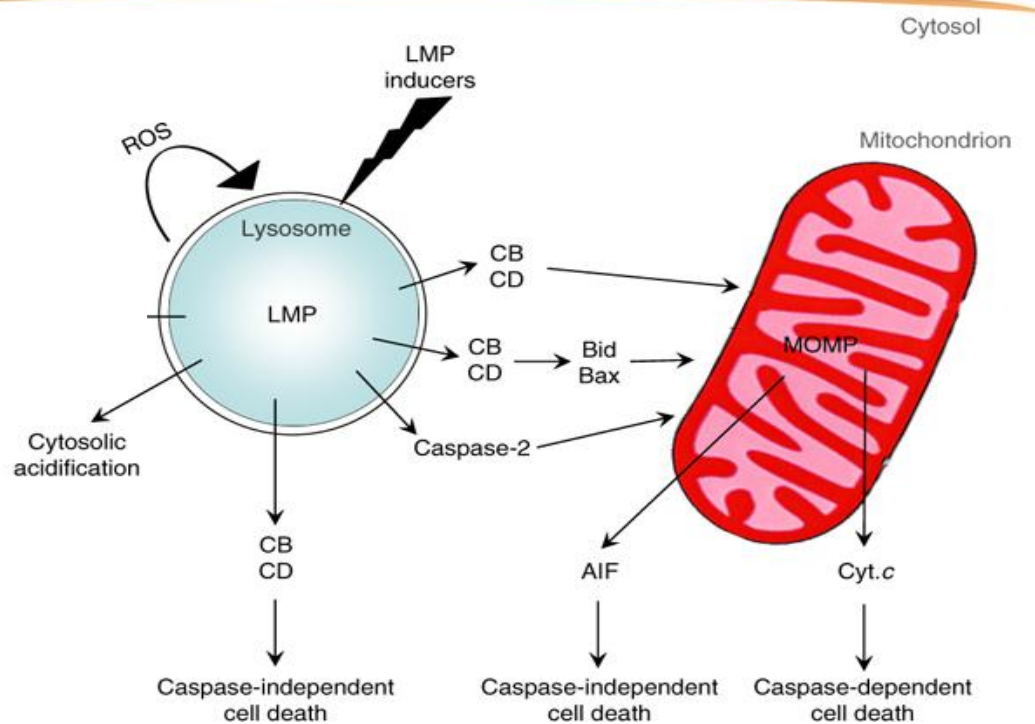
Figure 62. Lysosomal membrane permeabilization as apoptosis mediator. LMP takes part in both caspase-dependent and –independent apoptosis. LMP is able to trigger the classical MOMP-caspase cascade, by cathepsins-mediated cleavage of the Bcl-2 family proteins such as Bid and Bax. During MOMP, the release of AIF from the mitochondria may also result in caspase-independent apoptosis. On the other hand, cytosolic release of cathepsins may result in caspase-independent apoptosis (AIF, apoptosis-inducing factor; CB, cathepsin B; CD, cathepsin D; Cyt. *c*, cytochrome *c*; LMP, lysosomal membrane permeabilization; MOMP, mitochondrial outer membrane permeabilization). (Figure adapted from P Boya and G Kroemer, 2008[203])

In our study, we presented an unconventional lysosomal pathway leading to caspase 3 activation. There are two major differences between our pathway and the conventional lysosomal apoptotic pathway. Firstly, there was no apoptosis in our system, indicating that LMP does not necessarily result in apoptosis or cell death. Secondly, caspase 3 activation happened without the involvement of mitochondrial event.

Although it seems that LMP is a potentially dangerous event to the cells, it could have a physiological function. The evidence of partial and massive LMP shows that LMP is actually a regulated event because the cells seem to respond to the stress intensities and decide how much LMP to induce. However, the intensity of LMP, whether classified as partial or massive, is usually dependent on the final outcome. Although the prevailing views favours linking LMP to cell death, this could be biased due to unreported negative results. The occurrence of so called "low LMP" was often ignored, because cells continue to survive without inducing apoptosis or necrosis. The intensity of LMP may be low but significant; however, this is usually not recognized or reported as LMP under the prevailing model.

The most common method to measure LMP is by staining of cells with Acridine Orange. An increase in cytosolic green fluorescence indicates the occurrence of LMP. In our study, we found that LMP was induced at 2-4h, with an increase of average of 105-120% from the control. The maximum of green fluorescence was detected at 4h. After 4h, the green fluorescence of Acridine Orange decreased and was decreased gradually to basal level by 12h. Essentially, this could mean that LMP is recoverable. Unlike MOMP, LMP is not a point of no return for apoptosis. This is best illustrated

by a study showing that different intensity of LMP could be triggered by different degree of photo-oxidative damage[204]. In the study, cells were irradiated with blue light for different length of time (2, 4, and 8min). Cells irradiated for 4 min recorded an increase in the Acridine Orange green fluorescence of 400-600% over the control, and were apoptotic. Cells irradiated for 2 min showed a "considerable less" increase in green fluorescence and were viable. Cells irradiated for 8 min showed a "more pronounced" increase in green fluorescence and were necrotic. The actual increase in green fluorescence for cells irradiated for 2 min was unreported because it was considered as a negative result. However, the so called "considerable less" Acridine Orange relocation could be a physiologically important event, because cells remained viable after blue light irradiation[204].

We proposed that, beside the intensities of LMP, the lack of mitochondrial event could be one of the key determinants of whether the cells undergo apoptosis or not. In our study, the absence of MOMP as well as caspase 9 activation could mean that LMP could bypass MOMP to be directly involved in effector caspase activation. Our study provided two new findings; firstly, LMP is not a point of no return for cell death. Unlike MOMP, LMP is not an all-or-none event; this is evident by the recovery of LMP in our study. We deduced that LMP could be regulated event and could even be physiological-relevant because the release of lysosomal content seems to be a controlled event. In this case, we believe that the intensity of stress could be an important factor to induce a low and reversible LMP. The regulation of LMP in turn, is important in the regulation of caspase 3 activation via our proposed alternate pathway.

The actual mechanism of LMP is still largely unknown. Similarly, its regulatory mechanism remains elusive. It was reported that during partial LMP, not all lysosomes were permeabilized. The selectivity of LMP occurrence is dependent on the sizes and location of the lysosomes. For example, it has been shown that large lysosomes are more susceptible to LMP induction[205]. Also, the selectivity of lysosomal content release is still a mystery. As we have shown that LMP is reversible, it is more likely that lysosomal content release is mediated through specific pore formation rather than unspecific lysosomal membrane rupture. In addition, LMP can also be regulated via modulation of lysosome membrane stability. Studies have suggested Hsp70[206] and lysosome-associated membrane proteins 1 and 2 (LAMP-1, -2)[207] can protect lysosomes from destabilization.

4.2.2   Cathepsin B and L in caspase 3 activation

The activation of caspases requires proteolytic processing of the proenzyme to active fragments that further oligomerize to form the active enzyme conformation. Activation of the initiator caspases involves autocatalytic intrachain cleavage with the aid of an adaptor, as described by the induced proximity[9], proximity-driven dimerization[10,11], or induced conformation model[12]. Activation of effector caspases requires intrachain cleavage by the initiator caspases. In this study, we showed that, instead of the initiator caspases 8 and 9, Cathepsin B and L, were the upstream activators of caspase 3. LMP was induced by H_2O_2 treatment at 2-4h. This provides an opportunity of cytoplasmic translocation of cathepsin B and L, which then cleaved and activated caspase 3.

The involvement of cathepsins in caspase 3 activation, particularly in the context of apoptosis, has been reported[202,208,209]. It has been shown that mitochondrial event is indispensable for cell death initiated by LMP because cell death was inhibited by absence of Bax or Bak or over-expression of Bcl-2[210]. Also, purified cathepsins cleave Bid but not caspases *in vitro*[211]. These reports favour indirect activation of caspases through a LMP-MOMP functional hierarchy pathway. Nevertheless, there are opposing studies that support direct activation of caspases, in particular the effector caspases, by cathepsins. Studies have shown *in vitro* cleavage of caspase 3 by digitonin-treated lysosomal fractions and such cleavage was pH-dependent and was inhibited by cathepsin inhibitors[212,213]. In P39 cells treated with etoposide, apoptosis and caspase 3 was activated in the absence of MOMP and cytochrome c release[190]. The authors proposed that a lysosome pathway was activated as the activation of caspase 3 was suppressed by E64d (inhibitor for cathepsin and calpain), and a time-dependent cytosolic release of cathepsin L was observed[190]. Besides caspase 3, direct activation of caspase 8 by cathepsin D in neutrophil apoptosis was also reported[214]. The contradictory and controversial results suggest that the pathway activated could be dependent on apoptotic trigger and cell type. The mechanisms by which cathepsins activate caspase and trigger apoptosis are summarized in Figure 63.
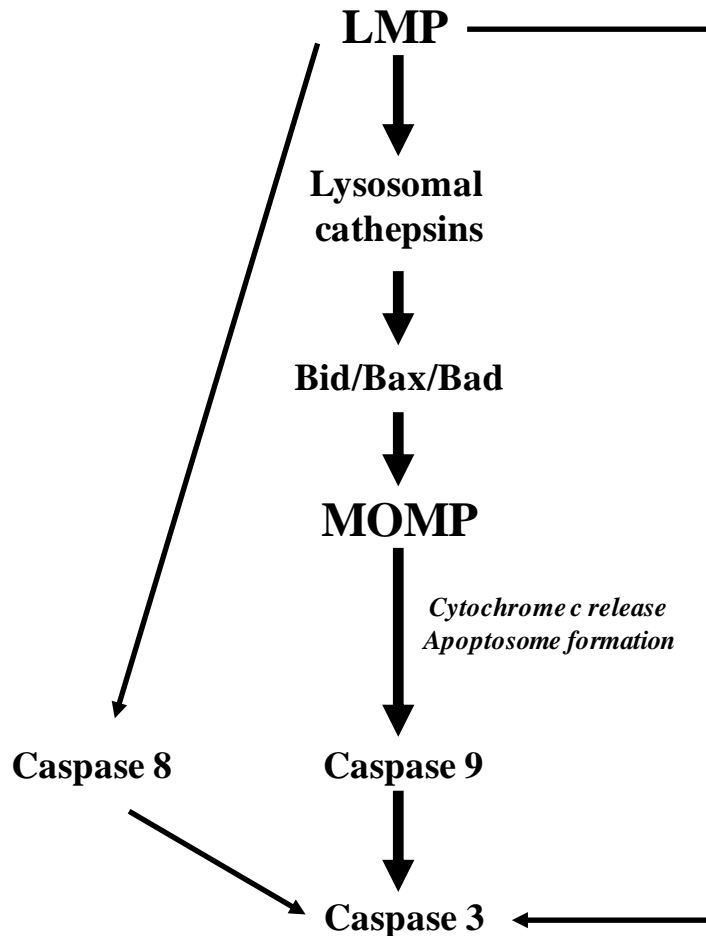
Figure 63. Lysosome-mediated pathway to caspase 3 activation. Upon lysosomal membrane permeabilization, cathepsins are released into the cytoplasm. In most studies, cathepsin-mediated activation of caspase 3 is based on their ability to induce MOMP by cleavage of the Bcl-2 family proteins, such as Bid. MOMP resulted in cytochrome c release followed by activation of caspase cascade and caspase 3 activation. On the other hand, the direct cleavage of caspase 8 and caspase 3 by cathepsins has also been reported. (LMP: lysosomal membrane permeabilization; MOMP: mitochondrial outer membrane permeabilization)

Instead of a single cathepsin, we found that both cathepsin B and L are involved in caspase 3 activation. Compared to caspases, cathepsins have less stringent specificity for substrate cleavage. Therefore, they have always been regarded as simple housekeeping proteases that take part in general proteolysis in the lysosome and have significant redundancy in substrate cleavage. Despite the redundancy in roles, recent studies have also shown that cathepsins have regulated expression and could play

important roles in specific biological function[215]. Furthermore, the deficiency or mutation of cathepsins gene have been linked to inherited genetic diseases[216-218].

In our study, silencing of cathepsin B only partially inhibited caspase 3 activity, suggesting that both cathepsin B and L are important in caspase 3 activation in our system. Cathepsin B and L are ubiquitous and constitutively expressed[219]. It is believed that cathepsin B and L share partial overlapping substrate repertoires and play have redundancy roles in many biological functions[220-222], although they may have different potency in substrate cleaving as regulated by stability in different pH[202]. Nevertheless, opposing actions of cathepsin B and L that support their non-redundancy roles were also reported[223,224]. Both cathepsin B and L have been shown to cleave caspases *in vitro*[137,213], and cathepsin L was proposed to cleave caspase 3 directly *in vivo*. Instead of unspecific proteolytic digestion, the cleavage of caspases by cathepsins results in caspases activation, probably due to the recognition of the canonical caspase recognition sites by cathepsins[225,226].

The involvement of both cathepsin B and L supports a redundancy roles of cathepsins in caspase activation. On the other hand, H_2O_2-induced caspase 3 activation was unaffected by inhibition of cathepsin G (Appendix D) and cathepsin D. This suggested that the redundancy in role could be limited to the same protease family. Cathepsin B and L are cysteine proteases, while cathepsin G is serine protease and cathepsin D is an aspartate protease. It is not known if other cysteine cathepsin, e.g. cathepsin S, has a role to play in caspase 3 activation. This is yet to be investigated in our system.

4.3   Role of iron in H$_2$O$_2$-induced caspase 3 activation

Iron is essential for cells proliferation and viability. It is an important component for key enzymes such as mitochondrial respiratory chain enzymes or essential cofactors for non-heme enzyme such as ribonucleotide reductase. Given the importance of iron, it is not surprising that iron deficiency could result in dysfunction in cellular processes, leading to decreased proliferation and apoptosis. It has been shown that iron deprivation by treatment with iron chelators could induce apoptosis in a caspase-dependent manner[227,228], Nevertheless, it is also shown that iron overload can also induce apoptosis[229]. As a transition metal, iron can take part in redox reaction due to its ability to accept and donate electrons readily. Therefore, excess iron may be potentially dangerous to cells as they catalyse the production of ROS, e.g. OH• via Fenton reactions. The production of excessive ROS could have deleterious effect on cells by inducing DNA damage or oxidation of proteins or lipid peroxidation[230-232].

In our study, we showed that iron was involved in both LMP and caspase 3 activation. Chelation of iron inhibited both LMP and caspase 3 activation. It was also found that only iron chelation at 0h could inhibit caspase activation. Also, extracellular iron was not required in the activation pathway.

Based on this result, we postulated that H$_2$O$_2$ reacts with iron to give rise to a second ROS to initiate the whole system. While it is a known fact that H$_2$O$_2$ can react with iron, it is also possible that H$_2$O$_2$ react with other transition metals in the cells[233 234 235,236]. This is best illustrated in our system that HO-1 expression is not completely decreased by iron chelation. This suggests that the H$_2$O$_2$ signalling is more complicated than expected, there could be a parallel redox pathway (besides the iron

pathway) or there could even be multiple redox pathways which are activated concomitantly upon H_2O_2 treatment. Moreover, it is also not surprising that these pathways could crosstalk with each other at some points along the way. Nevertheless, it would appear that the iron-mediated pathway was directly linked to caspase 3 activation in our system. This is outlined by the fact that iron chelation was able to completely prevent LMP and caspase 3 activation.

The participation of iron at 0h was a crucial finding, because it eliminates the possibility of the iron-mediated reaction in directly inducing LMP, or directly acting on the upstream protease or caspase 3. It has been shown that intralysosomal iron could react with H_2O_2 to generate OH• that initiate peroxidation of lysosomal membrane, leading to LMP[140,198,237,238]. Also, iron chelation was shown to inhibit caspase activation by benzo[a]pyrene as this iron chelation directly inhibits the iron-dependent protease lactoferrin[239]. However, this is unlikely the case in our study because iron chelation after 0h did not affect both LMP and caspase 3 activation, which happened at 2-4h, and 8-48h respectively.

We therefore hypothesized that iron is only involved in the production of a second ROS. While the extracellular iron was of no importance, we deduced that the intracellular labile iron pool (LIP), a pool of chelatable and redox-active iron, is important in our system. Essentially, iron chelation at 0h quenches the availability of LIP to react with H_2O_2. It has been shown that the presence of iron was crucial for intracellular ROS generation upon drug treatment. For example, NADPH-dependent ROS formation after treatment with simvastatin alone or with simvastatin plus lipopolysaccharide was abrogated by pre-treatment with iron chelator

deferoxamine[240]. Furthermore, gentamicin-induced ROS production and apoptosis was prevented in the presence of deferoxamine[241]. On the other hand, iron-mediated ROS generation could be important not only in cell death pathway, but also in physiological-relevant conditions. For example, increased generation of free radicals or reactive oxygen intermediates in the presence of iron was reported to enhance the anti-leishmanial activity of Artemisinin in *Leishmania donovani* promastigotes[242].

For our study, preliminary data in our lab have shown that iron chelation partially prevented the increase in DCF fluorescence. This, together with the effect of iron chelation on HO-1 expression, strongly supports that while iron is not a must for H_2O_2 treatment to induced oxidative stress; it is involved in a pathway specifically for caspase activation.

4.4   Role of peroxynitrite and nitric oxide in caspase 3 activation

In our study, we showed that H_2O_2 treatment resulted in a sustained increase in ROS and RNS level. By using the $ONOO^-$ decomposition catalyst, FeTPPS, LMP and caspase 3 activation was prevented. Beside FeTPPS, the nitric oxide chelator cPTIO was able to partially inhibit LMP and caspase 3 activation. On the other hand, LMP and caspase 3 activation was unaffected by the OH• chelator DMTU. We proposed that upon H_2O_2 treatment, the pathway leading to LMP and caspase 3 activation was redox-regulated, with peroxynitrite and nitric oxide being the main players involved.

NO• is one of the most important second messengers in a variety of cellular functions, particularly in neuronal function[243] and vasodilation[244]. One of the biological characteristics that makes NO• suitable as a second messenger is its ability to traverse across cell membranes rapidly to its targeted signalling complexes. Despite the high motility, NO• is a less reactive as compared to its free radical derivatives generated from NO•'s reaction with other oxygen radicals. $ONOO^-$, generated by the reaction of NO• with $O_2^{•-}$, is the most important free radical derivatives of NO•. $ONOO^-$ shares most of the same biological reaction of NO•, in direct and indirect reactions with cellular macromolecules, but with a higher reactivity. It is believed to be the important mediator of NO• in cell signaling pathway, as well as causing oxidative damage and cytotoxicity.

In our study, we showed that both NO• and $ONOO^-$ are responsible for LMP induction and caspase 3 activation. Dual role of NO• has been reported as inhibitor or activator of apoptosis, depending on the concentration of NO•, free cysteine and the cell type[245,246]. NO• and $ONOO^-$ are capable of s-nitrosylate caspase 3 on the its

active site cysteine, leading to its inactivation and inhibition of apoptosis[247,248]. On the other hand, exogenous addition of NO• has been shown to induce apoptosis via a caspase-dependent mechanism[249]. The dual effect of NO• on caspase activation is said to dependent on the availability of iron or iron-sulfur complexes[250].

Although it is well known that ROS is one of the common mediators of LMP [140,241], ONOO$^-$ or nitric oxide-induced LMP is not reported. We deduced that they are capable of inducing LMP in a way similar to their ability to induce MOMP. NO• and ONOO$^-$ was shown to activate the caspase cascade by induction of MOMP through multiple pathways, such as p53 and MAPK-mediated pathways. Direct modulation of the mitochondrial membrane stability by nitric oxide or ONOO$^-$ has also been shown. A study has shown that high concentration of spermine NONOate (NO• donor) resulted in opening of mitochondrial permeability transition pore via ONOO$^-$ and disulfide bonds formation[251]. Another study shows that when in high concentration, NO• can disrupt the mitochondrial membrane to release cytochrome c, which subsequently activates the caspase cascade and results in apoptosis[252]. Therefore, it is possible that NO• and ONOO$^-$ can also induce LMP by indirect or direct mechanisms similar to their induction of MOMP.

While we have shown that ONOO$^-$ and NO• were involved in our system, several questions remained unanswered: Firstly, how does a bolus dose of H_2O_2 lead to a sustained production of ONOO$^-$ and NO•? Secondly, what is the effect of this sustained increase in ONOO$^-$ and NO• concentration?

The sustained production of nitric oxide in our system could be due to an increased in nitric oxide synthase (NOS) activity. It has been shown that H_2O_2 treatment could result in short term and chronic increase of intracellular NO• level by modulating NOS activity and increased expression of NOS. In endothelial cells, H_2O_2 induced a rapid increase in the endothelial NOS (eNOS) serine 1177 phosphorylation and eNOS activation in a calcium-dependent manner[253]. Another group found that physiological concentrations of H_2O_2 activated eNOS, but not the neuronal NOS (nNOS), via a AMP-activated protein kinase and Akt-dependent pathway[254]. In this study, eNOS was phosphorylated at serine 1177 15 min after exposure to 10μM H_2O_2. On the other hand, long term activation of eNOS by H_2O_2 was mediated by increase gene transcription and increased mRNA stability[255]. Finally, *in vivo* study showed that rats administered intravenously with H_2O_2 showed increased eNOS and nNOS expressions in the renal cortex and medulla in a H_2O_2 dose-dependent manner[256].

Of the three isoforms of NOS, only the neuronal NOS (nNOS) is expressed in L6 myoblasts, the cell line used in our study (Appendix E). The three isoforms of NOS are encoded by different genes and are expressed in different cell types[257]. Given the similarity in protein structures, requirement for post-translational modification mechanisms and cofactors, similar mechanisms of H_2O_2 on eNOS (i.e. via increased phosphorylation or increased gene expression) could be applied on nNOS. We speculate that the initial increase in NO• level upon H_2O_2 treatment was due to increased nNOS activity by modulation of its phosphorylation status. Subsequently, sustained NO• production was achieved by increased nNOS protein level.

Although ONOO⁻ was involved in LMP and caspase 3 activation, it is not sure whether its production was sustained up to 48h, because the DCF dye also detects other ROS. Notably, FeTPPS and cPTIO has differential effect on LMP and caspase 3 activation. FeTPPS efficiently inhibit both LMP and caspase 3 activation while inhibition by cPTIO is only partial. The question here is whether the ONOO⁻ and NO• mediated two separate pathways leading to caspase 3 activation. It is more likely that cPTIO was inefficient to chelate all intracellular NO•, and hence the partial inhibition of LMP and caspase 3 activation. In the presence of superoxide, NO• react quickly to generate ONOO⁻. Preliminary data in lab shows that, upon H_2O_2 treatment, there was an increase in dihydroethidium fluorescence staining, which is specific for superoxide. The production of superoxide upon H_2O_2 treatment could be mediated by NO•. It has been shown that NO• stimulated mitochondrial production of $O2•^-$, H_2O_2 and ONOO⁻ by inhibition of mitochondrial cytochrome c oxidase[258]. Also, all three NOS isoforms are known to produce $O2•^-$ as a by-product, although this usually happen during non-physiological condition, for example, under the condition of L-arginine depletion[259].

In our system, although there was a sustained production of NO• and ROS, cells did not undergo apoptosis. The effect of this sustained oxidative stress is yet to be investigated. Although it is well known that ROS is a classical inducer of apoptosis and necrosis, chronic increase in ROS level has been associated with cell fate other than apoptosis (Figure 64). A few studies reported that pro-oxidant state of the cells favours cell survival. Sustained increased in intracellular ROS level "pre-conditioned" the cells to defence against apoptotic inducer, as ROS inhibit proteasome and Hsp70 expression[260]. Another study showed that resveratrol inhibited H_2O_2-induced

apoptosis by increase in intracellular $O_2^{\bullet-}$ concentration. They proposed that a pro-oxidant state is non-conducive for apoptotic execution[261]. It was also found that cells that have sustained oxidative stress encountered premature senescence as evident by β-galactosidase staining, while not cytotoxic or cytostatic effect was observed[262]. In the long term, increased in ROS level may disrupt the redox homeostasis and signalling in cells, allowing the cells to develop flexible machinery that can adapt to and survive oxidative stress. The dysfunction of redox signalling, together with oncogene activation and loss of p53 allow the cells to evade apoptosis and senescence, thereby leading to tumourigenesis[96].
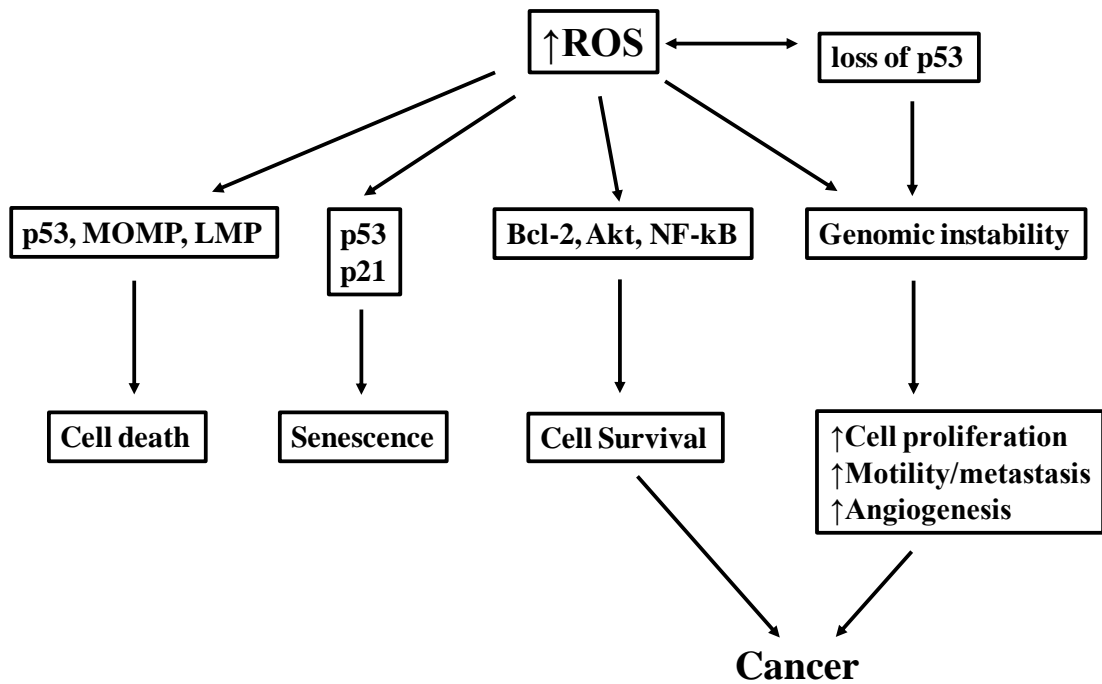
Figure 64. ROS as important determinant of cell fates. Elevated intracellular ROS by exogenous stimuli or endogenous stress resulted in increased oxidative stress. In most cases, such increase in oxidative stress results in cellular senescence and cell death. The development of adaptation mechanisms, such as up-regulation of survival proteins, allows the cells to continue to survive. The increased oxidative stress can induce genomic instability, such as loss of function of the tumour suppressor p53. A vicious cycle is formed when loss of p53 function further contribute to ROS production and genomic instability, leading to abnormal cell proliferation, enhanced cell motility and cancer development. (Adapted from Dunyaporn Trachootham, 2008[96])

4.5   Role of p53 in caspase 3 activation

The role of p53 on caspase 3 activation is well established. Currently, there are two models of p53-mediated caspase 3 activation that centralized on the transcriptional-dependent or –independent mechanisms of p53. In brief, the transcriptional-dependent mechanisms of p53 in apoptosis involves gene regulatory roles in up or down-regulation of apoptotic-related genes. The transcriptional-independent mechanism requires physical association of cytoplasmic p53 with apoptotic-related proteins that activates or inactivates the protein's function. Ultimately, both model result in MOMP, release of cytochrome c and caspase cascade activation.

In our study, we showed that knocking down of p53 partially inhibited LMP and caspase 3 activation. The absence of MOMP in our system led us to propose a new pathway of p53 in caspase 3 activation through LMP and bypassing MOMP.

4.5.1   p53 in LMP and caspase 3 activation

A number of studies have demonstrated the role of LMP as in integral event in p53-mediated apoptosis. In p53-mediated apoptosis, LMP was important as initiator event that triggered mitochondrial event and caspase cascade activation[197]. The inhibition of LMP also inhibited p53-mediated apoptosis, suggesting that LMP could be a common pathway and indispensible to p53-mediated apoptosis[197,263] The importance of LMP was further illustrated by the involvement of cathepsins in p53-mediated apoptosis[264].

The direct role of p53 on LMP induction was highlighted by studies showing that over-expression of p53 could trigger lysosomal membrane destabilization, and result in apoptosis[197]. It is natural to assume that the p53 induced-LMP could have bimodal

178

mechanisms via transcriptional-dependent or transcriptional-independent mode. Currently, the data favoured a transcriptional-independent role of p53 in LMP induction. It was discovered that the p53 protein translocates to the lysosomes during TNF-α induced apoptosis with the aid of Lysosome-associated apoptosis-inducing protein containing the pleckstrin homology and FYVE domains (LAPF) as an adaptor protein[265]. For this translocation, phosphorylation of p53 at serine 15 is of particular importance because LAPF recognized the phosphorylated homology. The co-localization of phospho-p53 (ser15) to lysosomes was also shown to be crucial for LMP induction and cathepsins release in Δ^9-tetrahydrocannabiol[266], or β-amyloid[267]– induced apoptosis. Furthermore, the transcriptional-deficient mutant of p53, p53R175H was able to induce apoptosis through LMP, confirming that p53 does not require its transcriptional function in LMP-mediated apoptosis[265].

Nevertheless, there are studies that supported a transcriptional-dependent role of p53 in LMP induction. For example, p53-dependent LMP induced by ultraviolet B treatment is accompanied by increase Puma and Noxa expression with absence of p53 translocation at the lysosomal membrane. At the same time, both LMP and cathepsins release was inhibited by the p53 transcriptional inhibitor, PFT[268].

PFT is a transcriptional inhibitor of p53 as it was shown to reduce the activation of p53-regulated genes, such as *cyclin G*, *p21*$^{CIP1/WAF1}$ and *mdm2* [154] . It has been used in various studies that addressed the transcriptional dependent/independent role of p53 in apoptosis[269,270]. The exact mechanisms of PFT-α on p53 inhibition remains elusive, although it was suggested that it could modulate the nuclear localization of p53 or the stability of nuclear p53[154]. Notably, PFT has also been shown to inhibit Heat Shock

and Glucocorticoid Signalling Pathways, suggesting it may target HSP complexes that sequestrate inactive HSF1, GR, and p53 proteins in the cytoplasm[271].

In our study, LMP and caspase 3 activation was partially inhibited by molecular knock-down of p53. While PFT effectively decreased p53-mediated p21 expression, it had no effect on caspase 3 activation. This suggests that p53 induced caspase 3 activation via a transcriptional-independent pathway. Furthermore, cytoplasmic phosphorylation of p53 on serine 15 was also detected at time points preceded LMP. We deduced that the cytoplasmic phospho-p53 (ser 15) might translocate to the lysosomal membrane and trigger LMP.

It should be noted the increase in serine 15 phosphorylation was also detected with the nuclear pool of p53. As master gene of cell regulatory mechanism, p53 is tightly regulated through modulation of its localization, post-translational modification and protein stability. In normal, unstressed cells, p53 shuttle between the nucleus and cytoplasm and was maintained at low level through MDM2-dependent degradation[272]. The localization of p53 is variable, depending on the cell type[273] and cell cycle phase[274,275]. In L6 myoblasts, p53 localizes predominantly in the nucleus. Upon H_2O_2 treatment, p53 protein is quickly stabilized and phosphorylated at serine 15. While we deduced that the cytoplasmic phospho-p53 (ser15) was important for LMP induction, we do not yet know the function of nuclear phospho-p53 (ser15). Serine 15 phosphorylation is important for p53 protein stability as it reduces the binding of p53-MDM2 complex. Serine 15 phosphorylation also enhances p53 transcriptional activity as it promotes p53 DNA binding and recruitment of transcriptional co-activators[276].

One important transcription target of p53 regulated by ser15 phosphorylation is p21, the main regulator of cell cycle checkpoint and progression[277,278].

Interestingly, p21 expression remained unchanged after H_2O_2 treatment. Furthermore, H_2O_2-induced cell growth arrest was dependent on p53 but was independent of cell cycle regulation, as no arrest at any phase of the cell cycle was observed. How p53 exert its role in cell growth independently of p21 and cell cycle control is unknown. One possible explanation is that the cells experienced a generalized slow down in all cell cycle phases and hence an overall decrease in proliferation. Such idea was proposed by Tao et al., where they showed that hyposmosis induced growth arrest in two pancreatic (AsPC-1 and PaCa-2) carcinoma cell lines without any change to the cell cycle profile[279]. They proposed that a "generalized cell cycle arrest" has occurred and this together with the formation of giant cells and cytoplasmic vacuolation in absence of apoptosis, are markers for a global cell cycle catastrophe. They also proposed that cell cycle catastrophe was due to decreased cell cycle-related proteins expression (Cdc2, cdk2, Cdk4, cyclin B1, and cyclin D3) as well as an overall decrease in cellular protein synthesis[279].

4.5.2 Redox-regulation of p53

The activation of p53 by oxidative signal, either endogenous or exogenous has been reported. Microarray analysis of H_2O_2-responsive genes in H_2O_2-treated human cells share significant overlapping with p53 target genes[280]. During oxidative stress, sensor molecules detect oxidative stress in cells and trigger signalling transduction pathways which determine the effect of oxidative stress, whether it is reversible, or leading to cell cycle arrest, senescence or apoptosis. In oxidative stress-mediated DNA damage,

the Ataxia Telangiectasia Mutated (ATM) kinase is the major sensor that effect through p53-mediated signal transduction network[281]. Phosphorylation of p53 by ATM is crucial in initiating the p53-mediated DNA Damage Response. Besides ATM, other sensors that phosphorylate p53 include DNA-dependent protein kinase (DNA-PK)[281] and the Ataxia Telangiectasia and Rad-3-related (ATR) kinase[282]. Together, ATM, DNA-PK and ATR constitute a myriad of p53 signalling transduction in response to DNA damage[149].

Other than DNA damage stress-signalling pathway, increase in cellular oxidative stress can trigger the activation of the MAPK that subsequently activated p53 through phosphorylation at distinct residues. The three MAPK, c-Jun N-terminal kinase (JNK)[283], Extracellular-signal-regulated kinases (ERK)[284], and p38 MAPK[285], have been shown to activate p53. It is important to note that activation of MAPK-p53 signalling are not limited to ROS, but also common pathway in other stress-inducing pathway such as in induced-genotoxicity by ultra-violet B[286,287]. Also, although phosphorylation is important for p53 activation, there are other covalent post-translational modifications, such as ubiquitylation[288], acetylation[289], neddylation[290], sumoylation[291] , and methylation[292] , that are critical to p53 protein stability and function. Some of the post-translational modifications, such as acetylation[293] and sumoylation[294], are associated with oxidative stress.

Notably, p53 itself is redox-sensitive due to the presence of conserved cysteine residues. These cysteine residues contain redox-sensitive thiol groups (-SH) and are prone to oxidative modification. The effect of such oxidative modification is variable and dependent on the residue modified and the type of modification[295]. Most of the

time, thiol oxidation of p53 induce conformational change that affects its DNA binding ability and hence transcriptional role, as well as p53 protein stability[296]. It has been suggested that redox modification of p53 is a mean of regulation of p53 transcriptional function that allows it to preferential binding to individual target genes[297]. For example, changes in the Cys 277 redox state in the DNA binding domain of p53 decreases its binding to GADD45 but not to p21[297].

It is important to recognize that p53 does not just act downstream of ROS. Within the p53 signaling transduction network, cross talk between p53 and ROS pathway regulates redox balance and determine the cell fate. p53 could have anti-oxidant or pro-oxidant role depending on the degree of oxidative stress[145]. It was also suggested that how p53 responses to ROS depends on its protein level[295]. In response to different amount of stress, distinct p53 signalling pathways are activated, resulting in different cell fate. Under normal physiological condition or low level of oxidative stress, p53 exert its anti-oxidant role by transcriptionally activating several antioxidant genes, such as mammalian sestrin homologs 1 and 2, glutathione peroxidase 1 (GPX1), and mitochondrial SOD2[298-301]. The transcription of these genes is important to bring down or maintain the ROS level at a physiological level. On the other hand, high oxidative stress level results in p53 activation of pro-oxidant genes, such as PIG3 and proline oxidase[298,302], or inhibition of anti-oxidant genes, such as SOD2 and Nrf2[303-305]. Furthermore, p53 induces the expression of pro-apoptotic genes, Noxa, Bax and Puma that mediate cytochrome c release from the mitochondria and caspase cascade activation[306,307].

The overall effect of the pro-oxidant function of p53 is a further accumulation of ROS

accumulation and this contribute to p53-induced cell death or cell senescence. Figure

65 summarizes the context-dependent roles of p53 during oxidative stress.
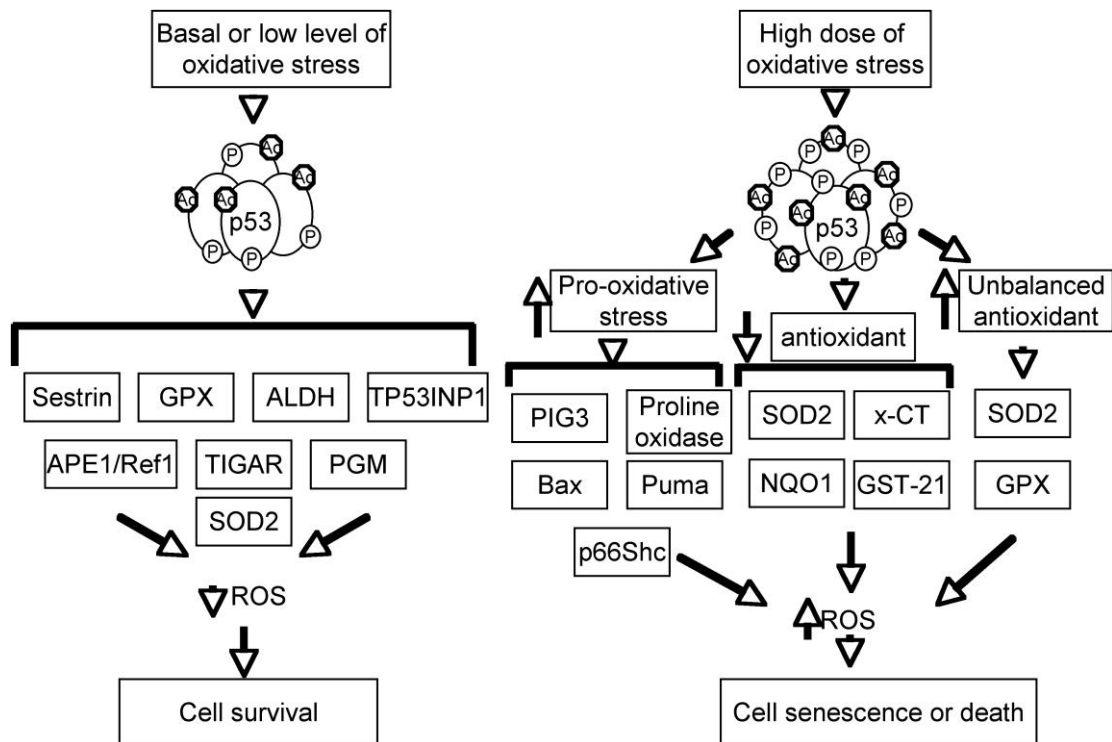
Figure 65. Context-dependent roles of p53 during oxidative stress. p53 could have anti-oxidant or pro-oxidant roles depending on the level of oxidative stress. By transcriptionally regulating distinct target genes, p53 is key determinant in cell fate during oxidative stress. At basal or low level of oxidative stress, p53 induces the expression of anti-oxidant genes, to decrease ROS and promote cell survival. At high level of oxidative stress, p53 induces the expression of pro-oxidant genes while inhibits the expression of anti-oxidant genes. This results in increase ROS level and promotes cell senescence or cell death. (Diagram adapted from Dongping Liu and Yang Xu, 2011[145])

In our study, while we have shown that p53 is redox-dependent, the increase of DCF and DAF fluorescence was independent of p53. We also found that knock down of p53 further elevated the ROS level, suggesting that p53 may have an anti-oxidant role in our system. There is a question that remains unanswered: chelation of iron and $ONOO^-$ inhibited p53 phosphorylation. It is not known whether it is due to a direct effect of ROS on p53 or through ROS-mediated signalling. We found that chelation of iron and $ONOO^-$ could also inhibit γ-H2AX phosphorylation and prevented DNA damage (Appendix F). Therefore, p53 could be phosphorylated by ATM, or other DNA damage response protein. The MAPK are also possible candidates because their phosphorylation in the presence of oxidative/nitrosative stress is well known. Secondly, whether p53 has an anti-oxidant role and how it exerts this anti-oxidant function in our system is yet to be explored in detail.

4.6   A novel role of caspase 3 in lysosome biogenesis through regulation of TFEB

Where caspase 3 is activated but apoptosis is not induced, it is of great interest what the role played by caspase 3. In our study, caspase 3 could play an important role in lysosomal biogenesis in absence of apoptosis. H_2O_2 treatment resulted in a dramatic increase in the numbers and sizes of lysosome. At the same time, we discovered that H_2O_2 induced the expression and nuclear localization of Transcriptional Factor for EB (TFEB), the master gene for lysosome biogenesis. The increase in lysosome biogenesis as well as TFEB regulation was found to be caspase 3-dependent. In view of the results, we proposed a novel role of caspase 3 in regulating lysosome biogenesis, through modulation of TFEB gene expression and localization.

Current model of lysosome biogenesis by TFEB

In the cells, lysosomes are specialized organelles that are critical in pH-dependent macromolecules degradation endocytic, heterophagy and autophagy pathways. Besides this catabolic function, lysosomes are also involved in other physiological functions, such as cholesterol homeostasis, plasma membrane repair, bone and tissue remodelling, pathogen defence and cell death[308]. The process of lysosome biogenesis involves systematic co-expression and co-localization of lysosome soluble and membrane proteins that integrated with the cellular endocytic pathway[308]. Furthermore, lysosomal functions and compositions vary depending on cell type, age, and exogenous stimulus[309]. Therefore, it has been postulated that lysosome biogenesis is controlled and coordinated by a centralized cellular program.

In fact, it is recently discovered that lysosome biogenesis is controlled by a master gene TFEB[155]. TFEB is a basic Helix-Loop-Helix leucine zipper transcription factor that belongs to the microphatalmia-transcription factor E family[310]. It has been shown that TFEB over-expression increased lysosomes size and numbers per cells, as well as the transcription of lysosomal targeted genes[155]. Among the lysosomal targeted genes regulated by TFEB are lysosome resident proteins, such as lysosomal hydrolases, cathepsins, lysosomal membrane proteins, and components of the vacuolar H+-ATPase. These proteins carry out important functions of lysosomes, such as substrate degradation, lysosomal acidification[155,311]. The role of TFEB in autophagy was demonstrated when knock down of TFEB inhibited autophagy while over expression increased the number of autophagosomes[312]. Autophagy-related genes, including *RRAGC* and *UVRAG*, which are non lysosomal proteins and are key factors regulators of autophagy[313,314], were up-regulated after TFEB over-expression[312].

It is shown that the phosphorylation status of TFEB is critical for its regulation[312]. Under physiological condition, phosphorylation of serine 142 is critical for the sequestration of TFEB in the cytoplasm and to keep the protein in inactive state[312,315]. Upon nutrient deprivation, serine 142 of TFEB is dephosphorylated and this enables TFEB to translocate to the nucleus to initiate its gene transcription. Currently, two kinases are identified to phosphorylate TFEB at ser142: ERK2[312] and mTOR[315]. The ERK2-TFEB complex was found in starved cells, but not normal cells. Knock down of ERK2 induced TFEB nuclear translocation, while constitutive activated ERK pathway resulted in down-regulation of TFEB target gene expression during starvation[312]. The mTOR model depends on the ability of TFEB to shuffle between lysosomal compartment and cytoplasm compartment. When TFEB binds to the

lysosomal surface, it is phosphorylated by mTOR complex 1 (mTORC1), which is held in place by the RagGTPase and Ragulator complex[315]. In case of nutrient deprivation and lysosomal stress, RagGTPase is inactivated, resulting in mTORC1 dissociation from lysosome. Displace mTORC1 is unable to re-phosphorylate TFEB, and this results in translocation of unphosphorylated TFEB into the nucleus. This model links TFEB regulation with lysosomal stress where lysosome itself acts as a sensor for its own defect and activates the repair of defective nutrient and/or pH status of the lysosome[315]. The two model of TFEB regulation is depicted in Figure 66.

A)

B)
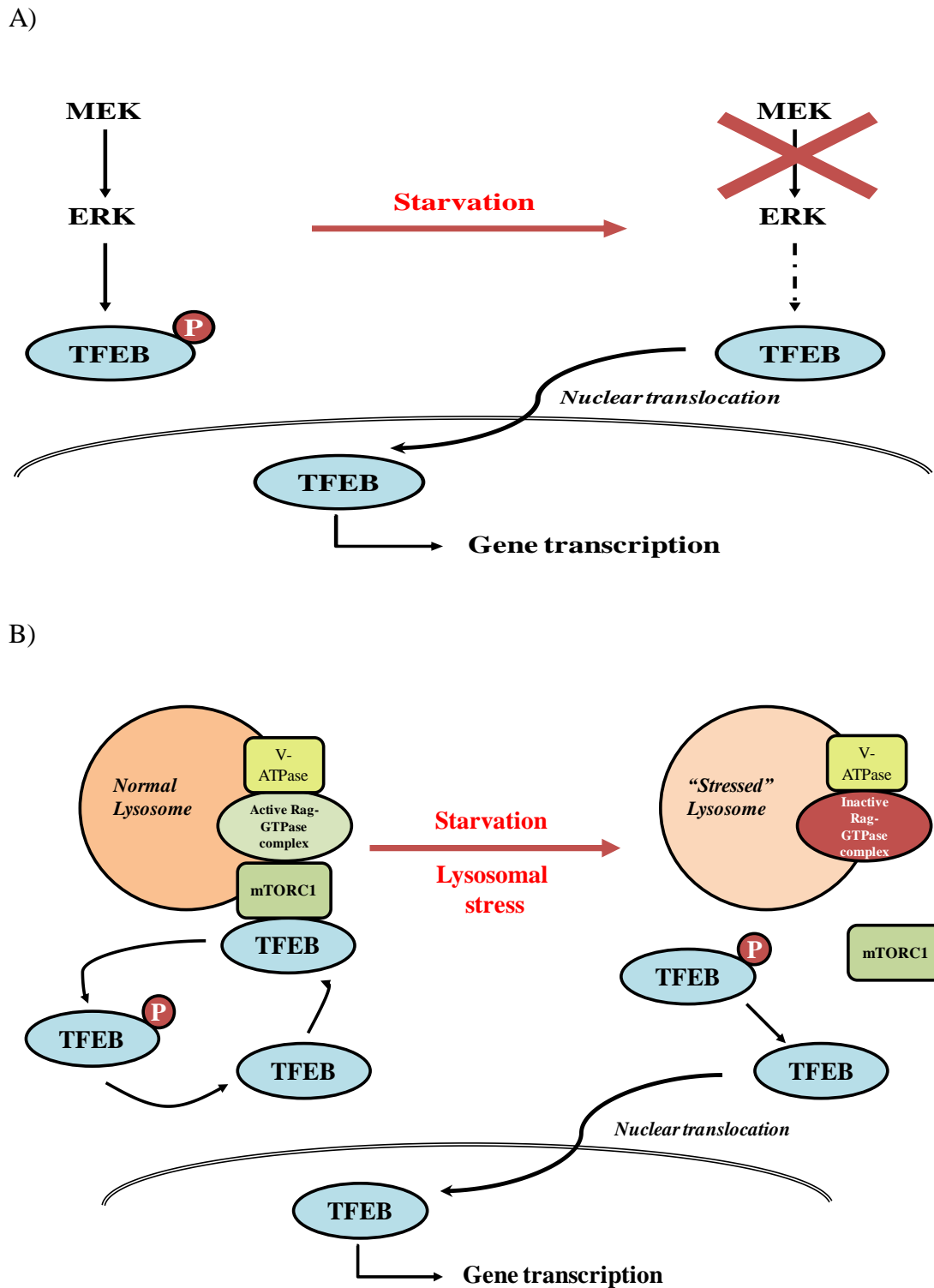
Figure 66. Models depicting regulation of TFEB localization and activation by ERK and mTOR. In both models, the phosphorylation on TFEB residue serine 142 is of great importance for its cytoplasmic sequestration. (A) The MEK-ERK pathway regulates TFEB by ERK-mediated phosphorylation. Upon starvation, shut down of MEK-ERK pathway resulting in dephosphorylation of TFEB and its nuclear translocation. (B) Under physiological condition, mTORC1 is recruited by V-ATPase and active Rag complex (consists of RagGTPases and Ragulator) to the lysosome

surface. TFEB binds to mTORC1 and is re-phosphorylated. Upon starvation and lysosomal stress, the Rag complex is inactivated, resulting in dissociation of mTORC1 from the lysosome surface. Dissociated mTORC1 is unable to phosphorylate TFEB. This results in TFEB dephosphorylation and translocation into the nucleus. (Adapted from Settembre 2011[312], and Settembre 2012[315])

How caspase 3 regulates TFEB is unknown. We speculate that caspase 3 could be involved in cleaving one of the members of the mTORC1 associated with TFEB, leading to complex dissociation and TFEB dephosphorylation. Alternatively, caspase 3 could be disrupting the upstream pathway leading to mTOR and ERK activation. Caspase 3 cleavage of mTORC1 or ERK is unreported. However, caspase 3 could cleave MEK, the upstream kinase of ERK[316], or Kinase suppressor of Ras1 (KSR1), the protein scaffold that facilitates ERK pathway[317]. While the regulation of TFEB seems to be a cytoplasmic event, it should be noted that H_2O_2-induced activated caspase 3 is sustained in nucleus, hence a nuclear substrate should be cleaved that leads to dephosphorylation of TFEB. How a nuclear-localized caspase 3 is able to regulate a cytoplasmic event is again a challenging question that remains without an answer. We believe this is the first study reporting on caspase 3's role in lysosome biogenesis.

It should be noted that H_2O_2 has been shown to be involved in the regulation of PI3K-AKT-mTOR pathway in a number of studies. H_2O_2 has been shown to inhibit mTOR through AMPKα activation[318] or through a Bcl-2/E1B 19kDa interacting protein 3 (BNIP3)-dependent pathway[319], leading to autophagy or cell death. On the other hand, it has also been shown that activation of the PI3K-AKT-mTOR pathway is crucial in H_2O_2-induced mitogenic signalling[320]. Therefore, H_2O_2 could regulate mTOR through multiple pathways resulting in different cellular outcome. Correspondingly, H_2O_2-

induced TFEB activation and lysosome biogenesis could be caspase-dependent, or caspase-independent, as a result of mTOR suppression by H_2O_2.

In our study, we found increase in lysosomal volume increase after 8h and cathepsin B expression after 24h. This is in correlation to the increased expression and nuclear localization of TFEB, However, the implication of increased TFEB signalling pathway and lysosome biogenesis in our system is unknown. It has been shown that in the cells of Lysosome Storage Disorders mouse model, TFEB has a predominant nuclear localization[155]. This indicates that the TFEB signalling is important in the intralysosomal storage of undegraded molecules, because activation of TFEB enhance lysosome-dependent degradation pathways[155]. On the other hand, increase in lysosome and autophagosome numbers is associated with senescence and autophagy respectively. Senescence associated-β-gal activity that is usually detected in senescent cells is attributed to increased lysosomal-β-galactosidase activity[321]. Also, TFEB nuclear translocation is associated with the induction of autophagy[312]. In our system, H_2O_2 treatment does not induce apoptosis, but could be potentiating the cells to premature senescence or autophagy. Future work regarding our study could include biochemical analysis of markers of senescence and autophagy. This is essential in understanding the cell fate induced by H_2O_2.

4.7   Conclusion

In summary, we have identified an unconventional pathway of caspase 3 activation during H_2O_2-induced oxidative stress. By comparing the activation of caspase 3 in our system to that induced by the classical apoptotic trigger, STS, we proposed three possible mechanisms for caspase's non-apoptotic roles regulation: a threshold for caspase 3 activation, sustained nuclear localization of activated caspase 3, and an alternative pathway for caspase 3 activation.

Also, we have presented a lysosome-mediated pathway of caspase 3 activation that involves ROS and p53. Starting with a redox reaction involving iron, the H_2O_2-induced caspase 3 activation involved $ONOO^-$, $NO•$, and p53 as the upstream signals to induce LMP. The activation of p53 was peroxynitrite-dependent but nitric oxide-independent. We postulated that LMP could be induced directly by $ONOO^-$ and/or $NO•$, and it could also be induced by p53 in a peroxynitrite-dependent manner. LMP resulted in cathepsin B and L release into the cytoplasm. Cathepsin B and L activated caspase 3 and activated caspase 3 was translocated into the nucleus.

Lastly, we discovered a novel role of caspase 3 in lysosome biogenesis. For the first time, caspase 3 was found to regulate the gene expression as well as the nuclear localization of TFEB, the master gene for lysosome biogenesis. Although we do not yet know the outcome of this caspase 3-mediated TFEB gene regulation, we postulate that it may potentiate the cells to cellular senescence or autophagy. The discovery of caspase 3 role in lysosome biogenesis adds on to its non-apoptotic physiological role. How caspase 3 regulate TFEB gene expression and nuclear localization is another

story that is of great interest as this provides new insides to caspase function and regulation.

The pathway of H_2O_2-induced caspase 3 activation is presented in Figure 67.
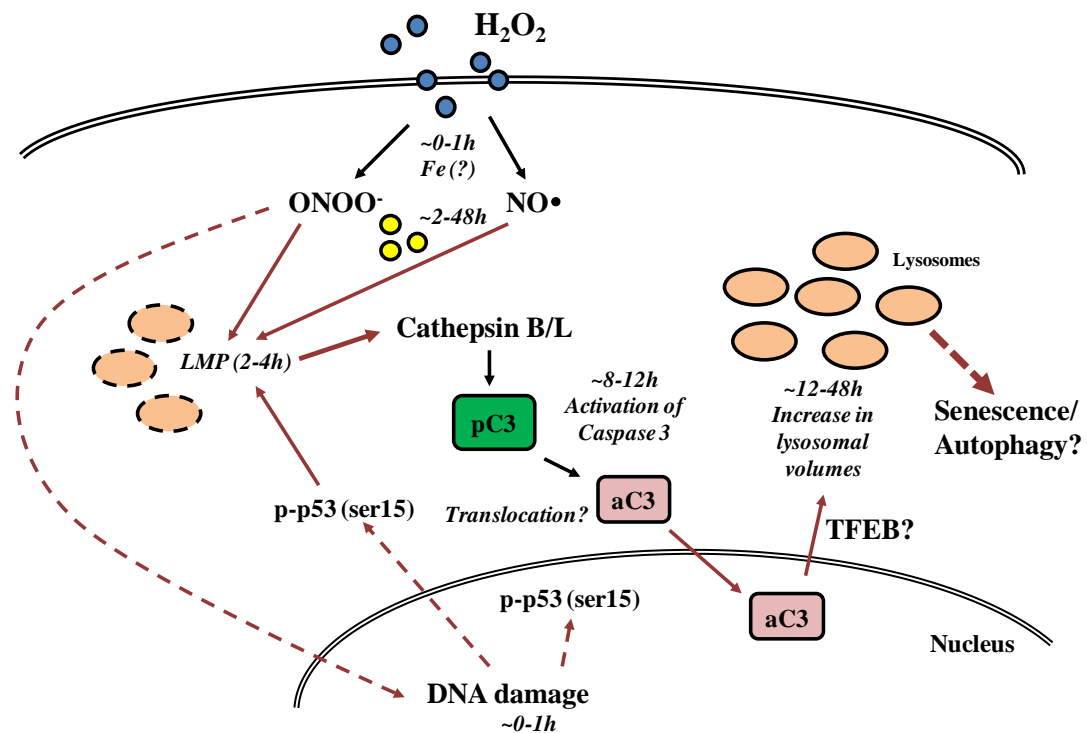
Figure 67. Summary of H_2O_2-induced caspase 3 activation. Upon H_2O_2 treatment in the presence of iron, $ONOO^-$ and $NO\bullet$ were produced. At the same time, p53 was phosphorylated in $ONOO^-/NO\bullet$ – dependent manner. Together, $ONOO^-$, $NO\bullet$, and p53 could induce LMP at 2-4h. This resulted in cathepsin B and L release from the lysosome and activates caspase 3. After activation, cleaved caspase 3 was translocated into the nucleus. While not inducing apoptosis, caspase 3 was found to regulate lysosome biogenesis through regulation of TFEB gene expression and localization. The final outcome of caspase 3 activation and increased lysosome biogenesis is yet to be investigated. (pC3: procaspase 3, aC3: activated caspase 3)

REFERENCES

1. Chowdhury I, Tharakan B, Bhat GK. Caspases - an update. Comp Biochem Physiol B Biochem Mol Biol. 2008;151(1):10-27.

2. Deveraux QL, Roy N, Stennicke HR, Van Arsdale T, Zhou Q, Srinivasula SM et al. IAPs block apoptotic events induced by caspase-8 and cytochrome c by direct inhibition of distinct caspases. EMBO J. 1998;17(8):2215-23.

3. Fuentes-Prior P, Salvesen GS. The protein structures that shape caspase activity, specificity, activation and inhibition. Biochem J. 2004;384(Pt 2):201-32.

4. Lamkanfi M, Declercq W, Kalai M, Saelens X, Vandenabeele P. Alice in caspase land. A phylogenetic analysis of caspases from worm to man. Cell Death Differ. 2002;9(4):358-61.

5. Muzio M, Chinnaiyan AM, Kischkel FC, O'Rourke K, Shevchenko A, Ni J et al. FLICE, a novel FADD-homologous ICE/CED-3-like protease, is recruited to the CD95 (Fas/APO-1) death--inducing signaling complex. Cell. 1996;85(6):817-27.

6. Sprick MR, Rieser E, Stahl H, Grosse-Wilde A, Weigand MA, Walczak H. Caspase-10 is recruited to and activated at the native TRAIL and CD95 death-inducing signalling complexes in a FADD-dependent manner but can not functionally substitute caspase-8. EMBO J. 2002;21(17):4520-30.

7. Sakamaki K, Satou Y. Caspases: evolutionary aspects of their functions in vertebrates. Journal of fish biology. 2009;74(4):727-53.

8. MacKenzie SH, Clark AC. Death by caspase dimerization. Adv Exp Med Biol. 2012;747:55-73.

9. Salvesen GS, Dixit VM. Caspase activation: the induced-proximity model. Proc Natl Acad Sci U S A. 1999;96(20):10964-7.

10. Boatright KM, Renatus M, Scott FL, Sperandio S, Shin H, Pedersen IM et al. A unified model for apical caspase activation. Mol Cell. 2003;11(2):529-41.

11. Renatus M, Stennicke HR, Scott FL, Liddington RC, Salvesen GS. Dimer formation drives the activation of the cell death protease caspase 9. Proc Natl Acad Sci U S A. 2001;98(25):14250-5.

12. Shi Y. Caspase activation: revisiting the induced proximity model. Cell. 2004;117(7):855-8.

13. Launay S, Hermine O, Fontenay M, Kroemer G, Solary E, Garrido C. Vital functions for lethal caspases. Oncogene. 2005;24(33):5137-48.

14. Häcker G. The morphology of apoptosis. Cell Tissue Res. 2000;301(1):5-17.

15. Ozben T. Oxidative stress and apoptosis: impact on cancer therapy. J Pharm Sci. 2007;96(9):2181-96.

16. Scheller C, Knöferle J, Ullrich A, Prottengeier J, Racek T, Sopper S et al. Caspase inhibition in apoptotic T cells triggers necrotic cell death depending on the cell type and the proapoptotic stimulus. J Cell Biochem. 2006;97(6):1350-61.

17. Fernandes-Alnemri T, Litwack G, Alnemri ES. CPP32, a novel human apoptotic protein with homology to Caenorhabditis elegans cell death protein Ced-3 and mammalian interleukin-1 beta-converting enzyme. J Biol Chem. 1994;269(49):30761-4.

18. Cohen GM. Caspases: the executioners of apoptosis. Biochem J. 1997;326 (Pt 1):1-6.

19. Geng YJ, Azuma T, Tang JX, Hartwig JH, Muszynski M, Wu Q et al. Caspase-3-induced gelsolin fragmentation contributes to actin cytoskeletal collapse, nucleolysis, and apoptosis of vascular smooth muscle cells exposed to proinflammatory cytokines. Eur J Cell Biol. 1998;77(4):294-302.

20. Jänicke RU, Ng P, Sprengart ML, Porter AG. Caspase-3 is required for alpha-fodrin cleavage but dispensable for cleavage of other death substrates in apoptosis. J Biol Chem. 1998;273(25):15540-5.

21. Slee EA, Adrain C, Martin SJ. Executioner caspase-3, -6, and -7 perform distinct, non-redundant roles during the demolition phase of apoptosis. J Biol Chem. 2001;276(10):7320-6.

22. Chang J, Xie M, Shah VR, Schneider MD, Entman ML, Wei L et al. Activation of Rho-associated coiled-coil protein kinase 1 (ROCK-1) by caspase-3 cleavage plays an essential role in cardiac myocyte apoptosis. Proc Natl Acad Sci U S A. 2006;103(39):14495-500.

23. Kato K, Yamanouchi D, Esbona K, Kamiya K, Zhang F, Kent KC et al. Caspase-mediated protein kinase C-delta cleavage is necessary for apoptosis of vascular smooth muscle cells. Am J Physiol Heart Circ Physiol. 2009;297(6):H2253-61.

24. Jänicke RU, Sprengart ML, Wati MR, Porter AG. Caspase-3 is required for DNA fragmentation and morphological changes associated with apoptosis. J Biol Chem. 1998;273(16):9357-60.

25. Kivinen K, Kallajoki M, Taimen P. Caspase-3 is required in the apoptotic disintegration of the nuclear matrix. Exp Cell Res. 2005;311(1):62-73.

26. Yang XH, Sladek TL, Liu X, Butler BR, Froelich CJ, Thor AD. Reconstitution of caspase 3 sensitizes MCF-7 breast cancer cells to doxorubicin- and etoposide-induced apoptosis. Cancer Res. 2001;61(1):348-54.

27. Blanc C, Deveraux QL, Krajewski S, Jänicke RU, Porter AG, Reed JC et al. Caspase-3 is essential for procaspase-9 processing and cisplatin-induced apoptosis of MCF-7 breast cancer cells. Cancer Res. 2000;60(16):4386-90.

28. de Bruin EC, Medema JP. Apoptosis and non-apoptotic deaths in cancer development and treatment response. Cancer Treat Rev. 2008;34(8):737-49.

29. Schneider P, Bodmer JL, Thome M, Hofmann K, Holler N, Tschopp J. Characterization of two receptors for TRAIL. FEBS Lett. 1997;416(3):329-34.

30. Youle RJ, Strasser A. The BCL-2 protein family: opposing activities that mediate cell death. Nat Rev Mol Cell Biol. 2008;9(1):47-59.

31. Gu Q, Wang JD, Xia HHX, Lin MCM, He H, Zou B et al. Activation of the caspase-8/Bid and Bax pathways in aspirin-induced apoptosis in gastric cancer. Carcinogenesis. 2005;26(3):541-6.

32. Gdynia G, Grund K, Eckert A, Böck BC, Funke B, Macher-Goeppinger S et al. Basal caspase activity promotes migration and invasiveness in glioblastoma cells. Mol Cancer Res. 2007;5(12):1232-40.

33. Ohsawa S, Hamada S, Yoshida H, Miura M. Caspase-mediated changes in histone H1 in early apoptosis: prolonged caspase activation in developing olfactory sensory neurons. Cell Death Differ. 2008;15(9):1429-39.

34. Bassnett S, Mataic D. Chromatin degradation in differentiating fiber cells of the eye lens. J Cell Biol. 1997;137(1):37-49.

35. Dahm R, Gribbon C, Quinlan RA, Prescott AR. Changes in the nucleolar and coiled body compartments precede lamina and chromatin reorganization during fibre cell denucleation in the bovine lens. Eur J Cell Biol. 1998;75(3):237-46.

36. Lee A, Morrow JS, Fowler VM. Caspase remodeling of the spectrin membrane skeleton during lens development and aging. J Biol Chem. 2001;276(23):20735-42.

37. Zermati Y, Garrido C, Amsellem S, Fishelson S, Bouscary D, Valensi F et al. Caspase activation is required for terminal erythroid differentiation. J Exp Med. 2001;193(2):247-54.

38. Kolbus A, Pilat S, Husak Z, Deiner EM, Stengl G, Beug H et al. Raf-1 antagonizes erythroid differentiation by restraining caspase activation. J Exp Med. 2002;196(10):1347-53.

39. Fernando P, Megeney LA. Is caspase-dependent apoptosis only cell differentiation taken to the extreme? FASEB journal : official publication of the Federation of American Societies for Experimental Biology. 2007;21(1):8-17.

40. Miura M, Chen XD, Allen MR, Bi Y, Gronthos S, Seo BM et al. A crucial role of caspase-3 in osteogenic differentiation of bone marrow stromal stem cells. J Clin Invest. 2004;114(12):1704-13.

41. Fernando P, Brunette S, Megeney LA. Neural stem cell differentiation is dependent upon endogenous caspase 3 activity. FASEB J. 2005;19(12):1671-3.

42. Janzen V, Fleming HE, Riedt T, Karlsson G, Riese MJ, Lo Celso C et al. Hematopoietic stem cell responsiveness to exogenous signals is limited by caspase-3. Cell stem cell. 2008;2(6):584-94.

43. Morioka K, Toné S, Mukaida M, Takano-Ohmuro H. The apoptotic and nonapoptotic nature of the terminal differentiation of erythroid cells. Exp Cell Res. 1998;240(2):206-17.

44. Zandy AJ, Lakhani S, Zheng T, Flavell RA, Bassnett S. Role of the executioner caspases during lens development. J Biol Chem. 2005;280(34):30263-72.

45. De Botton S, Sabri S, Daugas E, Zermati Y, Guidotti JE, Hermine O et al. Platelet formation is the consequence of caspase activation within megakaryocytes. Blood. 2002;100(4):1310-7.

46. Arama E, Agapite J, Steller H. Caspase activity and a specific cytochrome C are required for sperm differentiation in Drosophila. Dev Cell. 2003;4(5):687-97.

47. Okuyama R, Nguyen BC, Talora C, Ogawa E, Tommasi di Vignano A, Lioumi M et al. High commitment of embryonic keratinocytes to terminal differentiation through a Notch1-caspase 3 regulatory mechanism. Dev Cell. 2004;6(4):551-62.

48. Fernando P, Kelly JF, Balazsi K, Slack RS, Megeney LA. Caspase 3 activity is required for skeletal muscle differentiation. Proc Natl Acad Sci U S A. 2002;99(17):11025-30.

49. Fujita J, Crane AM, Souza MK, Dejosez M, Kyba M, Flavell RA et al. Caspase activity mediates the differentiation of embryonic stem cells. Cell stem cell. 2008;2(6):595-601.

50. Sordet O, Rébé C, Plenchette S, Zermati Y, Hermine O, Vainchenker W et al. Specific involvement of caspases in the differentiation of monocytes into macrophages. Blood. 2002;100(13):4446-53.

51. Oomman S, Strahlendorf H, Dertien J, Strahlendorf J. Bergmann glia utilize active caspase-3 for differentiation. Brain Res. 2006;1078(1):19-34.

52. Yan XX, Najbauer J, Woo CC, Dashtipour K, Ribak CE, Leon M. Expression of active caspase-3 in mitotic and postmitotic cells of the rat forebrain. J Comp Neurol. 2001;433(1):4-22.

53. Alam A, Cohen LY, Aouad S, Sékaly RP. Early activation of caspases during T lymphocyte stimulation results in selective substrate cleavage in nonapoptotic cells. J Exp Med. 1999;190(12):1879-90.

54. Woo M, Hakem R, Furlonger C, Hakem A, Duncan GS, Sasaki T et al. Caspase-3 regulates cell cycle in B cells: a consequence of substrate specificity. Nat Immunol. 2003;4(10):1016-22.

55. Wong SH, Santambrogio L, Strominger JL. Caspases and nitric oxide broadly regulate dendritic cell maturation and surface expression of class II MHC proteins. Proc Natl Acad Sci U S A. 2004;101(51):17783-8.

56. Posmantur R, Wang KK, Gilbertsen RB. Caspase-3-like activity is necessary for IL-2 release in activated Jurkat T-cells. Exp Cell Res. 1998;244(1):302-9.

57. Zhang Y, Center DM, Wu DM, Cruikshank WW, Yuan J, Andrews DW et al. Processing and activation of pro-interleukin-16 by caspase-3. J Biol Chem. 1998;273(2):1144-9.

58. Acarin L, Villapol S, Faiz M, Rohn TT, Castellano B, González B. Caspase-3 activation in astrocytes following postnatal excitotoxic damage correlates with cytoskeletal remodeling but not with cell death or proliferation. Glia. 2007;55(9):954-65.

59. Huesmann GR, Clayton DF. Dynamic role of postsynaptic caspase-3 and BIRC4 in zebra finch song-response habituation. Neuron. 2006;52(6):1061-72.

60. Li Z, Jo J, Jia JM, Lo SC, Whitcomb DJ, Jiao S et al. Caspase-3 activation via mitochondria is required for long-term depression and AMPA receptor internalization. Cell. 2010;141(5):859-71.

61. Droin N, Cathelin S, Jacquel A, Guéry L, Garrido C, Fontenay M et al. A role for caspases in the differentiation of erythroid cells and macrophages. Biochimie. 2008;90(2):416-22.

62. Bassnett S. On the mechanism of organelle degradation in the vertebrate lens. Exp Eye Res. 2009;88(2):133-9.

63. Rohn TT, Cusack SM, Kessinger SR, Oxford JT. Caspase activation independent of cell death is required for proper cell dispersal and correct morphology in PC12 cells. Exp Cell Res. 2004;295(1):215-25.

64. Walsh JG, Cullen SP, Sheridan C, Lüthi AU, Gerner C, Martin SJ. Executioner caspase-3 and caspase-7 are functionally distinct proteases. Proc Natl Acad Sci U S A. 2008;105(35):12815-9.

65. Gibson S, Widmann C, Johnson GL. Differential involvement of MEK kinase 1 (MEKK1) in the induction of apoptosis in response to microtubule-targeted drugs versus DNA damaging agents. J Biol Chem. 1999;274(16):10916-22.

66. Yang JY, Michod D, Walicki J, Murphy BM, Kasibhatla S, Martin SJ et al. Partial cleavage of RasGAP by caspases is required for cell survival in mild stress conditions. Mol Cell Biol. 2004;24(23):10425-36.

67. Yang JY, Widmann C. Antiapoptotic signaling generated by caspase-induced cleavage of RasGAP. Mol Cell Biol. 2001;21(16):5346-58.

68. Yang JY, Widmann C. The RasGAP N-terminal fragment generated by caspase cleavage protects cells in a Ras/PI3K/Akt-dependent manner that does not rely on NFkappa B activation. J Biol Chem. 2002;277(17):14641-6.

69. Darnowski JW, Goulette FA, Guan YJ, Chatterjee D, Yang ZF, Cousens LP et al. Stat3 cleavage by caspases: impact on full-length Stat3 expression, fragment formation, and transcriptional activity. J Biol Chem. 2006;281(26):17707-17.

70. Kim HS, Chang I, Kim JY, Choi KH, Lee MS. Caspase-mediated p65 cleavage promotes TRAIL-induced apoptosis. Cancer Res. 2005;65(14):6111-9.

71. Pétrilli V, Herceg Z, Hassa PO, Patel NSA, Di Paola R, Cortes U et al. Noncleavable poly(ADP-ribose) polymerase-1 regulates the inflammation response in mice. J Clin Invest. 2004;114(8):1072-81.

72. Lamkanfi M, Declercq W, Vanden Berghe T, Vandenabeele P. Caspases leave the beaten track: caspase-mediated activation of NF-kappaB. J Cell Biol. 2006;173(2):165-71.

73. Allan LA, Morrice N, Brady S, Magee G, Pathak S, Clarke PR. Inhibition of caspase-9 through phosphorylation at Thr 125 by ERK MAPK. Nat Cell Biol. 2003;5(7):647-54.

74. Jiang ZL, Fletcher NM, Diamond MP, Abu-Soud HM, Saed GM. S-nitrosylation of caspase-3 is the mechanism by which adhesion fibroblasts manifest lower apoptosis. Wound Repair Regen. 2009;17(2):224-9.

75. Deveraux QL, Takahashi R, Salvesen GS, Reed JC. X-linked IAP is a direct inhibitor of cell-death proteases. Nature. 1997;388(6639):300-4.

76. Roy N, Deveraux QL, Takahashi R, Salvesen GS, Reed JC. The c-IAP-1 and c-IAP-2 proteins are direct inhibitors of specific caspases. EMBO J. 1997;16(23):6914-25.

77. Cardone MH, Roy N, Stennicke HR, Salvesen GS, Franke TF, Stanbridge E et al. Regulation of cell death protease caspase-9 by phosphorylation. Science. 1998;282(5392):1318-21.

78. Walter J, Schindzielorz A, Grünberg J, Haass C. Phosphorylation of presenilin-2 regulates its cleavage by caspases and retards progression of apoptosis. Proc Natl Acad Sci U S A. 1999;96(4):1391-6.

79. Dawson BA, Lough J. Immunocytochemical localization of transient DNA strand breaks in differentiating myotubes using in situ nick-translation. Dev Biol. 1988;127(2):362-7.

80. Coulton GR, Rogers B, Strutt P, Skynner MJ, Watt DJ. In situ localisation of single-stranded DNA breaks in nuclei of a subpopulation of cells within regenerating skeletal muscle of the dystrophic mdx mouse. J Cell Sci. 1992;102 (Pt 3):653-62.

81. Larsen BD, Rampalli S, Burns LE, Brunette S, Dilworth FJ, Megeney LA. Caspase 3/caspase-activated DNase promote cell differentiation by inducing DNA strand breaks. Proc Natl Acad Sci U S A. 2010;107(9):4230-5.

82. Sies H. Oxidative stress: oxidants and antioxidants. Exp Physiol. 1997;82(2):291-5.

83. Jones DP. Redefining oxidative stress. Antioxid Redox Signal. 2006;8(9-10):1865-79.

84. Davies KJ. The broad spectrum of responses to oxidants in proliferating cells: a new paradigm for oxidative stress. IUBMB Life. 1999;48(1):41-7.

85. Matés JM, Sánchez-Jiménez FM. Role of reactive oxygen species in apoptosis: implications for cancer therapy. Int J Biochem Cell Biol. 2000;32(2):157-70.

86. Valko M, Leibfritz D, Moncol J, Cronin MTD, Mazur M, Telser J. Free radicals and antioxidants in normal physiological functions and human disease. Int J Biochem Cell Biol. 2007;39(1):44-84.

87. Dröge W. Free radicals in the physiological control of cell function. Physiol Rev. 2002;82(1):47-95.

88. Cejas P, Casado E, Belda-Iniesta C, De Castro J, Espinosa E, Redondo A et al. Implications of oxidative stress and cell membrane lipid peroxidation in human cancer (Spain). Cancer Causes Control. 2004;15(7):707-19.

89. Perez-Cruz I, Carcamo JM, Golde DW. Vitamin C inhibits FAS-induced apoptosis in monocytes and U937 cells. Blood. 2003;102(1):336-43.

90. Devadas S, Hinshaw JA, Zaritskaya L, Williams MS. Fas-stimulated generation of reactive oxygen species or exogenous oxidative stress sensitize cells to Fas-mediated apoptosis. Free Radic Biol Med. 2003;35(6):648-61.

91. Goossens V, Stangé G, Moens K, Pipeleers D, Grooten J. Regulation of tumor necrosis factor-induced, mitochondria- and reactive oxygen species-dependent cell death by the electron flux through the electron transport chain complex I. Antioxid Redox Signal. 1999;1(3):285-95.

92. Lee MW, Park SC, Kim JH, Kim IK, Han KS, Kim KY et al. The involvement of oxidative stress in tumor necrosis factor (TNF)-related apoptosis-inducing ligand (TRAIL)-induced apoptosis in HeLa cells. Cancer Lett. 2002;182(1):75-82.

93. Gil J, Almeida S, Oliveira CR, Rego AC. Cytosolic and mitochondrial ROS in staurosporine-induced retinal cell apoptosis. Free Radic Biol Med. 2003;35(11):1500-14.

94. Matsura T, Kai M, Fujii Y, Ito H, Yamada K. Hydrogen peroxide-induced apoptosis in HL-60 cells requires caspase-3 activation. Free Radic Res. 1999;30(1):73-83.

95. Zuo Y, Xiang B, Yang J, Sun X, Wang Y, Cang H et al. Oxidative modification of caspase-9 facilitates its activation via disulfide-mediated interaction with Apaf-1. Cell Res. 2009;19(4):449-57.

96. Trachootham D, Lu W, Ogasawara MA, Nilsa RDV, Huang P. Redox regulation of cell survival. Antioxid Redox Signal. 2008;10(8):1343-74.

97. Takahashi A, Masuda A, Sun M, Centonze VE, Herman B. Oxidative stress-induced apoptosis is associated with alterations in mitochondrial caspase activity and Bcl-2-dependent alterations in mitochondrial pH (pHm). Brain Res Bull. 2004;62(6):497-504.

98. Petersén A, Castilho RF, Hansson O, Wieloch T, Brundin P. Oxidative stress, mitochondrial permeability transition and activation of caspases in calcium ionophore A23187-induced death of cultured striatal neurons. Brain Res. 2000;857(1-2):20-9.

99. He Y, Leung KW, Zhang YH, Duan S, Zhong XF, Jiang RZ et al. Mitochondrial complex I defect induces ROS release and degeneration in trabecular meshwork cells of POAG patients: protection by antioxidants. Invest Ophthalmol Vis Sci. 2008;49(4):1447-58.

100. Seaton TA, Cooper JM, Schapira AH. Cyclosporin inhibition of apoptosis induced by mitochondrial complex I toxins. Brain Res. 1998;809(1):12-7.

101. Madesh M, Hajnóczky G. VDAC-dependent permeabilization of the outer mitochondrial membrane by superoxide induces rapid and massive cytochrome c release. J Cell Biol. 2001;155(6):1003-15.

102. Kagan VE, Tyurina YY, Bayir H, Chu CT, Kapralov AA, Vlasova II et al. The "pro-apoptotic genies" get out of mitochondria: oxidative lipidomics and redox activity of cytochrome c/cardiolipin complexes. Chem Biol Interact. 2006;163(1-2):15-28.

103. Sato T, Machida T, Takahashi S, Iyama S, Sato Y, Kuribayashi K et al. Fas-mediated apoptosome formation is dependent on reactive oxygen species derived from mitochondrial permeability transition in Jurkat cells. J Immunol. 2004;173(1):285-96.

104. Kumar AP, Chang MKX, Fliegel L, Pervaiz S, Clément MV. Oxidative repression of NHE1 gene expression involves iron-mediated caspase activity. Cell Death Differ. 2007;14(10):1733-46.

105. Putney LK, Barber DL. Na-H exchange-dependent increase in intracellular pH times G2/M entry and transition. J Biol Chem. 2003;278(45):44645-9.

106. Toyokuni S, Okamoto K, Yodoi J, Hiai H. Persistent oxidative stress in cancer. FEBS Lett. 1995;358(1):1-3.

107. Behrend L, Henderson G, Zwacka RM. Reactive oxygen species in oncogenic transformation. Biochem Soc Trans. 2003;31(Pt 6):1441-4.

108. Yang W, Dyck JR, Fliegel L. Regulation of NHE1 expression in L6 muscle cells. Biochim Biophys Acta. 1996;1306(1):107-13.

109. Forman HJ. Use and abuse of exogenous H2O2 in studies of signal transduction. Free Radic Biol Med. 2007;42(7):926-32.

110. Hampton MB, Orrenius S. Dual regulation of caspase activity by hydrogen peroxide: implications for apoptosis. FEBS Lett. 1997;414(3):552-6.

111. Omura S, Iwai Y, Hirano A, Nakagawa A, Awaya J, Tsuchya H et al. A new alkaloid AM-2282 OF Streptomyces origin. Taxonomy, fermentation, isolation and preliminary characterization. J Antibiot (Tokyo). 1977;30(4):275-82.

112. Tamaoki T, Nomoto H, Takahashi I, Kato Y, Morimoto M, Tomita F. Staurosporine, a potent inhibitor of phospholipid/Ca++dependent protein kinase. Biochem Biophys Res Commun. 1986;135(2):397-402.

113. Kase H, Iwahashi K, Matsuda Y. K-252a, a potent inhibitor of protein kinase C from microbial origin. J Antibiot (Tokyo). 1986;39(8):1059-65.

114. Qiao L, Koutsos M, Tsai LL, Kozoni V, Guzman J, Shiff SJ et al. Staurosporine inhibits the proliferation, alters the cell cycle distribution and induces apoptosis in HT-29 human colon adenocarcinoma cells. Cancer Lett. 1996;107(1):83-9.

115. Antonsson A, Persson JL. Induction of apoptosis by staurosporine involves the inhibition of expression of the major cell cycle proteins at the G(2)/m checkpoint accompanied by alterations in Erk and Akt kinase activities. Anticancer Res. 2009;29(8):2893-8.

116. Bruno S, Ardelt B, Skierski JS, Traganos F, Darzynkiewicz Z. Different effects of staurosporine, an inhibitor of protein kinases, on the cell cycle and chromatin structure of normal and leukemic lymphocytes. Cancer Res. 1992;52(2):470-3.

117. Zhang XD, Gillespie SK, Hersey P. Staurosporine induces apoptosis of melanoma by both caspase-dependent and -independent apoptotic pathways. Mol Cancer Ther. 2004;3(2):187-97.

118. Belmokhtar CA, Hillion J, Ségal-Bendirdjian E. Staurosporine induces apoptosis through both caspase-dependent and caspase-independent mechanisms. Oncogene. 2001;20(26):3354-62.

119. Bidère N, Lorenzo HK, Carmona S, Laforge M, Harper F, Dumont C et al. Cathepsin D triggers Bax activation, resulting in selective apoptosis-inducing factor (AIF) relocation in T lymphocytes entering the early commitment phase to apoptosis. J Biol Chem. 2003;278(33):31401-11.

120. Johansson AC, Steen H, Ollinger K, Roberg K. Cathepsin D mediates cytochrome c release and caspase activation in human fibroblast apoptosis induced by staurosporine. Cell Death Differ. 2003;10(11):1253-9.

121. Kabir J, Lobo M, Zachary I. Staurosporine induces endothelial cell apoptosis via focal adhesion kinase dephosphorylation and focal adhesion disassembly independent of focal adhesion kinase proteolysis. Biochem J. 2002;367(Pt 1):145-55.

122. Ricci JE, Muñoz-Pinedo C, Fitzgerald P, Bailly-Maitre B, Perkins GA, Yadava N et al. Disruption of mitochondrial function during apoptosis is mediated by caspase cleavage of the p75 subunit of complex I of the electron transport chain. Cell. 2004;117(6):773-86.

123. Khosravi-Far R, Zakeri Z, Lockshin RA. Methods in Enzymology, Volume 442. Academic Press; 2008.

124. Hoffmann JC, Pappa A, Krammer PH, Lavrik IN. A new C-terminal cleavage product of procaspase-8, p30, defines an alternative pathway of procaspase-8 activation. Mol Cell Biol. 2009;29(16):4431-40.

125. Rideout HJ, Zang E, Yeasmin M, Gordon R, Jabado O, Park DS et al. Inhibitors of trypsin-like serine proteases prevent DNA damage-induced neuronal death by acting upstream of the mitochondrial checkpoint and of p53 induction. Neuroscience. 2001;107(2):339-52.

126. de Bruin EC, Meersma D, de Wilde J, den Otter I, Schipper EM, Medema JP et al. A serine protease is involved in the initiation of DNA damage-induced apoptosis. Cell Death Differ. 2003;10(10):1204-12.

127. Dong Z, Saikumar P, Patel Y, Weinberg JM, Venkatachalam MA. Serine protease inhibitors suppress cytochrome c-mediatedcaspase-9 activation and apoptosis during hypoxia-reoxygenation. Biochem J. 2000;347 Pt 3:669-77.

128. Kritis A, Pourzitaki C, Klagas I, Chourdakis M, Albani M. Proteases inhibition assessment on PC12 and NGF treated cells after oxygen and glucose deprivation reveals a distinct role for aspartyl proteases. PloS one. 2011;6(10):e25950.

129. Schotte P, Declercq W, Van Huffel S, Vandenabeele P, Beyaert R. Non-specific effects of methyl ketone peptide inhibitors of caspases. FEBS Lett. 1999;442(1):117-21.

130. Chauvier D, Ankri S, Charriaut-Marlangue C, Casimir R, Jacotot E. Broad-spectrum caspase inhibitors: from myth to reality? Cell Death Differ. 2007;14(2):387-91.

131. Chwieralski CE, Welte T, Bühling F. Cathepsin-regulated apoptosis. Apoptosis. 2006;11(2):143-9.

132. Nozaki K, Das A, Ray SK, Banik NL. Calpeptin attenuated apoptosis and intracellular inflammatory changes in muscle cells. J Neurosci Res. 2011;89(4):536-43.

133. Chua BT, Guo K, Li P. Direct cleavage by the calcium-activated protease calpain can lead to inactivation of caspases. J Biol Chem. 2000;275(7):5131-5.

134. Mandic A, Viktorsson K, Strandberg L, Heiden T, Hansson J, Linder S et al. Calpain-mediated Bid cleavage and calpain-independent Bak modulation: two separate pathways in cisplatin-induced apoptosis. Mol Cell Biol. 2002;22(9):3003-13.

135. Sharma AK, Rohrer B. Calcium-induced calpain mediates apoptosis via caspase-3 in a mouse photoreceptor cell line. J Biol Chem. 2004;279(34):35564-72.

136. Hentze H, Lin XY, Choi MSK, Porter AG. Critical role for cathepsin B in mediating caspase-1-dependent interleukin-18 maturation and caspase-1-independent necrosis triggered by the microbial toxin nigericin. Cell Death Differ. 2003;10(9):956-68.

137. Vancompernolle K, Van Herreweghe F, Pynaert G, Van de Craen M, De Vos K, Totty N et al. Atractyloside-induced release of cathepsin B, a protease with caspase-processing activity. FEBS Lett. 1998;438(3):150-8.

138. Vile GF, Basu-Modak S, Waltner C, Tyrrell RM. Heme oxygenase 1 mediates an adaptive response to oxidative stress in human skin fibroblasts. Proc Natl Acad Sci U S A. 1994;91(7):2607-10.

139. Le WD, Xie WJ, Appel SH. Protective role of heme oxygenase-1 in oxidative stress-induced neuronal injury. J Neurosci Res. 1999;56(6):652-8.

140. Johansson AC, Appelqvist H, Nilsson C, Kågedal K, Roberg K, Ollinger K. Regulation of apoptosis-associated lysosomal membrane permeabilization. Apoptosis. 2010;15(5):527-40.

141. Glickstein H, El RB, Shvartsman M, Cabantchik ZI. Intracellular labile iron pools as direct targets of iron chelators: a fluorescence study of chelator action in living cells. Blood. 2005;106(9):3242-50.

142. Evans MD, Dizdaroglu M, Cooke MS. Oxidative DNA damage and disease: induction, repair and significance. Mutat Res. 2004;567(1):1-61.

143. Burney S, Caulfield JL, Niles JC, Wishnok JS, Tannenbaum SR. The chemistry of DNA damage from nitric oxide and peroxynitrite. Mutat Res. 1999;424(1-2):37-49.

144. Caulfield JL, Wishnok JS, Tannenbaum SR. Nitric oxide-induced deamination of cytosine and guanine in deoxynucleosides and oligonucleotides. J Biol Chem. 1998;273(21):12689-95.

145. Liu D, Xu Y. p53, oxidative stress, and aging. Antioxid Redox Signal. 2011;15(6):1669-78.

146. Fritsche M, Haessler C, Brandner G. Induction of nuclear accumulation of the tumor-suppressor protein p53 by DNA-damaging agents. Oncogene. 1993;8(2):307-18.

147. Siliciano JD, Canman CE, Taya Y, Sakaguchi K, Appella E, Kastan MB. DNA damage induces phosphorylation of the amino terminus of p53. Genes Dev. 1997;11(24):3471-81.

148. Shieh SY, Ikeda M, Taya Y, Prives C. DNA damage-induced phosphorylation of p53 alleviates inhibition by MDM2. Cell. 1997;91(3):325-34.

149. Chen K, Albano A, Ho A, Keaney JF. Activation of p53 by oxidative stress involves platelet-derived growth factor-beta receptor-mediated ataxia telangiectasia mutated (ATM) kinase activation. J Biol Chem. 2003;278(41):39527-33.

150. Fridman JS, Lowe SW. Control of apoptosis by p53. Oncogene. 2003;22(56):9030-40.

151. Hoffman WH, Biade S, Zilfou JT, Chen J, Murphy M. Transcriptional repression of the anti-apoptotic survivin gene by wild type p53. J Biol Chem. 2002;277(5):3247-57.

152. Chipuk JE, Kuwana T, Bouchier-Hayes L, Droin NM, Newmeyer DD, Schuler M et al. Direct activation of Bax by p53 mediates mitochondrial membrane permeabilization and apoptosis. Science. 2004;303(5660):1010-4.

153. Mihara M, Erster S, Zaika A, Petrenko O, Chittenden T, Pancoska P et al. p53 has a direct apoptogenic role at the mitochondria. Mol Cell. 2003;11(3):577-90.

154. Komarov PG, Komarova EA, Kondratov RV, Christov-Tselkov K, Coon JS, Chernov MV et al. A chemical inhibitor of p53 that protects mice from the side effects of cancer therapy. Science. 1999;285(5434):1733-7.

155. Sardiello M, Palmieri M, di Ronza A, Medina DL, Valenza M, Gennarino VA et al. A gene network regulating lysosomal biogenesis and function. Science. 2009;325(5939):473-7.

156. Simon HU, Haj-Yehia A, Levi-Schaffer F. Role of reactive oxygen species (ROS) in apoptosis induction. Apoptosis. 2000;5(5):415-8.

157. Conde de la Rosa L, Schoemaker MH, Vrenken TE, Buist-Homan M, Havinga R, Jansen PLM et al. Superoxide anions and hydrogen peroxide induce hepatocyte death by different mechanisms: involvement of JNK and ERK MAP kinases. J Hepatol. 2006;44(5):918-29.

158. Rayner BS, Duong TTH, Myers SJ, Witting PK. Protective effect of a synthetic anti-oxidant on neuronal cell apoptosis resulting from experimental hypoxia re-oxygenation injury. J Neurochem. 2006;97(1):211-21.

159. Pirlich M, Kiok K, Sandig G, Lochs H, Grune T. Alpha-lipoic acid prevents ethanol-induced protein oxidation in mouse hippocampal HT22 cells. Neurosci Lett. 2002;328(2):93-6.

160. Chan WH, Wu HJ, Hsuuw YD. Curcumin inhibits ROS formation and apoptosis in methylglyoxal-treated human hepatoma G2 cells. Ann N Y Acad Sci. 2005;1042:372-8.

161. Izeradjene K, Douglas L, Tillman DM, Delaney AB, Houghton JA. Reactive oxygen species regulate caspase activation in tumor necrosis factor-related apoptosis-inducing ligand-resistant human colon carcinoma cell lines. Cancer Res. 2005;65(16):7436-45.

162. Liu B, Chen Y, St Clair DK. ROS and p53: a versatile partnership. Free Radic Biol Med. 2008;44(8):1529-35.

163. Hampton MB, Fadeel B, Orrenius S. Redox regulation of the caspases during apoptosis. Ann N Y Acad Sci. 1998;854:328-35.

164. Karin M, Lin A. NF-kappaB at the crossroads of life and death. Nat Immunol. 2002;3(3):221-7.

165. Alexandre J, Batteux F, Nicco C, Chéreau C, Laurent A, Guillevin L et al. Accumulation of hydrogen peroxide is an early and crucial step for paclitaxel-induced cancer cell death both in vitro and in vivo. Int J Cancer. 2006;119(1):41-8.

166. Schröder E, Eaton P. Hydrogen peroxide as an endogenous mediator and exogenous tool in cardiovascular research: issues and considerations. Curr Opin Pharmacol. 2008;8(2):153-9.

167. Lamkanfi M, Festjens N, Declercq W, Vanden Berghe T, Vandenabeele P. Caspases in cell survival, proliferation and differentiation. Cell Death Differ. 2007;14(1):44-55.

168. Martinon F, Burns K, Tschopp J. The inflammasome: a molecular platform triggering activation of inflammatory caspases and processing of proIL-beta. Mol Cell. 2002;10(2):417-26.

169. Salmena L, Lemmers B, Hakem A, Matysiak-Zablocki E, Murakami K, Au PYB et al. Essential role for caspase 8 in T-cell homeostasis and T-cell-mediated immunity. Genes Dev. 2003;17(7):883-95.

170. Beisner DR, Ch'en IL, Kolla RV, Hoffmann A, Hedrick SM. Cutting edge: innate immunity conferred by B cells is regulated by caspase-8. J Immunol. 2005;175(6):3469-73.

171. Florentin A, Arama E. Caspase levels and execution efficiencies determine the apoptotic potential of the cell. J Cell Biol. 2012;196(4):513-27.

172. Rosado JA, Lopez JJ, Gomez-Arteta E, Redondo PC, Salido GM, Pariente JA. Early caspase-3 activation independent of apoptosis is required for cellular function. J Cell Physiol. 2006;209(1):142-52.

173. Woo M, Hakem R, Soengas MS, Duncan GS, Shahinian A, Kägi D et al. Essential contribution of caspase 3/CPP32 to apoptosis and its associated nuclear changes. Genes Dev. 1998;12(6):806-19.

174. Zheng TS, Schlosser SF, Dao T, Hingorani R, Crispe IN, Boyer JL et al. Caspase-3 controls both cytoplasmic and nuclear events associated with Fas-mediated apoptosis in vivo. Proc Natl Acad Sci U S A. 1998;95(23):13618-23.

175. Earnshaw WC, Martins LM, Kaufmann SH. Mammalian caspases: structure, activation, substrates, and functions during apoptosis. Annu Rev Biochem. 1999;68:383-424.

176. Fischer U, Jänicke RU, Schulze-Osthoff K. Many cuts to ruin: a comprehensive update of caspase substrates. Cell Death Differ. 2003;10(1):76-100.

177. Faleiro L, Lazebnik Y. Caspases disrupt the nuclear-cytoplasmic barrier. J Cell Biol. 2000;151(5):951-9.

178. Kamada S, Kikkawa U, Tsujimoto Y, Hunter T. A-kinase-anchoring protein 95 functions as a potential carrier for the nuclear translocation of active caspase 3 through an enzyme-substrate-like association. Mol Cell Biol. 2005;25(21):9469-77.

179. Luo M, Lu Z, Sun H, Yuan K, Zhang Q, Meng S et al. Nuclear entry of active caspase-3 is facilitated by its p3-recognition-based specific cleavage activity. Cell Res. 2010;20(2):211-22.

180. Noyan-Ashraf MH, Brandizzi F, Juurlink BHJ. Constitutive nuclear localization of activated caspase 3 in subpopulations of the astroglial family of cells. Glia. 2005;49(4):588-93.

181. Charvet C, Alberti I, Luciano F, Jacquel A, Bernard A, Auberger P et al. Proteolytic regulation of Forkhead transcription factor FOXO3a by caspase-3-like proteases. Oncogene. 2003;22(29):4557-68.

182. Ferrando-May E. Nucleocytoplasmic transport in apoptosis. Cell Death Differ. 2005;12(10):1263-76.

183. Kothakota S, Azuma T, Reinhard C, Klippel A, Tang J, Chu K et al. Caspase-3-generated fragment of gelsolin: effector of morphological change in apoptosis. Science. 1997;278(5336):294-8.

184. Zhang J, Reedy MC, Hannun YA, Obeid LM. Inhibition of caspases inhibits the release of apoptotic bodies: Bcl-2 inhibits the initiation of formation of apoptotic bodies in chemotherapeutic agent-induced apoptosis. J Cell Biol. 1999;145(1):99-108.

185. Elmore S. Apoptosis: a review of programmed cell death. Toxicol Pathol. 2007;35(4):495-516.

186. Mandal D, Moitra PK, Saha S, Basu J. Caspase 3 regulates phosphatidylserine externalization and phagocytosis of oxidatively stressed erythrocytes. FEBS Lett. 2002;513(2-3):184-8.

187. Fadok VA, de Cathelineau A, Daleke DL, Henson PM, Bratton DL. Loss of phospholipid asymmetry and surface exposure of phosphatidylserine is required for phagocytosis of apoptotic cells by macrophages and fibroblasts. J Biol Chem. 2001;276(2):1071-7.

188. Stennicke HR, Jürgensmeier JM, Shin H, Deveraux Q, Wolf BB, Yang X et al. Pro-caspase-3 is a major physiologic target of caspase-8. J Biol Chem. 1998;273(42):27084-90.

189. Slee EA, Harte MT, Kluck RM, Wolf BB, Casiano CA, Newmeyer DD et al. Ordering the cytochrome c-initiated caspase cascade: hierarchical activation of caspases-2, -3, -6, -7, -8, and -10 in a caspase-9-dependent manner. J Cell Biol. 1999;144(2):281-92.

190. Hishita T, Tada-Oikawa S, Tohyama K, Miura Y, Nishihara T, Tohyama Y et al. Caspase-3 activation by lysosomal enzymes in cytochrome c-independent apoptosis in myelodysplastic syndrome-derived cell line P39. Cancer Res. 2001;61(7):2878-84.

191. Cummings BS, Schnellmann RG. Cisplatin-induced renal cell apoptosis: caspase 3-dependent and -independent pathways. J Pharmacol Exp Ther. 2002;302(1):8-17.

192. Murray TVA, McMahon JM, Howley BA, Stanley A, Ritter T, Mohr A et al. A non-apoptotic role for caspase-9 in muscle differentiation. J Cell Sci. 2008;121(Pt 22):3786-93.

193. Turk B, Turk V. Lysosomes as "suicide bags" in cell death: myth or reality? J Biol Chem. 2009;284(33):21783-7.

194. Guicciardi ME, Deussing J, Miyoshi H, Bronk SF, Svingen PA, Peters C et al. Cathepsin B contributes to TNF-alpha-mediated hepatocyte apoptosis by promoting mitochondrial release of cytochrome c. J Clin Invest. 2000;106(9):1127-37.

195. Brunk UT, Svensson I. Oxidative stress, growth factor starvation and Fas activation may all cause apoptosis through lysosomal leak. Redox Rep. 1999;4(1-2):3-11.

196. Oberle C, Huai J, Reinheckel T, Tacke M, Rassner M, Ekert PG et al. Lysosomal membrane permeabilization and cathepsin release is a Bax/Bak-dependent, amplifying event of apoptosis in fibroblasts and monocytes. Cell Death Differ. 2010;17(7):1167-78.

197. Yuan XM, Li W, Dalen H, Lotem J, Kama R, Sachs L et al. Lysosomal destabilization in p53-induced apoptosis. Proc Natl Acad Sci U S A. 2002;99(9):6286-91.

198. Lin Y, Epstein DL, Liton PB. Intralysosomal iron induces lysosomal membrane permeabilization and cathepsin D-mediated cell death in trabecular meshwork cells exposed to oxidative stress. Invest Ophthalmol Vis Sci. 2010;51(12):6483-95.

199. Choi JH, Kim DH, Yun IJ, Chang JH, Chun BG, Choi SH. Zaprinast inhibits hydrogen peroxide-induced lysosomal destabilization and cell death in astrocytes. Eur J Pharmacol. 2007;571(2-3):106-15.

200. Blomgran R, Zheng L, Stendahl O. Cathepsin-cleaved Bid promotes apoptosis in human neutrophils via oxidative stress-induced lysosomal membrane permeabilization. J Leukoc Biol. 2007;81(5):1213-23.

201. Cirman T, Oresić K, Mazovec GD, Turk V, Reed JC, Myers RM et al. Selective disruption of lysosomes in HeLa cells triggers apoptosis mediated by cleavage of Bid by multiple papain-like lysosomal cathepsins. J Biol Chem. 2004;279(5):3578-87.

202. Droga-Mazovec G, Bojic L, Petelin A, Ivanova S, Romih R, Repnik U et al. Cysteine cathepsins trigger caspase-dependent cell death through cleavage of bid and antiapoptotic Bcl-2 homologues. J Biol Chem. 2008;283(27):19140-50.

203. Boya P, Kroemer G. Lysosomal membrane permeabilization in cell death. Oncogene. 2008;27(50):6434-51.

204. Brunk UT, Dalen H, Roberg K, Hellquist HB. Photo-oxidative disruption of lysosomal membranes causes apoptosis of cultured human fibroblasts. Free Radic Biol Med. 1997;23(4):616-26.

205. Ono K, Kim SO, Han J. Susceptibility of lysosomes to rupture is a determinant for plasma membrane disruption in tumor necrosis factor alpha-induced cell death. Mol Cell Biol. 2003;23(2):665-76.

206. Nylandsted J, Gyrd-Hansen M, Danielewicz A, Fehrenbacher N, Lademann U, Høyer-Hansen M et al. Heat shock protein 70 promotes cell survival by inhibiting lysosomal membrane permeabilization. J Exp Med. 2004;200(4):425-35.

207. Fehrenbacher N, Bastholm L, Kirkegaard-Sørensen T, Rafn B, Bøttzauw T, Nielsen C et al. Sensitization to the lysosomal cell death pathway by oncogene-induced down-regulation of lysosome-associated membrane proteins 1 and 2. Cancer Res. 2008;68(16):6623-33.

208. Ben-Ari Z, Mor E, Azarov D, Sulkes J, Tor R, Cheporko Y et al. Cathepsin B inactivation attenuates the apoptotic injury induced by ischemia/reperfusion of mouse liver. Apoptosis. 2005;10(6):1261-9.

209. Kågedal K, Johansson U, Ollinger K. The lysosomal protease cathepsin D mediates apoptosis induced by oxidative stress. FASEB journal : official publication of the Federation of American Societies for Experimental Biology. 2001;15(9):1592-4.

210. Boya P, Andreau K, Poncet D, Zamzami N, Perfettini JL, Metivier D et al. Lysosomal membrane permeabilization induces cell death in a mitochondrion-dependent fashion. J Exp Med. 2003;197(10):1323-34.

211. Stoka V, Turk B, Schendel SL, Kim TH, Cirman T, Snipas SJ et al. Lysosomal protease pathways to apoptosis. Cleavage of bid, not pro-caspases, is the most likely route. J Biol Chem. 2001;276(5):3149-57.

212. Ishisaka R, Utsumi T, Yabuki M, Kanno T, Furuno T, Inoue M et al. Activation of caspase-3-like protease by digitonin-treated lysosomes. FEBS Lett. 1998;435(2-3):233-6.

213. Ishisaka R, Utsumi T, Kanno T, Arita K, Katunuma N, Akiyama J et al. Participation of a cathepsin L-type protease in the activation of caspase-3. Cell Struct Funct. 1999;24(6):465-70.

214. Conus S, Perozzo R, Reinheckel T, Peters C, Scapozza L, Yousefi S et al. Caspase-8 is activated by cathepsin D initiating neutrophil apoptosis during the resolution of inflammation. J Exp Med. 2008;205(3):685-98.

215. Riese RJ, Chapman HA. Cathepsins and compartmentalization in antigen presentation. Curr Opin Immunol. 2000;12(1):107-13.

216. Hart TC, Hart PS, Bowden DW, Michalec MD, Callison SA, Walker SJ et al. Mutations of the cathepsin C gene are responsible for Papillon-Lefèvre syndrome. J Med Genet. 1999;36(12):881-7.

217. Gelb BD, Shi GP, Chapman HA, Desnick RJ. Pycnodysostosis, a lysosomal disease caused by cathepsin K deficiency. Science. 1996;273(5279):1236-8.

218. Toomes C, James J, Wood AJ, Wu CL, McCormick D, Lench N et al. Loss-of-function mutations in the cathepsin C gene result in periodontal disease and palmoplantar keratosis. Nat Genet. 1999;23(4):421-4.

219. Turk V, Turk B, Turk D. Lysosomal cysteine proteases: facts and opportunities. EMBO J. 2001;20(17):4629-33.

220. Deussing J, Roth W, Saftig P, Peters C, Ploegh HL, Villadangos JA. Cathepsins B and D are dispensable for major histocompatibility complex class II-mediated antigen presentation. Proc Natl Acad Sci U S A. 1998;95(8):4516-21.

221. Nakagawa T, Roth W, Wong P, Nelson A, Farr A, Deussing J et al. Cathepsin L: critical role in Ii degradation and CD4 T cell selection in the thymus. Science. 1998;280(5362):450-3.

222. Roth W, Deussing J, Botchkarev VA, Pauly-Evers M, Saftig P, Hafner A et al. Cathepsin L deficiency as molecular defect of furless: hyperproliferation of keratinocytes and pertubation of hair follicle cycling. FASEB journal : official publication of the Federation of American Societies for Experimental Biology. 2000;14(13):2075-86.

223. Reiser J, Adair B, Reinheckel T. Specialized roles for cysteine cathepsins in health and disease. J Clin Invest. 2010;120(10):3421-31.

224. Klein DM, Felsenstein KM, Brenneman DE. Cathepsins B and L differentially regulate amyloid precursor protein processing. J Pharmacol Exp Ther. 2009;328(3):813-21.

225. Pratt MR, Sekedat MD, Chiang KP, Muir TW. Direct measurement of cathepsin B activity in the cytosol of apoptotic cells by an activity-based probe. Chem Biol. 2009;16(9):1001-12.

226. Yakovlev AA, Gorokhovatsky AY, Onufriev MV, Beletsky IP, Gulyaeva NV. Brain cathepsin B cleaves a caspase substrate. Biochemistry (Mosc). 2008;73(3):332-6.

227. Greene BT, Thorburn J, Willingham MC, Thorburn A, Planalp RP, Brechbiel MW et al. Activation of caspase pathways during iron chelator-mediated apoptosis. J Biol Chem. 2002;277(28):25568-75.

228. Kim BS, Yoon KH, Oh HM, Choi EY, Kim SW, Han WC et al. Involvement of p38 MAP kinase during iron chelator-mediated apoptotic cell death. Cell Immunol. 2002;220(2):96-106.

229. Salvador GA, Oteiza PI. Iron overload triggers redox-sensitive signals in human IMR-32 neuroblastoma cells. Neurotoxicology. 2011;32(1):75-82.

230. Emerit J, Beaumont C, Trivin F. Iron metabolism, free radicals, and oxidative injury. Biomed Pharmacother. 2001;55(6):333-9.

231. Galaris D, Cadenas E, Hochstein P. Redox cycling of myoglobin and ascorbate: a potential protective mechanism against oxidative reperfusion injury in muscle. Arch Biochem Biophys. 1989;273(2):497-504.

232. Yamaguchi K, Mandai M, Toyokuni S, Hamanishi J, Higuchi T, Takakura K et al. Contents of endometriotic cysts, especially the high concentration of free iron, are a possible cause of carcinogenesis in the cysts through the iron-induced persistent oxidative stress. Clin Cancer Res. 2008;14(1):32-40.

233. Klotz LO, Kröncke KD, Buchczyk DP, Sies H. Role of copper, zinc, selenium and tellurium in the cellular defense against oxidative and nitrosative stress. J Nutr. 2003;133(5 Suppl 1):1448S-51S.

234. do Lago LCC, Matias AC, Nomura CS, Cerchiaro G. Radical production by hydrogen peroxide/bicarbonate and copper uptake in mammalian cells: modulation by Cu(II) complexes. J Inorg Biochem. 2011;105(2):189-94.

235. Lee DH, O'Connor TR, Pfeifer GP. Oxidative DNA damage induced by copper and hydrogen peroxide promotes CG-->TT tandem mutations at methylated CpG dinucleotides in nucleotide excision repair-deficient cells. Nucleic Acids Res. 2002;30(16):3566-73.

236. Lloyd DR, Phillips DH. Oxidative DNA damage mediated by copper(II), iron(II) and nickel(II) fenton reactions: evidence for site-specific mechanisms in the formation of double-strand breaks, 8-hydroxydeoxyguanosine and putative intrastrand cross-links. Mutat Res. 1999;424(1-2):23-36.

237. Yu Z, Persson HL, Eaton JW, Brunk UT. Intralysosomal iron: a major determinant of oxidant-induced cell death. Free Radic Biol Med. 2003;34(10):1243-52.

238. Castino R, Fiorentino I, Cagnin M, Giovia A, Isidoro C. Chelation of lysosomal iron protects dopaminergic SH-SY5Y neuroblastoma cells from hydrogen peroxide toxicity by precluding autophagy and Akt dephosphorylation. Toxicol Sci. 2011;123(2):523-41.

239. Gorria M, Tekpli X, Rissel M, Sergent O, Huc L, Landvik N et al. A new lactoferrin- and iron-dependent lysosomal death pathway is induced by benzo[a]pyrene in hepatic epithelial cells. Toxicol Appl Pharmacol. 2008;228(2):212-24.

240. Hsieh CH, Jeng SF, Hsieh MW, Chen YC, Rau CS, Lu TH et al. Statin-induced heme oxygenase-1 increases NF-kappaB activation and oxygen radical production in cultured neuronal cells exposed to lipopolysaccharide. Toxicol Sci. 2008;102(1):150-9.

241. Denamur S, Tyteca D, Marchand-Brynaert J, Van Bambeke F, Tulkens PM, Courtoy PJ et al. Role of oxidative stress in lysosomal membrane permeabilization and apoptosis induced by gentamicin, an aminoglycoside antibiotic. Free Radic Biol Med. 2011;51(9):1656-65.

242. Sen R, Saha P, Sarkar A, Ganguly S, Chatterjee M. Iron enhances generation of free radicals by Artemisinin causing a caspase-independent, apoptotic death in Leishmania donovani promastigotes. Free Radic Res. 2010;44(11):1289-95.

243. Garthwaite J. Concepts of neural nitric oxide-mediated transmission. Eur J Neurosci. 2008;27(11):2783-802.

244. Beckman JS, Koppenol WH. Nitric oxide, superoxide, and peroxynitrite: the good, the bad, and ugly. Am J Physiol. 1996;271(5 Pt 1):C1424-37.

245. Kim PK, Zamora R, Petrosko P, Billiar TR. The regulatory role of nitric oxide in apoptosis. Int Immunopharmacol. 2001;1(8):1421-41.

246. Chung HT, Pae HO, Choi BM, Billiar TR, Kim YM. Nitric oxide as a bioregulator of apoptosis. Biochem Biophys Res Commun. 2001;282(5):1075-9.

247. Rössig L, Fichtlscherer B, Breitschopf K, Haendeler J, Zeiher AM, Mülsch A et al. Nitric oxide inhibits caspase-3 by S-nitrosation in vivo. J Biol Chem. 1999;274(11):6823-6.

248. Li J, Bombeck CA, Yang S, Kim YM, Billiar TR. Nitric oxide suppresses apoptosis via interrupting caspase activation and mitochondrial dysfunction in cultured hepatocytes. J Biol Chem. 1999;274(24):17325-33.

249. Hirst DG, Robson T. Nitrosative stress as a mediator of apoptosis: implications for cancer therapy. Curr Pharm Des. 2010;16(1):45-55.

250. Kim YM, Chung HT, Simmons RL, Billiar TR. Cellular non-heme iron content is a determinant of nitric oxide-mediated apoptosis, necrosis, and caspase inhibition. J Biol Chem. 2000;275(15):10954-61.

251. Ohtani H, Katoh H, Tanaka T, Saotome M, Urushida T, Satoh H et al. Effects of nitric oxide on mitochondrial permeability transition pore and thiol-mediated responses in cardiac myocytes. Nitric Oxide. 2012;26(2):95-101.

252. Persichini T, Mazzone V, Polticelli F, Moreno S, Venturini G, Clementi E et al. Mitochondrial type I nitric oxide synthase physically interacts with cytochrome c oxidase. Neurosci Lett. 2005;384(3):254-9.

253. Thomas SR, Chen K, Keaney JF. Hydrogen peroxide activates endothelial nitric-oxide synthase through coordinated phosphorylation and dephosphorylation via a

phosphoinositide 3-kinase-dependent signaling pathway. J Biol Chem. 2002;277(8):6017-24.

254. Sartoretto JL, Kalwa H, Pluth MD, Lippard SJ, Michel T. Hydrogen peroxide differentially modulates cardiac myocyte nitric oxide synthesis. Proc Natl Acad Sci U S A. 2011;108(38):15792-7.

255. Drummond GR, Cai H, Davis ME, Ramasamy S, Harrison DG. Transcriptional and posttranscriptional regulation of endothelial nitric oxide synthase expression by hydrogen peroxide. Circ Res. 2000;86(3):347-54.

256. Cao P, Ito O, Guo Q, Ito D, Muroya Y, Rong R et al. Endogenous hydrogen peroxide up-regulates the expression of nitric oxide synthase in the kidney of SHR. J Hypertens. 2011;29(6):1167-74.

257. Förstermann U, Sessa WC. Nitric oxide synthases: regulation and function. Eur Heart J. 2012;33(7):829-37, 837a.

258. Yuyama K, Yamamoto H, Nishizaki I, Kato T, Sora I, Yamamoto T. Caspase-independent cell death by low concentrations of nitric oxide in PC12 cells: involvement of cytochrome C oxidase inhibition and the production of reactive oxygen species in mitochondria. J Neurosci Res. 2003;73(3):351-63.

259. Xia Y. Superoxide generation from nitric oxide synthases. Antioxid Redox Signal. 2007;9(10):1773-8.

260. Costa VM, Silva R, Ferreira R, Amado F, Carvalho F, de Lourdes Bastos M et al. Adrenaline in pro-oxidant conditions elicits intracellular survival pathways in isolated rat cardiomyocytes. Toxicology. 2009;257(1-2):70-9.

261. Ahmad KA, Clement MV, Pervaiz S. Pro-oxidant activity of low doses of resveratrol inhibits hydrogen peroxide-induced apoptosis. Ann N Y Acad Sci. 2003;1010:365-73.

262. Kurz DJ, Decary S, Hong Y, Trivier E, Akhmedov A, Erusalimsky JD. Chronic oxidative stress compromises telomere integrity and accelerates the onset of senescence in human endothelial cells. J Cell Sci. 2004;117(Pt 11):2417-26.

263. Lotem J, Sachs L. Different mechanisms for suppression of apoptosis by cytokines and calcium mobilizing compounds. Proc Natl Acad Sci U S A. 1998;95(8):4601-6.

264. Wu GS, Saftig P, Peters C, El-Deiry WS. Potential role for cathepsin D in p53-dependent tumor suppression and chemosensitivity. Oncogene. 1998;16(17):2177-83.

265. Li N, Zheng Y, Chen W, Wang C, Liu X, He W et al. Adaptor protein LAPF recruits phosphorylated p53 to lysosomes and triggers lysosomal destabilization in apoptosis. Cancer Res. 2007;67(23):11176-85.

266. Gowran A, Campbell VA. A role for p53 in the regulation of lysosomal permeability by delta 9-tetrahydrocannabinol in rat cortical neurones: implications for neurodegeneration. J Neurochem. 2008;105(4):1513-24.

267. Fogarty MP, McCormack RM, Noonan J, Murphy D, Gowran A, Campbell VA. A role for p53 in the beta-amyloid-mediated regulation of the lysosomal system. Neurobiol Aging. 2010;31(10):1774-86.

268. Wäster PK, Ollinger KM. Redox-dependent translocation of p53 to mitochondria or nucleus in human melanocytes after UVA- and UVB-induced apoptosis. J Invest Dermatol. 2009;129(7):1769-81.

269. Steele AJ, Prentice AG, Hoffbrand AV, Yogashangary BC, Hart SM, Nacheva EP et al. p53-mediated apoptosis of CLL cells: evidence for a transcription-independent mechanism. Blood. 2008;112(9):3827-34.

270. Vaseva AV, Marchenko ND, Moll UM. The transcription-independent mitochondrial p53 program is a major contributor to nutlin-induced apoptosis in tumor cells. Cell Cycle. 2009;8(11):1711-9.

271. Komarova EA, Neznanov N, Komarov PG, Chernov MV, Wang K, Gudkov AV. p53 inhibitor pifithrin alpha can suppress heat shock and glucocorticoid signaling pathways. J Biol Chem. 2003;278(18):15465-8.

272. O'Keefe K, Li H, Zhang Y. Nucleocytoplasmic shuttling of p53 is essential for MDM2-mediated cytoplasmic degradation but not ubiquitination. Mol Cell Biol. 2003;23(18):6396-405.

273. Dippold WG, Jay G, DeLeo AB, Khoury G, Old LJ. p53 transformation-related protein: detection by monoclonal antibody in mouse and human cells. Proc Natl Acad Sci U S A. 1981;78(3):1695-9.

274. Shaulsky G, Ben-Ze'ev A, Rotter V. Subcellular distribution of the p53 protein during the cell cycle of Balb/c 3T3 cells. Oncogene. 1990;5(11):1707-11.

275. David-Pfeuty T, Chakrani F, Ory K, Nouvian-Dooghe Y. Cell cycle-dependent regulation of nuclear p53 traffic occurs in one subclass of human tumor cells and in untransformed cells. Cell Growth Differ. 1996;7(9):1211-25.

276. Toledo F, Wahl GM. Regulating the p53 pathway: in vitro hypotheses, in vivo veritas. Nat Rev Cancer. 2006;6(12):909-23.

277. Wu W, Kehn-Hall K, Pedati C, Zweier L, Castro I, Klase Z et al. Drug 9AA reactivates p21/Waf1 and Inhibits HIV-1 progeny formation. Virol J. 2008;5:41.

278. Inoue N, Yahagi N, Yamamoto T, Ishikawa M, Watanabe K, Matsuzaka T et al. Cyclin-dependent kinase inhibitor, p21WAF1/CIP1, is involved in adipocyte differentiation and hypertrophy, linking to obesity, and insulin resistance. J Biol Chem. 2008;283(30):21220-9.

279. Tao GZ, Rott LS, Lowe AW, Omary MB. Hyposmotic stress induces cell growth arrest via proteasome activation and cyclin/cyclin-dependent kinase degradation. J Biol Chem. 2002;277(22):19295-303.

280. Desaint S, Luriau S, Aude JC, Rousselet G, Toledano MB. Mammalian antioxidant defenses are not inducible by H2O2. J Biol Chem. 2004;279(30):31157-63.

281. Formichi P, Battisti C, Tripodi SA, Tosi P, Federico A. Apoptotic response and cell cycle transition in ataxia telangiectasia cells exposed to oxidative stress. Life Sci. 2000;66(20):1893-903.

282. Tibbetts RS, Brumbaugh KM, Williams JM, Sarkaria JN, Cliby WA, Shieh SY et al. A role for ATR in the DNA damage-induced phosphorylation of p53. Genes Dev. 1999;13(2):152-7.

283. Fuchs SY, Adler V, Pincus MR, Ronai Z. MEKK1/JNK signaling stabilizes and activates p53. Proc Natl Acad Sci U S A. 1998;95(18):10541-6.

284. Persons DL, Yazlovitskaya EM, Pelling JC. Effect of extracellular signal-regulated kinase on p53 accumulation in response to cisplatin. J Biol Chem. 2000;275(46):35778-85.

285. Bragado P, Armesilla A, Silva A, Porras A. Apoptosis by cisplatin requires p53 mediated p38alpha MAPK activation through ROS generation. Apoptosis. 2007;12(9):1733-42.

286. Moiseeva O, Mallette FA, Mukhopadhyay UK, Moores A, Ferbeyre G. DNA damage signaling and p53-dependent senescence after prolonged beta-interferon stimulation. Mol Biol Cell. 2006;17(4):1583-92.

287. Kurz EU, Lees-Miller SP. DNA damage-induced activation of ATM and ATM-dependent signaling pathways. DNA Repair (Amst). 2004;3(8-9):889-900.

288. Dai MS, Jin Y, Gallegos JR, Lu H. Balance of Yin and Yang: ubiquitylation-mediated regulation of p53 and c-Myc. Neoplasia. 2006;8(8):630-44.

289. Gu W, Roeder RG. Activation of p53 sequence-specific DNA binding by acetylation of the p53 C-terminal domain. Cell. 1997;90(4):595-606.

290. Xirodimas DP, Saville MK, Bourdon JC, Hay RT, Lane DP. Mdm2-mediated NEDD8 conjugation of p53 inhibits its transcriptional activity. Cell. 2004;118(1):83-97.

291. Kim KI, Baek SH. SUMOylation code in cancer development and metastasis. Mol Cells. 2006;22(3):247-53.

292. Chuikov S, Kurash JK, Wilson JR, Xiao B, Justin N, Ivanov GS et al. Regulation of p53 activity through lysine methylation. Nature. 2004;432(7015):353-60.

293. Furukawa A, Tada-Oikawa S, Kawanishi S, Oikawa S. H2O2 accelerates cellular senescence by accumulation of acetylated p53 via decrease in the function of SIRT1 by NAD+ depletion. Cell Physiol Biochem. 2007;20(1-4):45-54.

294. Li T, Santockyte R, Shen RF, Tekle E, Wang G, Yang DCH et al. Expression of SUMO-2/3 induced senescence through p53- and pRB-mediated pathways. J Biol Chem. 2006;281(47):36221-7.

295. Vurusaner B, Poli G, Basaga H. Tumor suppressor genes and ROS: complex networks of interactions. Free Radic Biol Med. 2012;52(1):7-18.

296. Rainwater R, Parks D, Anderson ME, Tegtmeyer P, Mann K. Role of cysteine residues in regulation of p53 function. Mol Cell Biol. 1995;15(7):3892-903.

297. Buzek J, Latonen L, Kurki S, Peltonen K, Laiho M. Redox state of tumor suppressor p53 regulates its sequence-specific DNA binding in DNA-damaged cells by cysteine 277. Nucleic Acids Res. 2002;30(11):2340-8.

298. Polyak K, Xia Y, Zweier JL, Kinzler KW, Vogelstein B. A model for p53-induced apoptosis. Nature. 1997;389(6648):300-5.

299. Budanov AV, Sablina AA, Feinstein E, Koonin EV, Chumakov PM. Regeneration of peroxiredoxins by p53-regulated sestrins, homologs of bacterial AhpD. Science. 2004;304(5670):596-600.

300. Hussain SP, Amstad P, He P, Robles A, Lupold S, Kaneko I et al. p53-induced up-regulation of MnSOD and GPx but not catalase increases oxidative stress and apoptosis. Cancer Res. 2004;64(7):2350-6.

301. Tan M, Li S, Swaroop M, Guan K, Oberley LW, Sun Y. Transcriptional activation of the human glutathione peroxidase promoter by p53. J Biol Chem. 1999;274(17):12061-6.

302. Donald SP, Sun XY, Hu CA, Yu J, Mei JM, Valle D et al. Proline oxidase, encoded by p53-induced gene-6, catalyzes the generation of proline-dependent reactive oxygen species. Cancer Res. 2001;61(5):1810-5.

303. Pani G, Bedogni B, Anzevino R, Colavitti R, Palazzotti B, Borrello S et al. Deregulated manganese superoxide dismutase expression and resistance to oxidative injury in p53-deficient cells. Cancer Res. 2000;60(16):4654-60.

304. Faraonio R, Vergara P, Di Marzo D, Pierantoni MG, Napolitano M, Russo T et al. p53 suppresses the Nrf2-dependent transcription of antioxidant response genes. J Biol Chem. 2006;281(52):39776-84.

305. Drane P, Bravard A, Bouvard V, May E. Reciprocal down-regulation of p53 and SOD2 gene expression-implication in p53 mediated apoptosis. Oncogene. 2001;20(4):430-9.

306. Liu Z, Lu H, Shi H, Du Y, Yu J, Gu S et al. PUMA overexpression induces reactive oxygen species generation and proteasome-mediated stathmin degradation in colorectal cancer cells. Cancer Res. 2005;65(5):1647-54.

307. Macip S, Igarashi M, Berggren P, Yu J, Lee SW, Aaronson SA. Influence of induced reactive oxygen species in p53-mediated cell fate decisions. Mol Cell Biol. 2003;23(23):8576-85.

308. Saftig P, Klumperman J. Lysosome biogenesis and lysosomal membrane proteins: trafficking meets function. Nat Rev Mol Cell Biol. 2009;10(9):623-35.

309. Groth-Pedersen L, Ostenfeld MS, Høyer-Hansen M, Nylandsted J, Jäättelä M. Vincristine induces dramatic lysosomal changes and sensitizes cancer cells to lysosome-destabilizing siramesine. Cancer Res. 2007;67(5):2217-25.

310. Carr CS, Sharp PA. A helix-loop-helix protein related to the immunoglobulin E box-binding proteins. Mol Cell Biol. 1990;10(8):4384-8.

311. Palmieri M, Impey S, Kang H, di Ronza A, Pelz C, Sardiello M et al. Characterization of the CLEAR network reveals an integrated control of cellular clearance pathways. Hum Mol Genet. 2011;20(19):3852-66.

312. Settembre C, Di Malta C, Polito VA, Garcia Arencibia M, Vetrini F, Erdin S et al. TFEB links autophagy to lysosomal biogenesis. Science. 2011;332(6036):1429-33.

313. Sancak Y, Peterson TR, Shaul YD, Lindquist RA, Thoreen CC, Bar-Peled L et al. The Rag GTPases bind raptor and mediate amino acid signaling to mTORC1. Science. 2008;320(5882):1496-501.

314. Liang C, Lee JS, Inn KS, Gack MU, Li Q, Roberts EA et al. Beclin1-binding UVRAG targets the class C Vps complex to coordinate autophagosome maturation and endocytic trafficking. Nat Cell Biol. 2008;10(7):776-87.

315. Settembre C, Zoncu R, Medina DL, Vetrini F, Erdin S, Erdin S et al. A lysosome-to-nucleus signalling mechanism senses and regulates the lysosome via mTOR and TFEB. EMBO J. 2012;31(5):1095-108.

316. Widmann C, Gerwins P, Johnson NL, Jarpe MB, Johnson GL. MEK kinase 1, a substrate for DEVD-directed caspases, is involved in genotoxin-induced apoptosis. Mol Cell Biol. 1998;18(4):2416-29.

317. McKay MM, Morrison DK. Caspase-dependent cleavage disrupts the ERK cascade scaffolding function of KSR1. J Biol Chem. 2007;282(36):26225-34.

318. Chen L, Xu B, Liu L, Luo Y, Yin J, Zhou H et al. Hydrogen peroxide inhibits mTOR signaling by activation of AMPKalpha leading to apoptosis of neuronal cells. Lab Invest. 2010;90(5):762-73.

319. Byun YJ, Kim SK, Kim YM, Chae GT, Jeong SW, Lee SB. Hydrogen peroxide induces autophagic cell death in C6 glioma cells via BNIP3-mediated suppression of the mTOR pathway. Neurosci Lett. 2009;461(2):131-5.

320. Radisavljevic ZM, González-Flecha B. TOR kinase and Ran are downstream from PI3K/Akt in H2O2-induced mitosis. J Cell Biochem. 2004;91(6):1293-300.

321. Lee BY, Han JA, Im JS, Morrone A, Johung K, Goodwin EC et al. Senescence-associated beta-galactosidase is lysosomal beta-galactosidase. Aging Cell. 2006;5(2):187-95.

APPENDICES
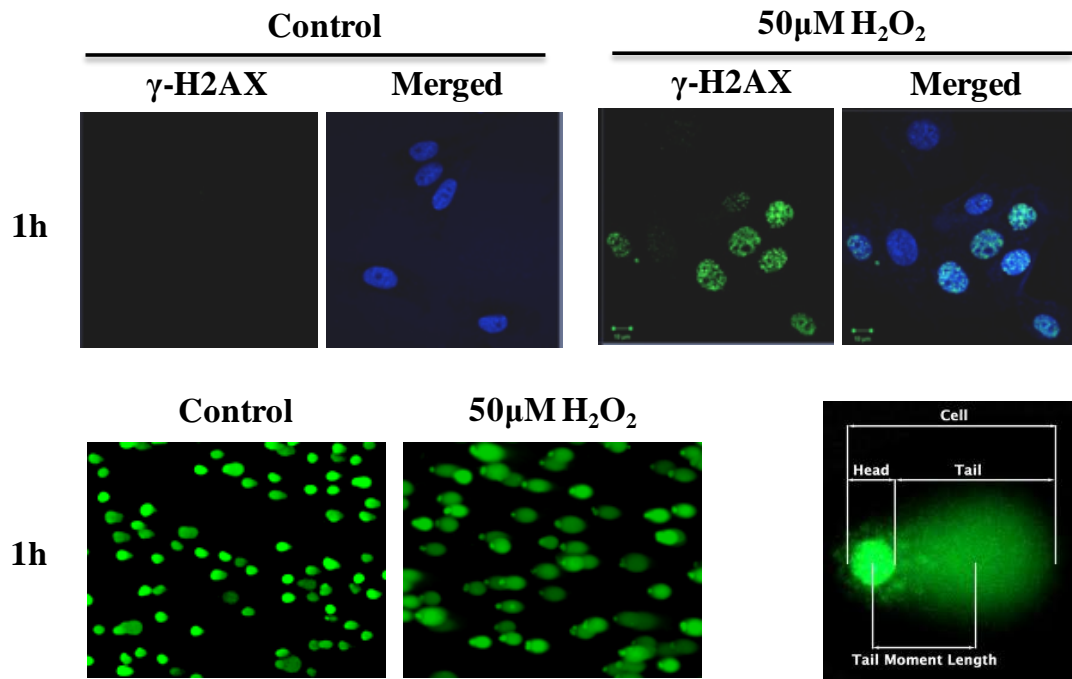
Appendix A. H₂O₂ treatment resulted in DNA damage. L6 myoblasts were treated with 50μM H$_2$O$_2$ for 1h. (A) After fixation, cells were stained with antibody specific to γ-H2AX, a DNA double strand break marker, in green. Nuclei were stained blue with Hoechst 34580. (B) Comet tail moment measurements using alkaline comet assay. (Courtesy of Gireedhar Venkatachalam)
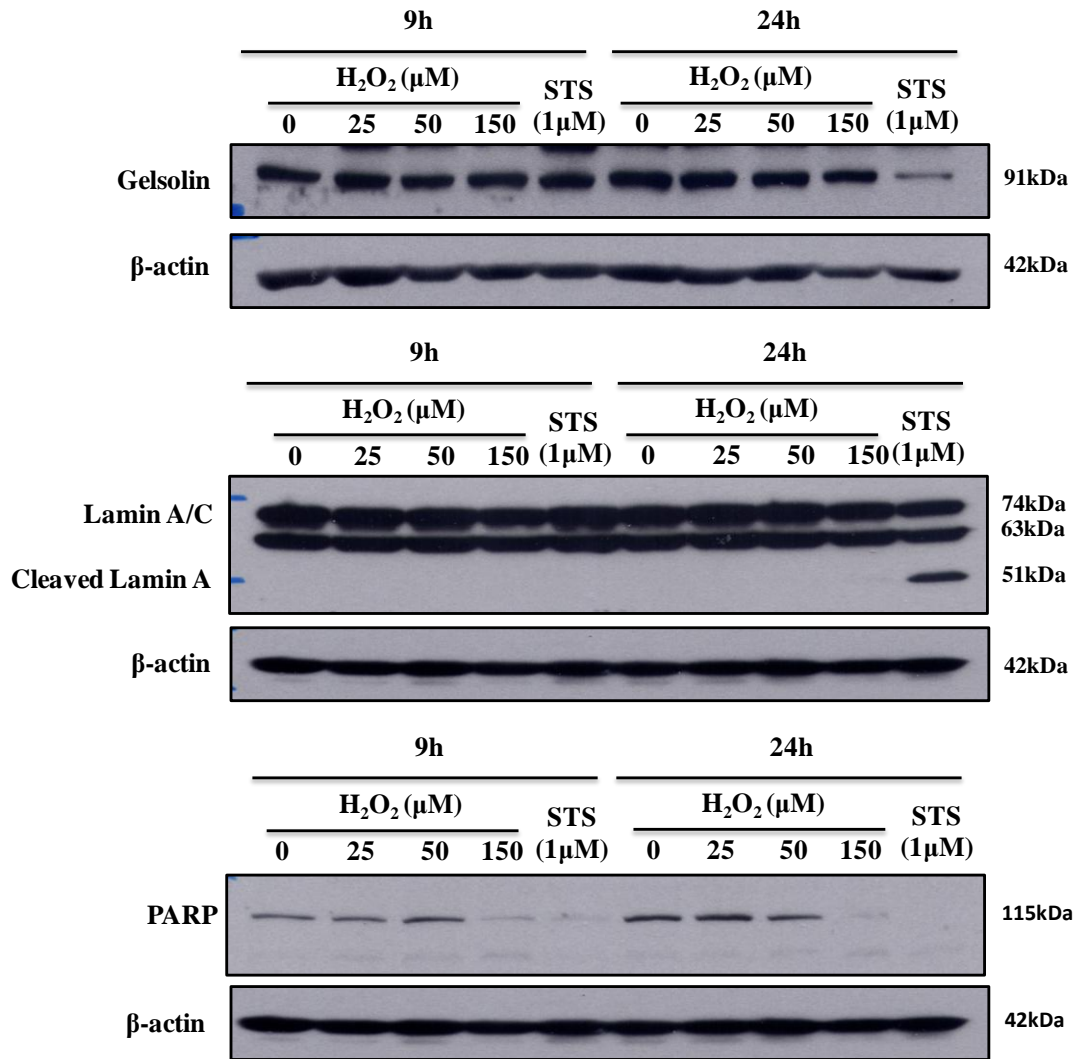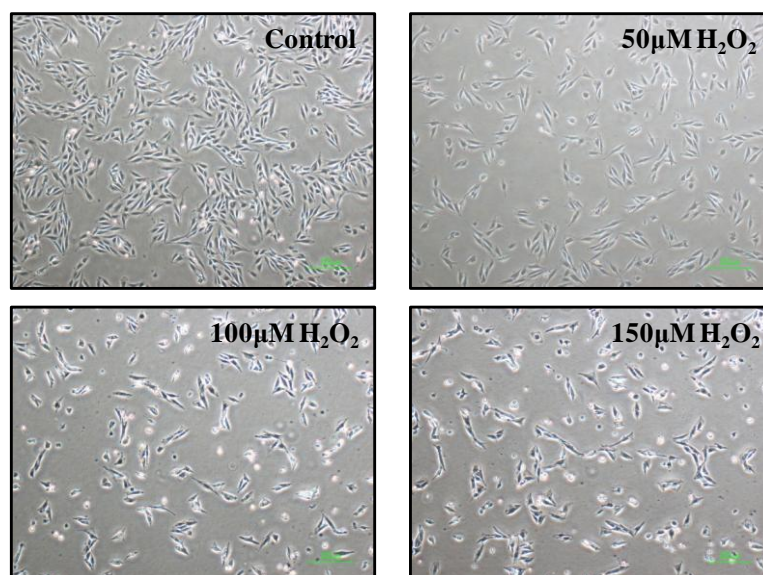
Appendix B. Effect of H₂O₂ and STS treatment on classic caspase 3 substrates cleavage. L6 myoblasts were treated with 25, 50, 150 μM H_2O_2 or 1μM STS. Cells were harvested at 9 hours and 24 hours for Western Blot analysis of cleavage of structural proteins: Gelsolin and Lamin A/C, and DNA damage repair protein: PARP. (Adapted from Deng 2011, Dissertation)
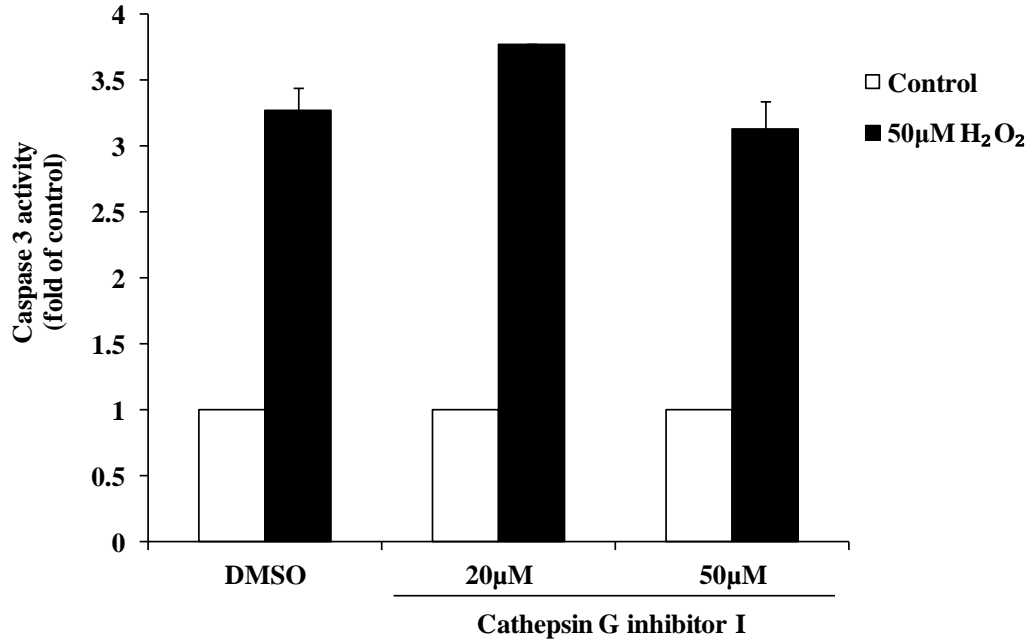
A)
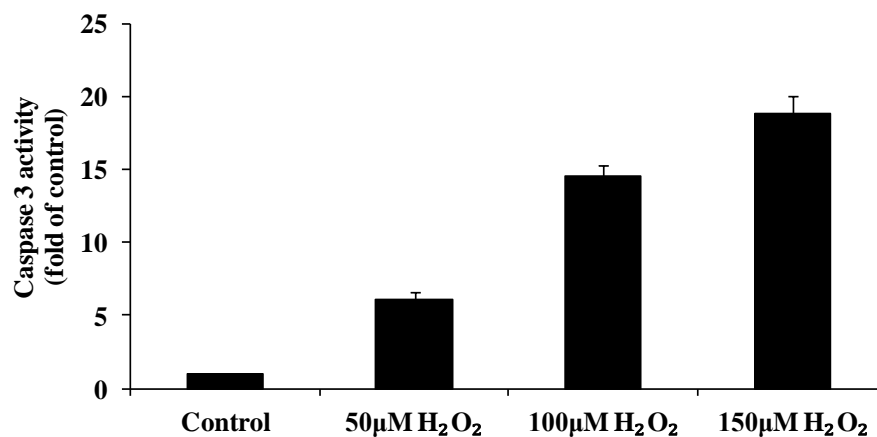
B)

Appendix C. Effect of different dose of H_2O_2 on caspase 3 activity and cell morphology. Cells were treated with increasing dose of H_2O_2 for 24 hours. (A) Cells were harvested for caspase 3 activity assay. The data are the means of three independent experiments ± S.E.M. (B) Cell morphology was observed under a phase contrast microscope.

Appendix D. Caspase 3 activation upon H₂O₂ treatment was independent of cathepsin G. Cells were pre-treated with 20 or 50μM cathepsin G inhibitor I before exposure to 50μM H₂O₂. At 24h post-H₂O₂ treatment, cells were harvested for caspase 3 activity analysis.
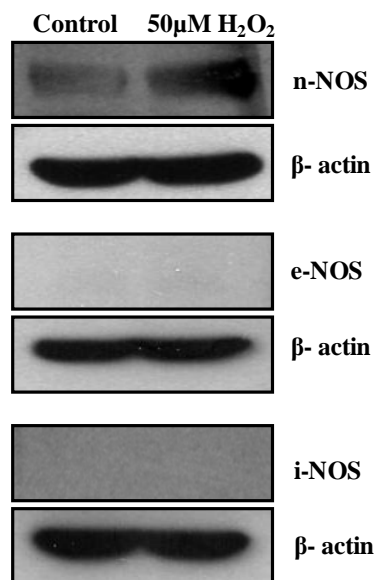
Appendix E. nNOS is expressed in L6 myoblasts. Cells were treated with 50μM H₂O₂ for 24 hours and were harvested for Western Blot analysis of NOS isoforms. (Adapted from Chang 2009, Dissertation)
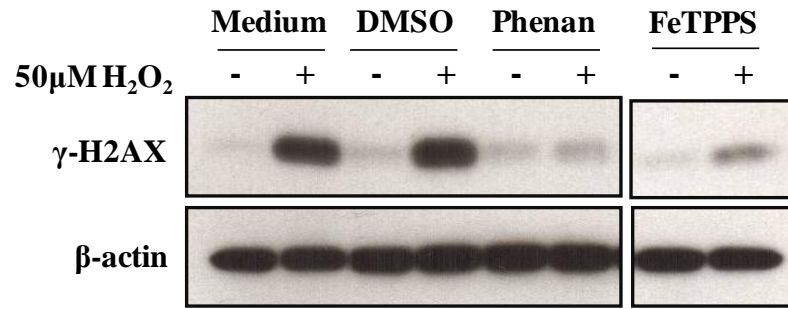
Appendix F. Phosphorylation of γ-H2AX was inhibited by iron and ONOO⁻ chelation. Cells were pre-treated with iron chelator, phenanthroline (Phenan), and peroxynitrite decomposition catalyst, FeTPPS for 2 hours before exposure with 50μM H_2O_2. At 1h post-H_2O_2 treatment, cells were harvested for Western Blot analysis of γ-H2AX. (DMSO: vehicle control). (Courtesy of Gireedhar Venkatachalam)

PUBLICATION AND PRESENTATION

Publication

Leow San Min, Gireedhar Venkatachalam and Marie-Véronique Clément
A new caspase 3-mediated signalling in lysosome biogenesis via TFEB regulation
(In preparation)

Poster presentation

Leow San Min, Michelle Chang Ker Xing and Marie-Véronique Clément
Redox regulation of Na^+/H^+ exchanger (NHE1) gene expression by hydrogen peroxide is p38MAPK- HO-1 dependent
Poster presented at the 2nd Biochemistry Student Symposium, held at the Clinical Research Centre, National University of Singapore (2009).

Leow San Min, Michelle Chang Ker Xing and Marie-Véronique Clément
Redox regulation of Na^+/H^+ exchanger (NHE1) gene expression by hydrogen peroxide is p38MAPK- HO-1 dependent
Poster presented at The Society for Free Radical Biology and Medicine's (SFRBM) 16th Annual Meeting, held at San Francisco, CA, USA (2009).

Leow San Min, Gireedhar Venkatachalam and Marie-Véronique Clément
Accumulation of active caspase 3 in the nucleus of cells exposed to non-toxic dose of H_2O_2 is associated with cells' growth arrest and DNA damage
Poster presented at European Cell Death Organization (ECDO) 19th Euroconference, held at Stockholm, Sweden (2011).

Oral presentation

Leow San Min and Marie-Véronique Clément
Regulation of caspase 3 activation during mild oxidative stress
Presented at Department of Biochemistry "Research in Progress" Seminar for post-graduates. National University of Singapore (2009).